

Scour at Contracted Bridges

DETAILS

0 pages | | PAPERBACK

ISBN 978-0-309-43168-2 | DOI 10.17226/21995

AUTHORS

BUY THIS BOOK

FIND RELATED TITLES

Visit the National Academies Press at NAP.edu and login or register to get:

- Access to free PDF downloads of thousands of scientific reports
- 10% off the price of print titles
- Email or social media notifications of new titles related to your interests
- Special offers and discounts



Distribution, posting, or copying of this PDF is strictly prohibited without written permission of the National Academies Press. (Request Permission) Unless otherwise indicated, all materials in this PDF are copyrighted by the National Academy of Sciences.

Scour at Contracted Bridges

Prepared for:

National Cooperative Highway Research Program

TRANSPORTATION RESEARCH BOARD

OF THE NATIONAL ACADEMIES

Submitted by:

C.R. Wagner, D.S. Mueller,

A.C. Parola, D.J. Hagerty, and S. T. Benedict

U.S. Geological Survey and University of Louisville

Louisville, Kentucky

March 2006

ACKNOWLEDGMENT

This work was sponsored by the American Association of State Highway and Transportation Officials (AASHTO), in cooperation with the Federal Highway Administration, and was conducted in the National Cooperative Highway Research Program (NCHRP), which is administered by the Transportation Research Board (TRB) of the National Academies.

COPYRIGHT PERMISSION

Authors herein are responsible for the authenticity of their materials and for obtaining written permissions from publishers or persons who own the copyright to any previously published or copyrighted material used herein.

Cooperative Research Programs (CRP) grants permission to reproduce material in this publication for classroom and not-for-profit purposes. Permission is given with the understanding that none of the material will be used to imply TRB, AASHTO, FAA, FHWA, FMCSA, FTA, or Transit Development Corporation endorsement of a particular product, method, or practice. It is expected that those reproducing the material in this document for educational and not-for-profit uses will give appropriate acknowledgment of the source of any reprinted or reproduced material. For other uses of the material, request permission from CRP.

DISCLAIMER

The opinion and conclusions expressed or implied in the report are those of the research agency. They are not necessarily those of the TRB, the National Research Council, AASHTO, or the U.S. Government.

This report has not been edited by TRB.

THE NATIONAL ACADEMIES

Advisers to the Nation on Science, Engineering, and Medicine

The **National Academy of Sciences** is a private, nonprofit, self-perpetuating society of distinguished scholars engaged in scientific and engineering research, dedicated to the furtherance of science and technology and to their use for the general welfare. On the authority of the charter granted to it by the Congress in 1863, the Academy has a mandate that requires it to advise the federal government on scientific and technical matters. Dr. Ralph J. Cicerone is president of the National Academy of Sciences.

The **National Academy of Engineering** was established in 1964, under the charter of the National Academy of Sciences, as a parallel organization of outstanding engineers. It is autonomous in its administration and in the selection of its members, sharing with the National Academy of Sciences the responsibility for advising the federal government. The National Academy of Engineering also sponsors engineering programs aimed at meeting national needs, encourages education and research, and recognizes the superior achievements of engineers. Dr. William A. Wulf is president of the National Academy of Engineering.

The **Institute of Medicine** was established in 1970 by the National Academy of Sciences to secure the services of eminent members of appropriate professions in the examination of policy matters pertaining to the health of the public. The Institute acts under the responsibility given to the National Academy of Sciences by its congressional charter to be an adviser to the federal government and, on its own initiative, to identify issues of medical care, research, and education. Dr. Harvey V. Fineberg is president of the Institute of Medicine.

The **National Research Council** was organized by the National Academy of Sciences in 1916 to associate the broad community of science and technology with the Academy's purposes of furthering knowledge and advising the federal government. Functioning in accordance with general policies determined by the Academy, the Council has become the principal operating agency of both the National Academy of Sciences and the National Academy of Engineering in providing services to the government, the public, and the scientific and engineering communities. The Council is administered jointly by both the Academies and the Institute of Medicine. Dr. Ralph J. Cicerone and Dr. William A. Wulf are chair and vice chair, respectively, of the National Research Council.

The **Transportation Research Board** is a division of the National Research Council, which serves the National Academy of Sciences and the National Academy of Engineering. The Board's mission is to promote innovation and progress in transportation through research. In an objective and interdisciplinary setting, the Board facilitates the sharing of information on transportation practice and policy by researchers and practitioners; stimulates research and offers research management services that promote technical excellence; provides expert advice on transportation policy and programs; and disseminates research results broadly and encourages their implementation. The Board's varied activities annually engage more than 5,000 engineers, scientists, and other transportation researchers and practitioners from the public and private sectors and academia, all of whom contribute their expertise in the public interest. The program is supported by state transportation departments, federal agencies including the component administrations of the U.S. Department of Transportation, and other organizations and individuals interested in the development of transportation.
www.TRB.org

www.national-academies.org

TABLE OF CONTENTS

LIST OF FIGURES	ii
LIST OF TABLES	v
ACKNOWLEDGMENTS	vii
ABSTRACT	viii
CHAPTER 1 Introduction and Research Approach	1
Purpose and Objectives	
Scope and Approach of Research	
CHAPTER 2 Findings	7
Executive Summary of Literature Review and Field Data	
Scour at Bridge Contractions	
Contraction Scour	
Abutment Scour	
Scour with Debris	
Applying Numerical Models for Scour Analysis	
Erodibility and Geotechnical Properties of Materials	
CHAPTER 3 Interpretation, Appraisal, and Applications	92
Recommended Modifications to Scour Prediction Methodology	
Guidelines for Numerical Modeling	
Erodibility and Geotechnical Properties of Materials	
CHAPTER 4 Conclusions and Suggested Research	101
Conclusions	
Recommendations	
Modification to Strategic Research Plan	
REFERENCES	113
APPENDIX A: Case Study Reports	A-1

LIST OF FIGURES

1.	Example of single scour hole at shorter bridges, as shown at U.S. Route 301, crossing Douglas Swamp in Florence County, South Carolina, July 31, 1996.....	15
2.	Example of separate left and right abutment-scour holes at longer bridges, as shown at Road S-87 bridge, crossing the Coosawhatchie River in Jasper County, South Carolina, November 12, 1997.....	16
3.	Plot of abutment scour measurements at the C.R. 22 bridge over the Pomme De Terre River near Fairfield, Minnesota in April 1997.....	18
4.	Plot of contraction scour measurements at (A) Conehoma Creek at State Highway 35, near Kosciusko, Mississippi, April 1979 and (B) Beaver Creek Overflow at US 2, 7 miles West of Saco, Montana...	19
5.	Relation of observed and theoretical clear-water contraction-scour depth for the 100-year flow, in the Piedmont of South Carolina. (Theoretical contraction scour calculated with the Laursen (1963) equation.).....	29
6.	Example of scour-hole low point located upstream of S.R. 218 over the Cedar River near Janesville, Iowa.....	32
7.	Example of scour-hole low point located downstream of S.R. 25 over the Minnesota River near Belle Plaine, Minnesota.....	33
8.	Site configuration, flow patterns and approach section location for S.R. 37 over the James River near Mitchell, South Dakota.....	34
9.	Relation of longitudinal location for the low point of the abutment-scour hole and the 100-year-flow top width at the bridge for (A) shallow and deep scour holes in the Piedmont of South Carolina, and (B) sites in the Coastal Plain of South Carolina.....	36
10.	Example of scour-hole low point located upstream of Road S-299, crossing Cannons Creek in Newberry County, South Carolina, November 24, 1997.....	37
11.	Example of scour-hole low point located downstream of S.C. Route 41, crossing Maiden Down Swamp in Marion County, South Carolina, December 3, 1996.....	37
12.	Illustration of flow contracted by an embankment constructed in a floodplain.....	43

13.	Relation of observed clear-water abutment-scour depth and the 100-year-flow embankment length, normalized by the 100-year-flow depth near the abutment toe, for the Piedmont and Coastal Plain of South Carolina with (A) a complete horizontal axis, and (B) a truncated horizontal axis.....	46
14.	Comparison of the embankment-length envelope for field observations of abutment-scour depth in South Carolina with the observed abutment-scour for selected sites from the National Bridge Scour Database (BSDMS).....	49
15.	Comparison of field observations of abutment-scour depth with the theoretical abutment-scour depth computed with the original Froehlich (1989) and modified Froehlich (2001) equations for selected sites from the National Bridge Scour Database (BSDMS).....	51
16.	Comparison of field observations of abutment-scour depth with theoretical abutment-scour depth computed with the HEC-18 (2001) Sturm equation (with and without the safety factor) for selected sites from the National Bridge Scour Database (BSDMS).....	52
17.	Aerial photograph of State Route 25 over the Minnesota River near Belle Plaine, Minnesota.....	60
18.	Comparison of observed and model-velocity distributions at U.S. Route 12 over the Pomme de Terre River, Minnesota for (A) April 5, 1997 and (B) April 9, 1997.....	71
19.	Comparison of observed and model velocity distributions at County Route 22 over the Pomme de Terre River, Minnesota for (A) April 5, 1997 and (B) April 9, 1997.....	72
20.	Plan view of topography and channel alignment for County Route 22 over the Pomme De Terre River near Fairfield, Minnesota.....	74
21.	Sketch of the hydrodynamics observed during bridge scour measurements at County Route 22 over the Pomme de Terre River on April 5, 1997.....	76
22.	Modeled flow field for County Route 22 over the Pomme de Terre River for conditions on April 5, 1997	77
23.	Computational mesh for the two-dimensional model of County Route 22 over the Pomme de Terre River.....	78

24.	Comparison of the velocity distribution for the two-dimensional model and field measurements at the upstream bridge face of County Route 22 over the Pomme de Terre River on (A) April 5, 1997 and (B) April 9, 1997.....	79
25.	Difference in bed elevation (in meters) between two-dimensional sediment-transport model output and field data collected during flood conditions on the Pomme de Terre River at County Route 22, April 4-9, 1997.....	81
26.	Comparison of the velocity distribution for the two-dimensional model, one-dimensional models and field measurements at the upstream bridge face of County Route 22 over the Pomme de Terre River on (A) April 5, 1997 and (B) April 9, 1997.....	82
27.	Comparison of the original one-dimensional and two-dimensional model-approach section location with an approach section in a location more representative of the actual blocked and main channel hydraulics at County Route 22 over the Pomme de Terre River	83
28.	Looking upstream from the east-bound bridge deck of Highway 70 over Bear Creek near Lagrange, North Carolina during low-low.....	90

LIST OF TABLES

1.	Summary of live-bed contraction-scour equation exponents.....	22
2.	Comparison of observed and theoretical contraction-scour depth (clear-water and live-bed) for bridge sites in the National Bridge Scour Database (BSDMS).....	26
3.	Comparison of observed abutment scour with scour calculated using the HEC-18 (2001) Froehlich and Sturm prediction equations using HEC-RAS modeled hydraulics for eight abutment scour sites in the National Bridge Scour Database (BSDMS).....	53
4.	Comparison of observed abutment scour with scour calculated using the HEC-18 (2001) prediction equations using hydraulic parameters measured in the field for two sites in the National Bridge Scour Database (BSDMS).....	55
5.	Comparison of measured and modeled abutment-tip velocities for use in the HIRE abutment scour prediction equation.....	57
6.	Comparison of observed abutment scour with scour calculated using the HEC-18 (2001) Froehlich and HIRE prediction equations using modeled and field hydraulics for two abutment scour sites in the National Bridge Scour Database (BSDMS).	58
7.	Comparison of observed abutment scour with scour calculated using the HEC-18 (2001) Sturm and Maryland prediction equations using modeled and field hydraulics for two abutment scour sites in the National Bridge Scour Database (BSDMS).....	59
8.	Comparison of observed abutment scour with scour calculated using the HEC-18 (2001) Froehlich and HIRE prediction equations using flood and pre-flood geometry for four abutment scour sites in the National Bridge Scour Database (BSDMS).....	62
9.	Comparison of observed abutment scour with scour calculated using the HEC-18 (2001) Sturm and Maryland prediction equations using flood and pre-flood geometry for four abutment scour sites in the National Bridge Scour Database (BSDMS).....	63
10.	Comparison of Melville's debris scour estimating procedure with HEC-18 procedures and observed debris scour at S.R. 129 over the Chariton River near Prairie Hill, Missouri.....	67

11.	Comparison of debris-width design-criteria relation (Diehl, 1997) and measured debris raft diameters for S.R. 129 over the Chariton River near Prairie Hill, Missouri.....	68
12.	Comparison of HEC-18 scour estimates (Froehlich, HIRE, and live-bed equations) from the one-dimensional and two-dimensional models (original and adjusted approach-section locations) relative to the sediment transport model results and observed scour at County Route 22 over the Pomme de Terre River on April 9, 1997.....	84

ACKNOWLEDGMENTS

The research reported herein was conducted under NCHRP Project 24-14 by the U.S. Geological Survey and University of Louisville, Department of Civil Engineering. University of Louisville was the contractor for this study. The work undertaken by the U.S. Geological Survey was under a subcontract with the University of Louisville. Arthur C. Parola, Professor of Civil Engineering, University of Louisville, was the principal investigator. David S. Mueller, Hydrologist, U.S. Geological Survey was co-principal investigator. The other authors of this report are Chad R. Wagner, Hydrologist, U.S. Geological Survey; Stephen T. Benedict, Hydrologist, U.S. Geological Survey; and D. J. Hagerty, Professor of Civil Engineering, University of Louisville. The field work of the U.S. Geological Survey was conducted with assistance from Ed Puckett, Hydrologic Technician; Brian Moore, Hydrologic Technician; and Harry Hitchcock, retired Hydrologic Technician. The work at the University of Louisville was completed under the supervision of Professor Parola with the assistance of Michelle Matherly, Research Assistant and Andrea Curini, Research Engineer.

ABSTRACT

The main purpose of NCHRP Project 24-14 was to collect field data from which processes affecting scour magnitude in contracted bridge openings could be identified, to support verification of physical and numerical model studies, and to improve guidelines for applying scour-prediction methods at contracted bridge sites. The objectives were accomplished by the collection and analysis of data at 15 bridge sites. A combination of real-time and post-flood data collection activities provided comprehensive field data sets. Detailed directional velocity data were collected throughout the reaches affected by the bridge where flood and site conditions permitted (4 of 15 sites). In addition, streambed, stream bank and floodplain material properties were described. Raw data were reduced and assembled into a database accessible through the World Wide Web (http://ky.water.usgs.gov/Bridge_Scour/BSDBMS/index.htm).

Scour predictions based on the methods provided in HEC-18 were compared to the observed scour at each site. Flow velocity and depth data obtained from real-time investigations along with post-flood topographic surveys were used to develop and calibrate two-dimensional hydraulic models (RMA-2 and FESWMS) at two sites. One-dimensional hydraulic models (HEC-RAS or WSPRO) were developed for all sites where sufficient cross sectional data were collected or available. The velocities obtained from numerical simulations were compared to measured velocities.

The observations and measured data demonstrate the inaccuracies of the current scour prediction methods as specified in HEC-18 related to contraction scour and abutment and the effectiveness of the Melville and Dongol method for predicting scour at a pier with debris. Measured flow-velocity distributions and those computed from the one-dimensional and two-dimensional models were compared. Scour topography computed with the two-dimensional hydraulic model and two-dimensional sediment-transport model were compared. Recommendations for future research that will advance scour-prediction methods were provided including suggested modifications to the Strategic Plan for Scour Research (NCHRP Project 24-8). Appendix A, 10 case studies, is provided.

CHAPTER 1: INTRODUCTION

Current application of scour prediction methods overestimates scour depths around abutments and in contracted openings at many locations. Such excessive scour depth prediction results in construction of unnecessarily deep foundations or installation of unnecessary countermeasures. State Departments of Transportation are using methods recommended in HEC-18 (Richardson and Davis, 2001) to estimate the potential for scour at bridges. These scour-prediction methods are based primarily on simplified small-scale model studies conducted in laboratory flumes. These laboratory investigations typically model straight, rectangular channels with uniform approach-flow velocities, approach-flow depths, and non-cohesive bed material. The floodplains represented in the model studies are often of uniform roughness and are typically of a roughness similar to the main channel; however, variable width compound channels, floodplains with highly non-uniform roughness and non-uniform sediments with varying degrees of cohesiveness, are typical of most bridge sites.

The concept of scour components, which can be summed to obtain total scour, was derived from observations of scour in laboratory studies. These components consist of local scour at piers and abutments and contraction scour caused by the overall contraction of flow at the bridge. Long-term degradation associated with the streambed adjustments over long river reaches, considered independent of the bridge, also contributes to changes in streambed elevations at the bridge; therefore, long-term degradation is considered as a component of total scour.

Error in prediction of scour components stems from three sources: (1) estimation of hydraulic parameters, typically through hydraulic modeling; (2) selection of scour-prediction parameters; and (3) scour-prediction equations. The hydraulic parameters usually are estimated from a one-dimensional hydraulic model that distributes flow across the approach and bridge opening by conveyance (combination of roughness and flow area); however, the flow distribution at a bridge or in its approach is typically non-uniform because of cross-stream flow caused by channel bends, complex roughness patterns, irregular valley topography, and obstructions in the floodplain. Bridges and approach embankments not aligned perpendicular to the approach flow further complicate flow patterns and velocity distributions. The empirical scour-depth prediction equations developed from laboratory studies use average flow parameters such as approach velocity, flow depth, and embankment length. A high degree of subjectivity is often required to select these parameters. The simplifications involved in using laboratory experiments to develop scour-prediction methods and the subjectivity required to extract average representative parameters from non-uniform and heterogeneous field conditions contribute to the uncertainty and error of scour-depth prediction.

A well-recognized source of scour-prediction error is the inadequate representation of erosion resistance of soils. The scour-prediction equations recommended in HEC-18 were developed for uniform, unstratified, non-cohesive sediments that are representative of the most severe scour conditions. The erosional resistance of typical soils found at bridge sites is a combination of stratified soils with varying degrees of cohesiveness. In addition, the surface soils often are protected and reinforced by vegetation or armored by the largest size fractions of the

bed material. The complexity of the erosion resistance of bed material has been marginally included into scour-prediction equations.

Three comparisons are necessary to evaluate the current design guidance and to form the basis of significant improvement in scour-prediction accuracy. First, comparison of scour depth predicted by the current guidance with field measured scour depth is needed to provide an overall assessment of the state-of-practice. Second, comparison of the hydraulics from one-dimensional numerical models with the measured hydraulics is required to evaluate the adequacy of those models for estimating the hydraulics at contracted sites. Third, comparison of scour computed using measured hydraulics with the observed depth of scour is needed to provide a direct evaluation of the scour-prediction equations. These comparisons are the basis for determining the source of inaccuracies associated with the scour-prediction methods.

PURPOSE AND OBJECTIVES

The main purpose of NCHRP Project No. 24-14 was to collect field data from which processes affecting scour magnitude in contracted openings could be identified, to support verification of physical and numerical model studies, and to improve guidelines for applying scour-prediction methods at contracted bridge sites.

The specific objectives of this research are as follows:

- (1) to describe and quantify the influence of processes affecting scour magnitude in contracted openings using field data;
- (2) to provide field data for use in verification of physical- and numerical-model studies;
- (3) to develop interim guidelines for applying scour-prediction methodology at contracted bridge sites for a wide range of common field situations; and
- (4) to provide recommendations for future research that will advance scour-prediction methodology in accordance with the Strategic Plan for Scour Research as modified by the findings of this research (Parola et al, 1996).

SCOPE AND APPROACH OF RESEARCH

The objectives were accomplished by the collection and analysis of data at 15 bridge sites. A combination of real-time and post-flood data-collection activities provided comprehensive field data sets. Real-time measurements are measurements of flow velocities and channel bathymetry during the flood event. Post-flood data collection consists of detailed bathymetric, geotechnical, and geomorphologic measurements obtained after the floodwaters recede. Emphasis was placed on collection of comprehensive real-time and post-flood data sets to quantify the non-uniform and time-dependent flow and geotechnical conditions at the sites and to define the processes responsible for total scour. Scour that forms within bridge contractions and around bridge abutments is dependent on the entire flow field approaching, within and exiting the bridge area; therefore, detailed directional velocity data were collected throughout the

reach affected by the bridge where flood and site conditions permitted (4 of 15 sites). In addition, streambed, stream bank, and floodplain-material properties were described.

Raw data were reduced and assembled into a database. The database interface was developed such that the information is easily accessible by both researchers and highway engineers. The database is accessible through the World Wide Web at the following location: http://ky.water.usgs.gov/Bridge_Scour/BSDMS/index.htm.

The scour predictions based on the methods provided in HEC-18 were compared to the observed scour at each site. Flow velocity and depth data obtained from real-time investigations along with post-flood topographic surveys were used to develop and calibrate two-dimensional models such as RMA-2 and FESWMS at two sites. The one-dimensional hydraulic models HEC-RAS or WSPRO were developed for all sites where sufficient cross-sectional data were collected or available. The velocities obtained from numerical simulations were compared to measured velocities.

The research team identified processes that substantially affect scour, but are not represented in HEC-18. The observations and measured data demonstrate inaccuracies of the current scour-prediction methods as specified in HEC-18; however, there were insufficient data to support the reliability of recommended changes without additional research.

The research team provided recommendations for future research that will advance scour prediction methods. These recommendations include suggested modifications to the Strategic Plan for Scour Research to reflect the findings of this research.

CHAPTER 2: FINDINGS

EXECUTIVE SUMMARY OF LITERATURE REVIEW AND FIELD DATA

Scour at contracted bridge openings results from the complex interaction of hydraulics, bridge geometry, soils characteristics, and other site-specific conditions. The current understanding of bridge-scour processes, largely have been derived from laboratory investigations consisting of physical models in straight, rectangular flumes with uniform non-cohesive bed material. These models simplify the complexities of field conditions, but allow researchers to gain insights about scour processes under controlled conditions. Observations from these studies have led to the development of simplified concepts of scour processes and various methods for evaluating scour at bridges. The concepts and methods for evaluating scour derived from these studies may not accurately account for scour processes in the field, because of the simplifications inherent in these laboratory investigations.

The literature divides bridge scour into various components that are considered independent and additive. The most common components include long-term streambed aggradation or degradation, contraction scour, and local scour. Most research has focused on the last two components, and a summary of contraction and local scour as it relates to this study follows.

Contraction scour is the erosion of material from the bed and banks across all or most of the channel width, resulting from the contraction of flow area. The literature presents various

methods for estimating contraction scour including (1) regime equations, (2) hydraulic-geometry equations, (3) numerical sediment-transport models, and (4) contraction-scour equations.

Regime and hydraulic-geometry equations are empirical equations that are used to assess changes in channel geometry for given hydraulic conditions. Although originally developed to assist in the design or assessment of channel shape, these methods can be used for estimating contraction scour at bridges. The assumption implied by use of these equations is that changes in unit discharge cause a unique change in channel depth. These equations must be calibrated with local or regional field data, which limits their application to sites with characteristics similar to those used for calibration.

Numerical sediment-transport models combine various sediment-transport equations with numerical hydraulic models to simulate scour processes in streams. Hydraulic conditions estimated with these models are used to drive the sediment-transport equations. The literature shows that the various sediment transport equations provide significantly different estimates of sediment discharge for the same site. Given adequate topographic and channel data, numerical models have been shown to provide reasonable estimates of hydraulic parameters at some sites. Adequate representation of sediment transport and scour requires selection of specific sediment-transport equations developed for the specific conditions of the site and may require site calibration. To assure that the results from the sediment-transport numerical model are reasonable, the model should be calibrated and verified with observed field data. Sediment transport models are rarely used to estimate contraction scour because of the time and cost associated with data collection necessary to construct, calibrate and verify these models.

The literature describes a number of semi-empirical contraction-scour equations that were developed by use of conservation of flow and sediment in a control volume, in conjunction with laboratory derived concepts of sediment transport. These equations can be readily applied to a given site, which may account for their common use.

Laboratory researchers have found that the transport or lack of transport of sediment in the flow approaching an obstruction or contraction is critical in assessing scour at bridges. Contraction scour has traditionally been classified as live-bed or clear-water, which reflects the bed material sediment-transport conditions of approaching flows. Researchers have used similar approaches to derive the various equations. In the case of live-bed scour, the common assumption is that scour will cease when the load of sediment transport into the contraction is equal to the load transported from the contraction. The major difference in the various equations stems from the use of different sediment-transport relations. Though differences exist within the derivations, the format and exponents of the various live-bed equations generally are similar. In the case of clear-water scour, the common assumption is that scour will cease when the bed-shear stress in the contraction equals the critical shear stress for the bed material. The critical shear stress is typically determined from Shield's diagram that represents a laboratory-derived shear stress for incipient motion of uniform, noncohesive sediments. The Shield's relation and other similar relations represent laboratory-derived shear stress for incipient motion of uniform, noncohesive sediments. Other common assumptions used in the derivation of live-bed and clear-water contraction-scour equations include steady-uniform flow, noncohesive bed material, and sufficient time to achieve equilibrium conditions. To the degree that field conditions deviate

from these and other assumptions, it is likely that the contraction-scour equations may not provide reasonable scour depths under field conditions.

Local scour is the removal of bed material from around flow obstructions such as piers, abutments, spurs, and embankments caused by the local flow field induced by a pier or abutment. Analytical equations for predicting abutment scour primarily have been derived from observations obtained from small-scale physical-model studies conducted in laboratory flumes. As with contraction scour, abutment-scour equations have been classified as live-bed or clear-water, reflecting the approaching sediment-transport conditions. The equations can be subdivided further into empirical and semi-empirical equations. The empirical equations were developed from envelope curves or regression analysis of dimensionless variables obtained from laboratory investigations. The semi-empirical equations were derived in a similar manner to the contraction-scour equations by use of conservation of flow and sediment in a control volume in conjunction with laboratory-derived concepts of sediment transport. Abutment-scour depth is often assumed to be a function of contraction-scour depth and the contraction-scour equation is adjusted to reflect the increased scour potential at the abutment. In addition to laboratory-derived equations, there are several abutment-scour equations derived from field observations. These field-derived equations were developed from limited data sets for site-specific conditions; therefore, they may not be applicable to other sites. Numerical sediment-transport models also have been used to investigate abutment scour, and results from these models are subject to the same limitations described for contraction scour.

Complete and reliable field data sets are rare, although there have been more than 100 laboratory studies in which detailed and complete data sets have been published (Melville and

Coleman, 2000). A survey of the literature located 30 references with potential field data for abutment and contraction scour. Of the 30 references reviewed, 4 are potential sources of data for abutment scour and 22 are potential sources for contraction scour. Most of the scour data presented in these references were collected during post-flood investigations, and flow conditions that created the scour were estimated from hydraulic models. Nearly all of the sites identified in the literature review required the compilation of raw data and additional analysis to obtain complete abutment and contraction-scour data sets. An exception to this is data collected by the U.S. Geological Survey (USGS) at 146 bridges in South Carolina. Hydraulic models were developed for these sites and hydraulic variables were compiled into a database and associated with field observations of scour. This database was developed to assess clear-water contraction and abutment-scour equations. It should be noted that the South Carolina data were not just post-flood measurements, but were often remnant scour after several years or decades of recovery and there was often no knowledge of what flood event caused the scour.

Studies found in some of the references compare field observations with computed scour. Contraction- and abutment-scour comparisons frequently predict scour depths greater than those observed and often this bias can be three to four times the measured scour depth; however, some comparisons indicate that there are conditions under which some equations will predict scour depths less than those observed. These comparisons indicate that the current methods for predicting contraction and abutment scour at bridges are unreliable.

SCOUR AT BRIDGE CONTRACTIONS

Field observations of scour at many bridges indicate that conceptual separation of contraction and abutment scour as described in Hydraulic Engineering Circular-18 (HEC-18) (Richardson and Davis, 2001) is problematic because the hydrodynamic mechanisms that induce the individual scour components work together. It is clear from the field observations of this study that the scour that occurs near the ends of the abutment is the result of a complex combination of flow contraction and flow curvature.

Scour-prediction methods published in HEC-18 indicate that contraction and abutment scour are separate and additive for all contracted bridge openings. HEC-18 follows a conservative approach of adding the scour components to create a scour prism for design and assessment purposes, because of an insufficient amount of field data to develop an understanding of the interaction of scour components. Therefore, to compute the total scour at an abutment, the individual components of long-term streambed change, contraction scour, and abutment scour within the abutment region must be estimated and then summed. Isolating the effect of an individual scour component is difficult because the various components interact in the development of the total depth of scour. Laboratory investigations typically have focused on understanding each scour component in isolation, necessitating the approach for estimating total scour as outlined in HEC-18. Analyses of field observations, in conjunction with the theory of flow patterns in short contractions, indicate that this view of scour in the abutment region may be inappropriate.

Consideration of contraction and local-abutment scour as independent and separate processes in the abutment region is a particular concern. The assessment of contraction scour is often based on the simplifying assumption of uniform-flow distributions within a long contraction. By simplifying the hydraulics in a contraction to uniform flow, the current patterns are assumed rectilinear and equations for predicting scour can be derived following the procedure applied by Laursen (1963), which utilized the concept of critical bed-shear stress for rectilinear flow. As the abutment-to-abutment width of the contracted bridge increases for a given depth, local flow patterns through the structure trend toward becoming approximately rectilinear and the assumptions used to develop Laursen's (1963) equation are more appropriate. The highly curvilinear velocities near the abutment promote vortices, which are the primary mechanism for the development of scour in the abutment region (Dongol, 1993). The absence of rectilinear flow patterns in the abutment region indicate that it may be reasonable to assume that scour produced by this flow pattern is absent as well. Following this logic, contraction scour produced by rectilinear flow should not be considered a component of total scour within the abutment region; therefore, the total scour in an abutment region should consist of long-term streambed change, local abutment scour generated from the highly curvilinear-flow patterns, and local scour generated from any piers within this same flow field (Benedict, 2003).

Reference conditions from which the abutment scour and contraction-scour depth can be measured at field sites are difficult to determine because, unlike the planar initial conditions of laboratory experiments, field sites have a complex bed topography that reflects site history including bridge and roadway construction. When attempting to compare field observations and scour predictions from various abutment-scour equations derived from laboratory data, it is

necessary to understand how the depth of abutment scour or contraction scour was measured in the laboratory. In the laboratory, observed contraction scour that has occurred beyond the abutment region is subtracted from the total observed scour depth at a simulated abutment. For example, laboratory investigations by Dongol (1993) measured contraction scour at a flume wall opposite from an abutment, and subtracted it from the total scour at the abutment in an attempt to isolate the scour created by the abutment alone. A parallel reference condition rarely exists under complex field conditions making comparisons of data difficult.

Analysis of field data has shown that the interaction between what has been called contraction and abutment scour is highly complex. It is sometimes difficult to separate the two components in the region adjacent to abutments. Using data collected at 146 sites in South Carolina, Benedict (2003) found that bridges approximately 240 ft or less in length tend to form a large, single scour hole (Figure 1) rather than separate left and right abutment-scour holes (Figure 2). This phenomenon may be caused by the highly rotational flow separating from the channel boundary at the left and right abutments. Scour holes at these shorter bridges could be classified as abutment scour hole, because highly rotational flow is typically associated with abutment scour; however, the scour hole could instead be classified as contraction scour because it is separated from the abutment and is a single scour hole near the center of the channel. Scour holes at bridges shorter than 240 ft were classified as abutment scour by Benedict (2003), although the bed was degraded across the entire channel, characteristic of contraction scour. Field data collected throughout the United States for NCHRP Project 24-14 did not show the same consistent breakpoint at 240 ft as was observed in South Carolina; however, the data collected

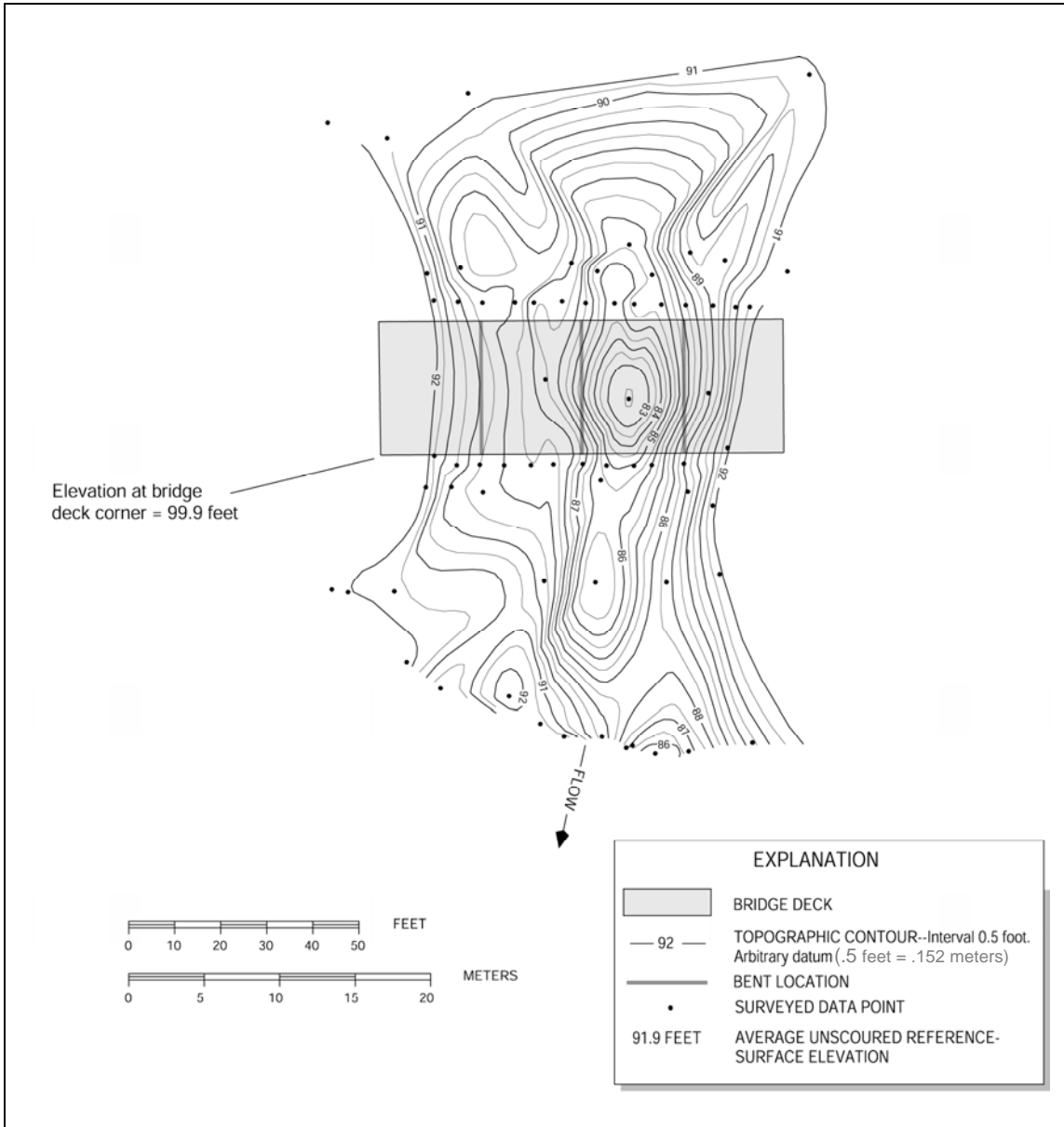


Figure 1. Example of single scour hole at shorter bridges, as shown at U.S. Route 301, crossing Douglas Swamp in Florence County, South Carolina, July 31, 1996.

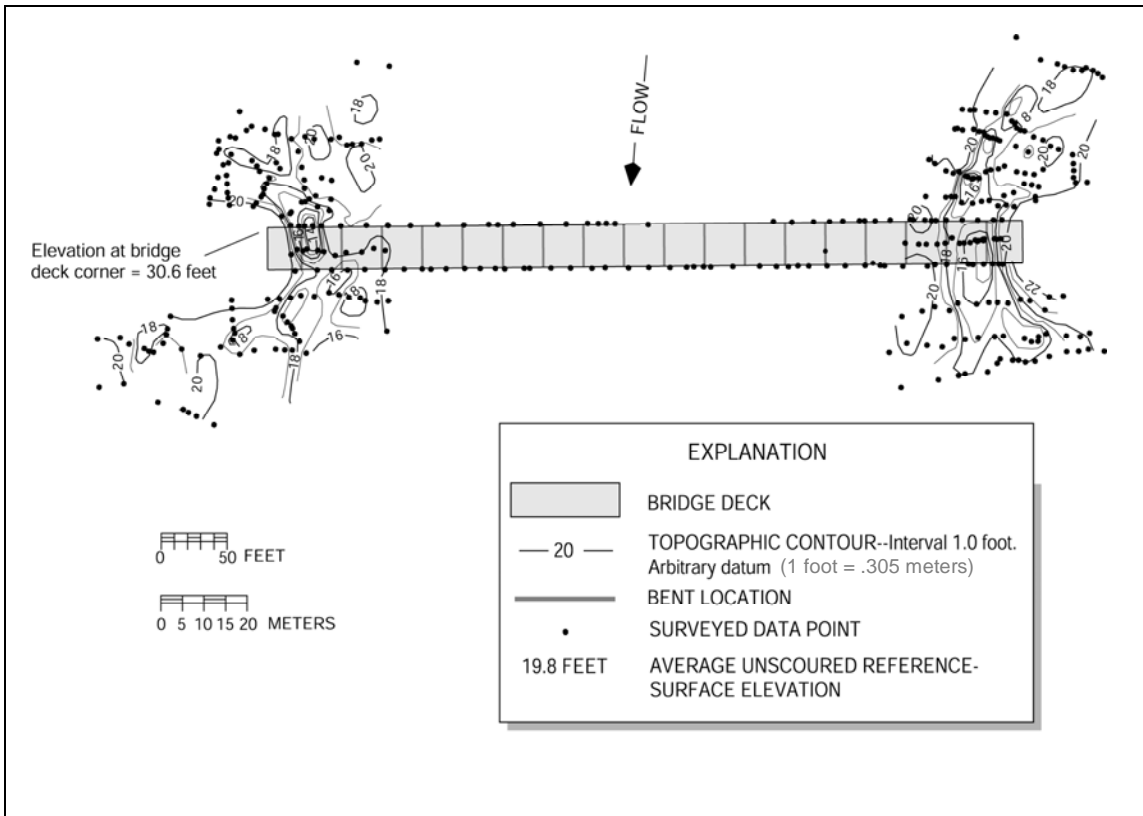


Figure 2. Example of separate left and right abutment-scour holes at longer bridges, as shown at Road S-87 bridge, crossing the Coosawhatchie River in Jasper County, South Carolina, November 12, 1997.

showed some bridges with abutment scour and no contraction scour (Figure 3) and other bridges (Figures 4) with apparent contraction scour and no abutment scour. Thus, development of contraction and (or) abutment scour is highly dependent up on the site and approach flow conditions (see Appendix A, case studies No.1 and No. 5, for a discussion of site and approach conditions for the bridges shown in Figures 3 and 4), and the presence of a contracted bridge opening does not guarantee that either or both types of scour will occur.

Although the overall effects of flow contraction and the local flow curvature that occurs around abutments can be conveniently separated conceptually, the resulting scour pattern cannot be separated into contraction- and abutment-scour components. The cause of the specific scour patterns is believed to be highly sensitive to local field conditions. The field observations collected during this study are not adequate to develop a definitive classification system based on site characteristics that could indicate the expected scour pattern. For the purposes of this report, we will consider scour that occurs adjacent to an abutment to be abutment scour and any other general scour not occurring adjacent to a pier or abutment to be contraction scour or some other type of scour resulting from unique site characteristics. The depth of abutment scour is always measured from the adjacent bed unaffected by local scour, which will include any contraction scour that occurred at the site. The depth of contraction scour will be measured relative to an uncontracted surface usually defined by cross sections collected upstream and downstream from the bridge beyond the hydraulic affect of the bridge.

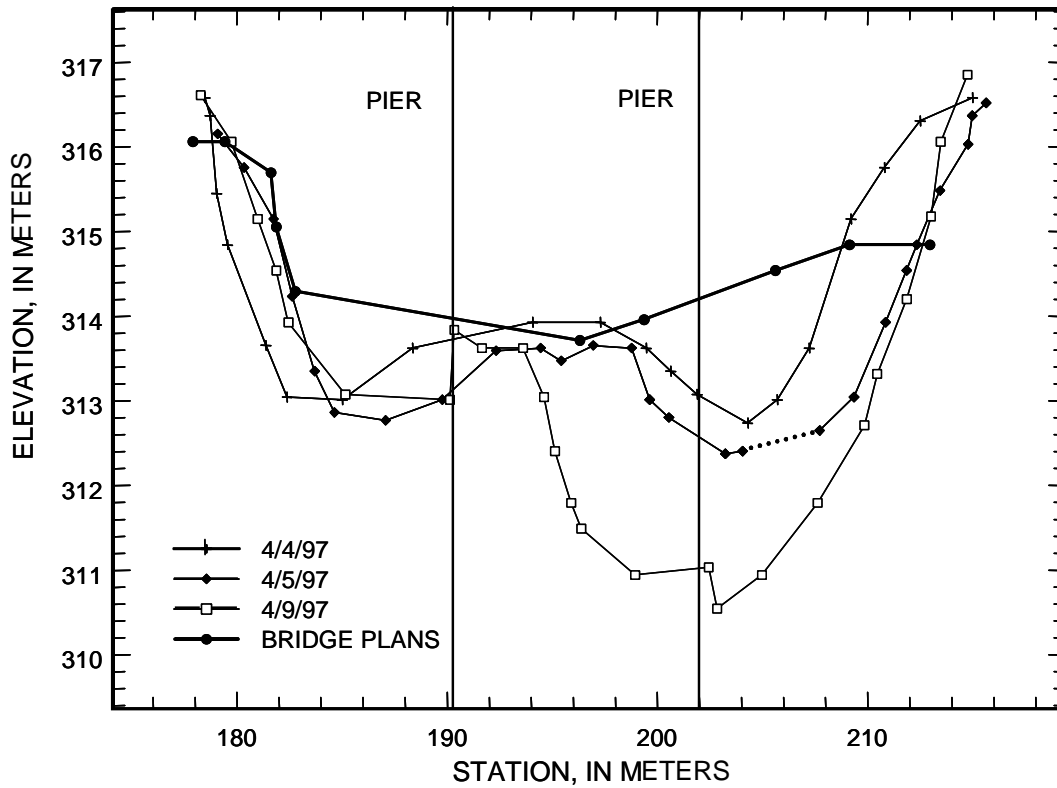


Figure 3. Plot of abutment scour measurements at the C.R. 22 bridge over the Pomme De Terre River near Fairfield, Minnesota in April 1997.

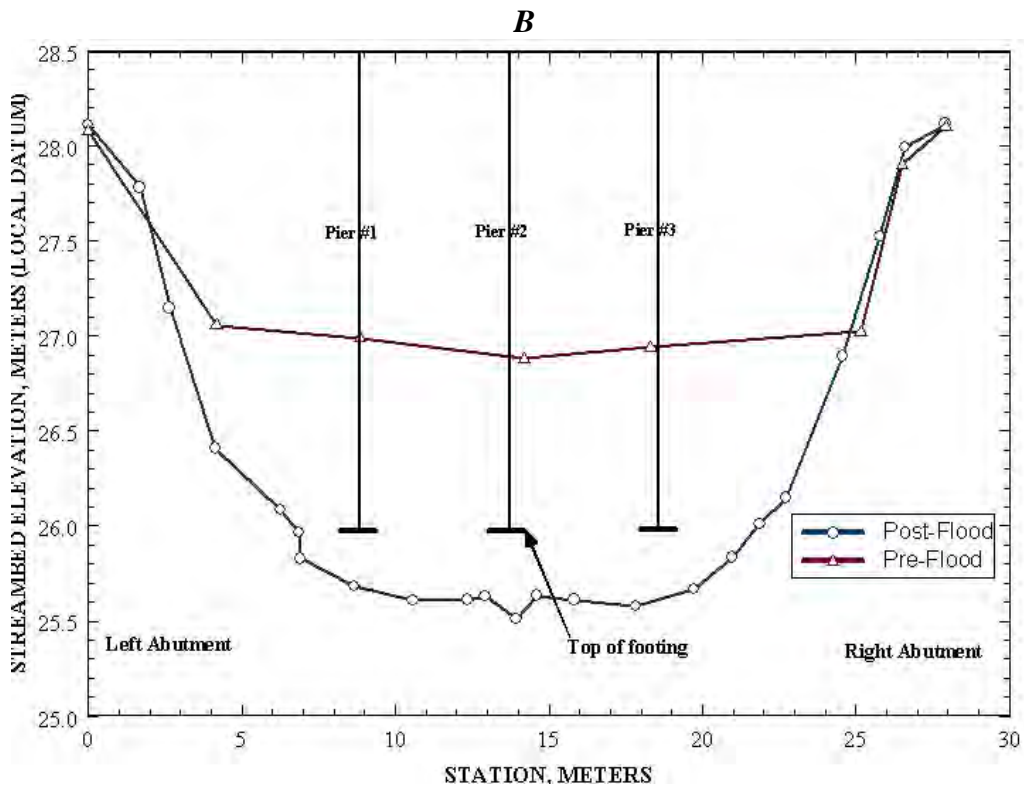
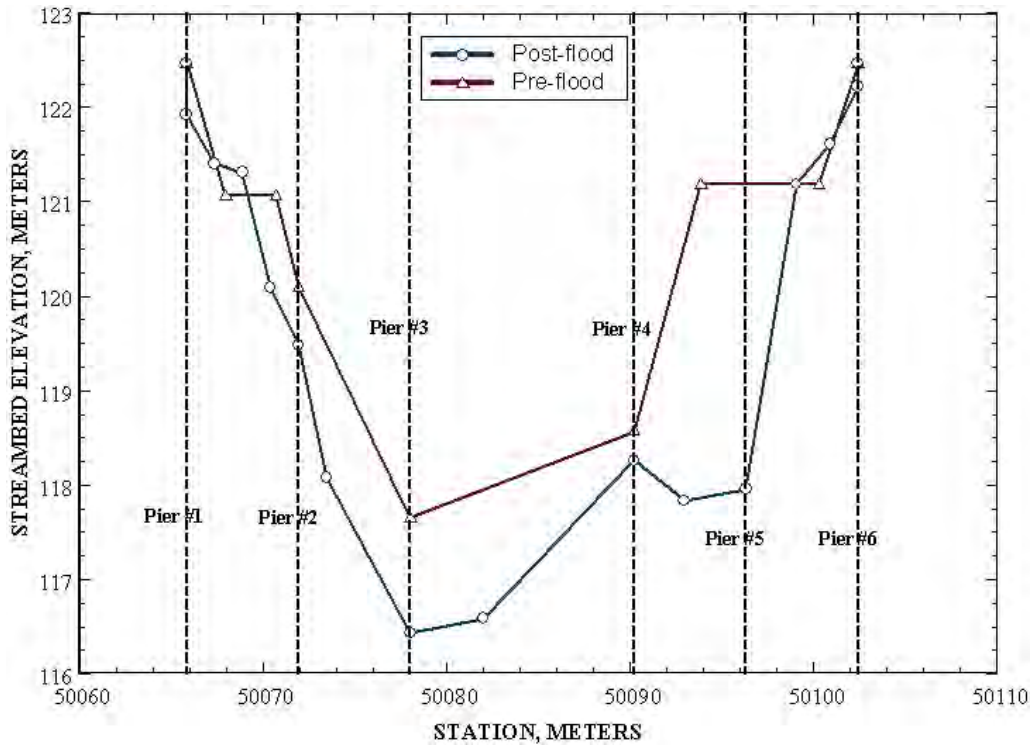


Figure 4. Plot of contraction scour measurements at (A) Conehoma Creek at State Highway 35, near Kosciusko, Mississippi, April 1979 and (B) Beaver Creek Overflow at US 2, 7 miles West of Saco, Montana.

CONTRACTION SCOUR

Contraction scour traditionally has been classified as live-bed or clear-water. The live-bed condition is characterized by bed material being transported into the contracted opening from upstream of the bridge. Live-bed scour is typical of scour that occurs in the main channel portion of a waterway in high-flow conditions. Clear-water contraction scour occurs when the flow conveyed to the bridge crossing is not transporting bed material; thus, all material that is transported from the contracted section is sediment being scoured. Scour occurring on vegetated floodplains may be classified as clear-water scour despite the potential for the shear stress in the approach section to be greater than the critical shear stress of the material comprising the floodplains.

Discussion of Live-Bed Contraction-Scour Equations

Straub (1935) was the first to develop an approach to predict contraction scour that most others would follow. He assumed that the bed in the contracted section would scour until it reached a depth at which the local transport capacity was equal to the amount of material being supplied from upstream (sediment-discharge continuity). He selected the DuBoys sediment-transport equation to compute the amount of material supplied to the reach and the local transport capacity in the contraction. Straub estimated the energy-dissipation rate (friction slope) in the contracted and uncontracted reaches by use of Manning's equation. This assumption is reasonable where flow curvature is small and pressure gradients are small compared to boundary stresses. The hydraulics in a short contraction, such as a bridge crossing, require the

consideration of additional energy losses not accounted for in a roughness coefficient based on the channel composition and configuration (Matthai 1968; Schneider and others, 1977; Shearman and others, 1986). Straub's equation, based on sediment discharge-continuity, water-discharge continuity, and the Manning equation has the general form of equation 1:

$$\frac{y_2}{y_1} = \left(\frac{Q_2}{Q_1} \right)^{E_Q} \left(\frac{b_1}{b_2} \right)^{E_b} \left(\frac{n_2}{n_1} \right)^{E_n} f(\tau) \quad (1)$$

where

- y_2 is the depth in the contracted section;
- y_1 is the depth in the uncontracted section;
- b_1 is the bottom width in the uncontracted section;
- b_2 is the bottom width in the contracted section;
- n_2 is the Manning's n in the contracted section;
- Q_2 is the discharge in the contracted section;
- n_1 is the Manning's n in the uncontracted section;
- Q_1 is the discharge in the uncontracted section;
- τ represents one or more shear-stress variables;
- E_Q is the exponent on the ratio of discharges;
- E_b is the exponent on the ratio of bottom widths; and
- E_n is the exponent on the ratio of roughness coefficients.

For most applications the shear stress based function is assumed equal to unity.

TABLE 1. Summary of live-bed contraction scour equation exponents.

Equation	$(Q_2/b_2)/$		
	(Q_1/b_1)	b_1/b_2	Q_2/Q_1
Straub (1935)		0.43	0.86
Straub (1935)		.642	
Griffith (1939)		.637	
Neill (1973)	0.67-0.85		
Laursen (1962)		.6 – .7	.86
Komura (1966)		.85	
Komura (1966)		.667	
Culbertson and others (1967)		.667	

The approach to developing live-bed contraction-scour equations is similar among all researchers and differs primarily by the method of determining the sediment-transport capacity. A summary of the exponents of the ratios common to the equations developed by select researchers is shown in Table 1. There is good consistency in the exponents, considering that each researcher used a different sediment-transport equation. In the derivation of the live-bed contraction-scour equations the sediment-transport equation is applied to both the contracted and uncontracted sections and only the difference in the transport rates between these sections affects the computed depth of scour. Thus, the depth of computed contraction scour does not appear to be sensitive to the selection of the transport equation (Mueller and Wagner, 2002).

Richardson and Richardson (1994) modified Laursen's live-bed equation by removing the ratio of Manning's n in equation 1. They concluded that Laursen's equation did not correctly account for the increase in transport that would occur if a plane bed existed in the contracted opening with a dune-bed configuration in the approach section. For this situation, Laursen's equation would predict less scour than if the roughness coefficients were equal. The Manning's n ratio in Laursen's equation does, in fact, behave properly. The basic principle of estimating contraction scour is the assumption of achieving equilibrium sediment transport. With a plane bed configuration more sediment can be transported at a reduced depth than for a dune-bed configuration; therefore, equilibrium sediment transport can be achieved at a shallower depth. To achieve a plane bed configuration, the streambed had to progress through the dune bed configuration in the contracted section. A deeper scour may have occurred at a lower flow with a dune configuration in the contracted section than at a higher flow with a plane-bed configuration; therefore, to predict the maximum depth of scour for design purposes, a constant Manning's n should be assumed in the approach and bridge sections. This yields the same result as that proposed by Richardson and Richardson (1994).

Discussion of Clear-Water Contraction-Scour Equations

Clear-water scour occurs where the boundary-shear stress in the uncontracted section is less than or equal to the critical tractive force of the bed material, thus, preventing the supply of material into the contracted section. Laursen (1963) assumed that the maximum limit of clear-water scour occurs when the boundary shear stress is equal to the critical tractive force. This assumption is common among all of the proposed clear-water contraction equations. The critical

shear stress of noncohesive sediments with a specific grain size is commonly estimated from the Shield's diagram. The critical velocity for incipient motion can be computed from the Shield's parameter by substituting the Manning equation for the slope term of the shear-stress equation and then using Strickler (1923) to approximate Manning's n . By setting the velocity in the contracted section equal to the critical velocity and solving for depth, the following generic clear-water contraction-scour equation (2) is obtained:

$$y_2 = \left(\frac{V_2^2}{\theta (K_u 31.08)^2 D_m^{2/3}} \right)^3 \quad (2)$$

where:

y_2 is the average equilibrium depth in the contracted section after scour, in m;

V_2 is the average velocity in the contracted opening in m/s;

θ is the Shield's parameter for the bed material;

K_u is a constant (.025 in SI units, .0077 in English units); and

D_m is the mean grain size of the bed material, in m.

Based on research on the effective size of bed material for riprap design and resistance to erosion presented in Richardson and others (1990), Richardson and Richardson (1994) suggest that 1.25 D_{50} be used for D_m .

The critical velocity or critical shear stress and the corresponding scour is not well established for channels having cohesive bed material, bed material that varies with depth, heavily vegetated floodplains, previously developed scour holes, or armored beds. The clear-water scour equations were developed by use of flow variables obtained under initially flat bed

conditions; however, flow variables can change substantially after a scour develops. As a result large changes in flow area and backwater effects can affect the accuracy of scour-prediction equations. Clear-water scour prediction is highly sensitive to the critical conditions of the bed material; therefore, accurate representation of the bed material is essential. Bed-material samples should represent both the surface and subsurface material. Various agencies use different methods for determining the critical velocity. These inconsistencies can have a significant impact on clear-water scour estimates, especially in fine grained soils.

Summary of Observations

The data presented in this section were observed at 13 real-time sites included in the BSDMS and 146 sites in South Carolina (Benedict, 2003). The observed data represent a wide range of site characteristics (i.e., non-cohesive and cohesive soils, upstream channel meanders, spur dikes, varied geomorphic settings, and complex bridge configurations). A detailed description of the techniques and equipment used to collect real-time scour measurements can be found in Mueller and Wagner (2002). The procedure that was used to collect the post-flood scour measurements is detailed in Benedict (2003).

Comparison of Observed and Computed Scour Depths

In this study, observed depths of contraction scour were compared with computed depths based on the approach presented in HEC-18. Only three sites had sufficient data to allow computation of contraction scour based on field data alone. Thus, all computed scour used in the comparison

is based on hydraulic parameters from a one-dimensional model calibrated to the discharge and water-surface elevations observed in the field. The equations for live-bed contraction scour consistently overpredicted the observed scour (Table 2). This overprediction ranged from two to four times the observed scour. The equations for clear-water contraction scour substantially overpredicted the observed depths of scour (Table 2). Situations that fit into the clear-water scour regime are more likely to be in areas with cohesive bed material. Cohesive soils greatly reduce actual scour depths, and therefore, result in even larger overpredictions of scour when applying clear-water equations.

Contraction scour was not always observed in the field, even at sites with considerable contraction ratios and high velocities. Benedict (2003) observed no scour at about 25 percent of the sites in South Carolina; however, the HEC-18 approach predicted scour at all of these sites (Figure 5). Bed-material size and gradation, cohesion, armoring potential, and road overflow are common factors that can limit or prevent contraction scour, but other highly site-specific preventative factors have been discovered in the analysis of field measurements. Real-time measurements during an approximate 50-year event at the 247th Street bridge over the James River near Mitchell, South Dakota revealed no scour through the bridge opening and around .3 meters (m) of contraction scour 9 to 15 m downstream of the bridge. Intense velocities through the bridge, a considerable contraction of the left floodplain (about 610 m) and a silty bed material would indicate the occurrence of contraction scour using HEC-18 prediction techniques. Analysis of the data and bridge plans revealed that although there was minimal road-overflow, remnants of an old bridge under the existing structure were acting as scour protection.

Channel alignment upstream and through the bridge opening is another factor that can greatly affect the occurrence of contraction scour. The increase in flow conveyance caused by scour at an abutment can be sufficient to reduce overall velocities and shear stresses through the bridge opening, limiting scour to the area near the abutment. This phenomena has been observed

TABLE 2. Comparison of observed and theoretical contraction-scour depth (clear-water and live-bed) for bridge sites in the National Bridge Scour Database (BSDMS).

Site name	Scour type	Date	Contraction scour	
			Computed (meters)	Observed (meters)
Chehalis River at Galvin Road Overflow, Centralia, Washington	Clear-water	2/9/1996	9.32	0.92
Beaver Creek Overflow 7 miles West of Saco, Montana	Clear-water	Unknown	39.6	1.37
Beaver Creek Overflow 9 miles West of Saco, Montana	Clear-water	Unknown	21.0	.99
Bitterroot River at US 93 near Darby, Montana	Clear-water	6/11/1996	0	.21
Minnesota River at SR 25 near Belle Plaine, Minnesota	Live-Bed	4/17/2001	10.8	4.57
Conehoma Creek at SR 35 near Kosciusko, Mississippi	Live-Bed	4/5/2001	5.79	1.83
James River at SR 37 near Mitchell, South Dakota	Live-Bed	4/15/2001	4.48	1.68
Conehoma Creek at SR 35 near Kosciusko, Mississippi	Live-Bed	4/12/1979	5.79	1.22
Pomme De Terre River at US 12 near Holloway, Minnesota	Live-Bed	4/5/1997	1.40	.94
Cedar River at S.R. 218 near Janesville, Iowa	Live-Bed	7/23/1999	.76	.61
Pomme De Terre River at CR 22 near Fairfield, Minnesota	Live-Bed	4/9/1997	.00	.00

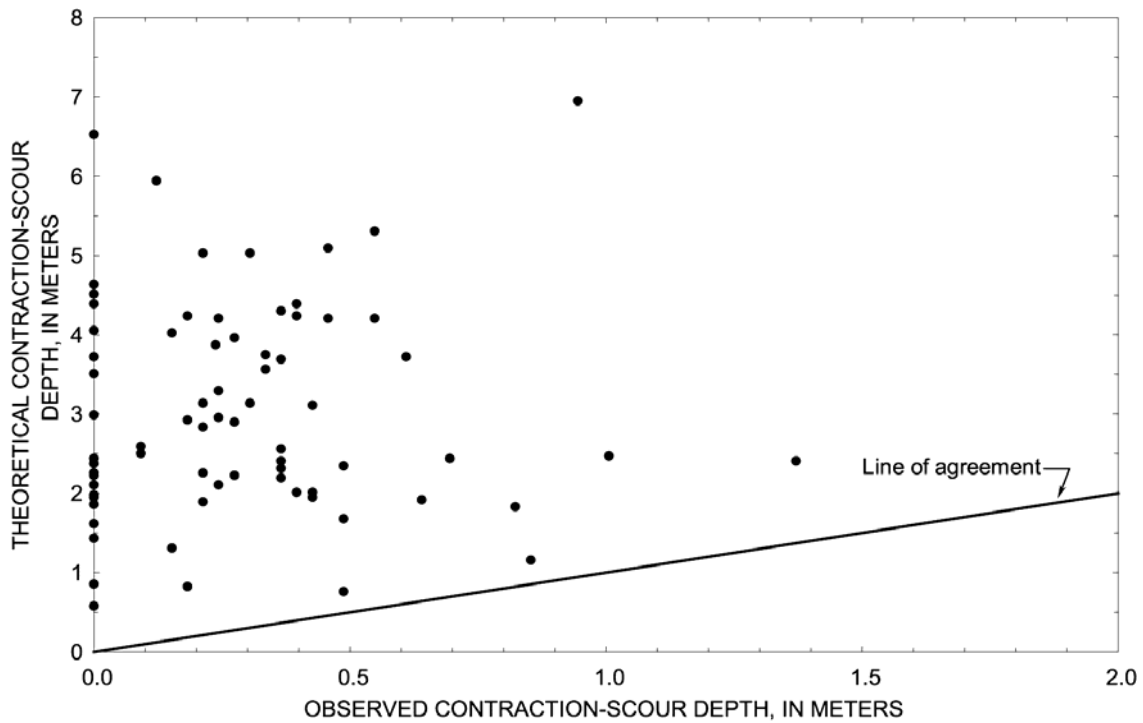


Figure 5. Relation of observed and theoretical clear-water contraction-scour depth for the 100-year flow, in the Piedmont of South Carolina. (Theoretical contraction scour calculated with the Laursen (1963) equation.)

at sites with long bridges that have extremely high rotational velocities at the abutments as a result of upstream meanders. Appreciable embankment skew and (or) expansive floodplains also have been shown to limit or exclude contraction scour in some situations. The County Route 22 bridge over the Pomme De Terre River near Fairfield, Minnesota is an example of a site where the upstream channel alignment and corresponding abutment scour precluded any contraction scour (see Appendix A, Case Study No. 1). Thus, development of contraction and (or) abutment scour is highly dependent upon the site and approach flow conditions. The presence of a contracted bridge opening does not guarantee that either or both types of scour will occur.

Location of Scour at Contracted Bridges

Analysis of the field data also has revealed that the location of scour in a contracted bridge opening is highly variable and does not follow the patterns typically reported from laboratory experiments. The longitudinal location of contraction scour can be dependent upon factors such as the configuration of scour protection, guide banks, bridge length, channel alignment, and bed material. The detailed data from two of the real-time scour sites clearly shows the variation in longitudinal location of contraction scour. The contraction scour at State Route 218 over the Cedar River near Janesville, Iowa is located upstream of the S.R. 218 Westbound Bridge in the region where the floodplain flow combines with the main channel flow (Figure 6) (also see Appendix A, Case Study No. 8). A spur dike extending upstream from the right abutment directs the right floodplain flow into the main channel approximately 35 m upstream of the bridge. The configuration of the scour pattern observed at State Route 25 over the Minnesota River at Belle Plaine, Minnesota (Figure7) (also see Appendix A, Case Study No. 3) is caused by a

combination of upstream approach alignment and riprap around the left abutment and piers. Abutment-scour holes were observed at both abutments and contraction scour was observed across the entire bridge section, but the deepest scour was observed downstream between the left abutment and the leftmost pier. The downstream location of the scour hole may be attributed to scour protection that was in place on the left abutment and leftmost pier that prevented degradation of the bed in the bridge opening.

The uncontracted approach section is commonly assumed to be one-bridge length upstream from the bridge. Field observations show that the location of the uncontracted approach section also can be highly variable depending upon site specific characteristics such as flow structures, geomorphic setting, floodplain topography and land cover, and upstream channel configuration. The berm and geomorphic setting of the S.R. 37 Bridge over the James River near Mitchell, South Dakota (see Appendix A, Case Study No. 4) induced hydraulic conditions that could not have been represented using the standard guidelines for locating the approach cross-section (approximately one-bridge length upstream). Inspection of the "approach" section (one-bridge length upstream) revealed a large discharge (334 cubic meters per second (m^3/s)) relative to that of the contracted opening (394 m^3/s). It was discovered that the blockage caused by the roadway embankment forced the majority of the left floodplain flow back into the main channel at the typical approach section (Figure 8). A cross section made further upstream showed much less discharge (191 m^3/s), which was consistent with channel discharge

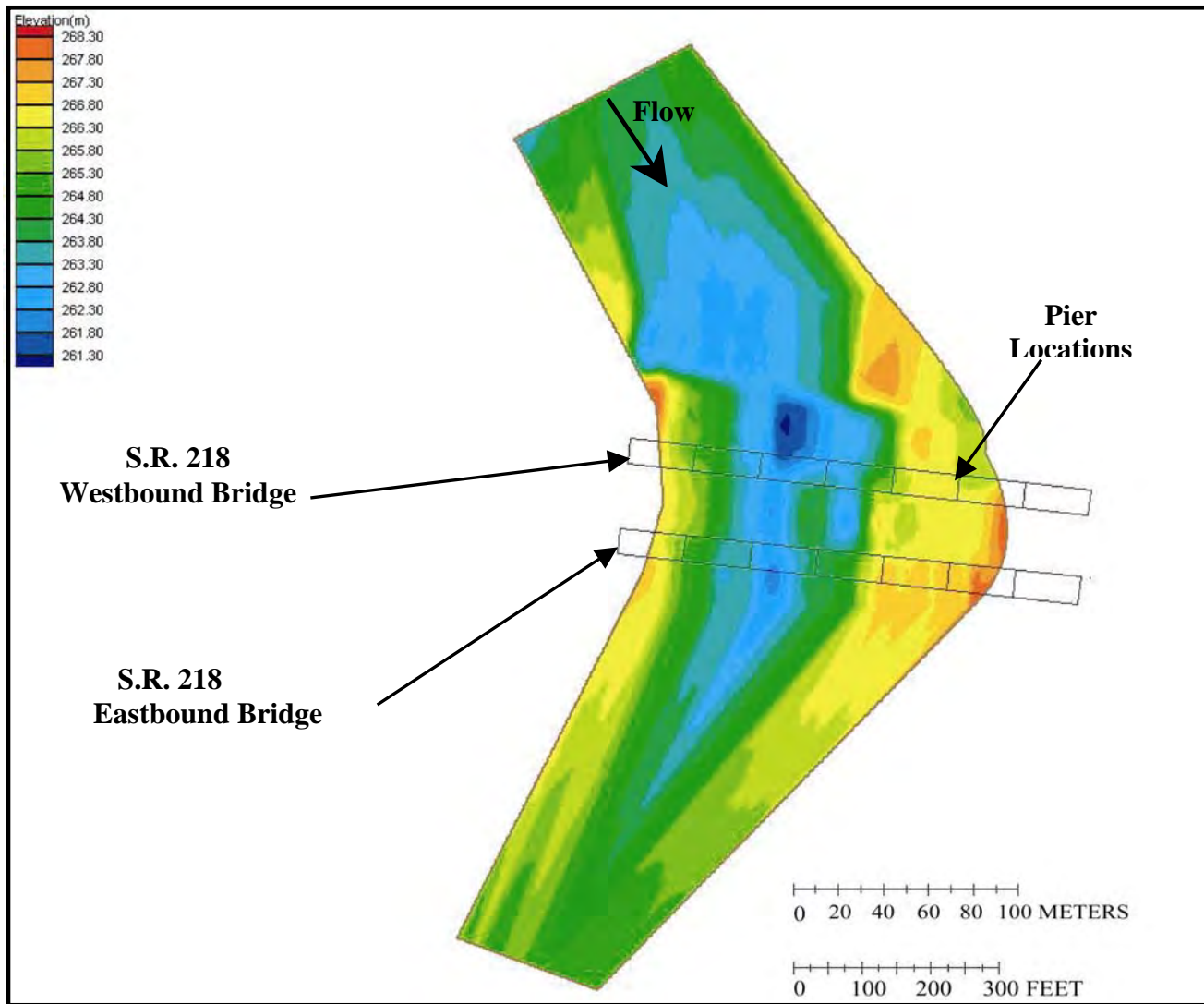


Figure 6. Example of scour-hole low point located upstream of S.R. 218 over the Cedar River near Janesville, Iowa.

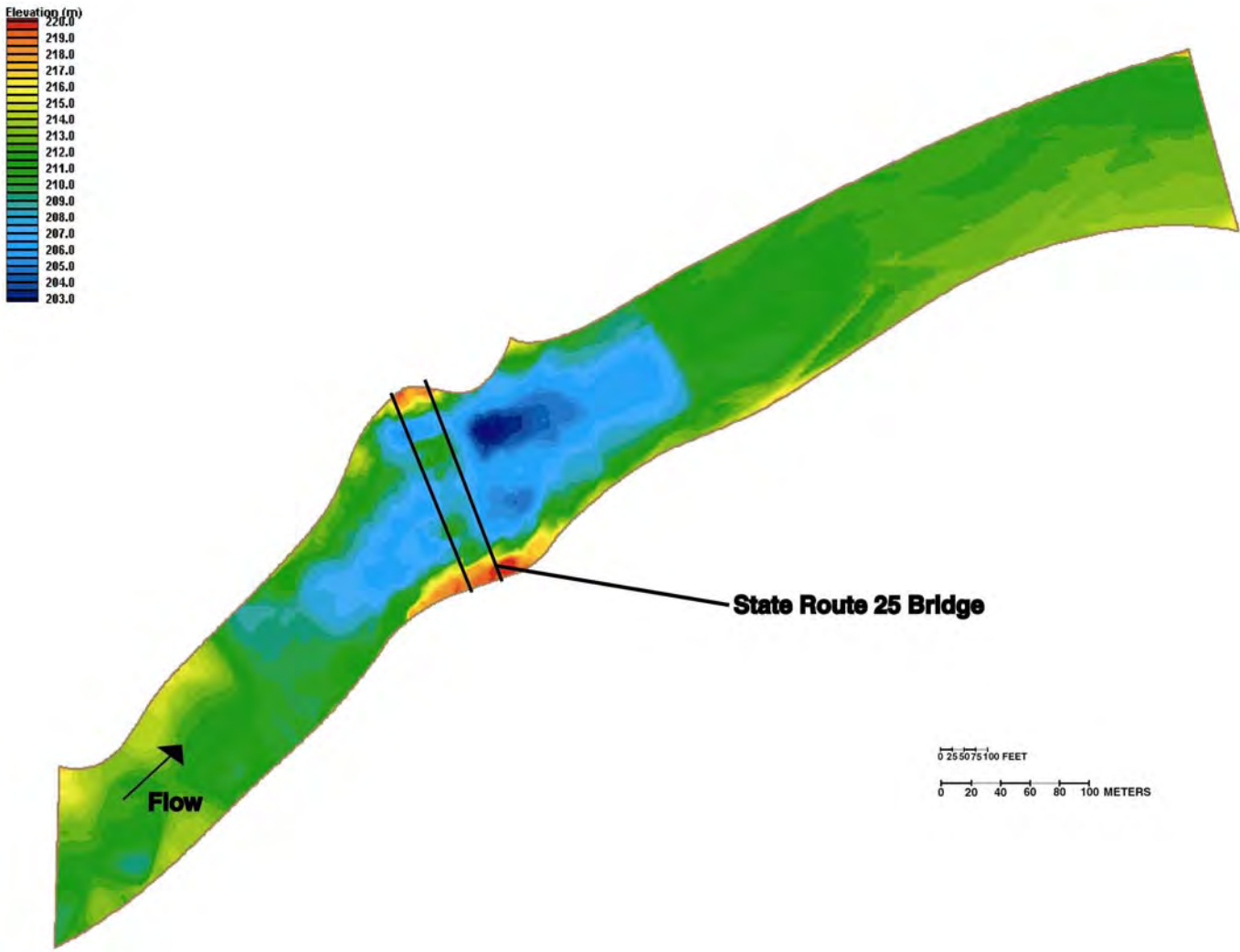


Figure 7. Example of scour-hole low point located downstream of S.R. 25 over the Minnesota River near Belle Plaine, Minnesota.

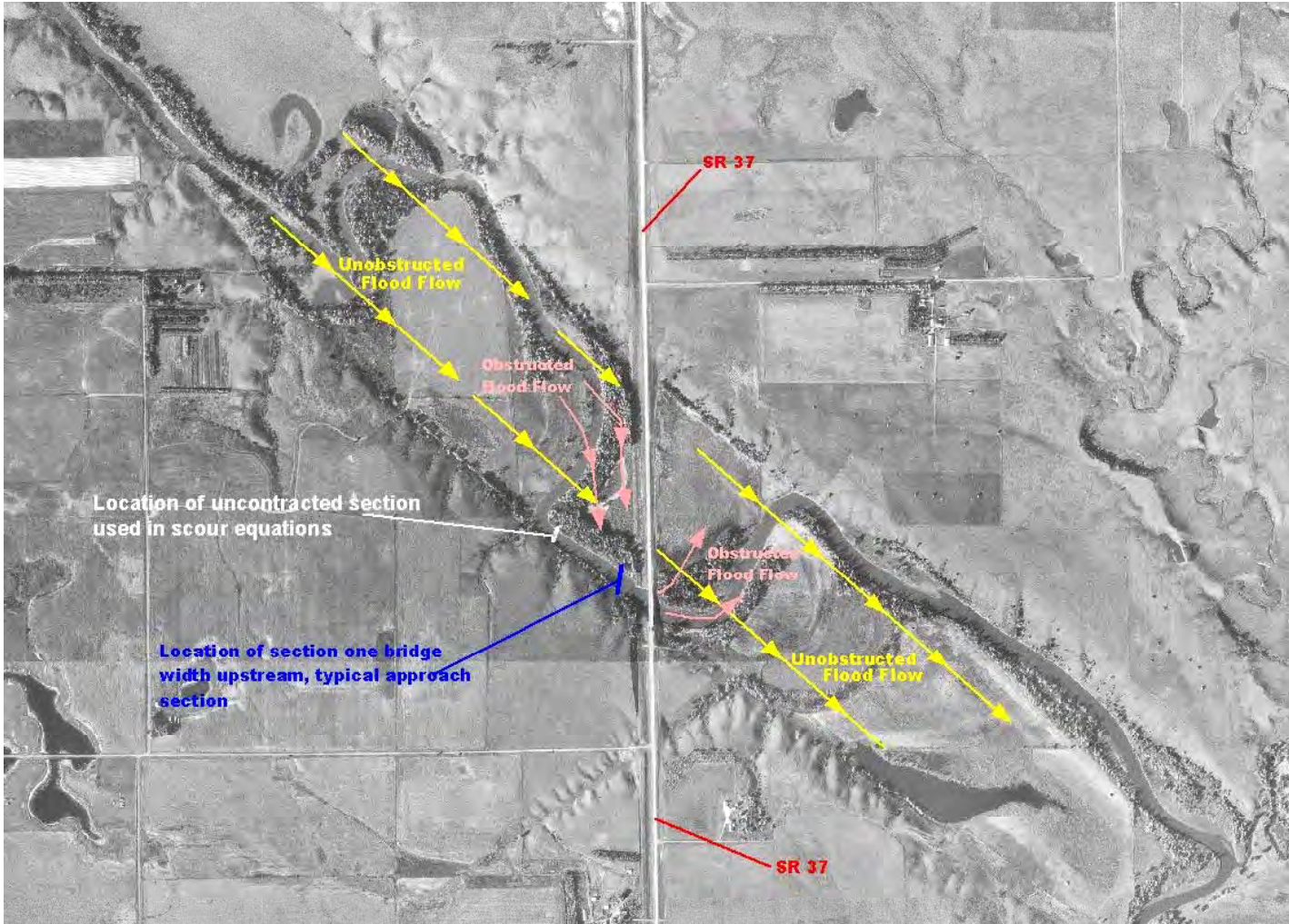


Figure 8. Site configuration, flow patterns and approach section location for S.R. 37 over the James River near Mitchell, SD

downstream of the bridge opening. Data from an ADCP section that cut-off the left floodplain flow accounted for all but 14 m³/s of the difference in discharge between the typical approach section and the section further upstream. The section furthest upstream was used as the uncontracted section because it was most representative of the flow naturally carried by the main channel had the roadway embankment not been present. A similar situation is present at the Minnesota River at Belle Plaine site in which an upstream bend forces much of the overbank flow into the main channel before the section located one bridge width upstream (see Appendix A, Case Study No. 3).

A summary of the longitudinal scour location for the contracted bridges surveyed in South Carolina (Benedict, 2003) showed that the location of maximum contraction scour varied appreciably (Figure 9). For the shallow scour depths (1.4 m or less) in the clayey soils of the Piedmont, the low point of the scour hole was typically found along the centerline of the roadway directly under the bridge (Figure 9A). For the Coastal Plain sites, the longitudinal location of the scour hole varied appreciably for 100-year-flow bridge top widths of 91.5 m or less (Figure 9B); however, beyond 91.5 m, the longitudinal location was close to the roadway centerline directly under the bridge. Although data for the deeper scour holes in the Piedmont were not as abundant as data in the Coastal Plain, a similar longitudinal location of the scour holes was observed (Benedict, 2003); however, for relatively short bridge lengths, bridges with 100-year-flow top widths approximately 91.5 m or less, Figure 9 illustrates that the low point of the scour hole may form outside of the bridge limits. In some cases, the low point of the scour hole was largely removed from the bridge so as to not significantly threaten bridge foundations (Figures 10 and 11). Interaction of highly rotational flow coming from the left and right

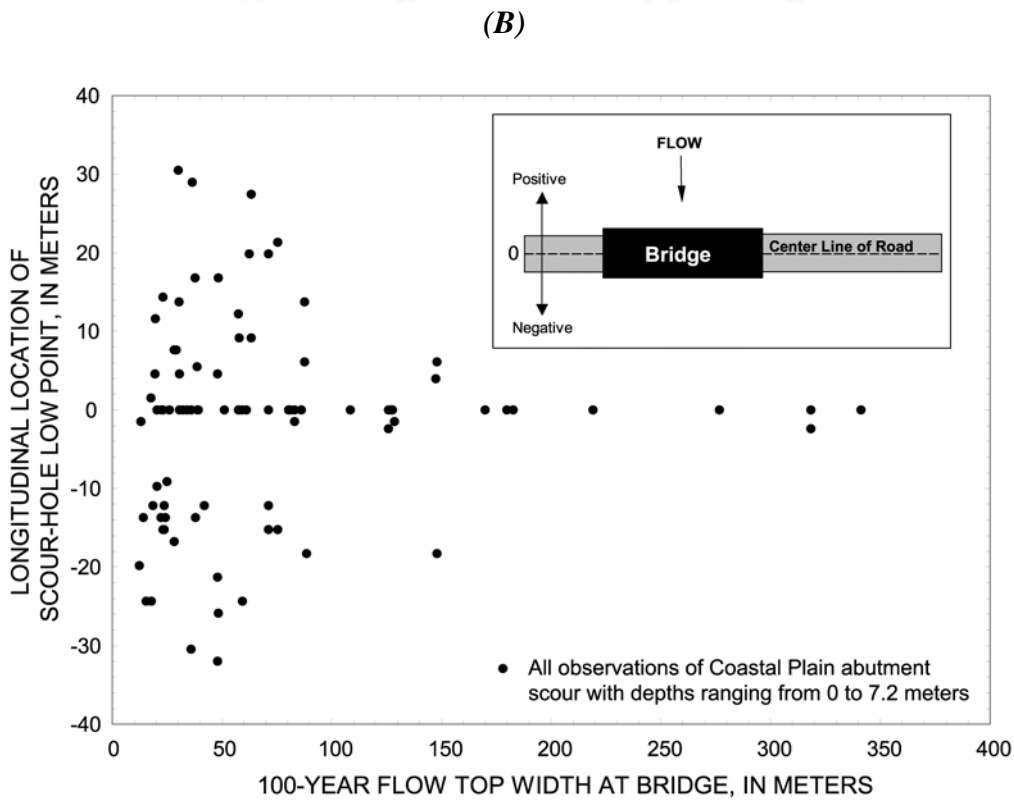
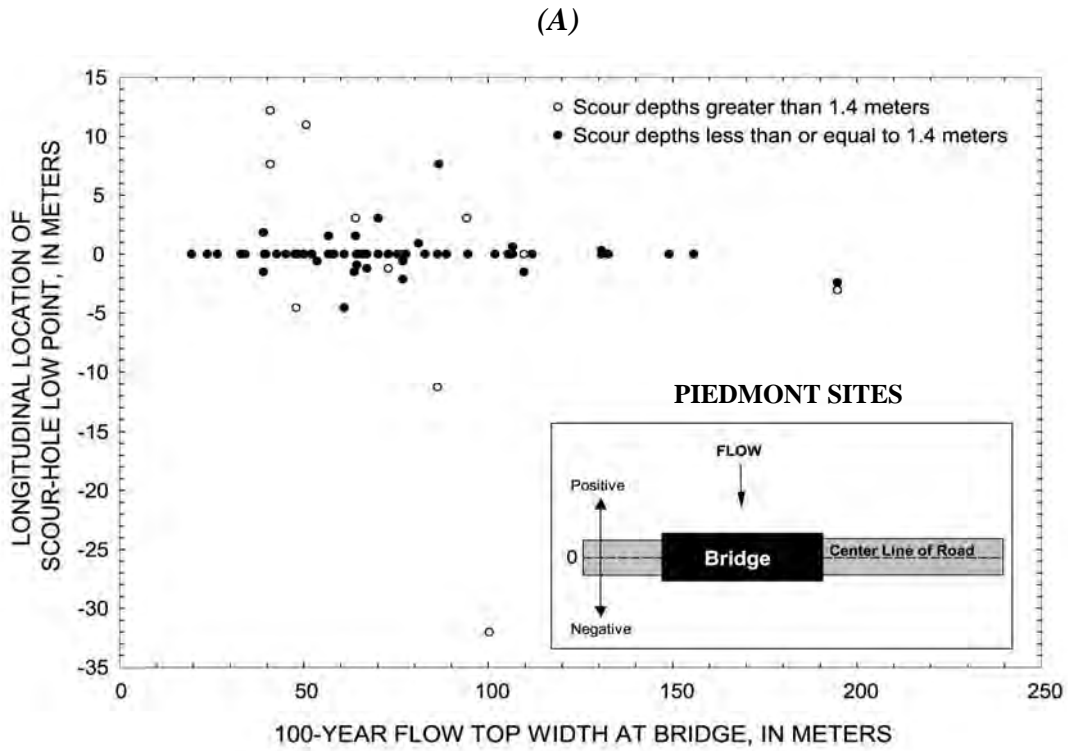


Figure 9. Relation of longitudinal location for the low point of the abutment-scour hole and the 100-year-flow top width at the bridge for (A) shallow and deep scour holes in the Piedmont of South Carolina, and (B) sites in the Coastal Plain of South Carolina.

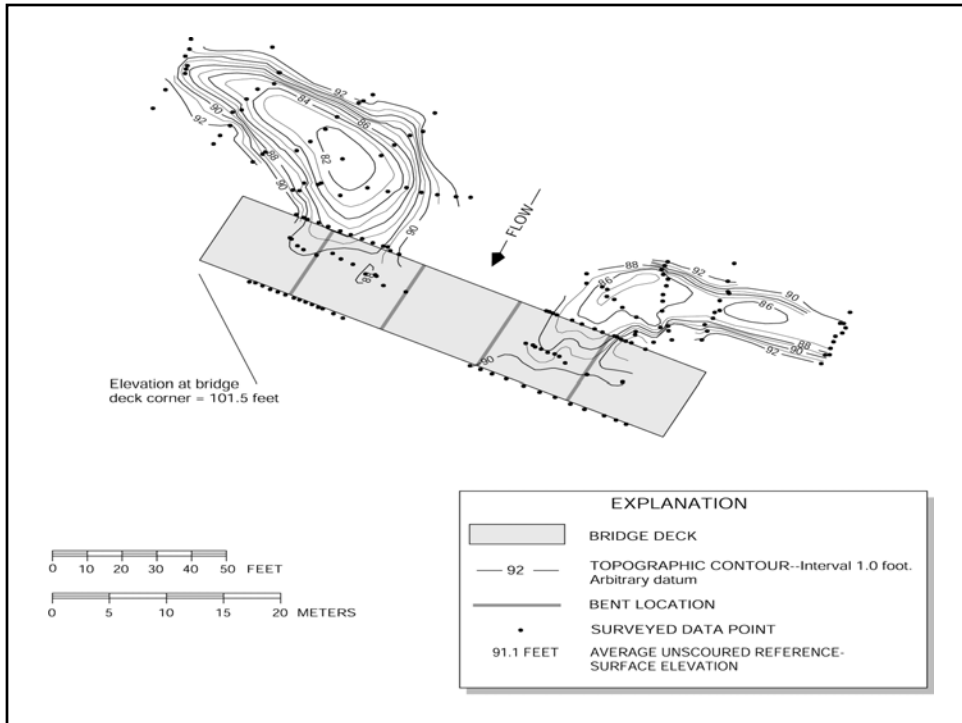


Figure 10. Example of scour-hole low point located upstream of Road S-299, crossing Cannons Creek in Newberry County, South Carolina, November 24, 1997.

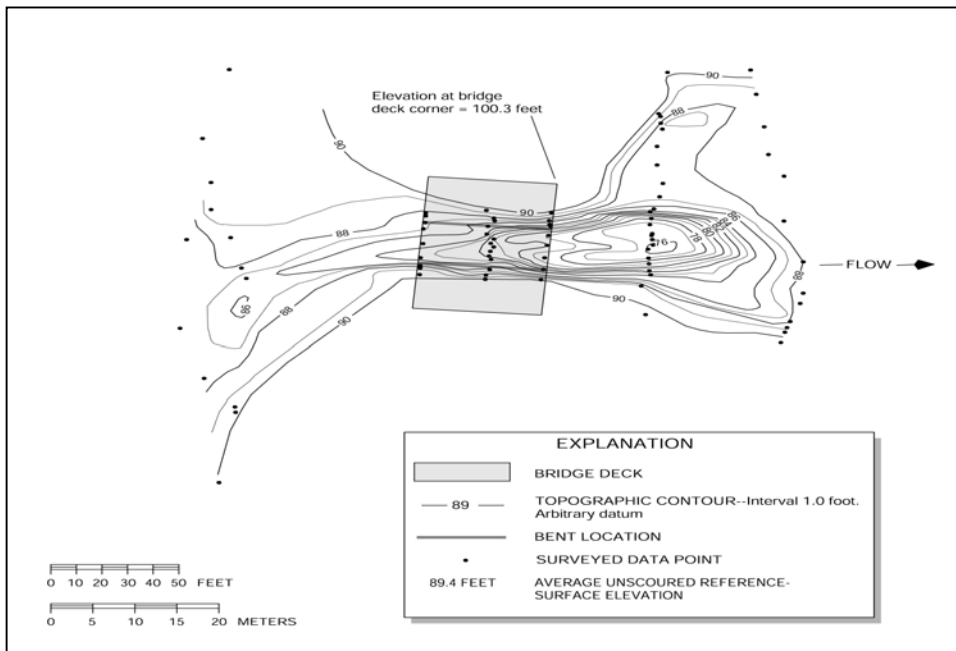


Figure 11. Example of scour-hole low point located downstream of S.C. Route 41, crossing Maiden Down Swamp in Marion County, South Carolina, December 3, 1996.

abutments likely causes complex, unsteady flow patterns for shorter bridge lengths and creates the scatter within the longitudinal pattern. As bridge length increases beyond approximately 91.5 m, the interaction of flow from left and right abutments is diminished and steadier flow patterns are established around each separate abutment. The steady flow patterns promote the creation of the classical abutment-scour hole pattern where the low point falls longitudinally near the bridge (Benedict, 2003). Although Benedict (2003) and others have discussed factors that contribute to the position of scour holes, no method for predicting the location has been developed. Consequently, the present scour-prediction methods found in HEC-18 recommend that the scour-hole low point be located at the bridge. Additional research and data collection is needed to determine the factors that control scour and to develop a method for predicting the location of scour holes.

Discussion of One-Dimensional Backwater Model Applications

The discharge in the contracted and uncontracted sections is typically determined by use of a one-dimensional step-backwater computer model such as Water-Surface Profile Computations (WSPRO) (Shearman, 1990) or Hydrologic Engineering Center–River Analysis System (HEC-RAS) (U.S. Army Corps of Engineers, 1998). Stream-tube and one-dimensional models distribute the flow in a cross section based on conveyance alone. The flow distribution upstream of a bridge has no effect on the flow distribution within the bridge opening, because one-dimensional backwater models compute solutions in the upstream direction. The observations in this study show that the flow distribution in a contracted opening is highly dependent upon flow distribution of the approaching flow in addition to roughness and topography of the approach

flow reach. Models based on cross-section conveyance distributions alone can be highly inaccurate where non-uniform approach-flow conditions exist at bridges.

Experience in applying backwater models in this study indicates that distribution of the flow by conveyance may lead to overestimating the depth of contraction scour. At the uncontracted approach cross section, a conveyance-based model distributes more flow in the floodplain than was measured, resulting in the computed main channel flow being too low. Increased flow in the floodplain may result because (1) the one-dimensional model assumes a constant friction slope for the whole cross section when, in reality, the downstream water-surface slope varies across the section; (2) the one-dimensional model does not account for flow-path lengths between main channel and the floodplains; and (3) the one-dimensional model does not account for the lateral resistance of the flow moving from the main channel to the floodplains. Conversely, the conveyance-based flow distribution may place too much flow in the main channel at the bridge because the conveyance tubes fail to represent the accelerating curvilinear flow separating from abutments and (or) road embankments. This problem could be partially addressed if ineffective areas were used to represent the flow-separation regions in the upstream and downstream ends of the bridge opening. The combination of a reduction of the main channel flow in the uncontracted section coupled with an increase of main channel flow at the bridge section could lead to an overprediction of depth of contraction scour. Analysis of the one-dimensional model outputs for contracted bridge sites of this study show that computed discharge ratios are not representative of field conditions. Too much flow is distributed to the floodplains in the approach and in the main channel through the bridge opening resulting in consistent overprediction of the observed contraction scour (Table 2).

ABUTMENT SCOUR

The current knowledge on prediction of scour at abutments is derived from regime theory equations, equations used to estimate the depth of scour for spur dikes, and equations developed from small-scale physical-model studies conducted in laboratory flumes. Unfortunately, none of these approaches have resulted in a satisfactory prediction equation. The inability of these approaches to accurately predict scour at abutments is a result of the simplifying assumptions on which the research is based and the complexity of abutment scour in field conditions. The configuration of bridge abutments and associated embankments is complex when placed in the context of river hydraulics.

Field Conditions

The geometric configuration of the bridge crossing, floodplain, and channel greatly affects the way flow is directed around the abutments. The abutment may be located in the channel, at or near the top bank, or on the floodplain. The configuration of the abutment may be vertical, have wing walls at various angles, or have a spill slope protected with riprap or some other armoring material. Although abutments with spill slopes are usually protected, the armoring can fail or be undermined by scour causing the abutment configuration to change during a flood. The embankments may not be perpendicular to the approach flow but may be angled either upstream or downstream. Drainage ditches along the toe of the embankment are common and complicate the flow patterns around the abutment.

The natural flow distribution in a river and its floodplain also can have an appreciable effect on the depth of scour at an abutment. The distribution of the approach flow blocked by the embankment is dependent upon the roughness and topography of the floodplain and alignment of the main channel. The flow distribution and direction can change appreciably during a flood hydrograph. Such complexity and the variability of these conditions between sites are major obstacles in developing a reliable method for predicting scour at abutments.

Discussion of Laboratory-Based Equations

Although some predictive equations are based on field observations, such as the HIRE (Richardson and others, 1990) equation (based on spur dikes on the Mississippi River), most of the equations for predicting scour at abutments are based on small-scale physical model studies. Literature documenting the laboratory experiments reveals that the approach section of the flume usually had a constant depth with a uniform velocity distribution except for a small boundary layer along the flume walls. The roughness of the channel also was typically uniform throughout the approach and bridge sections and the bed material generally was composed of uniform sand. The abutments were represented by solid, non-erodible obstructions protruding from the sides of the flume with ends that varied in configuration to represent typical shapes of embankments and abutments at contracted bridge openings. These conditions are different from the conditions that occur in the field.

Recently (2000), several researchers have attempted to account for some of the conditions commonly found in the field. Dongol (1993), Melville (1995), and Sturm and Janjua

(1994) have used models that incorporate the floodplain, some channel-geometry effects, and non-uniform flow distributions. Unfortunately, the amount of field data on abutment scour that can be used to evaluate the validity of the laboratory studies is limited.

The laboratory research, although not in agreement, typically has used some combination of the following variables to predict scour at abutments: (1) embankment length, (2) abutment shape, (3) depth of flow, (4) velocity, (5) sediment size, and (6) discharge. The variables in equations developed from these experiments are ambiguous when these equations are applied to field conditions, because of the simplicity of many of the laboratory experiments. In simple flume studies the flow depth is uniform everywhere, and there is no way to define what depth is controlling the depth of scour (the depth at the abutment, the depth in the approach upstream of the abutment, or an average depth of flow blocked by the abutment). In the field these all may be different values; however, in the laboratory with a uniform bed they are all the same. The representative or reference velocity also is a good example of potential ambiguous variables in the field. The local velocity in the contracted opening adjacent to the abutment (which would represent the peak-flow velocity near the region of highest flow curvature) would be different from the unobstructed approach velocity upstream of the abutment or the average velocity of the approach flow blocked by the length of the embankment. Flume studies often use the total length of the embankment from the flume wall to the abutment as the embankment length; however, this approach fails to account for the flow separation and recirculation zone that forms along the upstream edge of the embankment (Figure 12). The effective length of the embankment on the depth of scour is dependent upon the distribution of the approach flow and the floodplain roughness and geometry (Mueller and Wagner, 2002). It is important that laboratory research

emulates the conditions in the field so that the equations developed are more representative of field conditions.

Laboratory research on abutment scour has focused on equilibrium scour in non-cohesive materials. Floodplain soils typically contain fine-grained sediments sufficient to provide a degree of cohesion that makes them more resistant than non-cohesive soils. Vegetation also can appreciably increase soil resistance to scour. Cohesive sediments are present in many main channel streambeds.

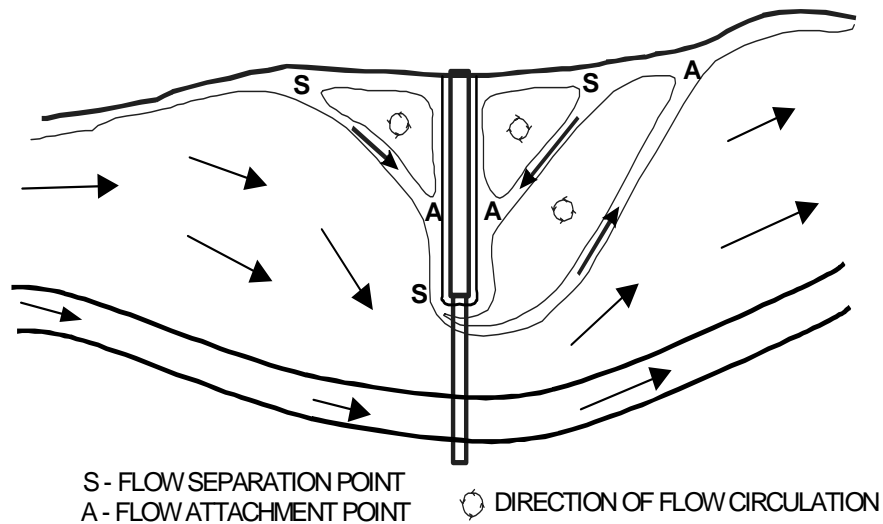


Figure 12. *Illustration of flow contracted by an embankment constructed in a floodplain.*

Research on scour in cohesive materials shows that, in general, cohesion increases the resistance of soils. In addition, the time required for maximum scour-depth conditions in cohesive soils is substantially longer than would occur with non-cohesive soils. Scour equations derived from small-scale laboratory experiments are incapable of providing accurate equations for cohesive soils because of scaling problems associated with fine-grained sediment entrainment. In many cases, cohesive fine-grained soils reinforced by vegetation root mats overlay non-cohesive sands or gravel and sand mixtures. Abutment scour in these complex but common soil conditions has not been addressed in model studies.

Summary of Observations

The data collected at the 12 sites with abutment scour for the NCHRP Project 24-14 have shown that the magnitude and location of abutment scour are highly site specific and dependent upon the geometry of the bridge crossing and the roughness of the channel and floodplains. The South Carolina data (Benedict 2003) indicate that scour through short contracted bridge openings is more often dominated by scour processes associated with “curvilinear flow” around the abutments rather than “rectilinear flow” associated with HEC-18 defined contraction scour. Although the length of the bridge and channel geometry are important factors in the development of abutment scour, there are a multitude of other parameters that must be considered when evaluating and (or) predicting scour in the abutment region including the following:

1. cohesion of soils;
2. geometric contraction ratio;
3. approach flow-velocity distribution including the effects of channel bends;

4. floodplain roughness and topographic variation;
5. floodplain-flow obstructions;
6. valley geometry, including valley width variation and slope;
7. roadway crossing geometry – roadway profile, embankment geometry and orientation, and bridge length;
8. embankment protection; and
9. duration and frequency of flood flows.

Appreciable limitations of extrapolating laboratory results to conditions in the field can be illustrated in a comparison of the relation between embankment length and scour depth, normalized by flow depth, for laboratory (Melville, 1992) and field data collected in South Carolina (Figure 13). The field data shown in Figure 13 exhibit a similar trend to the laboratory relation, but there is more scatter within the field data and the asymptotic limit of the field data (3.4) is appreciably lower than the Melville (1992) laboratory data limit (10).

A review of the primary scour factors specified by Dongol (1993) in the field data indicates that many of the factors likely have a minimal affect on abutment-scour depths for the prevailing field conditions in the NCHRP Project 24-14 sites and in South Carolina. Dongol (1993) classified the variables affecting abutment scour into the seven categories listed below:

(1) Variables describing the channel

channel width

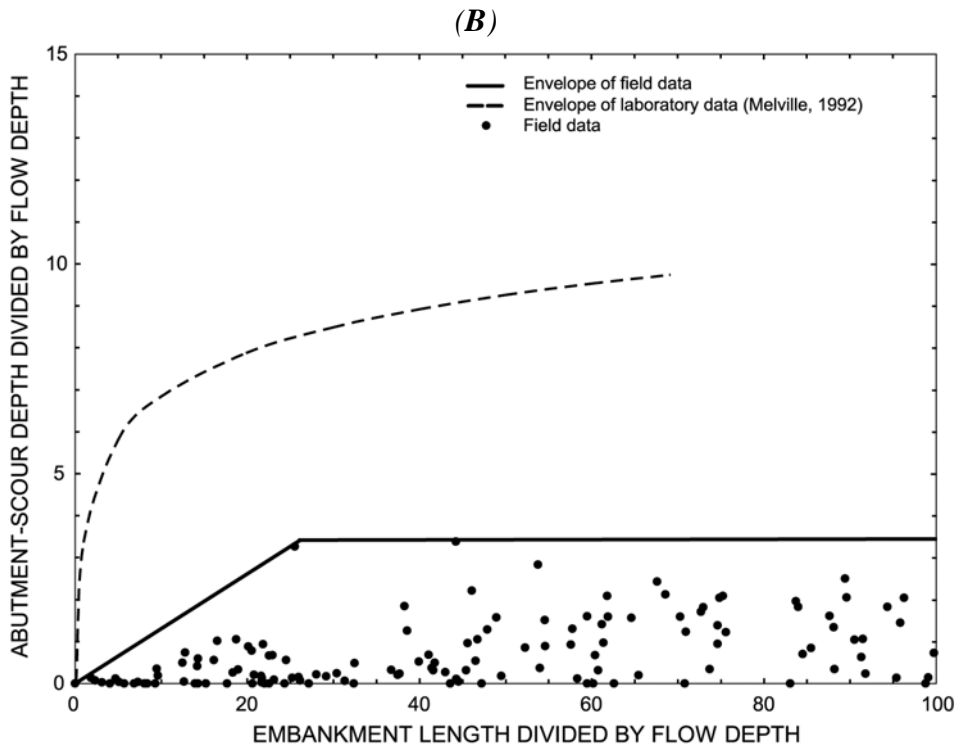
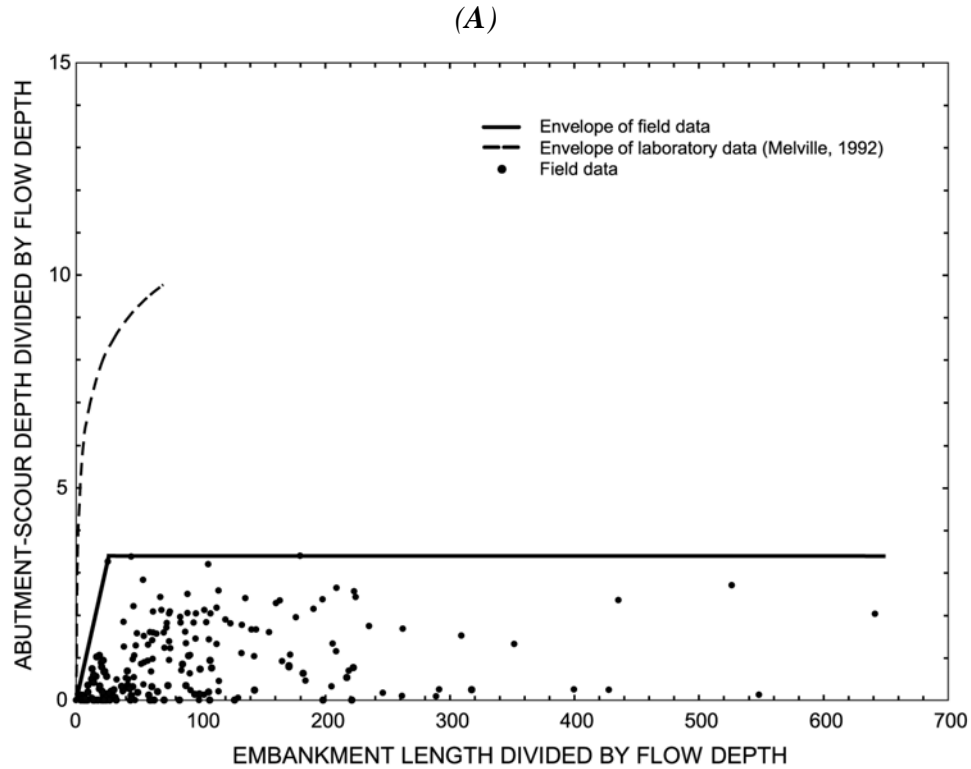


Figure 13. Relation of observed clear-water abutment-scour depth and the 100-year-flow embankment length, normalized by the 100-year-flow depth near the abutment toe, for the Piedmont and Coastal Plain of South Carolina with (A) a complete horizontal axis, and (B) a truncated horizontal axis.

channel slope

channel geometry

(2) Variables describing the abutment

embankment length

skew

abutment shape

(3) Variables describing the flow

flow depth

mean approach velocity

energy slope

gravitational acceleration

(4) Variables describing the bed material

median size

specific gravity

gradation

fall velocity

particle shape factor

angle of repose

cohesiveness

dimensionless critical-shear stress

particle Reynolds number

(5) Variables describing the fluid

density

dynamic viscosity

(6) Temperature

(7) Time

Inspection of the data compiled for the NCHRP Project 24-14 sites revealed that approach and contracted flow velocity, geomorphic setting (i.e., upstream channel alignment and valley configuration), bed-material cohesion and size, and geometric-contraction ratio are the factors that have the most affect on the measured scour. A review of the data collected in South Carolina revealed that the factors having the most appreciable effect on abutment-scour depth are embankment length, geometric-contraction ratio, flow velocity, and soil cohesion. The envelope curves plotting observed abutment scour versus embankment length for the South Carolina field data enveloped the observed scour at all the selected NCHRP Project 24-14 sites (Figure 14).

Comparisons of Observed Scour to HEC-18 Abutment-Scour Predictions

Abutment scour at 8 of the 12 NCHRP Project 24-14 sites was calculated using a one-dimensional model and 4 of the abutment-scour prediction equations (Froehlich, modified Froehlich, Sturm and HIRE) documented in HEC-18. The results of the predictive methods were compared to the real-time abutment-scour observations documented at the NCHRP Project 24-14 sites. Of the four NCHRP Project 24-14 sites not included in the comparison, two sites did not have models, one site had flow only in the channel, and one site had scour caused primarily by debris. The following comparisons should be viewed as comparisons of scour-prediction methods rather than simply comparisons of specific scour equations. The methods include the

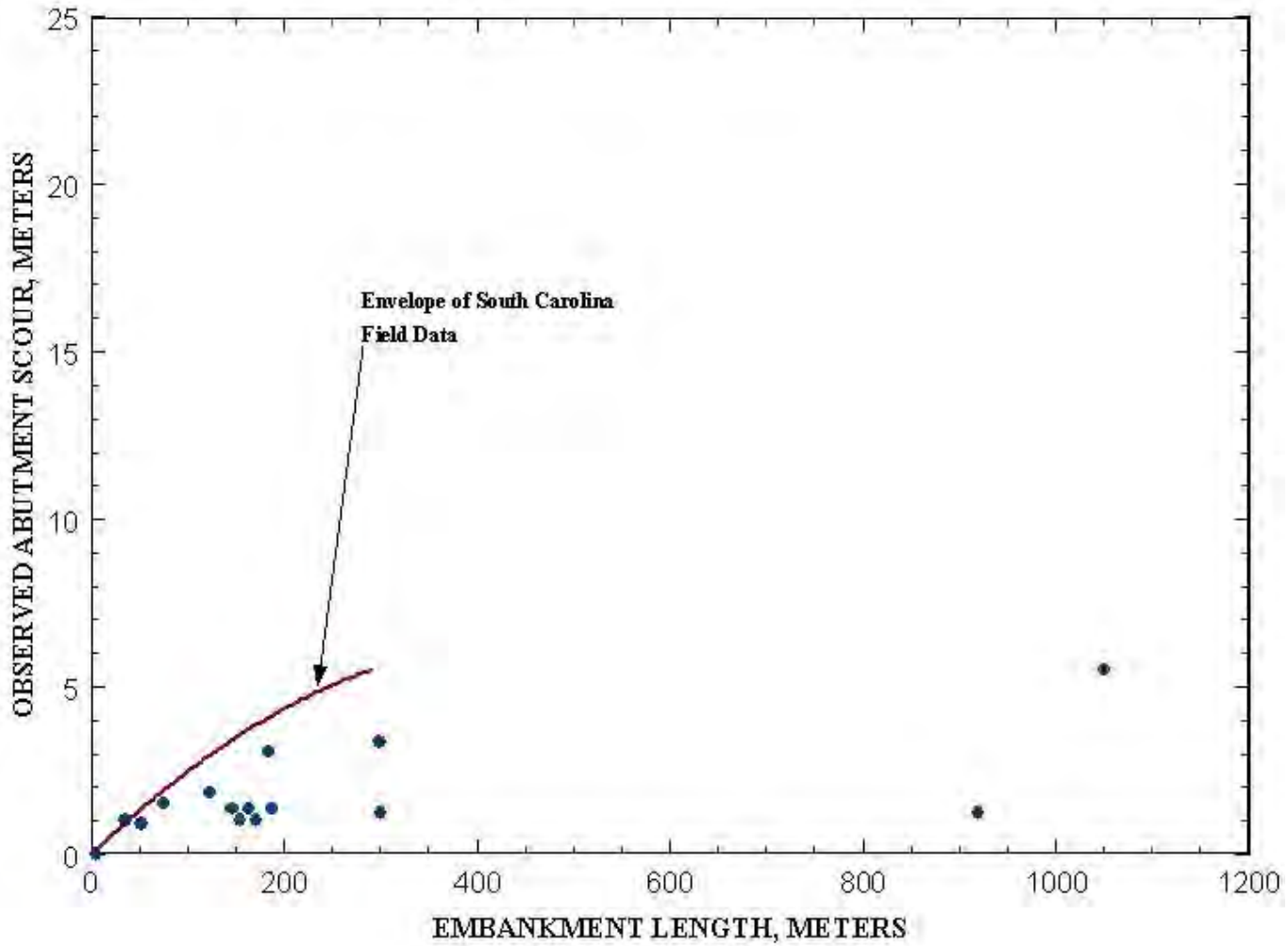


Figure 14. Comparison of the embankment-length envelope for field observations of abutment-scour depth in South Carolina with the observed abutment scour for selected sites from the National Bridge Scour Database (BSDMS).

application of one-dimensional hydraulic models and the selection of scour-prediction variables from these models. Errors in the hydraulic models or the selection of scour parameters from hydraulic models can lead to appreciable error in the scour predictions.

The results and comparisons of the scour-prediction method using Froehlich equations are shown in Figure 15. Recent (2001) adjustments to the embankment length term in the Froehlich equation have resulted in the modified Froehlich equation. An evaluation of the performance of the scour-prediction method using the Sturm equation, shown in Figure 16, reveals that the Sturm relation both over- and under-predicted the observed abutment scour at the sites in the BSDMS. An equation that excessively over-predicts scour is not a good tool and leads to excessive bridge-construction costs; however, an equation that under-predicts scour is a worse tool for design purposes because it can lead to bridge failures and potential loss of life. The data illustrated in figures 15 and 16 also are presented in Table 3.

A scour-prediction method that excessively over-predicts scour is not a good tool and leads to excessive bridge construction costs. The analysis of the Sturm, Froehlich, modified Froehlich and HIRE abutment-scour equations predictions of scour for the NCHRP Project 24-14 sites indicates that all four relations can appreciably over-predict scour when used in combination with standard one-dimensional models for the selection of hydraulic parameters.

Variability in Scour Predictions

A series of comparisons were developed to illustrate the relative effects of channel geometry, hydraulic parameters derived from one-dimensional models, and selected predictive

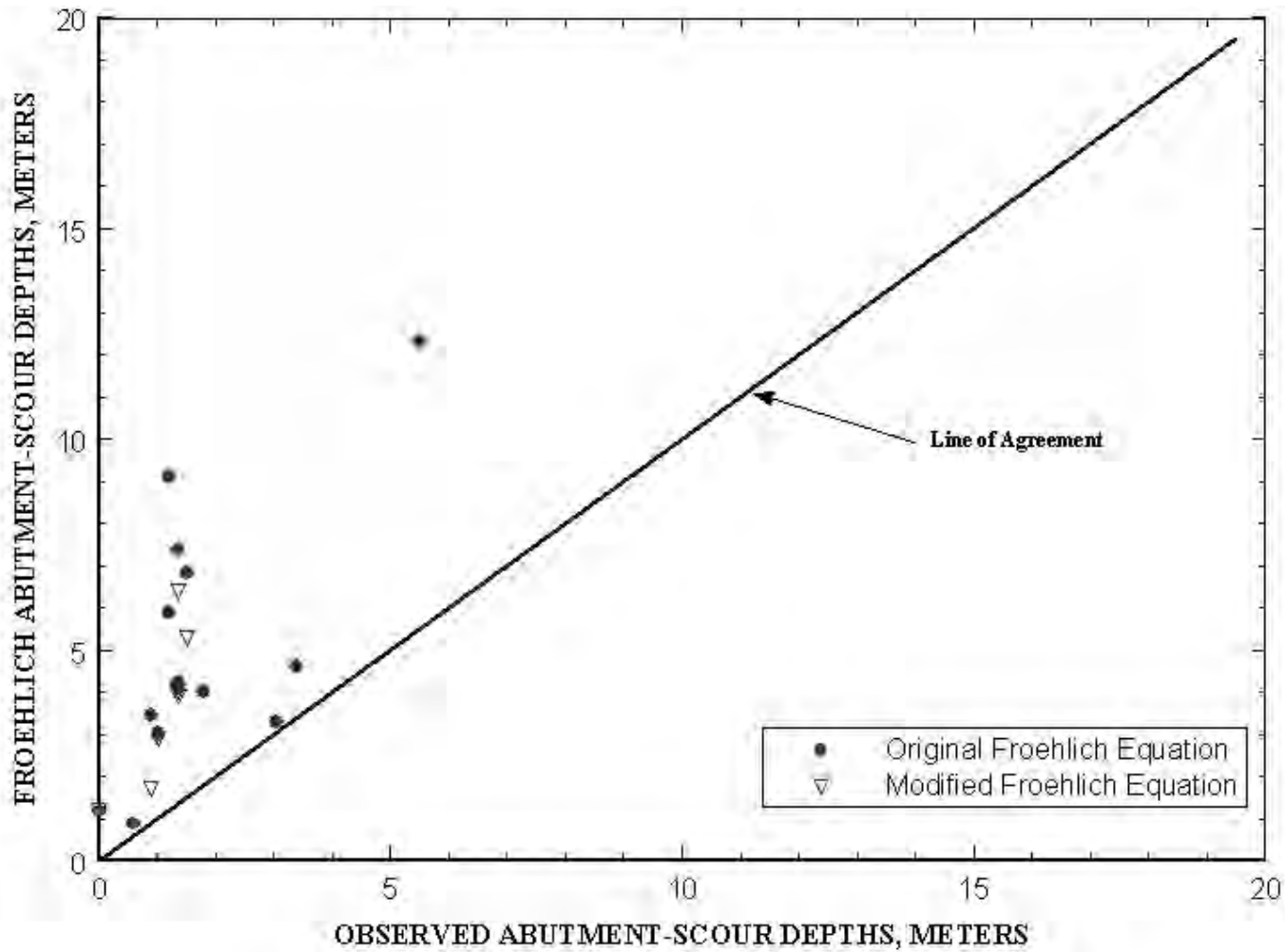


Figure 15. Comparison of field observations of abutment-scour depth with the theoretical abutment-scour depth computed with the original Froehlich (1989) and modified Froehlich (2001) equations for selected sites from the National Bridge Scour Database (BSDMS).

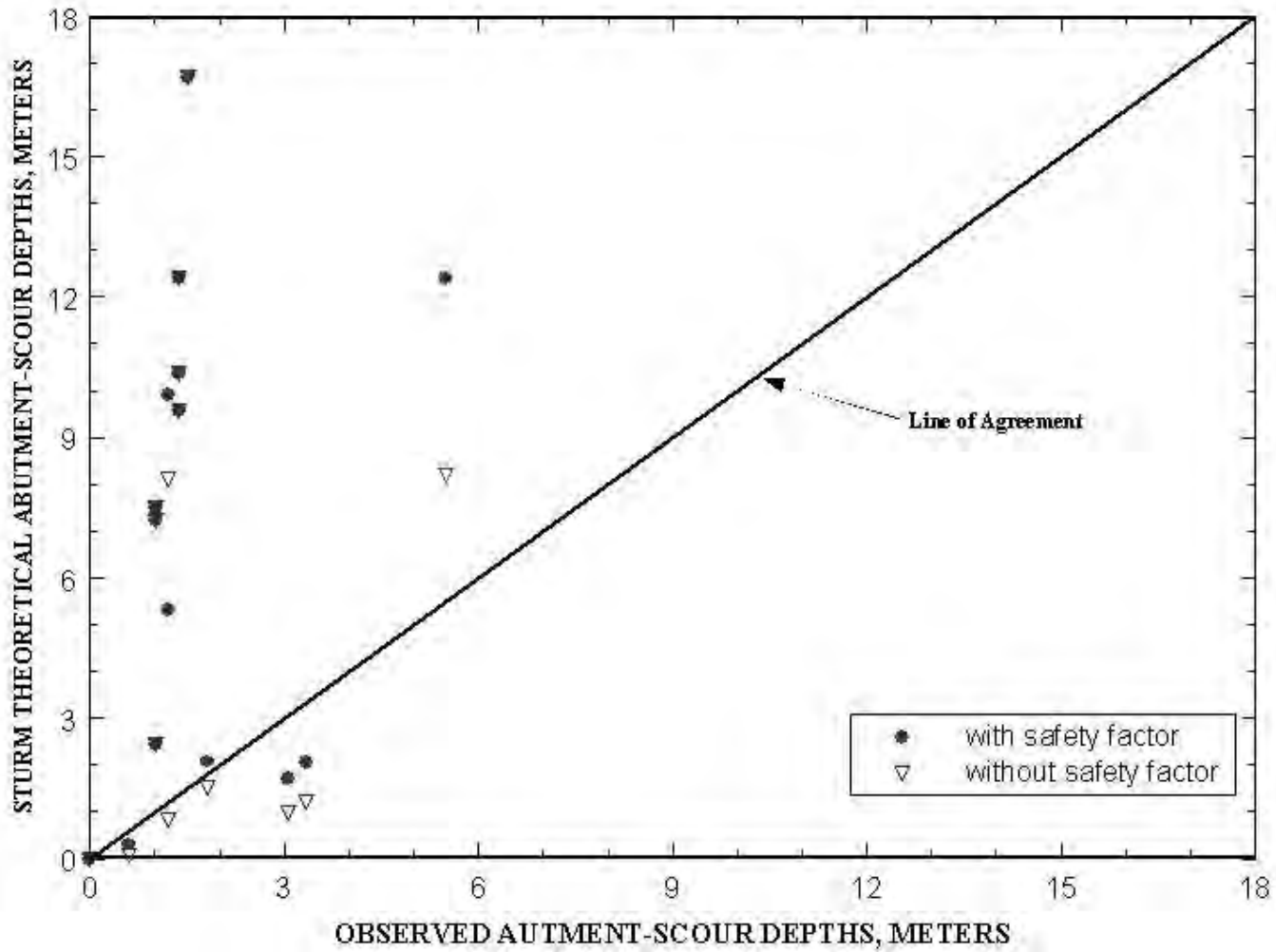


Figure 16. Comparison of field observations of abutment-scour depth with theoretical abutment-scour depth computed with the HEC-18 (2001) Sturm equation (with and without the safety factor) for selected sites from the National Bridge Scour Database (BSDMS).

TABLE 3. Comparison of observed abutment scour with scour calculated with the HEC-18 (2001) Froehlich and Sturm prediction equations using HEC-RAS modeled hydraulics for eight abutment scour sites in the National Bridge Scour Database (BSDMS). (-- not computed, m - meters)

Site Name	Location of Scour	Froehlich Scour Prediction (m)	Modified Froehlich Scour Prediction (m)	Sturm Scour Prediction (m)	Field Observed Scour (m)
James River at SR 37 near Mitchell, South Dakota	Left Abutment	5.9	--	9.9	1.2
Minnesota River at SR 25 near Belle Plaine, Minnesota	Left Abutment	12.3	--	12.4	5.5
Minnesota River at SR 25 near Belle Plaine, Minnesota	Right Abutment	9.1	--	5.3	1.2
Pomme De Terre River at US 12 Holloway, Minnesota	Left Abutment	4.0	--	2.1	1.8
Pomme De Terre River at US 12 Holloway, Minnesota	Right Abutment	4.6	--	2.1	3.4
Pomme De Terre River at CR22 Fairfield, Minnesota	Left Abutment	.88	--	.31	.61
Pomme De Terre River at CR22 Fairfield, Minnesota	Right Abutment	3.3		1.65	3.0
Bitterroot River near Belle Crossing, Montana	Left Abutment	6.8	5.3	16.7	1.5
Bitterroot River near Belle Crossing, Montana	Right Abutment	7.4	6.4	12.4	1.4
Beaver Creek Overflow 7 miles West of Saco, Montana	Left Abutment	4.1	3.9	10.4	1.4
Beaver Creek Overflow 7 miles West of Saco, Montana	Right Abutment	4.2	4.0	9.6	1.4
Beaver Creek Overflow 9 miles West of Saco, Montana	Left Abutment	3.0	2.9	7.2	1.0
Beaver Creek Overflow 9 miles West of Saco, Montana	Right Abutment	3.0	2.9	7.5	1.0
Gallatin River at I-90 near Manhattan, Montana	Left Abutment	1.2	1.2	0	0
Gallatin River at I-90 near Manhattan, Montana	Right Abutment	3.5	1.7	2.4	.91

equations when calculating scour by methods documented in HEC-18. Comparing the observed to computed depths of scour using field measured hydraulic parameters in the selected predictive equations allows evaluation of the accuracy of the predictive equations. Comparing the observed to computed depths of scour using hydraulic parameters derived from one-dimensional models allows an overall assessment of the accuracy of the methods recommended in HEC-18. A prerequisite to predicting scour from a one-dimensional model simulation is selecting the channel geometry to be modeled. The channel geometry that exists at the time of the flood may be appreciably different from the channel geometry that existed when the survey of the channel for modeling purposes was made. Scour resulting from use of both pre-flood and flood-channel geometry are compared to evaluate the effect of channel geometry on computed depth of scour. Analysis of these comparisons will highlight any deficiencies in the modeling approach and (or) the selected predictive equations.

The hydraulic parameters measured in the field were used in the selected prediction equations to directly evaluate the accuracy of the equations. Only two sites had detailed hydraulic measurements both through the bridge opening and in the approach section (Table 4), because of the difficulty of collecting data in the approach section and floodplain during major floods. The application of the HIRE (Richardson and others, 1990) equation showed the problems of using equations developed for simple geometries at bridge sites with complex geometry. The HIRE equation uses the velocity and depth of flow “at the abutment.” Current guidelines in HEC-18 indicate that when using one-dimensional models and the HIRE equation, it is acceptable to use the conveyance tube closest to the abutment for determining the velocity and depth at the abutment. However, the flow velocity in the conveyance tube closest to the

TABLE 4. Comparison of observed abutment scour with scour calculated by use of the HEC-18 (2001) prediction equations using hydraulic parameters measured in the field for two sites in the National Bridge Scour Database (BSDMS). (-- not applicable, $L'/y < 25$)

Site Name	Location of Scour	Date	Field Distributed Hydraulics Scour Calculations			Field Observed Scour (meters)
			(Froehlich) (meters)	(HIRE) (meters)	(Sturm) (meters)	
James River at SR 37 Mitchell, SD	Left Abutment	4/15/2001	9.7	10.8	16.8	1.2
Minnesota River at SR 25 Belle Plaine, MN	Left Abutment	4/17/2001	15.6	20.5	17.8	3.0
Minnesota River at SR 25 Belle Plaine, MN	Right Abutment	4/17/2001	6.0	--	3.0	1.2

abutment is always low compared to the rest of the flow field around the abutment and does not represent the acceleration of the high curvature flow especially near the point of flow separation (Table 5). The use of the field-measured velocity as defined by HEC-18 for the HIRE equation, results in gross over-prediction of abutment-scour depths. The HIRE equation was derived from scour measured at dikes on the Mississippi River using hydraulic variables measured in the flow approaching the dikes (Richardson and others, 1990); therefore, a more representative field-velocity measurement for use in the HIRE equation should be taken upstream of the abutment tip, near the approach section. The HIRE abutment-scour values found in Table 4 were calculated using velocity values measured at the approach section rather than directly adjacent to the abutment. None of the equations accurately predicted the scour using the measured hydraulic parameters at these sites.

Comparing the predicted depths of abutment scour using measured hydraulics and modeled hydraulics provides an evaluation of the adequacy of the one-dimensional modeling approach. Tables 6 and 7 show that the predicted depth of scour generally was larger for measured hydraulics than for modeled hydraulics. The hydraulics for the two sites used in this comparison are dominated by the alignment of the channels upstream of the bridges (Figures 8 and 17). These channel alignments and their effects are not captured in one-dimensional models that only extend one bridge-length upstream and downstream. Although the abutment-scour equations over-predicted the observed scour for both measured and modeled hydraulic parameters, it is possible that the modeled hydraulics could have resulted in underpredictions because of the failure of the one-dimensional model to account for the highly two-dimensional hydraulics occurring at these sites if the equations provided accurate scour predictions.

TABLE 5. Comparison of measured and modeled abutment-tip velocities for use in the HIRE abutment scour prediction equation (m/s, meters per second).

Site name	Location of scour	Date	Modeled abutment tip velocity (m/s)	Field abutment tip velocity (m/s)
James River at SR 37 Mitchell, South Dakota	Left Abutment	4/15/2001	0.20	1.8
Minnesota River at SR 25 Belle Plaine, Minnesota	Left Abutment	4/17/2001	.35	4.1
Minnesota River at SR 25 Belle Plaine, Minnesota	Right Abutment	4/17/2001	.62	1.7

TABLE 6. Comparison of observed abutment scour with scour calculated by use of the HEC-18 (2001) Froehlich and HIRE prediction equations using modeled and field hydraulics for two abutment scour sites in the National Bridge Scour Database (BSDMS). (-- not applicable, ($L'/y < 25$); m, meters)

Site name	Location of scour	Date	Modeled calculated scour (Froehlich) (m)	Field hydraulics scour calculation (Froehlich) (m)	Modeled calculated scour (HIRE) (m)	Field hydraulics scour calculation (HIRE) (m)	Field observed scour (m)
James River at SR 37 near Mitchell, South Dakota	Left Abutment	4/15/2001	5.2	9.7	2.6	10.8	1.2
Minnesota River at SR 25 Belle Plaine, Minnesota	Left Abutment	4/17/2001	11.6	15.6	10.9	20.5	3.0
Minnesota River at SR 25 Belle Plaine, Minnesota	Right Abutment	4/17/2001	9.0	6.0	--	--	1.2

TABLE 7. Comparison of observed abutment scour with scour calculated by use of the HEC-18 (2001) Sturm and Maryland prediction equations using modeled and field hydraulics for two abutment scour sites in the National Bridge Scour Database (BSDMS). (m, meters)

Site name	Location of scour	Date	Modeled calculated scour (Sturm) (m)	Field hydraulics scour calculation (Sturm) (m)	Field observed scour (m)
James River at SR 37 near Mitchell, South Dakota	Left Abutment	4/15/2001	6.3	16.8	1.2
Minnesota River at SR 25 Belle Plaine, Minnesota	Left Abutment	4/17/2001	11.6	17.8	3.0
Minnesota River at SR 25 Belle Plaine, Minnesota	Right Abutment	4/17/2001	9.2	3.0	1.2



Figure 17. Aerial photograph of State Route 25 over the Minnesota River near Belle Plaine, Minnesota

The effect of changes in channel geometry on the computed depth of scour is evaluated by comparing depth of scour computed from modeled hydraulic parameters for pre-flood and flood-channel geometry. Because this comparison does not require detailed measured flow data in the approach section and floodplain, additional sites can be used in this evaluation. The pre-flood geometry was approximated through inspection of bridge plans as well as upstream- and downstream-channel bathymetry. The flood geometry was taken directly from the detailed real-time scour measurements on the specified dates. The results of this comparison clearly show that channel geometry has an effect on the computed depth of scour, but the equations were unable to accurately predict the observed depth of scour using either geometry (Tables 8 and 9).

The comparisons presented in this section show that although geometry and the one-dimensional modeling approach can cause variations in the depth of predicted scour, the accuracy of the selected equations currently is the largest source of error in abutment-scour predictions. The channel and floodplain geometry both near the bridge and upstream play an important role in the distribution of flow at the bridge. Although these effects are not accounted for in the one-dimensional model, the use of field-measured hydraulics did not improve the accuracy with which the selected equations could predict the observed scour. Therefore, although the one-dimensional approach proposed in HEC-18 has limitations, the data, assumptions, and experiments on which the selected equations are based do not adequately represent complex field conditions and render the equations inaccurate.

TABLE 8. Comparison of observed abutment scour with scour calculated by use of HEC-18 (2001) Froehlich and HIRE prediction equations using flood and pre-flood geometry for four abutment scour sites in the National Bridge Scour Database (BSDMS).

(-- not applicable ($L'/y < 25$); m, meters)

Site name	Location of scour	Date	Pre-flood geometry modeled scour (Froehlich) (m)	Flood geometry modeled scour (Froehlich) (m)	Pre-flood geometry modeled scour (HIRE) (m)	Flood geometry modeled scour (HIRE) (m)	Field observed scour (m)
James River at SR 37 near Mitchell, South Dakota	Left Abutment	4/15/2001	5.9	5.2	3.4	2.6	1.2
Minnesota River at SR 25 Belle Plaine, Minnesota	Left Abutment	4/17/2001	12.3	11.6	9.5	10.9	5.5
Minnesota River at SR 25 Belle Plaine, Minnesota	Right Abutment	4/17/2001	9.1	9.0	--	--	1.2
Pomme De Terre River at US 12 Holloway, Minnesota	Left Abutment	4/9/1997	4.0	3.0	5.2	4.6	1.8
Pomme De Terre River at US 12 Holloway, Minnesota	Right Abutment	4/9/1997	4.6	4.3	10.8	4.3	3.4
Pomme De Terre River at CR 22 Fairfield, Minnesota	Left Abutment	4/9/1997	.88	1.8	--	--	.61
Pomme De Terre River at CR 22 Fairfield, Minnesota	Right Abutment	4/9/1997	3.3	4.4	4.2	1.4	3.0

TABLE 9. Comparison of observed abutment scour with scour calculated by use of the HEC-18 (2001) Sturm prediction equation using flood and pre-flood geometry for four abutment scour sites in the National Bridge Scour Database (BSDMS). (m, meters)

Site Name	Location of scour	Date	Pre-flood geometry modeled scour (Sturm) (m)	Flood geometry modeled scour (Sturm) (m)	Field observed scour (m)
James River at SR 37 near Mitchell, South Dakota	Left Abutment	4/15/2001	9.9	6.3	1.2
Minnesota River at SR 25 Belle Plaine, Minnesota	Left Abutment	4/17/2001	12.6	11.8	5.5
Minnesota River at SR 25 Belle Plaine, Minnesota	Right Abutment	4/17/2001	5.3	9.2	1.2
Pomme De Terre River at US 12 Holloway, Minnesota	Left Abutment	4/9/1997	2.1	1.6	1.8
Pomme De Terre River at US 12 Holloway, Minnesota	Right Abutment	4/9/1997	2.0	2.4	3.4
Pomme De Terre River at CR 22 Fairfield, Minnesota	Left Abutment	4/9/1997	.33	1.1	.61
Pomme De Terre River at CR 22 Fairfield, Minnesota	Right Abutment	4/9/1997	1.7	3.4	3.0

SCOUR WITH DEBRIS

In general, very little research has been done regarding bridge scour that is directly associated with woody-debris accumulation despite the fact that debris accumulations have contributed to one-third of all bridge failures in the United States (Chang, 1973). Woody-debris accumulations (also referred to as a debris raft) affect the scour depth and patterns at bridges in several ways: (a) they increase the effective size of piers and (or) abutments, which may lead to deeper local scour; (b) if they are large enough, they can contract the flow through the bridge sufficient enough to induce contraction scour; and (c) they can deflect flow into a neighboring pier or abutment causing deeper scour at nearby foundations.

Dongol (1989) experimentally investigated the effects that debris rafting had on scour depths at bridge piers and developed a procedure to estimate the equilibrium local scour depth associated with debris accumulation. The study provided a method for determining the effective diameter to be used in computing local scour depth for piers with floating-debris accumulation. Single cylindrical piers are considered the least likely to accumulate large debris rafts relative to other pier shapes and configurations. Piers consisting of multiple piles can be especially susceptible to appreciable debris accumulations because the free space between columns is not typically wide enough to pass floating debris and provides an excellent place for debris to lodge.

Predicting the probability and size of debris rafts is an issue of great importance for those responsible for the maintenance of bridges; however, little work has been done on this subject.

Current design guidelines treat debris rafts as a detriment to bridges, but do not provide methods for estimating the likelihood and size of debris accumulation. The majority of published information regarding debris scour is subjective and qualitative; although this information is useful, it is difficult to apply in bridge design. A report prepared for the Federal Highway Administration (Diehl and Bryan, 1997) attempted to provide more quantitative criteria on the likelihood and size of potential debris accumulation at bridges by reviewing published literature on drift, analyzing data from 2,577 reported drift accumulations, and conducting field investigations of 144 debris accumulations.

Summary of Observations

The current NCHRP Project 24-14 data set only contains one real-time measurement of scour appreciably affected by a debris accumulation (State Route 129 over the Chariton River near Prairie Hill, Missouri; see Appendix A, Case Study No. 10). A review of flood-measurement notes indicates that this site does not experience substantial scour of any form when there is no debris accumulation; however, for floods where a debris accumulation forms on the central pier, the streambed elevations drop by as much as 6.1 m in what appears to be a combination of contraction scour (caused by the reduced flow area as a result of the debris accumulation) and local scour effects caused by the debris and pier. The procedure for estimating scour at piers with a debris accumulation (Dongol, 1989 and Melville and Dongol, 1992) combined with contraction scour estimates using hydraulic parameters from WSPRO was compared to a series of five separate scour measurements at this site.

The local scour associated with the debris accumulation for each of the five measured floods was calculated using Melville and Dongol (1992) wherein the effect of a debris accumulation is converted to an effective pier diameter based on the thickness and diameter of the accumulation. The effective diameter was then substituted for the diameter term in the HEC-18 equations to predict the total scour. The total scour computed using the Melville and Dongol approach and the total scour observed in the field compared very closely (Table 10). Although data from one site is an insufficient basis for an overall validation of the proposed technique, it indicates that this technique has promise and that comparisons with additional field data would be useful.

The design debris-accumulation width criteria developed by Diehl and Bryan (1997) is based on the width of the approach channel. The channel width at this site was unchanged during the period of data collection so only one design debris-accumulation width was computed. The comparison of the design width to observed widths of the debris accumulation show close agreement (Table 11). As with the approach for determining scour depth, one site is insufficient for an overall validation of the proposed technique, but it indicates that this technique has promise and that comparisons with additional field data would be useful.

APPLYING NUMERICAL MODELS FOR SCOUR ANALYSIS

The use of one-dimensional models is currently (2004) the standard method to estimate the bridge hydraulics for scour computations by State and Federal highway agencies; however,

TABLE 10. Comparison of Melville's debris-scour-estimating procedure with HEC-18 procedures and observed debris scour at S.R. 129 over the Chariton River near Prairie Hill, Missouri. (m, meters)

Date	Pier scour		Contraction scour	Total scour		
	Melville (m)	HEC-18 (m)	Melville/HEC-18 (m)	Melville (m)	HEC-18 (m)	Observed (m)
3/29/1960	4.7	2.9	0.37 / 0.21	5.0	3.1	5.2
4/22/1973	5.2	2.6	0 / 0	5.2	2.6	5.2
5/8/1978	5.9	3.0	0 / 0	5.9	3.0	6.1
7/8/1993	6.4	3.1	.12 / 0	6.6	3.1	6.1
5/24/1995	3.9	2.9	0 / 0	3.9	2.9	3.6

TABLE 11. Comparison of debris width-design-criteria relationship (Diehl and Bryan, 1997) and measured debris raft diameters for S.R. 129 over the Chariton River near Prairie Hill, Missouri.

Measurement Date	Approach Channel Width (m)	Design Debris Width (m)	Measured Debris Width (m)
3/29/1960	74.7	24.0	13.4
4/22/1973	74.7	24.0	21.3
5/8/1978	74.7	24.0	21.3
7/8/1993	74.7	24.0	23.2
5/24/1995	74.7	24.0	9.1

flood flow contracting through bridge openings is an inherently two-dimensional and many times three-dimensional hydrodynamic situation. One of the most important factors in using numerical models at contracted bridges is the ability for the model to accurately represent the velocity distribution laterally across the stream and floodplain.

Summary of Observations

One-dimensional hydraulic models were developed for most of the sites included in the BSDMS. The hydraulic parameters estimated by the models were used to predict scour depths using the HEC-18 methods and to build comparisons with scour measurements. A two-dimensional hydrodynamic and sediment-transport model also was developed for a site with real-time detailed scour data. The results of the two-dimensional simulation were compared to the one-dimensional results and the field measurements.

One-Dimensional Numerical Models

One-dimensionally modeled velocity distributions for two contracted sites over the Pomme De Terre River in Minnesota are compared with real-time field measurements of velocity made during the 1997 flooding.

The velocity-distribution comparisons at both sites were made for channel geometry measured on 4/5/97, which was on the rising limb of the flow and for channel geometry measured on 4/9/97, which was just after the peak. The velocity distribution at U.S. Route 12 on 4/5/97 indicates that the flow in the field was skewed toward the right abutment (Figure 18A).

HEC-RAS did not duplicate this skewed flow pattern but rather computed a uniform flow distribution across the cross-section caused by the model assigning flow tubes of equal conveyance through the geometrically uniform bridge section. HEC-RAS was more accurate in reproducing the observed velocity distribution for the scoured channel geometry (Figure 18B). The one-dimensional model is not able to reproduce the region of reverse flow that occurred adjacent to the left abutment. HEC-RAS computed velocities are greater near the deeply scoured region adjacent to the right abutment because the slope and roughness are constant across the cross section, so the conveyance becomes dependent upon the depth of flow. The one-dimensional model results did not compare well with the 4/5/97 observations at County Route 22 (Figure 19A) because of its inability to replicate the two-dimensional features of the measured flow field. Although the model estimated the peak velocity near the right-most pier reasonably well, the modeled velocities were too high near the right bank and in the center of the main channel and too low along the left bank. The model once again did a better job redistributing the flow after the scour had fully developed (Figure 19B).

Although the current amount of field data in the approach sections of the surveyed bridges were inadequate to provide a comprehensive evaluation of the ability of a one-dimensional model to represent complex two-dimensional flow fields, the comparisons that could be made showed the limitations of the one-dimensional modeling approach. Where conveyance dominates the hydrodynamics, such as for fully developed scour-hole conditions, a one-dimensional model is able to provide a reasonable estimate of the velocity distribution; however, where two and three-dimensional effects caused by flow accelerations dominate the

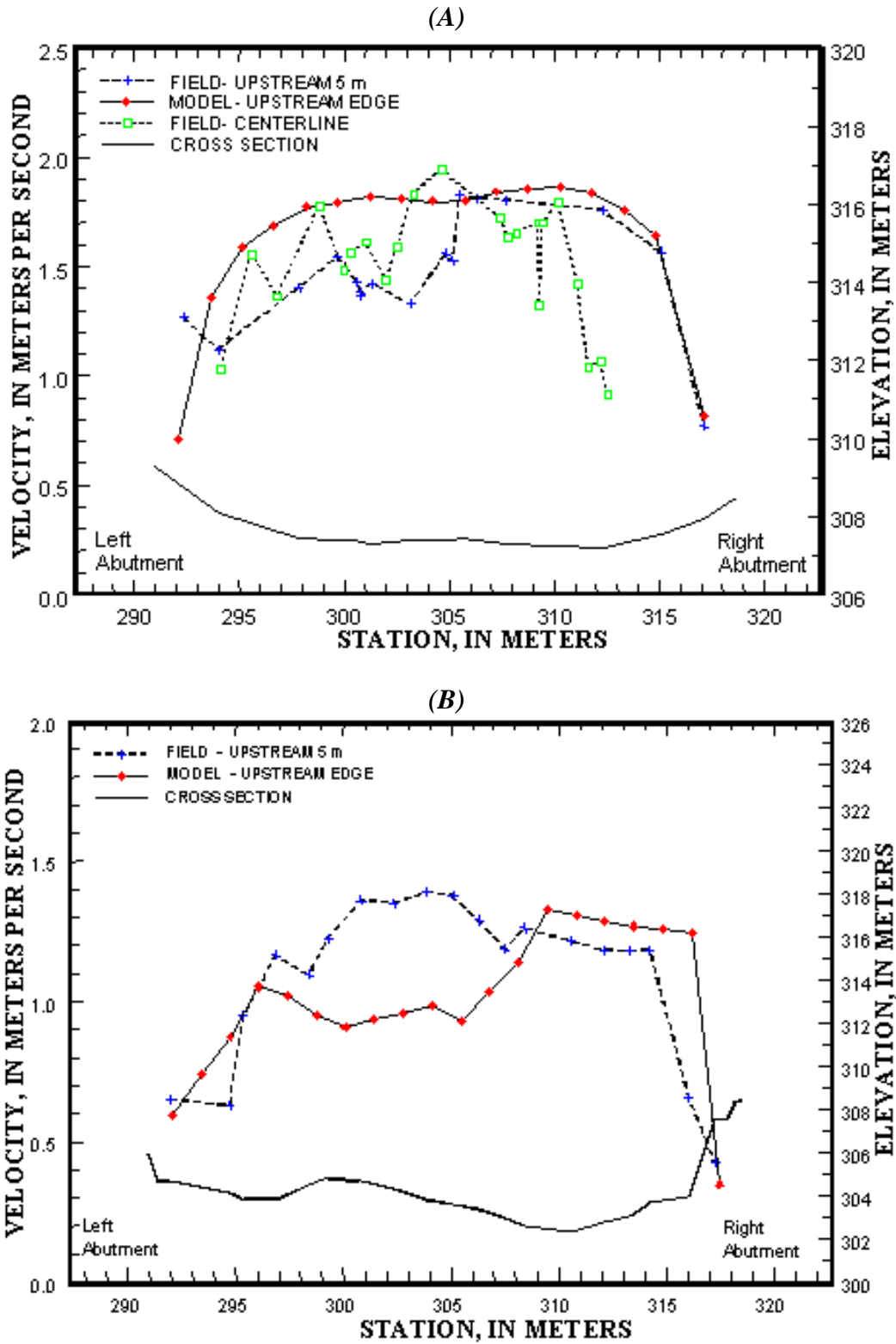


Figure 18. Comparison of observed- and model-velocity distributions at U.S. Route 12 over the Pomme de Terre River, Minnesota, for (A) April 5, 1997 and (B) April 9, 1997.

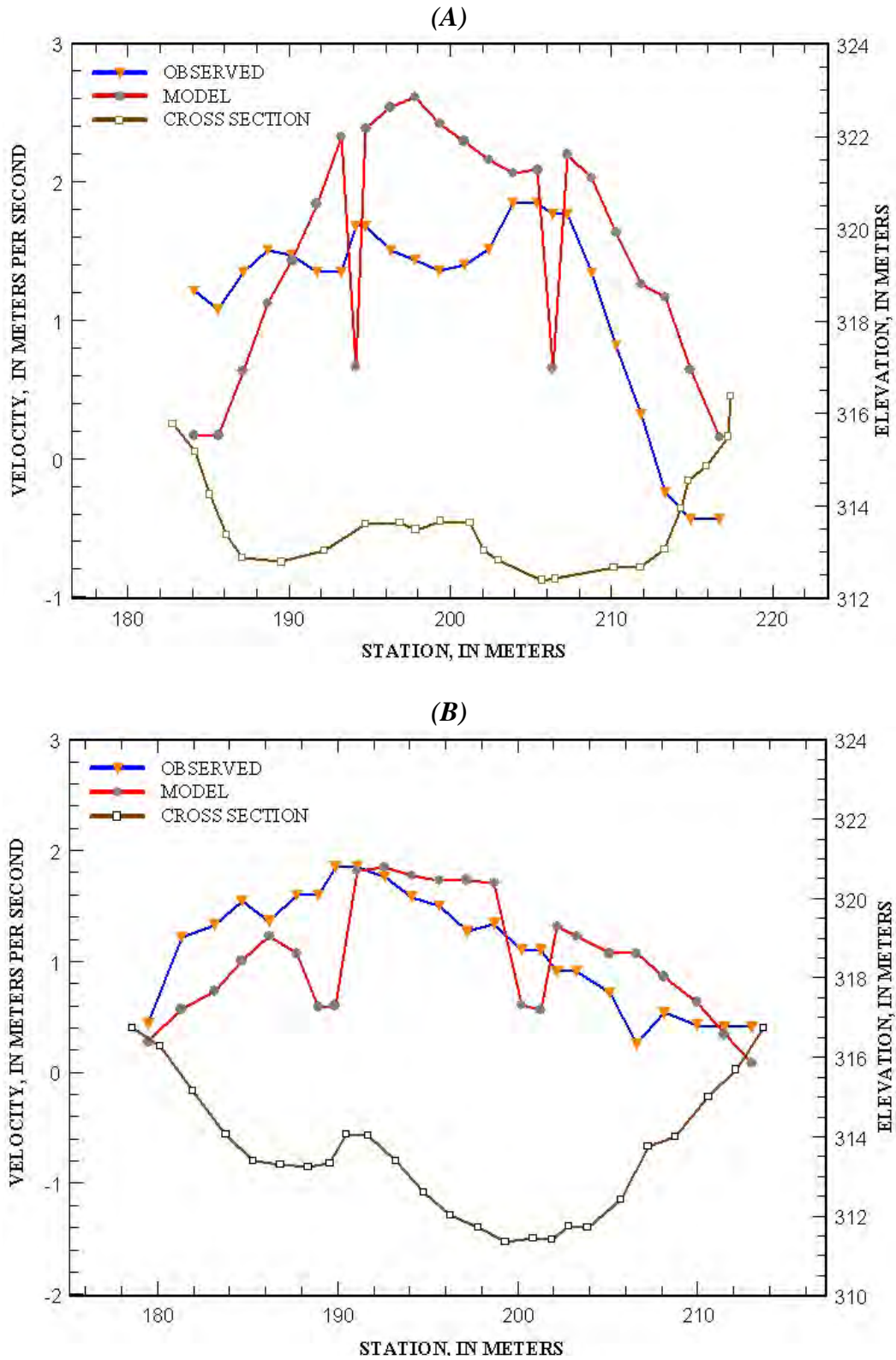


Figure 19. Comparison of observed- and model-velocity distributions at County Route 22 over the Pomme de Terre River, Minnesota, for (A) April 5, 1997 and (B) April 9, 1997.

flow field, such as at the beginning of a flood and during the scouring process, the one-dimensional model is severely limited in its ability to accurately distribute the flow.

An analysis of scour computations in HEC-RAS revealed that the approach channel alignment is not accounted for in calculations of abutment scour. Default HEC-RAS hydraulic parameters used for abutment-scour calculations can provide erroneous predictions based on incorrect projection of the bridge opening to the approach section. The HEC-RAS default scour parameters for the two Pomme De Terre river sites and the State Route 25 Bridge over the Minnesota River had to be adjusted. Without this adjustment the parameters such as the blocked discharge (Q_e), area of flow blocked (A_e) and average depth of blocked flow in the approach (Y_a) were inaccurately estimated because of upstream channel bends that were not considered in the HEC-RAS algorithms for determination of scour variables.

Two-Dimensional Numerical Models

A two-dimensional hydrodynamic model (Resource Management Associates – 2 (RMA-2)) also was developed for the County Route 22 site over the Pomme De Terre River near Fairfield, Minnesota in order to evaluate the flow distribution relative to the one-dimensional model and field measurements. The site has a large bend directly upstream of the bridge, which has a large affect on the flow distribution and scour processes at the bridge (Figure 20). Two separate measurements were made at County Route (C.R.) 22 during an appreciable flood event. The measurements produced velocity magnitudes and distributions primarily because of the

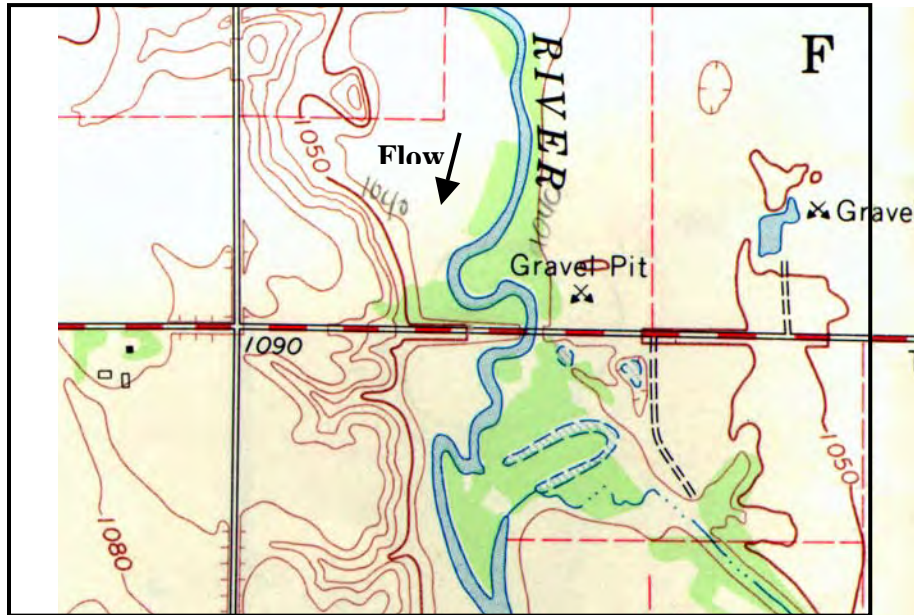


Figure 20. Plan view of topography and channel alignment for County Route 22 over the Pomme De Terre River near Fairfield, Minnesota (elevation referenced in feet above seal level; 1 ft = 3.2808 m).

formation of a large scour hole at the left abutment during the time between the measurements. A large standing wave and area of reverse flow was witnessed during the 4/5/97 measurement (Figure 21) because of the interaction of the main channel and floodplain flow contracting through the bridge opening. The modeled flow field for the 4/5/97 conditions is illustrated in Figure 22 and is representative of the field observations. The reverse flow and standing wave were absent during the 4/9/97 survey and modeled flow field.

The calibration of the two-dimensional model (Figure 23) to the field measurements was limited because of flow conditions through the bridge opening being inherently three dimensional, especially around the right abutment. On 4/9/97, flow was shifted from the left to the right abutment in the two-dimensional model relative to the field measurements (Figure 24). Detailed data were unable to be collected at the site during the flood because of heavy vegetation on the floodplain and near pressure-flow conditions at the bridge. Bathymetry data throughout the model reach was not collected until October 2001, over 4 years after the measured flood. Uncertainty in the geometry upstream of the bridge also is a likely a large contributor in the difference between the field measurements and the two-dimensional model results.

A two-dimensional sediment-transport model of C.R. 22 site also was developed utilizing the calibrated hydrodynamics from 4/5/97 and 4/9/97. The sediment-transport model was run for the period between measurements (4/5-4/9/97) at the site to evaluate its ability to replicate the observed scour through the bridge opening. To replicate the conditions that produced the observed scour, the discharge measured on 4/5/97 was run for 48 hours followed by 48 hours of the 4/9/97 discharge. Although steady-flow conditions were obviously not what occurred in the

field, the lack of data between 4/5/97 and 4/9/97 prevented a more accurate representation of the hydraulics. The bed elevations of the sediment-transport model relative to scour measurements made on 4/9/97 are illustrated in the difference map found in Figure 25. The model predicted more scour at the left abutment and less scour at the right abutment than were measured in the field (red contours indicate the model underpredicted scour, blue contours indicate the model overpredicted scour). The errors in the modeled-scour patterns can be directly associated with the differences in the modeled- and measured-velocity distributions. The model conveyed too much flow near the left abutment and not enough flow near the right abutment.

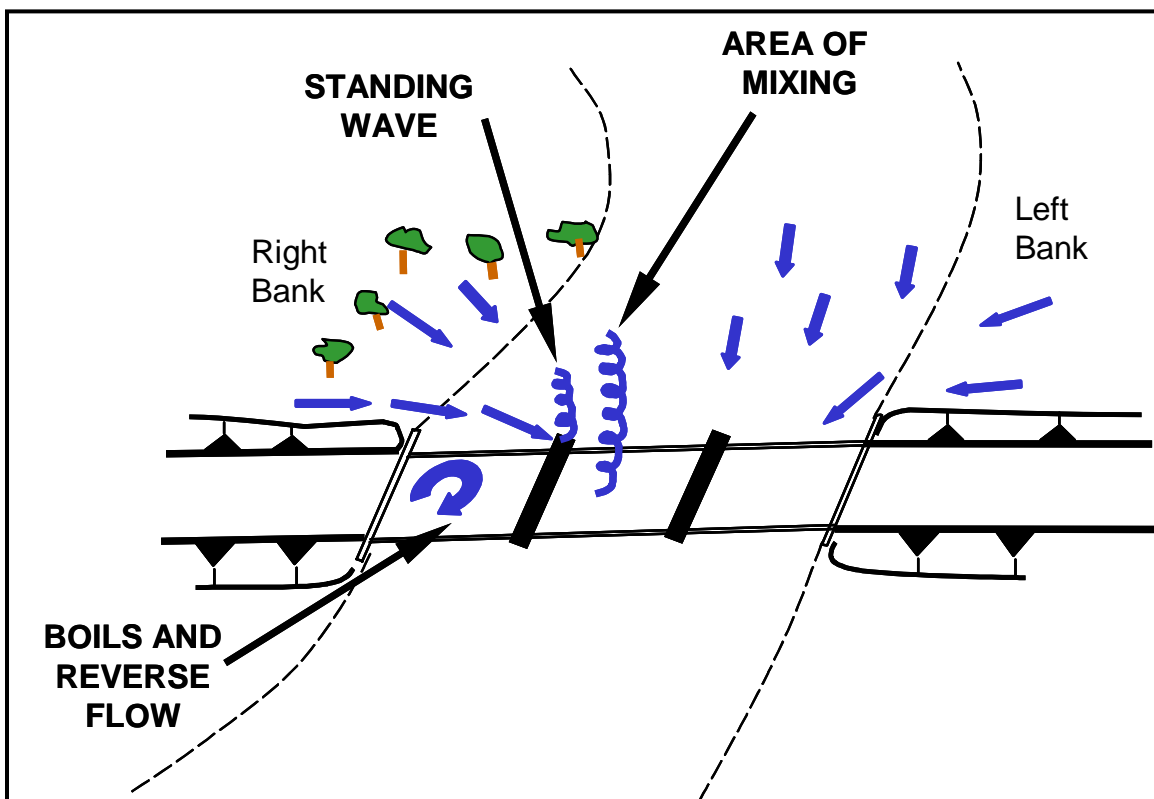


Figure 21. Sketch of the hydrodynamics observed during bridge scour measurements at County Route 22 over the Pomme de Terre River on April 5, 1997.

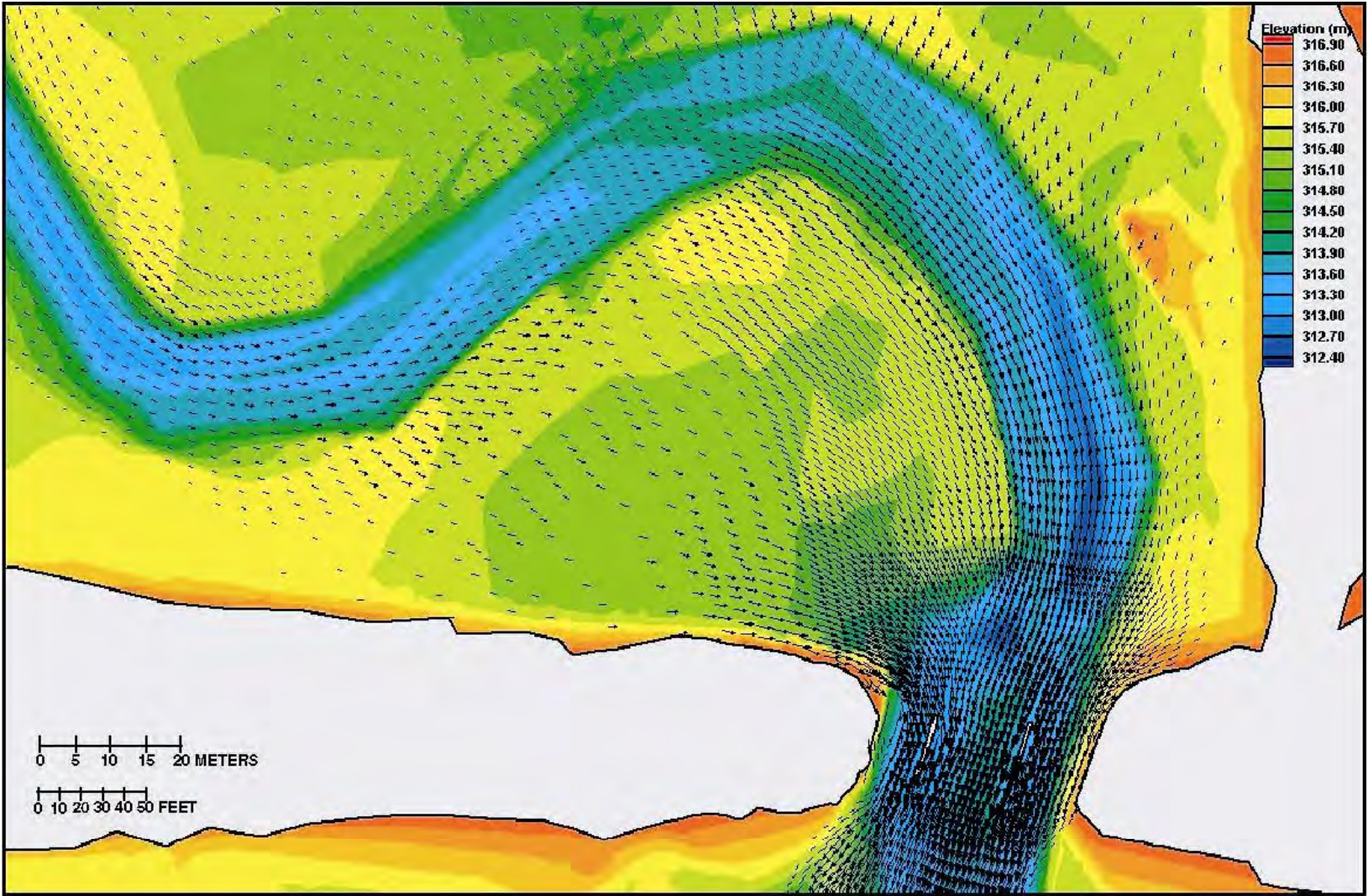


Figure 22. Modeled flow field for County Route 22 over the Pomme de Terre River for conditions on April 5, 1997.

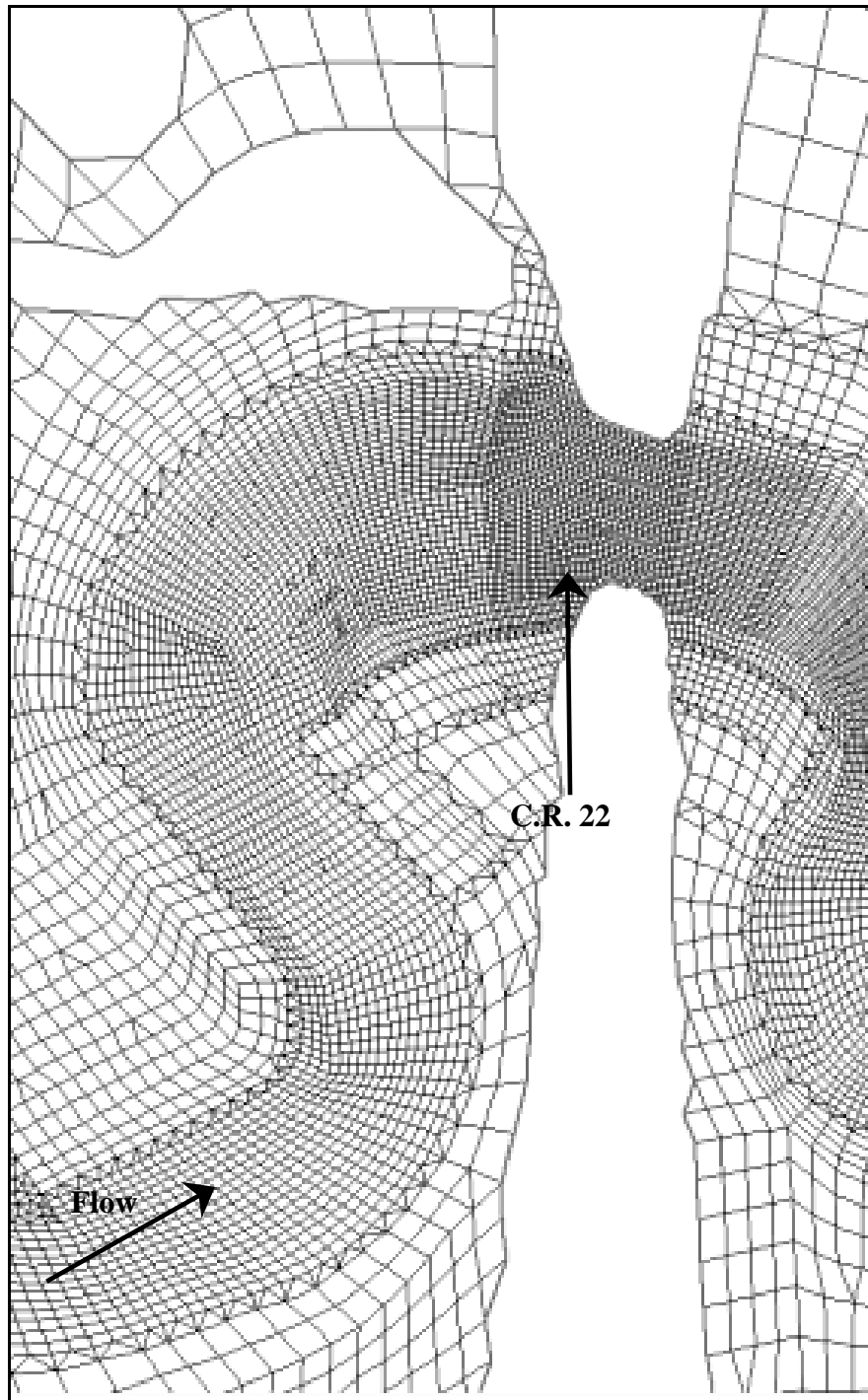


Figure 23. Computational mesh for the two-dimensional model of County Route 22 over the Pomme de Terre River.

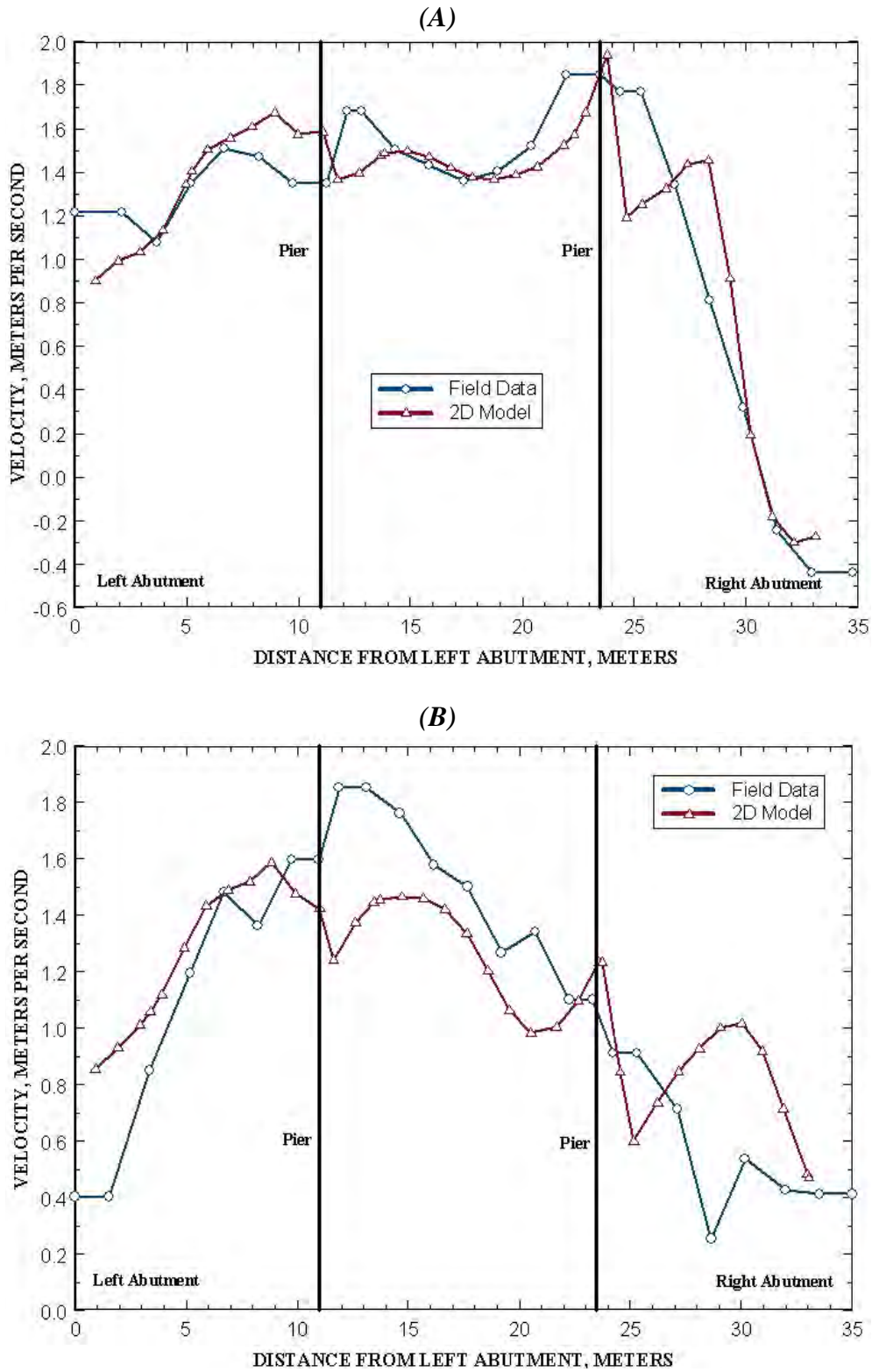


Figure 24. Comparison of the velocity distribution for the two-dimensional model and field measurements at the upstream bridge face of County Route 22 over the Pomme de Terre River on (A) 4/5/1997 and (B) 4/9/1997.

Discussion of One-Dimensional and Two-Dimensional Model Comparisons

Comparison of the output from the one- and two-dimensional models yielded surprising results. Despite the calibration complexities induced by geometry uncertainty and three-dimensional flow, the two-dimensional model was able to reproduce the hydraulics in the bridge opening for the conditions measured on 4/5/97 more accurately than the one-dimensional model (Figure 26). However, for the fully developed scour-hole condition on 4/9/97, the one-dimensional model provides a slightly better representation of the velocity distribution than does the two-dimensional model. A comparison of the HEC-18 scour estimates using the one-dimensional and two-dimensional models relative to the observed scour depths was complicated by the automatic approach section selected by HEC-RAS and the section selected from the two-dimensional model based on the modelers evaluation of the flow lines (Figure 27).

HEC-18 scour computations also were computed from the two-dimensional model hydraulics with the HEC-RAS selected and the manually selected approach cross-section and compared to scour depths calculated from the one-dimensional model, sediment-transport model, and those observed in the field (Table 12). The contraction scour and right-abutment scour estimated using the two-dimensional model hydraulics improved by adjusting the location of the approach cross section, however there was an increase in the difference between Froehlich's prediction and the observed depth of scour at the left abutment. The comparison shows that the one-dimensional model more accurately estimated the observed scour than did any of the two-dimensional model results. The equations in HEC-18 were developed and mostly based on data collected in a laboratory setting, which does not replicate the complex, site-specific hydraulic

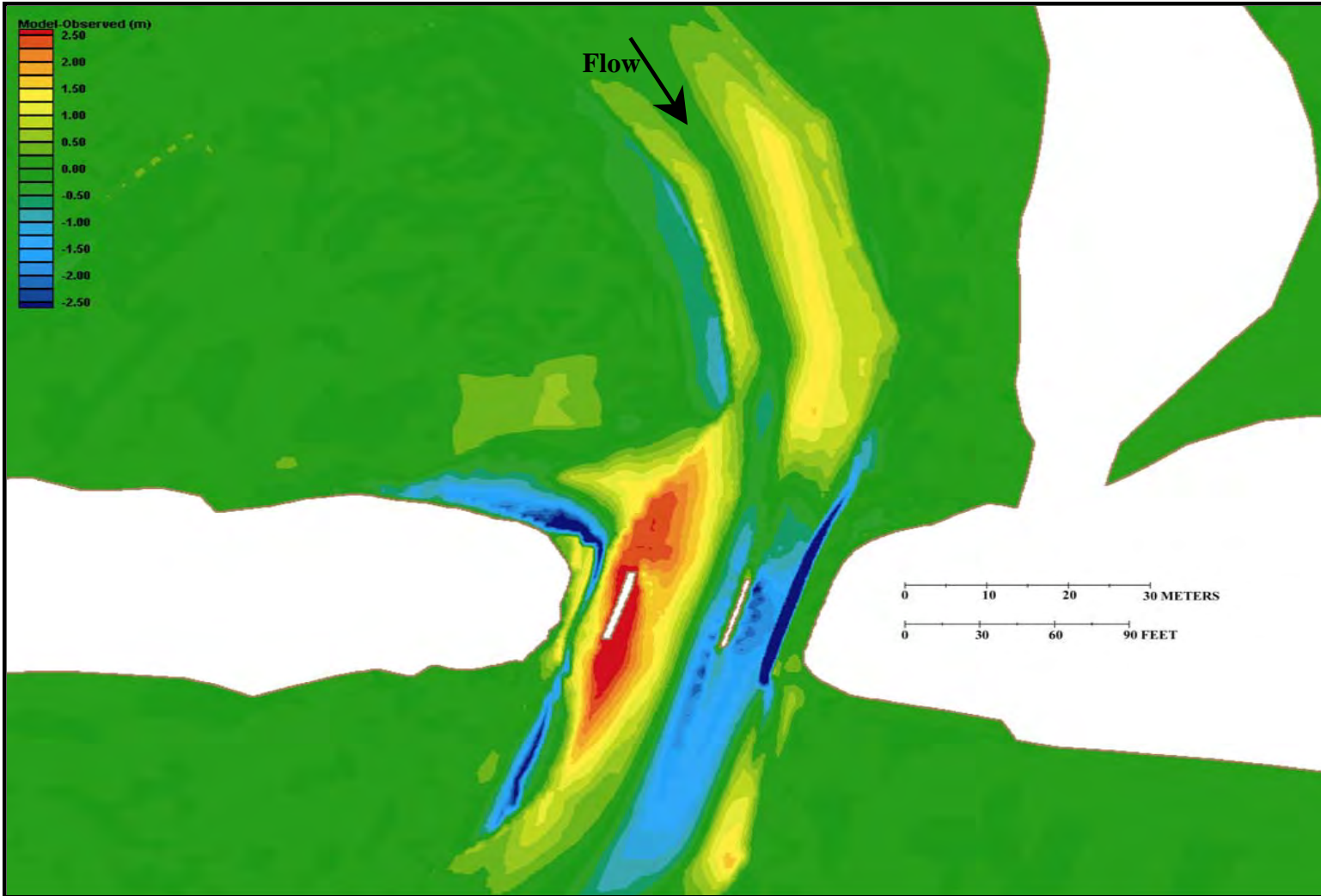


Figure 25. Difference in bed elevation (in meters) between two-dimensional sediment-transport model output and field data collected during flood conditions on the Pomme de Terre River at County Route 22, April 4-9, 1997.

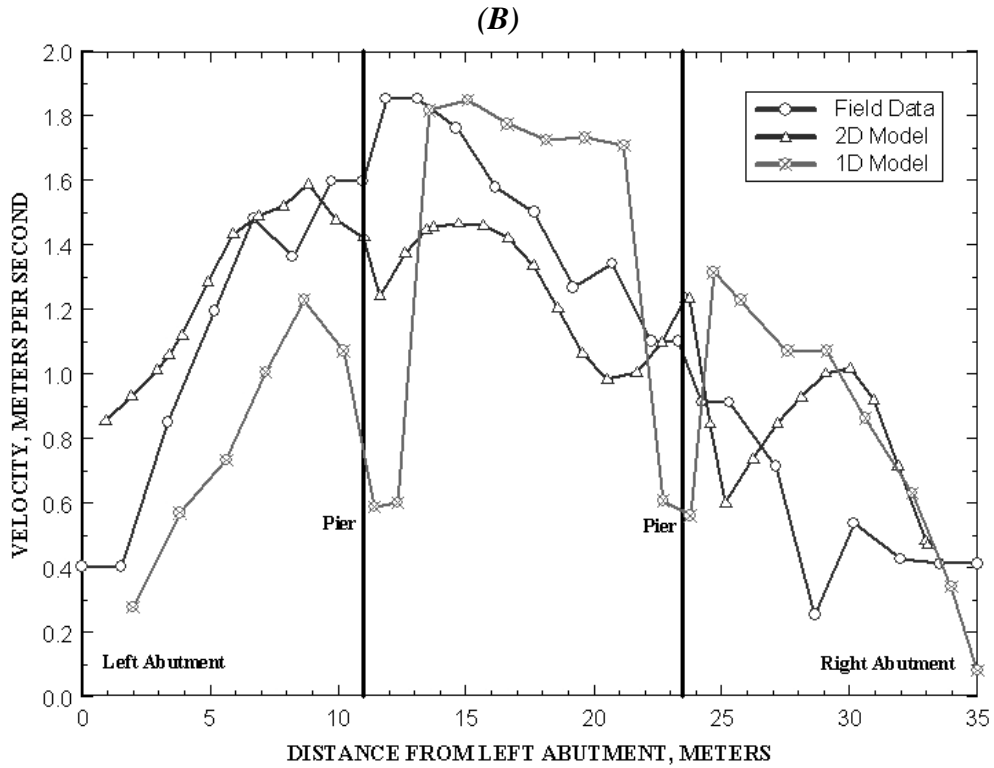
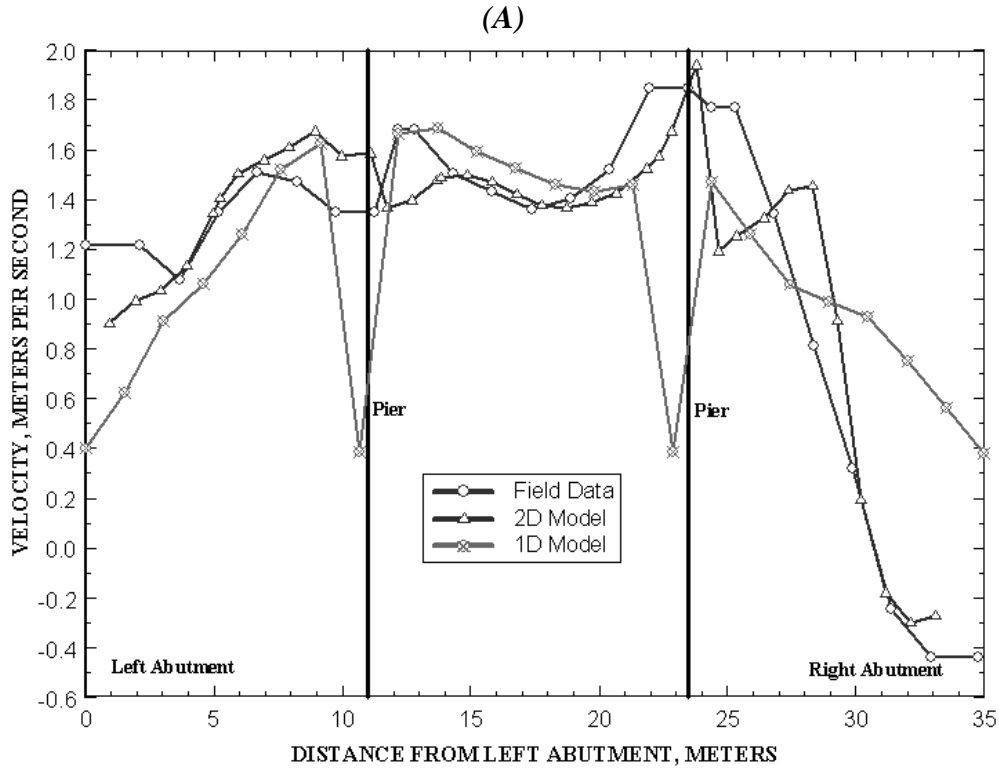


Figure 26. Comparison of the velocity distribution for the two-dimensional model, one-dimensional models and field measurements at the upstream bridge face of County Route 22 over the Pomme de Terre River on (A) 4/5/1997 and (B) 4/9/1997.

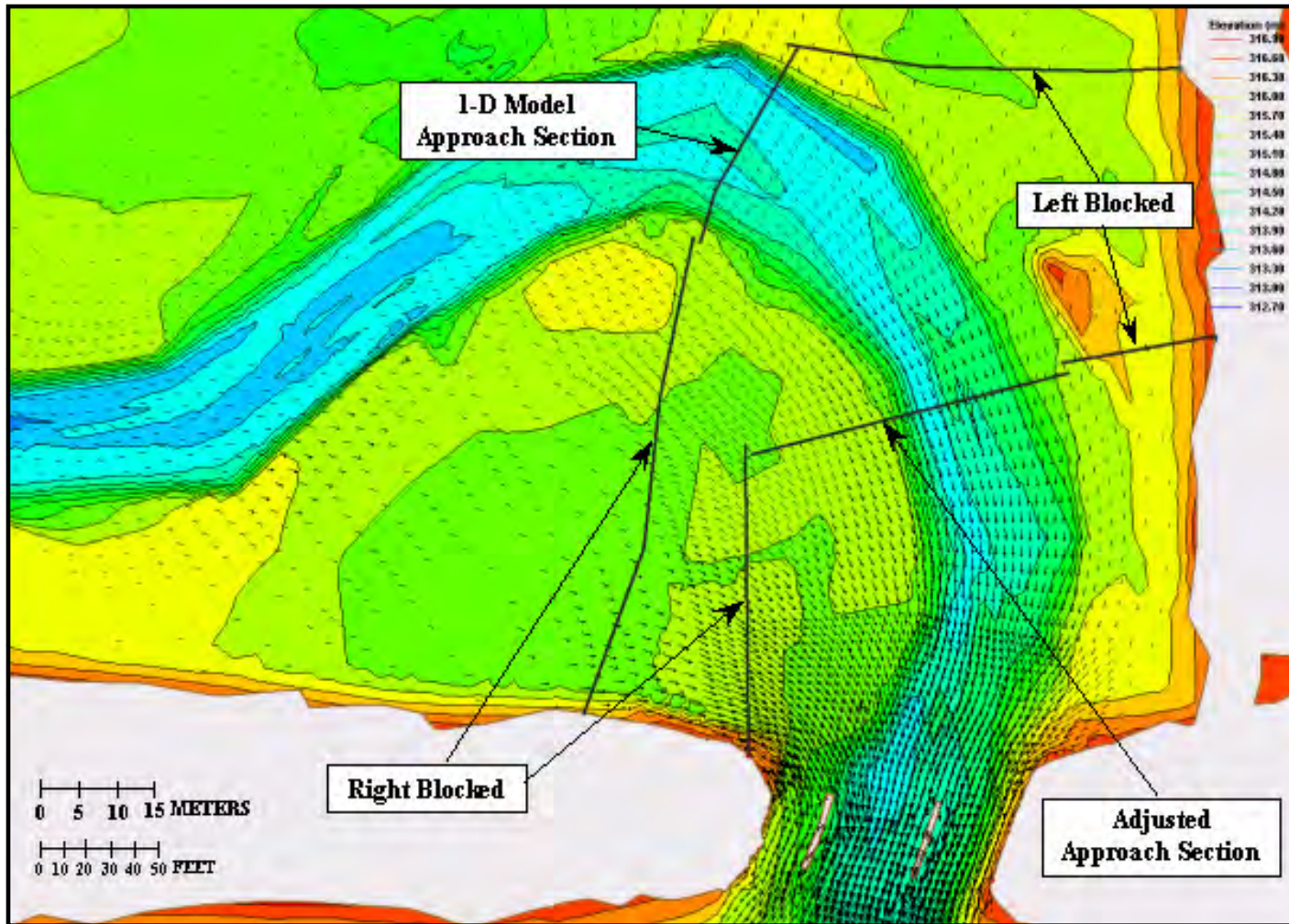


Figure 27. Comparison of the original one-dimensional and two-dimensional model approach section location with an approach section in a location more representative of the actual blocked and main channel hydraulics at County Route 22 over the Pomme de Terre River. (Velocity vectors are overlain to illustrate flow patterns through the bridge contraction for conditions on April 9, 1997).

TABLE 12. Comparison of HEC-18 scour estimates (Froehlich, HIRE, and Live-bed equations) from the one-dimensional and two-dimensional models (original and adjusted approach section locations) relative to the sediment transport model results and observed scour at County Route 22 over the Pomme de Terre River on April 9, 1997. (-- not applicable; m, meters)

Scour Type/Location	One-dimensional model results			Two-dimensional model results (original approach)			Two-dimensional model results (adjusted approach)			Sediment transport model	Observed Scour (m)
	Froehlich (m)	HIRE (m)	Live- Bed (m)	Froehlich (m)	HIRE (m)	Live- Bed (m)	Froehlich (m)	HIRE (m)	Live- Bed (m)	Sed2D Results (m)	
Left Abutment	0.95	--	--	6.8	--	--	2.9	--	--	5.5	0.61
Right Abutment	3.3	4.1	--	7.2	4.5	--	9.1	4.5	--	4.5	3.0
Contraction	--	--	0.40	--	--	8.7	--	--	2.5	0.94	0

processes that are present in the field. Field hydraulic measurements and two-dimensional models are more representative of the processes that induce scour than one-dimensional models; however, the scour depths at the selected field sites were more accurately estimated when using HEC-18 equations and the output from the one-dimensional models, which simulate hydraulic conditions similar to those of laboratory experiments.

ERODIBILITY AND GEOTECHNICAL PROPERTIES OF MATERIALS

Several factors contributed to the resistance to erosion and slope failure that was observed in the soils and sediments examined in this study. Unlike coarse-grained soils for which erodibility is primarily a function of grain-size distribution and secondarily a function of grain shape and packing, erodibility of fine-grained soil is dominated by other factors such as apparent or true cohesion, porewater pressure, and root reinforcement. True cohesion may occur because of cementation and (or) attractive forces developed in soils rich in very fine particles of clay minerals. Apparent cohesion is caused by development of negative pore-water pressure changes in all soils but is most important in fine-grained clay and silt soils. Roots provide reinforcing effects and growth of vegetation lowers pore-water pressures. All three of these factors affected the location and dimensions of scour holes observed in this study. These effects are not observed in laboratory flumes where cohesionless sands are tested without any vegetation present. The increases in resistance to both erosion and mass movement attributed to vegetation and soil strength appear to control many important aspects of scour. Despite the variability of fine-grained soil characteristics from site to site in floodplains (Benedict 2003), the increase in resistance of vegetated fine-grained floodplain soils over the resistance of coarse-grained

cohesionless soils has a profound affect on the initiation of scour, the development of scour holes, and the final geometry of scour holes near bridges.

Generally, at the sites examined in this study, the characteristics of sediments composing the streambed were different from those composing the upper layers of the floodplain and streambanks. An increase in soil resistance caused by vegetation and fine-grained soil effects appeared to affect the location, depth of scour and scour pattern. Most frequently, the combined effects of vegetation and fine-grained soil inhibited the initiation of scour holes on the surface of floodplains where erosion was anticipated; e.g., immediately adjacent to the sides of abutments. However, sections of floodplain adjacent to the main channel appeared to collapse into scour holes extending laterally from the main channel under resistant surface layers. Our observations indicate that scour was frequently initiated in (1) soils unprotected by vegetation under the shadow of the bridge, and along streambanks where coarse, cohesionless, and unvegetated soils could be eroded from the bank toe; or (2) at flow separation points at piers, at abutment walls, or near riprap edges.

Scour appear to be initiated at

- (1) Non-vegetated and unprotected areas in shadows under bridges;
- (2) Stream banks in the flow field of bridge abutments;
- (3) Around piers, especially those located in the high-velocity flow near bridge abutments; and
- (4) Locations where bends cause high-velocity zones in the bridge opening.

Scour propagates away from the initial erosion point by

- (1) Undermining of vegetated soils and fine-grained soils strengthened by cohesion effects;
- (2) Mass failure of scour protection because of undermining; and
- (3) Changes in flow patterns as scour holes developed.

Although main-channel sediments typically are treated as cohesionless soils, fine-grained sediments in the silt-size range or smaller were obtained from the channel bed in several of the river channels in this study (see Appendix A, Case Studies No. 1, 2, and 4). The sediments in three of the rivers examined in this study were derived from fluvial-glacial processes including reworked deposits from lakes formed by glacial moraines. Borings from some of these sites indicated the presence of silt layers beneath the streambed surface. Samples from all other sites indicated only small amounts silt- and clay-size particles on the surface of the streambed.

The effects of soil cohesion, both real and apparent, and of vegetation on soil erosion were observed at all sites examined. Scour patterns on floodplains and the shape of scour holes appear to have been affected by the increased soil strength and erosion resistance afforded by soils containing fine-grained particles and covered by vegetation. Increased resistance of soils to erosion and mass movement derived from undrained strength of dried or preconsolidated fine-grained soil (silt and clay) is termed soil cohesion here.

Examination of soils on floodplain surfaces, in scour holes, and in streambanks showed the affect of several factors that contributed to resistance to scour. Fine-grained soils such as silts and clays were observed near the surface of floodplain alluvium at all sites. Both woody and (or) herbaceous vegetation covered all floodplains.

The soils encountered at the sites visited during this research in all cases were layered, with appreciable variations in grain size and texture from layer to layer. At most of the sites, much of the soil profile consisted of layers containing fine-grained silts and clays. Also, at most sites, the fine-grained layers had been subjected to preloading from desiccation effects (soil drying) and (or) overburden pressures from pre-existing strata. Such preconsolidation effects caused those fine-grained soils to have medium to high undrained shear strengths (to be firm to very stiff). The time for pore-water pressure equilibration during shearing (during a scour episode) for these fine-grained soil layers far exceeded the time during which shear would have occurred, and in most cases would have exceeded the time during which a flood event would occur. Empirical evidence for the appreciable shear strength of the fine-grained soil layers at these sites was the exposure of nearly vertical faces in fine-grained layers whereas adjacent coarse-grained layers typically displayed gently sloping faces. In the long-term situation, drained strengths in these same layers would be much lower than the undrained strengths because of the low values of effective confining pressure at the shallow soil depths in the zone where scour typically occurred. Vegetation also contributed to the scour resistance at these sites by providing tensile reinforcement (roots) at shallow depths (0 to 1 m) and by developing soil suctions to contribute to both drained and undrained shear strengths.

The upstream edge of a scour hole formed during Hurricane Floyd at the U.S. 70 Bridge over Bear Creek in North Carolina (Appendix A, Case Study No. 6) is illustrated in Figure 28. The scour hole appeared to be initiated in the main channel and propagated across the stream and upstream. The fine-grained surface soils reinforced by the roots of woody vegetation did not appear to have been scoured; however, the toe of the bank appeared to have been scoured and the undermined soil block containing the fine-grained surface material failed (toppled) into the scour hole. The orientations and positions of trees in Figure 28 indicate the mechanism of mass failure. Complex flow patterns caused by the rapid vertical expansion of flow over the vegetated floodplain surface at the upstream end of the scour hole and into the scour hole may be responsible for erosion of the more vulnerable basal soils that typically containing higher components of coarse-grained sediments. Erosion of the basal soils at the edge of the scour hole caused mass instability of the upper layers eventually leading to their collapse and the upstream propagation of the scour hole.

The processes governing scour-hole formation are dependant on the vertical variation in soil characteristics and are not represented in laboratory experiments in which uniform and non-cohesive sediments are used to model floodplain soils. The scour processes involved in the scour of soils with non-uniform characteristics also may affect the distribution of scour including



Figure 28. Looking upstream from the east bound bridge deck of highway 70 over Bear Creek near LAGRANGE, North Carolina during low-flow.

the location and depth of the maximum point of scour and, more importantly, the scour around pier and abutment foundations. The upstream and lateral extension of the scour holes is one mechanism by which the non-uniform soil characteristics of floodplain sediments affect scour-hole formation processes; other effects of the variation of soil characteristics also probably exist.

CHAPTER 3: INTERPRETATIONS, APPRAISAL AND APPLICATION

RECOMMENDED MODIFICATIONS TO SCOUR PREDICTION METHODOLOGY

The analysis of field data collected at the 15 sites during the NCHRP 24-14 project, and 146 sites in South Carolina (Benedict, 2003) has provided further recognition of the complex nature of scour at contracted bridges and a basis to recommend modifications to the HEC-18 (Richardson and Davis, 2001) scour-prediction methodology.

Use of BSDMS in Bridge Evaluation

With the contributions of this study there are now 93 measures of scour at bridges in the BSDMS database. This database can be used by state highway agencies (and their consultants) to make comparisons between bridges being evaluated and those in the database where scour has been measured. The database should provide a basis for evaluating complex sites and how individual factors may contribute to limiting or causing scour. The case studies in Appendix A provide detailed information on methods of evaluation and observed scour. Appendix A and the BSDMS can both be used as a training tool.

Adding Abutment and Contraction Scour

Field observations of scour at many bridges indicate that conceptual separation of contraction and abutment scour as described in Hydraulic Engineering Circular-18 (HEC-18) (Richardson and Davis, 2001) is problematic because the hydrodynamic mechanisms that induce the individual scour components work together. It is clear from the field observations of this study that the scour that occurs near the ends of the abutment is the result of a complex combination of flow contraction and flow curvature.

Scour prediction methods published in HEC-18 indicate that contraction and abutment scour are separate and additive for all contracted bridge openings. HEC-18 follows a conservative approach of adding the scour components to create a scour prism for design and assessment purposes, because of an insufficient amount of field data to develop an understanding of the interaction of scour components. Therefore, to compute the total scour at an abutment, the individual components of long-term streambed change, contraction scour, and abutment scour within the abutment region must be estimated and then summed. Isolating the effect of an individual scour component is difficult because the various components interact in the development of the total depth of scour. Laboratory investigations typically have focused on understanding each scour component in isolation, necessitating the approach for estimating total scour outlined in HEC-18. Analyses of field observations, in conjunction with the theory of flow patterns in short contractions, indicate that this view of scour in the abutment region may be inappropriate.

Although the overall effects of flow contraction and the local flow curvature that occurs around abutments can be conveniently separated conceptually, the resulting scour pattern cannot be separated into contraction- and abutment-scour components. The cause of the specific scour patterns is believed to be highly sensitive to local field conditions. The field observations collected during this study are not adequate to develop a definitive classification system based on site characteristics that could indicate the expected scour pattern.

Effects of Channel Bends

Channel alignment and in particular, channel bends upstream of bridges can have an appreciable effect on the depth and distribution of scour, including the location of maximum scour. Hydraulic parameters should be adjusted to account for bend effects on flow distributions. Although the scour-prediction methodology provided in HEC-18 typically over-predicts scour depths, scour depths greater than those predicted can result where upstream channel bends centrifuge flow into floodplains and toward piers or abutments. Channel bends can present a unique, site-specific problem at bridges because approaching flow distributions at flood stage can be appreciably altered when flows leave a channel and enter a floodplain at a channel bend. When channel bends occur just upstream of a bridge, concentrated channel flows can be directed to a section of a bridge opening that would not typically experience this magnitude of flow if the channel were straight. Under these conditions, large scour holes can develop even when embankment lengths and geometric-contraction ratios are small (Benedict, 2003).

Two-dimensional models such as FESWMS-2DH can provide information on the bend effects on flow distribution; however, judgment in the adjustment of flow parameters may be required where two-dimensional models may not be cost effective. Considerations such as the relative amount of flow in the channel and floodplain, the bend radius of curvature, the position of the bend with respect to the bridge opening, and the flow velocity in the channel and floodplain are a few factors that influence the effect of bends on the flow distribution near a bridge.

Other factors such as the distribution of floodplain roughness, topographic variation, and features such as drainage ditches and flow obstructions can appreciably affect the distribution of flow approaching bridges and the depth and distribution of scour. Although one-dimensional backwater models can represent some of these effects, they are incapable of propagating these effects in the downstream direction.

In general, a detailed topographic map and aerial photography can be used to qualitatively assess the severity of flow contraction at bridge crossings as well as the location of contracted and uncontracted cross-sections. The use of these maps can provide valuable insight on site characteristics such as flow structures, geomorphic setting, floodplain topography and land cover, and upstream channel configuration; all of which greatly affect the potential for scour at a bridge site. Where the floodplain is narrow and embankments are short, potential for abutment scour is low. In contrast, when floodplains are wide and embankments are long, the potential for abutment scour is high. Although there are exceptions to these generalizations, qualitative assessments need to be taken into account during scour computations.

Location of Scour Holes

Analysis of the field data also has revealed that the location of scour in a contracted bridge opening is highly variable and does not follow the patterns typically reported from laboratory experiments. The longitudinal location of contraction and abutment scour holes can be dependent upon site specific factors such as the configuration of scour protection, guide banks, bridge length, channel alignment, and bed material. The location of scour holes observed at the 15 sites in this study and the 146 sites in the South Carolina study (Benedict, 2003) were highly variable, especially for shorter bridges (less than 91 m long). Field observations show contraction and abutment scour holes commonly are formed upstream and (or) downstream of the bridge. Although this study, Benedict (2003) and others have discussed factors that contribute to the position of scour holes, no method for predicting the location has been developed. Consequently, the present scour-prediction methods found in HEC-18 recommend that the scour hole low point be located at the bridge. Additional research and data collection is needed to determine the factors that control scour and to develop a method for predicting the location of scour holes.

Application of Contraction Scour Equations

All contraction-scour equations were shown to consistently over-predict observed scour depths; however, the clear-water scour equations grossly over-predicted field observations by 2 to 40 times the measured scour depth (Table 2). The collection and analysis of additional field data at clear-water scour sites, similar to what was collected as part of the South Carolina bridge

scour study (Benedict, 2003), may provide the information necessary to develop prediction equations that will more accurately represent field conditions and reduce the costs of over-designing bridge foundations. Clear-water scour equations should be used with the knowledge that the selection of the critical-shear stress for the bed material will substantially affect the computed depth of scour. Vegetation and soil cohesion, both of which are difficult to quantify, greatly affect the soil's ability to resist scour.

Predicting Abutment Scour

Analysis of the recommended methods for predicting abutment scour indicates that current methods are not reliable. The methods include procedures for assessing flow hydraulics using one-dimensional backwater models and abutment-scour prediction procedures recommended in HEC-18. Comparison of measured flow velocities and those computed using one-dimensional backwater programs showed that in most cases average and local velocities required for use in abutment scour equations were appreciably in error. Computed velocities near the abutment were always appreciably lower than the peak measured velocity near the upstream tip of the abutments. Despite the consistently low prediction of velocities near abutments, computed scour depths under most conditions were still high compared to measured scour depths. Under a few conditions where velocities were not measured, the scour depths computed using flow velocity from one-dimensional models were slightly lower than measured scour depths.

Comparison of abutment-scour predictions with observed scour depths showed that typically the abutment-scour equations over-predict the depth of scour, often substantially. Analysis of the cause of the inaccuracies of the predictions showed that the primary problem lies in the abutment-scour equations rather than in the model used to estimate the hydraulic parameters. Scour at contracted bridges is complex and is highly dependent upon site conditions and channel geometry (curvature and alignment). Simple equations based on simple experiments are not able to account for the complexities of typical field conditions. The current approach to predicting scour at abutments is unreliable.

Envelope curves from field observations of abutment scour can be useful tools for assessing abutment-scour depths; however, analysis of the envelope curves developed for South Carolina shows that these types of curves may be regionally specific and cannot be applied without sufficient consideration of the site conditions on which they are based.

Scour with Debris

The New Zealand debris scour prediction methodology (Dongol, 1989 and Melville and Dongol, 1992) worked well at the Chariton River site near Prairie Hill, Missouri (see Appendix A, Case Study No. 10) and may be appropriate for application at other sites. The methodology suggested by Diehl and Bryan (1997) for determining the design width of a debris accumulation based on channel characteristics also proved accurate predictions for the Chariton River site. Unfortunately, a single favorable comparison is not sufficient to prove general accuracy and

applicability of these methods. These methods should be applied with caution and substantiated with additional field observations.

GUIDELINES FOR NUMERICAL MODELING

When using HEC-RAS to predict scour at contracted bridge openings, engineers should closely inspect the model output and input parameters used for the internal scour computations especially in simulations with complex upstream channel configurations. The approach channel alignment is not accounted for in HEC-RAS calculations of abutment scour; default HEC-RAS hydraulic parameters used for abutment scour calculations can provide erroneous predictions based on incorrect projection of bridge opening to approach section. All default scour parameters in HEC-RAS should be closely inspected to assure they represent site configuration and any available field data. It also is important to note that because of the limitations of the model, it is extremely common for appreciable differences to exist between the contraction and abutment scour variables used in HEC-RAS and those measured in the field.

Multi-dimensional numerical models have the capability to provide a better representation of the complex flow conditions that exist at a contracted bridge site. Using such models requires more topographic information than one-dimensional models and hence more time to develop. The comparisons with field data showed that if the application of the abutment- and contraction-scour equations is the primary goal of the effort, a multi-dimensional model may not be worth the additional cost; however, where flow conditions are particularly complex a multi-dimensional model will likely provide insights into the flow patterns that cannot be identified with a one-dimensional model. The coupling of sediment transport with a multi-

dimensional model appears to be a better alternative to simply using the multi-dimensional model to determine the hydraulic parameters for the scour equations; therefore, the need for a multi-dimensional model is highly site specific but where applicable can provide valuable information on the expected flow and scour patterns.

ERODIBILITY AND GEOTECHNICAL PROPERTIES OF MATERIALS

The drastic overprediction of scour using HEC-18 methods on floodplains where no scour was observed at a large percentage of sites in the study of Benedict (2003) and of this study can be, at least in part, attributed to the treatment of soil-erosion resistance without the effects of fine-grained soil behavior and vegetation. On floodplains in low-gradient environments (valley slopes less than 0.5 percent) consideration should be given to increased erosion resistance afforded by vegetation and fine-grained soil properties. Unfortunately, the uncertainty in predicting erosion resistance caused by the variability in fine-grained characteristics of floodplain soils (Benedict 2003) may preclude complete reliance on apparent or true fine-grained soil cohesion; however, the combined effect of root reinforcement and fine grained soil behavior appears to be reliable, at least in humid environments. The effectiveness and reliability of vegetation in preventing scour should be developed on a regional basis such that regional climate, soils, bridge-design methods, and vegetation can be considered.

Typically vegetation is not a significant factor in the river main channel, in heavily shaded areas beneath the superstructure, or in arid climates where plant growth is unreliable. NCHRP Project 24-15 has developed techniques for predicting scour depths in cohesive soils that include temporal effects and variation in soil properties.

CHAPTER 4: CONCLUSIONS AND SUGGESTED RESEARCH

The main purpose of this research was to collect field data from which processes affecting scour magnitude in contracted openings could be identified, to support verification of physical- and numerical-model studies, and to improve guidelines for applying scour-prediction methods at contracted bridge sites. Field data collected from 15 sites in this study were added to the National Bridge Scour Database (BSDMS). These data, available through the World Wide Web, can currently (2004) be accessed by researchers and practitioners from a link on the USGS Kentucky District world wide web page (<http://ky.water.usgs.gov>) and eventually (2005) from a link on the USGS Office of Surface Water world wide web page (<http://water.usgs.gov/osw/techniques/bs/sed.bs.html>).

CONCLUSIONS

Conclusions about current HEC-18 scour-prediction methods, the use of hydraulic and sediment-transport models, and scour at piers with debris were developed through analysis of the field data. The most important finding is that the main sources of error in the abutment scour-prediction methods presented in HEC-18 (2001) are the scour prediction equations and not the hydraulic parameters typically obtained from one-dimensional models. Specific conclusions from this study are provided in the following sections.

Factors Not Included In Laboratory Models

- (1) To date (2004), laboratory research has failed to capture the complexity of typical field conditions, rendering the resulting equations unreliable for field applications. The concepts and methods for evaluating scour derived from these studies may not accurately account for scour processes in the field, because of the simplifications inherent in these studies. The inability of current (2004) scour-prediction methods to accurately predict scour at abutments is a result of the simplifying assumptions on which the research is based and the complexity of abutment scour in field conditions.
- (2) Channel alignment and, in particular, channel bends upstream of bridges can have an appreciable effect on the depth and distribution of scour, including the location of maximum scour.

Scour Components

- (3) When compared to field data, contraction- and abutment- scour equations predict scour depths greater than those observed and often this error can be 2 to 40 times the measured scour depth; however, some comparisons indicate that there are conditions under which some equations will predict scour depths less than those observed. These comparisons indicate that the current (2004) methods for predicting contraction and abutment scour at bridges are unreliable.
- (4) Field observations of scour at many bridges indicate that conceptual separation of contraction and abutment scour as described in HEC-18 (Richardson and Davis,

2001) is problematic because the hydrodynamic mechanisms that induce the individual scour components work together. Consideration should be given to an alternative provided by Benedict (2003) to the superposition procedure (addition of independently calculated contraction- and abutment-scour components) recommended in HEC-18. Benedict (2003) recommends that regions of high-flow curvature (abutment scour) and low-flow curvature (contraction scour) be separated and computation of scour made independently but not added. Development of contraction and (or) abutment scour is highly dependent upon the site and approach flow conditions.

- (5) The presence of a contracted bridge opening does not guarantee that either or both types of scour will occur. Bed-material size and gradation, cohesion, armoring potential, and road overflow are common factors that can limit or prevent contraction scour. In addition, highly site-specific factors such as channel alignment, large abutment-scour holes, obstruction in the bridge opening, embankment skew, wide floodplains in the bridge opening, and bed protection also can limit contraction scour.

Contraction Scour

- (6) Clear-water contraction scour prediction is highly sensitive to the critical conditions of the bed material; therefore, accurate representation of the bed material is essential. Bed-material samples should represent both the surface and subsurface material.

- (7) The clear-water scour equations grossly over-predicted field observations by 2 to 40 times the measured scour depth. Soil cohesion at most sites where clear-water scour was observed and the lack of a method to account for the increased soil resistance in currently (2004) accepted HEC-18 scour methods is considered to be the reason for the large range of over-prediction.
- (8) The longitudinal location of contraction scour is highly variable. The longitudinal location of contraction scour can be dependent upon factors such as the configuration of scour protection, guide banks, bridge length, channel alignment and bed material, and does not follow the patterns typically reported from laboratory experiments.
- (9) Judgment should be used in selecting the location of the approach cross-section used in the analysis of contraction scour. Site-specific characteristics such as flow structures, geomorphic setting, floodplain topography and land cover, and upstream channel configuration should be considered in the location of this analysis cross-section.

Abutment Scour

- (10) Although the length of the bridge and channel geometry are important factors that have been examined extensively in previous research and in the development of existing abutment-scour equations, there are a multitude of other parameters that must be considered when evaluating and (or) predicting scour in the abutment region including the following: cohesion of soils; geometric contraction ratio; approach flow velocity distribution including the effects of channel bends; floodplain

roughness and topographic variation; floodplain flow obstructions; valley geometry, including valley width variation and slope; roadway crossing geometry – roadway profile, embankment geometry and orientation, and bridge length; embankment protection; and duration and frequency of flood flows.

(11) Inspection of the data compiled for the NCHRP Project 24-14 sites revealed that approach and contracted flow velocity, geomorphic setting (i.e. upstream channel alignment and valley configuration), bed material cohesion and size, and geometric-contraction ratio are the factors that have the most affect on the measured abutment scour.

(12) Comparison of measured abutment scour depths and computed abutment scour depths by several of the methods (Sturm, Froehlich, modified Froehlich, and HIRE equations) provided in HEC-18 (2001) indicates that all methods can appreciably overpredict scour when used in combination with one-dimensional models for the selected hydraulic parameters. The comparisons of predicted versus observed scour in this report show that although geometry and the one-dimensional modeling approach can cause variations in the depth of predicted scour, the accuracy of the selected scour equations are currently (2004) the largest source of error in abutment scour predictions.

Numerical Models

- (13) The flow conditions and resulting scour patterns at contracted bridges are often too complex to be represented accurately by one-dimensional hydraulics and current (2004) scour equations.
- (14) Current (2004) guidelines in HEC-18 indicate that when using one-dimensional models and the HIRE equation, it is acceptable to use the conveyance tube closest to the abutment for determining the velocity and depth at the abutment. Comparison of field measurements with one-dimensional modeled flow shows that the velocity in the conveyance tube closest to the abutment is always low compared to the rest of the flow field around the abutment.
- (15) The use of the field-measured velocity as defined by HEC-18 for the HIRE equation, results in gross over-prediction of abutment-scour depths. A more representative field velocity measurement for use in the HIRE equation should be taken upstream of the abutment tip near the approach section.
- (16) Although the current (2004) amount of field data in the approach sections of the surveyed bridges were inadequate to provide a comprehensive evaluation of the ability of a one-dimensional model to represent complex two-dimensional flow fields, the comparisons that could be made showed the limitations of the one-dimensional modeling approach. Where conveyance dominates the hydrodynamics, such as for fully developed scour-hole conditions, a one-dimensional model is able to provide a reasonable estimate of the velocity distribution; however, where two and three-dimensional effects caused by flow accelerations dominate the flow field, such

as at the beginning of a flood and during the scouring process, the one-dimensional model is severely limited in its ability to accurately distribute the flow.

- (17) Default HEC-RAS hydraulic parameters used for abutment-scour calculations can provide erroneous predictions based on incorrect projection of the bridge opening to the approach section.
- (18) Despite the calibration complexities induced by geometry uncertainty and three-dimensional flow, the two-dimensional model was able to reproduce the hydraulics in the bridge opening for the conditions measured more accurately than the one-dimensional model for the early flood condition; however, for fully developed scour-hole conditions, the one-dimensional model provided a slightly better representation of the velocity distribution than did the two-dimensional model.
- (19) Using HEC-18 equations, scour computed using the hydraulics generated from a two-dimensional hydraulic model was less accurate (more conservative) than scour computed using a one-dimensional model.
- (20) Scour computed from a two-dimensional sediment transport model was found to be less accurate (more conservative) than scour computed using HEC-18 methods and hydraulics generated by a one-dimensional model.

Scour at Pier with Debris

- (21) The method for predicting scour with debris proposed by Melville and Dongol (1992) accurately predicted scour over several events and the method proposed by Deihl (1997) for estimating the width of debris rafts on piers accurately predicted the

observed width of debris accumulations on the observed pier; however this was based on data from only one site.

RECOMMENDATIONS

Although additional real-time data collection would be beneficial, the collection of large volumes of field data sufficient for developing regression or semi-empirical equations for abutment and contraction scour would be difficult and expensive. Therefore, the development of techniques for estimating scour at contracted bridges must be based on a combination of detailed field data sets and the study of these data using laboratory or multi-dimensional numerical models. A major limitation to physical models is the scale effect on the depth of scour, especially in the case of modeling cohesive soils. Numerical models should not have this same limitation, but are limited by the available sediment-transport algorithms. Regardless of the modeling approach selected, the model must be calibrated to field conditions, considering all of the complexities of channel alignment and the geometric and hydraulic configuration of the main channel, floodplain, and bridge crossing. Once these complexities are properly modeled, changes then can be made to the alignment and geometric and hydraulic conditions to study the corresponding effects on the depth of scour. It is unlikely that a simple computational equation could be developed, except for gross-envelope curves; however, it is likely that a procedure could be developed based on a series of computations or multidimensional models that would provide a more accurate estimate of scour than is currently (2004) available.

Post-flood field data collection and analysis similar to the approach used in South Carolina by Benedict (2003) also would be valuable. As shown by the research for NCHRP 24-

14, this approach is only appropriate for regional applications; however, a large data set with a broader range of conditions may provide a more detailed assessment of the limits of scour given a variety of different conditions. The result could be a simple method or family of curves that would provide the maximum observed scour for various site conditions. While this approach does not directly account for the site complexities and is only empirical in nature, where applicable, it would provide a conservative and low-cost approach for estimating scour at contracted bridges.

Additional research is needed to obtain information on flow patterns near bridges to improve numerical representation of flow conditions and to verify numerical models. Because of hazardous conditions that include debris in forested floodplains, submerged obstacles, and partially submerged superstructures, collection of approach flow velocity data from a manned boat requires very specific conditions that may not be representative of the wide spectrum of conditions where information is needed.

Specific recommendations developed from this research include the following:

- (1) Additional field observations are necessary to develop a definitive classification system based on site characteristics that could indicate the expected scour pattern. The classification system could be the basis for methods to determine the position of scour holes, especially in cases where the scour is likely to occur sufficiently far from the bridge such that it does not affect foundation stability.

- (2) No detailed real-time measurements were collected during conditions where the bridge superstructure is partially or completely submersed, because of the difficulty and hazards in measuring scour these conditions. Additional research is needed to evaluate this common condition.
- (3) Contraction scour in gravel-bed streams where sediment sorting occurs may affect the transport to the bridge opening. Limited field data is available for this common condition.
- (4) Only four sites had sufficient data to allow computation of contraction scour based on field data that includes measured upstream flow velocities. Additional research in which approach distribution of flow velocity upstream and within the bridge opening is measured is needed to improve understanding of flow contractions.
- (5) Detailed data was collected at only three sites in this study because of the difficulties and hazards of collecting data in floodplains upstream of bridges during flood events. If scour equations are to be based on hydraulic models, and meaningful improvements in flow modeling are a key component to accurate prediction of scour, then methods for collecting flow-velocity data in these difficult conditions are necessary. Additional approach flow data and research on methods for collecting flow velocity during flood events is needed.
- (6) This study indicates that distribution of the flow by conveyance used in one-dimensional models may lead to overestimating the depth of contraction scour. Methods for adjusting one-dimensional models to overcome this problem would increase the accuracy of computed scour depths.

- (7) Additional research should be conducted on the geometry of debris accumulations to extend and support the methods proposed by Diehl and Bryan (1997). Additional field data are necessary to verify the method by Melville and Dongol (1992) for predicting scour depth around debris accumulations.

MODIFICATION TO STRATEGIC RESEARCH PLAN

This research project was one of 37 projects recommended in the strategic research plan developed under NCHRP Project 24-8 (Parola et al, 1996) to improve scour-prediction methods. The findings of NCHRP 24-14 emphasize the need for information on scour related to soil cohesion, vegetation, channel alignment, addition of abutment and contraction scour, the location of scour holes, and debris effects. Studies similar to those recommended in the strategic plan that will address these issues are underway and include the following:

NCHRP Project 24-15: Abutment Scour in Cohesive Soils

NCHRP Project 24-20: Prediction of Scour at Abutments

NCHRP Project 24-24: Criteria for Selecting Numeric Hydraulic Modeling Software

NCHRP Project 24-26: Effects of Debris on Bridge Scour

Research on the effects of vegetation on scour, although recommended, was not given a high priority in the strategic plan for scour research. For low gradient systems, the combined effect of vegetation and fine-grained soil behavior may prevent the initiation of or limit scour at a

large number of bridges. The research on the effect of vegetation should be given a higher priority.

Other studies that should be considered are (see strategic research plan for details)

Total scour at bridge contractions

Post-flood evaluation of bridges (similar to Benedict, 2003)

Enhancement of one-dimensional modeling

Enhancement of two-dimensional modeling and sediment transport.

Bridges with superstructures partially or completely submersed are a common occurrence during design flood events. A project that should be added to the strategic research plan is one that includes both field and laboratory research on scour at partially and completely submersed bridges. Little is known about this common design condition.

REFERENCES

Richardson, E. V., and Davis, S. R., "Evaluating Scour at Bridges." *Hydraulic Engineering Circular No. 18 FHWA-NHI 01-001*, Federal Highway Administration, Washington, DC (2001) 378 pp.

Parola, A. C., Hagerty, D. J., Mueller, D. S., Usher, J. S., Parker, G., and Melville, B. W. "NCHRP Project 24-14 Scour at Bridge Foundations: Research Needs" *Transportation Research Board*, National Research Council, Washington D.C. (1996).

Melville, B.W. and Coleman, S.E., Bridge Scour. *Water Resources Publications*, LLC, Highlands, Colorado, (2000) 550 pp.

Laursen, E.M., "An analysis of relief bridge scour." *Journal of the Hydraulic Division*, American Society of Civil Engineering, Vol. 92, No. HY3 (1963) pp. 93-118.

Dongol, D.M.S., "Local scour at bridge abutments." University of Auckland, New Zealand, School of Engineering Report, No. 544 (1993) 410 pp.

Benedict, S.T., "Clear-water abutment and contraction scour in the Coastal Plain and Piedmont provinces of South Carolina, 1996-99." *Water-Resources Investigations Report 03-4064*, U.S. Geological Survey, Columbia, South Carolina (2003) 137 pp.

Straub, L.G., "Missouri River report: U.S. Department of the Army to 73rd United States Congress, 2nd Session." *House Document 238*, Appendix XV (1935) 1156 pp.

Matthai, H. F., "Measurement of peak discharge at width contractions by indirect methods." *Techniques of Water-Resources Investigations Book 3, Chapter A4*, U.S. Geological Survey (1968).

Schneider, V. R., Board, J. W., Colson, B. E., Lee, F. N., and Druffel, L., "Computation of backwater and discharge at width constrictions of heavily vegetated flood plains." *Water Resources Investigations Report 76-129*, U.S. Geological Survey (1977).

Shearman, J. O., Kirby, W. H., Schneider, V. R., and Flippo, H. N., "Bridge waterways analysis model." *Research Report FHWA-RD-86-108*, Federal Highway Administration, Washington DC (1986).

Griffith, W. M., "A theory of silt transportation." *Transactions of the American Society of Civil Engineers*, Vo. 104 (1939) pp. 1733-1786.

Neill, C. R., "Guide to bridge hydraulics." *Roads and Transportation Association of Canada*, ed., University of Toronto Press, Toronto (1973) 191 pp.

Laursen, E. M., "Scour at bridge crossings." *Transactions of the American Society of Civil Engineers*, Vol. 127, Pt. 1 (1962) pp. 166-209.

Komura, S., "Equilibrium depth of scour in long constrictions." *Journal of the Hydraulics Division*, Vol. 92, No. HY5 (1966) pp. 17-37.

Culbertson, D. M., Young, L. E., and Brice, J. C., "Scour and fill in alluvial channels." *Open-File Report*, U.S. Geological Survey (1967).

Mueller, D.S. and Wagner, C.R., "Field observations and evaluations of streambed scour at bridges." *Research Report FHWA-RD-01-041*, Federal Highway Administration, Washington, DC (November 2002) 117pp.

Richardson, E.V., and Richardson, J.R., "Practical method for calculating contraction scour." *Hydraulic Engineering '94*, American Society of Civil Engineers, Buffalo, New York (1994) pp. 6-10.

Strickler, A., "Beitrage zur Frage der Geschwindigkeitsformel und der Rauigkeitszahlen fur Strome, Kanale und Geschlossene Leitungen." *Mitteilungen des Eidgenossischer Amtes fur Wasserwirtschaft* (1923).

Richardson, E. V., Simons, D. B., and Julien, P. Y., "Highways in the river environment." *Publication FHWA-HI-90-016*, Federal Highway Administration, Washington, D.C (1990).

Shearman, J.O., User's manual for WSPRO—a computer model for water surface profile computations. *Publication FHWA-IP-89-027*, Federal Highway Administration, Washington, DC (1990) 187 pp.

U.S. Army Corps of Engineers, HEC-RAS river analysis system user's manual, version 3.0. *Report No. CPD-68*, Hydrologic Engineering Center, Davis, CA (2001) 320 pp.

Melville, B. W., "Bridge abutment scour in compound channels." *Journal of Hydraulic Engineering*, American Society of Civil Engineers, Vol. 121, No. 12 (1995) pp. 863-868.

Sturm, T. W., and Janjua, S., "Clear-water scour around abutments in floodplains." *Journal of Hydraulic Engineering*, Vol. 120, No. 8 (1994) pp. 956-972.

Melville, B. W., "Local scour at bridge abutments." *Journal of Hydraulic Engineering*, Vol. 118, No. 4 (1992) pp. 615-631.

Chang, F. F. M., "A statistical summary of the cause and cost of bridge failures." *Publication FHWA-RD-75-87*, Federal Highway Administration, Washington, D.C. (1973).

Dongol, D. M., "Effect of debris rafting on local scour at bridge piers." *Report No. 473*, University of Auckland School of Engineering, Auckland, New Zealand (1989).

Diehl, T., and Bryan, B. A., "Supply of large woody debris in a stream." *ASCE National Hydraulics Conference*, San Francisco, CA (1997) pp.1061-1066.

Melville, B. W., and Dongol, D. M., "Bridge pier scour with debris accumulation." *Journal of Hydraulic Engineering*, Vol. 118, No. 9 (1992) pp. 1306-1310.

APPENDIX A - CASE STUDY REPORT #1

Pomme de Terre River at County Route 22 near Fairfield, Minnesota

SITE OVERVIEW

Swift County Road 22 over the Pomme De Terre River is a three-span structure supported by round concrete-pile bents. The site is located in a rural / agricultural area and is 18 miles upstream of the US Geological Survey (USGS) Appleton streamflow-gaging station (05294000). During the upper Midwestern flooding in April 1997, the USGS visited this site three times (an additional site visit was made during low-flow on July 15, 1997) and collected real-time bridge-scour data. The cross-sections collected at the bridge face during each site visit show a progression of scour at the right abutment. During all three visits the floodplain flow was concentrated in the right floodplain. This concentration of flow in the right floodplain is likely caused by the sinuous channel alignment upstream of the bridge. The field crew searched for but could not define a location of flow reattachment along the right embankment. Flow was towards the main channel along the entire length of the embankment. The flow separated from the right embankment, nearly perpendicular to the main channel flow, and joined the main flow just left of the right-most pier. During the April 5, 1997 visit the flow from the right floodplain was so strong that a standing wave formed upstream of the bridge where the floodplain and main channel flow began mixing. The area from the rightmost pier to the right abutment was primarily slack and reverse flow. A scour hole beneath the abutment progressively deepened from 14.8 ft on April 4, 1997 to 19.5 feet on April 9, 1997. On April 9, 1997, a portion of the right embankment slumped, forcing the Swift Country officials to temporarily close the bridge until riprap was placed to protect the bridge. In July 1997 it was observed that riprap was used to fill scour at the right wingwall. A summary of the general site information is found in Table 1.

Cross-section data were collected using a chart-recording echo sounder with the transducer mounted on a kneeboard. The charts were digitized and scaled. Velocities were measured using standard discharge-measurement procedures and a Price AA cup meter. A step-backwater hydraulic model was developed and calibrated to field measurements at the CR 22 site and used to predict the amount of abutment and contraction scour using the techniques and equations from HEC-18.

Table 1. Site information

Site Characteristic	Description
County	Swift
Nearest City	Fairfield
State	Minnesota
Latitude	45°23'04''
Longitude	95°56'46''
Route Number	22
Route Class	County
Stream Name	Pomme De Terre River

Hydrologic Conditions

Record snowfall and snowpack-moisture content, combined with excessive soil moisture conditions in much of North Dakota, South Dakota, and Minnesota led to severe flooding during April 1997. During the winter of 1996-97, precipitation amounts in nearly all of the west-central portions of Minnesota were equal to or in the excess of the 90th percentile based on the 30-year period 1961-1990. Record or near-record amounts of snowfall occurred in most of the western portions of Minnesota during this period. Snowfall totals were particularly high in the upper Minnesota River valley. Warm temperatures in late March initiated snowmelt, producing record flooding; however, a late-spring storm and falling temperatures added more than 2 inches of precipitation in the form of rain and up to 23.5 inches of snow in some areas. Discharge exceeded the 200-year flood on the Pomme de Terre River near Appleton, Minn., and the 100-year flood on the Minnesota River at Montevideo, Minn.

Discharge measurements were made at the site during two of the three site visits. The total discharge at the C.R. 22 bridge increased from 4,570 cubic feet per second (ft³/s) on 4/5/97 to 5,150 ft³/s on 4/9/97.

DISCUSSION OF CONTRACTED SITE

The Pomme de Terre River has a high level of meander near the CR 22 bridge, which added complexity to the scour analysis. All of the floodplain flow contracted through the bridge opening from the right floodplain. A depiction of the hydraulics through the bridge opening during the April 1997 flood is shown in Figure 1.

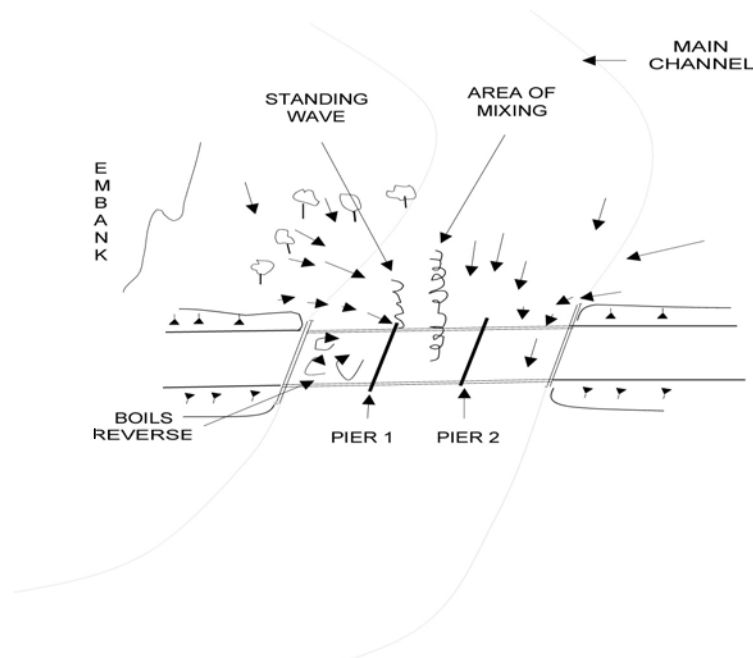


Figure 1. Sketch of the Pomme de Terre River at County Route 22 site hydraulics during the April 1997 flood.

Bridge Data

The bridge is a new structure with wide shoulders and concrete guardrails. The bridge is angled about 15 degrees to the low-flow channel. All cross-sections collected during the flood were collected approximately parallel to the bridge deck. The bridge has two piers in the main channel with the abutments set at the edge of the main channel. The spill-through abutments were protected by riprap and formed the banks of the main channel. The bridge characteristics pertinent to scour are summarized in Table 2.

Table 2. *Bridge data*

Bridge Characteristic	Description
Structure Number	76518
Length (ft)	120.8
Width (ft)	39.3
Spans	3
Vertical Configuration	Sloping
Low Chord Elev (ft)	1041.21
Upper Chord Elev (ft)	1041.57
Overtopping Elev (ft)	1043
Skew (degrees)	15
Guide Banks	None
Waterway Classification	Main
Year Built	1992
Avg. Daily Traffic	222
Plans on File	Yes
Parallel Bridges	No
Continuous Abutments	No

Geomorphic Setting

The bridge is located in a sinuous reach of the river with two large meanders immediately upstream and downstream of the bridge. The floodplains are comprised of farmland and densely populated forests with little topographic relief. During the three site visits in April 1997, the floodplain flow was concentrated in the right floodplain and contributed to the channel alignment upstream of the bridge. No defined point of reattachment along the right embankment was found during the flood; therefore, flow was toward the main channel along the entire length of the right embankment. Data characterizing the geomorphic setting is summarized in Table 3. A topographic map of the site is shown in Figure 2.

Table 3. Geomorphic data

Geomorphic Characteristic	Description
Drainage Area	836
Slope in Vicinity (ft/ft)	.0006
Flow Impact	Straight
Channel Evolution	Pre-modified
Armoring	Unknown
Debris Frequency	Unknown
Debris Effect	Unknown
Stream Size	Small
Flow Habit	Perennial
Bed Material	Sand
Valley Setting	Low relief
Floodplain Width	Wide
Natural Levees	Unknown
Apparent Incision	None
Channel Boundary	Alluvial
Banks Tree Cover	Medium
Sinuosity	Meandering
Braiding	None
Anabranching	Locally
Bars	Irregular
Stream Width Variability	Random

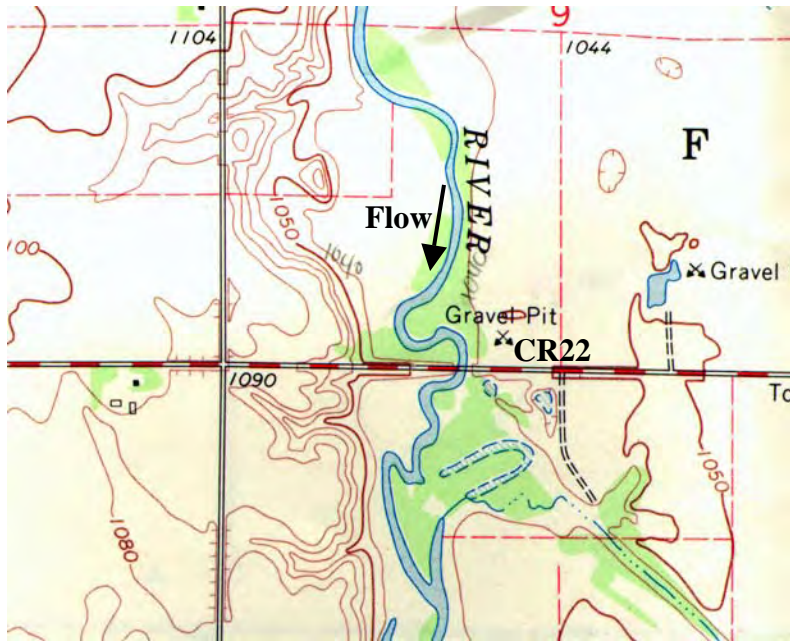


Figure 2. US Geological Survey 7.5-degree topographic map of the County Route 22 bridge-scour site.

Bed Material Data

The boring logs of the site generally indicate the bed material to be sand with some loam layers with fine gravel in the sub-bottom. Bed material samples at the site were collected from the upstream bridge face on 10/28/2001 with a USGS BM-54 grab sampler. The sampled material was a silty/sand with a $D_{50} = 0.15$ millimeters (mm). The grain size distribution of the bed material is shown in Figure 3.

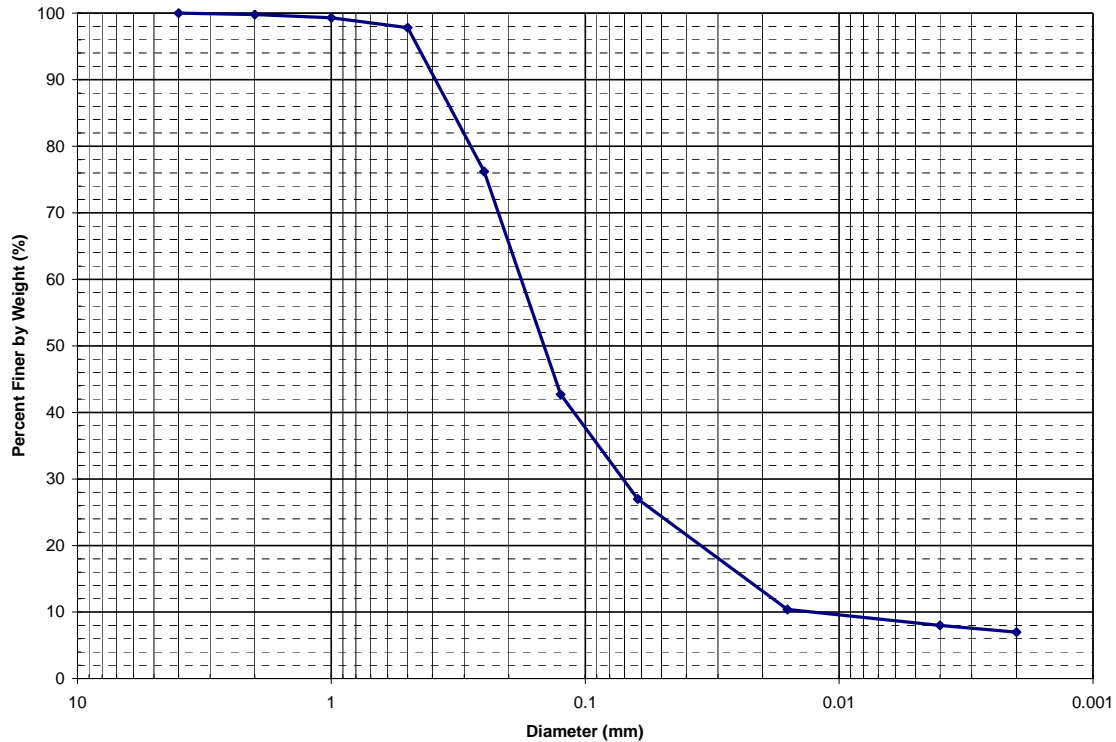


Figure 3. Grain size distribution for County Route 22 bed-material samples

Roughness Coefficients

A complete distribution of Manning's n values is provided in Table 4.

Table 4. Manning's n values upstream and downstream of the County Route 22 bridge. (fldpln, floodplain; chnl, channel; rt, right)

Upstream				Downstream			
Flow Type	Left Fldpln	Main Chnl	Rt Fldpln	Flow Type	Left Fldpln	Main Chnl	Rt Fldpln
High	0.12	0.035	0.13	High	0.09	0.035	0.09
Typical	0.10	0.030	0.12	Typical	0.08	0.030	0.08
Low	0.08	0.030	0.08	Low	0.07	0.030	0.07

Abutment Details

The bridge has spill-through abutments set at the edge of the main channel. The abutments were protected by riprap and formed the banks of the main channel. The abutment characteristics are summarized in Table 5.

Table 5. Abutment data

Abutment Characteristic	Description
Left Station	584
Right Station	705
Left Skew (degrees)	15
Right Skew (degrees)	15
Left Abutment Length (ft)	64
Right Abutment Length (ft)	64
Left Abutment to Channel Bank (ft)	0
Right Abutment to Channel Bank (ft)	0
Left Abutment Protection	Riprap
Right Abutment Protection	Riprap
Contracted Opening Type	III *
Embankment Skew (degrees)	-15
Embankment Slope (ft/ft)	2
Abutment Slope (ft/ft)	2
Wingwalls	Yes
Wingwall Angle (degrees)	90

* - Type III opening has sloping abutments and sloping spillthrough abutments.

Pier Details

The piers are pile bents consisting of five, 16-inch diameter concrete piles spaced 9-ft apart in a single line. Pier 1 is on the left and Pier 2 is on the right when looking downstream. The upstream and downstream piles are battered at 2 on 12. The pier characteristics are summarized in Table 6.

Table 6. Pier data. (--, not available)

Pier ID	Bridge Station (ft)	Alignment	Highway Station	Pier Type	# of Piles	Pile Spacing (ft)
1	666	15		Group	5	9
2	624	15		Group	5	9

Pier ID	Pier Width (ft)	Pier Shape	Shape Factor	Length (ft)	Protection	Foundation
1	1.33	Round	--	--	Unknown	Unknown
2	1.33	Round	--	--	Unknown	Unknown

Pier ID	Top Elevation (ft)	Bottom Elevation (ft)	Foot or Pile Cap Width (ft)	Cap Shape	Pile Tip Elevation (ft)
1	--	--	--	Unknown	--
2	--	--	--	Unknown	--

Surveyed Elevations

Water-surface elevations were measured from the bridge deck. The elevation of the bridge deck was determined from the bridge plans. All measurements were made between the leftmost pier and the left abutment. The datum for all measurements was mean sea level (MSL). A summary of the measured water-surface elevations is presented in the Table 7.

Table 7. Water-surface elevations measured from the County Route 22 bridge deck.

Date	Time	Upstream (ft)	Downstream (ft)
4/4/1997	----	1040.13	1039.85
4/5/1997	14:30	1040.57	1040.27
4/9/1997	18:00	1041.20	---
7/15/1997	14:10	1032.75	---

A local right-hand coordinate system was established with the positive y-axis in the upstream direction and the x-axis parallel to the upstream face of the bridge. This resulted in x-coordinates increasing from right to left. Since step-backwater models typically use left to right coordinates, stationing was added, which increases from left to right. The stationing on the two sections 500-ft upstream was adjusted so that the main channel aligned with the main channel at the bridge.

PHOTOS



Figure 4. Looking upstream from County Route 22 bridge deck during low flow.



Figure 5. Looking downstream from County Route 22 bridge deck during low flow.



Figure 6. Looking at scoured area on right upstream bank of County Route 22, during low flow.

MEASURED SCOUR

All bathymetry data were collected by floating an echo sounder attached to a knee-board across the river while being controlled by a hand line from the bridge. The board was allowed to float downstream and streambed elevations were collected as far as 100 ft downstream from the bridge. Data collected upstream of the bridge was restricted to the upstream edge of the bridge deck and the area around the upstream end of the right wing wall. Data could not be collected in the floodplains because of heavy vegetation.

Additional bathymetry data were collected 70-ft upstream and 100-ft downstream from the bridge after the flood during a low-water site visit on July 15, 1997. The development of the scour hole adjacent to the right abutment at the upstream bridge face from April 5, 1997 to April 9, 1997 is depicted in Figure 7.

Abutment Scour

The rightmost pier may have had some effect on the depth of scour at the right abutment, yet it is difficult to determine the effect of the pier on the depth of local abutment scour. The effect of the abutment is believed to be the dominant scouring factor; therefore, all scour is credited to the abutment with none reported for the pier. The observed velocity in the area of the right abutment dropped considerably as the scour-hole depth increased. The velocity at the left abutment held steady through the data-collection period, as did the depth and shape of the scour hole. All abutment-scour measurements were collected from the upstream edge of the bridge.

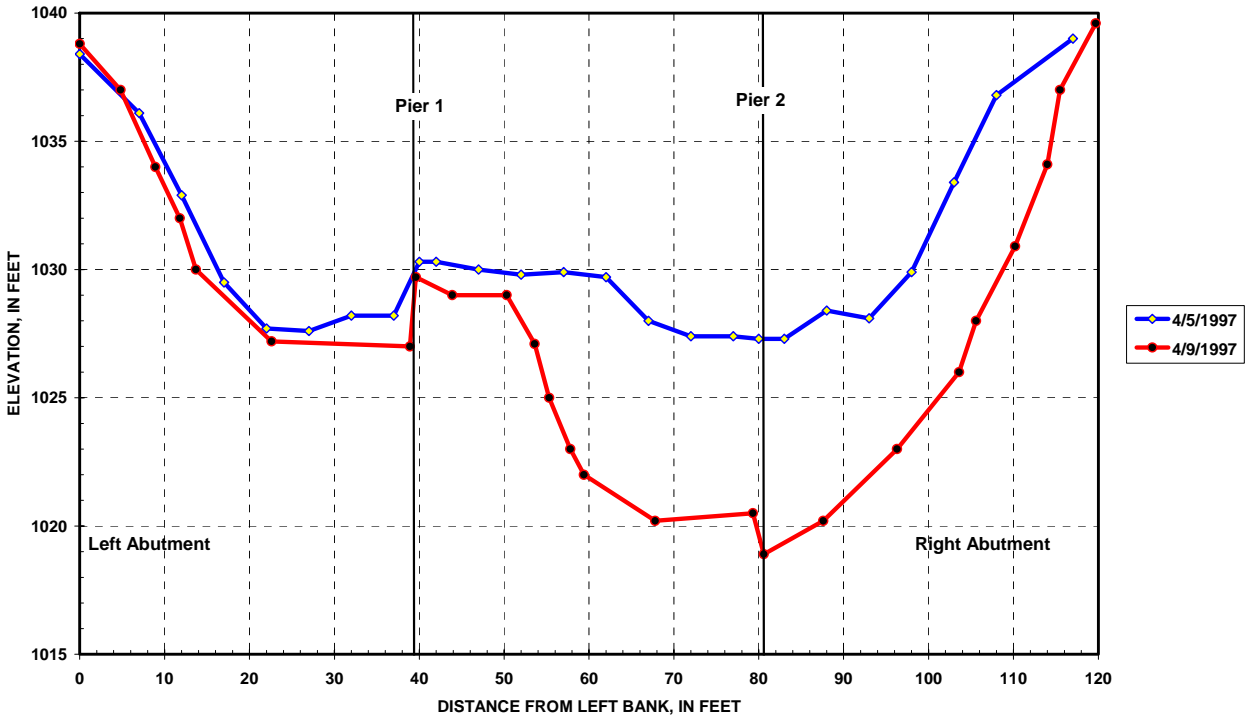


Figure 7. Cross-section data collected from the County Route 22 upstream bridge face during the April 1997 flood.

The reference surface used to determine the depth of abutment scour was the concurrent ambient bed. The concurrent ambient bed or reference surface is defined as the projected bed level around the abutment scour hole at the time of measurement; therefore, the depth of abutment scour reported is the additional local scour below the depth of contraction scour. Based on the cross sections from the bridge plans there appeared to be little contraction scour.

Elevation of reference surfaces used:

4-4-97 – 1030 ft

4-5-97 – 1029 ft

4-9-97 – 1029 ft

The velocity reported for “at the abutment” is the maximum velocity observed in the area of the scour hole. Note that the velocity dropped considerably at the right abutment as the scour hole depth increased causing an increase in the flow area. The velocity at the left abutment held steady as did the depth and shape of the scour hole. The site characteristics pertinent to abutment scour are summarized in Table 8.

Table 8. Abutment scour data (--, not available; ft/s, feet per second; cfs, cubic feet per second; Abut, abutment; Avg, average; US, upstream; DS, downstream)

Measurement Number	Abutment	Date	Time	US/DS	Scour Depth (ft)	Accuracy (ft)
1	Right	4/4/1997		Upstream	3.9	1
2	Right	4/5/1997		Upstream	4.1	1
3	Right	4/9/1997		Upstream	10.0	1.5
4	Left	4/4/1997		Upstream	3.0	1
5	Left	4/5/1997		Upstream	2.8	1
6	Left	4/9/1997		Upstream	2.0	1

Measurement Number	Sediment Transport	Velocity at Abut (ft/s)	Depth at Abut (ft)	Discharge Blocked (cfs)	Avg Velocity Blocked (ft/s)	Avg Depth Blocked (ft)
1	Live-bed	--	13.9	--	--	--
2	Live-bed	8.3	15.6	--	--	--
3	Live-bed	3.3	21.1	--	--	--
4	Live-bed	--	13	--	--	--
5	Live-bed	5.0	14.3	--	--	--
6	Live-bed	5.1	14	--	--	--

Measurement Number	Embankment Length (ft)	Bed Material Cohesion	D50 (mm)	Sigma	Debris Effect
1	516	None	0.15	--	Unknown
2	532	None	0.15	--	Unknown
3	546	None	0.15	--	Unknown
4	143	None	0.15	--	Unknown
5	154	None	0.15	--	Unknown
6	165	None	0.15	--	Unknown

Contraction Scour

No hydraulic measurements were made on 4/4/97; however, from the channel-geometry measurements no contraction scour was observed. From the data collected on 4/5/97 and 4/9/97, contraction scour was computed as the difference in average bed elevation between uncontracted and contracted sections, adjusted for bed slope.

Based on the elevation of the main channel between the abutment-scour holes there appears to be only 1 ft or less of contraction scour; therefore, a value of zero contraction scour is reported. No measurements in the uncontracted sections could be made; however, comparisons of the center of the contracted section with the cross section on the bridge plans collected in 1991 showed no change in elevation except in the areas affected by local scour. Thus, a zero contraction scour was reported.

The average depth and velocity of the contracted section were computed from the discharge measurements. The average depth included the abutment-scour holes. The site characteristics pertinent to contraction scour are summarized in Table 9.

Table 9. Contraction scour data (--, not available; ft/s, feet per second; cfs, cubic feet per second; US, upstream; DS, downstream; Avg, average)

Measurement Number	Contracted Date	Contracted Time	Uncontracted Date	Uncontracted Time	US/DS	Scour Depth (ft)
1	4/4/1997	--	--	--	--	0
2	4/5/1997	--	--	--	--	0
3	4/9/1997	--	--	--	--	0

Measurement Number	Accuracy (ft)	Contracted Avg Vel (ft/s)	Contracted Discharge (cfs)	Contracted Depth (ft)	Contracted Width (ft)
1	1	--	--	--	--
2	1	4.23	4570	10.1	107
3	1	3.79	5150	12.5	109

Measurement Number	Uncontracted Avg Vel (ft/s)	Uncontracted Discharge (cfs)	Uncontracted Depth (ft)	Uncontracted Width (ft)	Channel Contraction Ratio
1	---	---	---	---	---
2	---	---	---	---	---
3	---	---	---	---	---

Measurement Number	Pier Contraction Ratio	Scour Location	Eccentricity	Sediment Transport	Bed Form	Debris Effect
1	---	Main Channel	---	Live-Bed	Unknown	Unknown
2	---	Main Channel	---	Live-Bed	Unknown	Unknown
3	---	Main Channel	---	Live-Bed	Unknown	Unknown

Measurement Number	D95 (mm)	D84 (mm)	D50 (mm)	D16(m)	Sigma	Bed Material Cohesion
1	0.46	0.35	0.15	0.03	---	Non-cohesive
2	0.46	0.35	0.15	0.03	---	Non-cohesive
3	0.46	0.35	0.15	0.03	---	Non-cohesive

COMPUTED SCOUR

A calibrated HEC-RAS model of the site was developed to assess how accurately the scour for this flood could have been predicted. The original geometry of the bridge section was taken from the bridge plans and input into the calibrated HEC-RAS model. The approach and exit cross-sections were modified to be consistent with the streambed elevations from the bridge plans. The discharges from both April 5, 1997 and April 9, 1997 were then modeled with the original bathymetry to determine the hydraulic parameters needed for scour components. The analysis did not include data collected on April 4, 1997, because no hydraulic measurements were made on that date.

Abutment Scour

Abutment scour was computed in HEC-RAS by both the Froehlich equation and the HIRE equation. The data contained in Table 10 show that the Froehlich equation did a good job predicting abutment scour, when compared to the fully developed scour holes on April 9, 1997. The Froehlich equation correctly over-predicted the depth of scour when compared to the scour holes measured on April 5, 1997, which had not fully developed, because the equations predict maximum depth of scour. The HIRE equation overpredicted scour for all situations.

Table 10. Comparison of observed to computed abutment scour at County Route 22 over the Pomme de Terre River in Minnesota. (ft, feet)

Date	Abutment	Location	Equipment	Local Scour Depth		
				Observed (ft)	Froehlich Equation (ft)	HIRE Equation (ft)
4/5/97	Right	Upstream	Echo sounder	3.9	9.5	12.5
4/5/97	Left	Upstream	Echo sounder	2.6	2.3	9.2
4/9/97	Right	Upstream	Echo sounder	9.8	10.8	13.5
4/9/97	Left	Upstream	Echo sounder	2.0	3.0	10.2

Contraction Scour

The contraction scour was computed in HEC-RAS by allowing the model to use the default equation (live-bed or clear-water) depending upon the hydraulic conditions computed by the model. The model correctly predicted little or no contraction scour for the prescribed discharges.

REFERENCES

The data and subsequent analysis of the CR 22 site has been summarized in the following publications:

Mueller, D.S., and Hitchcock, H.A., 1998, Scour measurements at contracted highway crossings in Minnesota, 1997: Memphis, Tenn., ASCE, Water Resources Engineering '98, p. 210-215.

Mueller, D.S. and Wagner, C.R., "Field observations and evaluations of streambed scour at bridges." *Research Report FHWA-RD-01-041*, Federal Highway Administration, Washington, DC (November 2002) 117pp.

Wagner, C.R. and Mueller, D.S., 2002, Analysis of contraction and abutment scour at two sites in Minnesota, *in* International Conference on the Scour of Foundations, 1st, College Station, Tex., 2002, Proceedings: College Station, Tex., International Conference on the Scour of Foundations.

Any questions regarding the CR 22 bridge over the Pomme De Terre River should be directed to the following points of contact:

1. David Mueller, U.S. Geological Survey
9818 Bluegrass Parkway
Louisville, KY 40299
Phone: (502) 493-1935
e-mail: dmueller@usgs.gov

2. Chad Wagner, U.S. Geological Survey
3916 Sunset Ridge Road
Raleigh, NC 27607
(919) 571-4021
e-mail: cwagner@usgs.gov

SUPPORTING DATA

The following is a listing of supporting files that are associated with the CR 22 bridge:

PDT22-brgpln-profile.jpg - profile plot from bridge plan, includes bed material information.

Planview.wmf - is a file showing the bridge with a sketch of the channel and the locations of the cross sections. Note the location of the cross sections from the bridge plans located 500 ft upstream and downstream are approximate.

PDT22-pier-details.jpg - scan of bridge plan pier details

PDT22-topo.jpg

PDT22-brgpln-profile.jpg

Photos taken on 7-15-97:

PDT22-ds-bridge.jpg - photo along downstream edge of bridge

PDT22-ds-channel.jpg - photo of main channel downstream

PDT22-ds-lbnk.jpg - photo of left bank downstream from bridge

PDT22-ds-rbnk.jpg - photo of right bank downstream from bridge

PDT22-us-bridge.jpg - photo along upstream edge of bridge

Photos taken on 10/29/01

HWY220001.jpeg – Looking downstream at right bend from left upstream fldpln

HWY220002.jpeg – same as 0001

HWY220003.jpeg – Left upstream fldpln near bend closest to bridge

HWY220004.jpeg – Looking upstream at left fldpln, upstream of bridge, OP#2

HWY220005.jpeg – same as 0004

HWY220006.jpeg – same as 0004

HWY220007.jpeg – Looking at upstream right fldpln from roadway, OP#3

HWY220008.jpeg – same as 0007, looking at US x-secs 9 and 10.

HWY220009.jpeg – Looking downstream at right fldpln, OP#4
HWY220010.jpeg – Looking downstream from roadway, OP#4
HWY220011.jpeg – same as 0010
HWY220012.jpeg – USGS employee collecting bathymetry data with scour board
HWY220013.jpeg – Scour board collecting bathymetry data
HWY220014.jpeg – same as 0012
HWY220015.jpeg – Looking downstream from bridge deck
HWY220016.jpeg – same as 0015
HWY220017.jpeg – same as 0015
HWY220018.jpeg – Looking upstream from bridge deck
HWY220019.jpeg – Upstream bridge face and area of scour along right bank
HWY220020.jpeg – Looking upstream at channel and left overbank from deck
HWY220021.jpeg – Looking at right abutment from US left bank
HWY220022.jpeg – Looking at bridge from US left bank, in bend
HWY220023.jpeg – Looking upstream at upstream bend from left bank
HWY220024.jpeg – same as 0021
HWY220025.jpeg – Looking at DS right bank from left abutment
HWY220027.jpeg – same as 0025
HWY220028.jpeg – Looking DS from left abutment
HWY220029.jpeg – Looking US at right bank from left abutment
HWY220030.jpeg – Looking US from left abutment
HWY220031.jpeg – Upstream left floodplain, gravel pits
HWY220032.jpeg – same as 0031
HWY220033.jpeg – Downstream left floodplain
HWY220034.jpeg – Looking westward at upstream bridge face from roadway
HWY220035.jpeg – Upstream left overbank
HWY220036.jpeg – Looking eastward at upstream right overbank from roadway
HWY220037.jpeg – Looking westward at bridge from roadway
HWY220038.jpeg – Upstream bridge face / the source of 3 days of pleasant odors
HWY220039.jpeg – Upstream right overbank from bridge deck

CR22PDT.doc - MS Word summary of site, bridge and scour data

CR22PDT.xls - contains the following worksheets

cross sections are label by location upstream (us) or downstream (ds)

distance from bridge

date or source (bp is bridge plans)

See appropriate worksheet

us500_bp

us70_7-15

us50_7-15

us50_7-15(2)

usfv_bp

us0_4-4

us0_4-5
us0_4-9
us0Q_4-5
us0Q_4-9
us0Q_7-15
lsrtww_4-9 - longitudinal section along the right wing wall
lsp1p2_7-15 - longitudinal section between piers 1 and 2
ds0_4-4
ds0_4-5
ds0_7-15
dsfv_bp
ds10_4-9
ds15_4-5
ds20_4-9
ds25_4-4
ds40_4-5
ds50_4-4
ds50_4-9
ds50_7-15
ds80_4-5
ds80_4-5(2)
ds90_4-9
ds100_4-4
ds100_7-15
ds500_bp
Q4-5-97- velocities from discharge measurement on 4-5-97
Q4-9-97 - velocities from discharge measurement on 4-9-97
Q7-15-97 - velocities from discharge measurement on 7-15-97
Hydrograph - hydrograph from nearest gage

CASE STUDY #2

U.S. Route 12 over the Pomme De Terre River near Holloway, Minn.

SITE OVERVIEW

U.S. Route 12 crosses the Pomme de Terre River about 10.7 miles west of Danvers, Minnesota. The Appleton USGS streamflow-gaging station (05294000) is located approximately 12 miles downstream of the U.S. Route 12 bridge. The single-span steel-truss structure was constructed in 1933 with a maximum span length of 87.3 feet. The bridge has vertical-wall abutments with wing walls; each abutment and wing wall rests on concrete footings supported on timber piling. Neither abutment was riprapped nor was there any other scour protection measures. A field investigation conducted by BRW, Inc. (1995) prior to the flood revealed no evidence of significant scour at either of the abutments. The floodplains downstream of the bridge are more heavily wooded and classified on the maps as a wetland area. There is a park on the upstream left bank. A summary of the general site information on the site is found in Table 1.

During the April 1997 flood, where an estimated 200-year discharge was calculated at the USGS Appleton streamflow-gaging station, the USGS National Bridge Scour Team made real-time bridge scour measurements at the site. A manned boat was deployed to collect detailed scour data with a 1200 kHz acoustic Doppler current profiler (ADCP) on 4/5/1997 and additional limited-detail data was collected on 4/9/1997 from the bridge deck. The USGS measured considerable contraction and abutment scour at the U.S.12 bridge site. A large scour hole developed at the right abutment, scouring below the abutment cutoff wall resulting in failure of the fill material behind the abutment. Slumping of the embankment slope and some deformation of the approach highway were observed. Although scour measurements showed a scour hole 6.5 feet below the footing of the left abutment, no deformation was observed near the left abutment. These conditions resulted in closure of the bridge. Because of the age and scheduled replacement of the bridge, the bridge was not repaired but rather replaced with a new structure following the 1997 flood.

The compiled field data (channel and floodplain bathymetry, water discharge, water-surface elevations, roughness, and bridge geometry) were used to calibrate a step-backwater model at each site. Abutment and contraction scour were calculated in HEC-RAS (U.S. Army Corps of Engineers, 1998) using the equations and methods outlined in HEC-18 (Richardson and Davis, 2001) and then compared with the field measurements.

Hydrologic Conditions

Record snowfall and snowpack-moisture content, combined with excessive soil moisture conditions in much of North Dakota, South Dakota, and Minnesota led to severe flooding during April 1997. During the winter of 1996-97, precipitation amounts in nearly all of the west-central portions of Minnesota were equal to or in the excess of the 90th percentile based on the 30-year period from 1961 to 1990.

Table 1. Site information

Site Characteristic	Description
County	Swift
Nearest City	Holloway
State	Minnesota
Latitude	45°16'58''
Longitude	95°58'45''
Route Number	12
Route Class	US
Stream Name	Pomme De Terre

Record or near-record amounts of snowfall occurred in most of the western portions of Minnesota during this period. Snowfall totals were particularly high in the upper Minnesota River valley. Warm temperatures in late March initiated snowmelt, producing record flooding; however, a late-spring storm and falling temperatures added more than 2 inches of precipitation in the form of rain and up to 23.5 inches of snow in some areas. Discharge exceeded the 200-year flood on the Pomme de Terre River near Appleton, Minn. and the 100-year flood on the Minnesota River at Montevideo, Minn. A discharge measurement of 5750 ft³/s was made at the U.S. 12 bridge during the site visit on 4/9/97.

DISCUSSION OF CONTRACTED SITE

The bridge had a channel contraction ratio of around 0.48, with a most of the contracted flow coming from the left floodplain. A berm located approximately 100 feet upstream of the bridge on the left overbank directed the contracting flow into the channel upstream of the left abutment (see Figure 1).

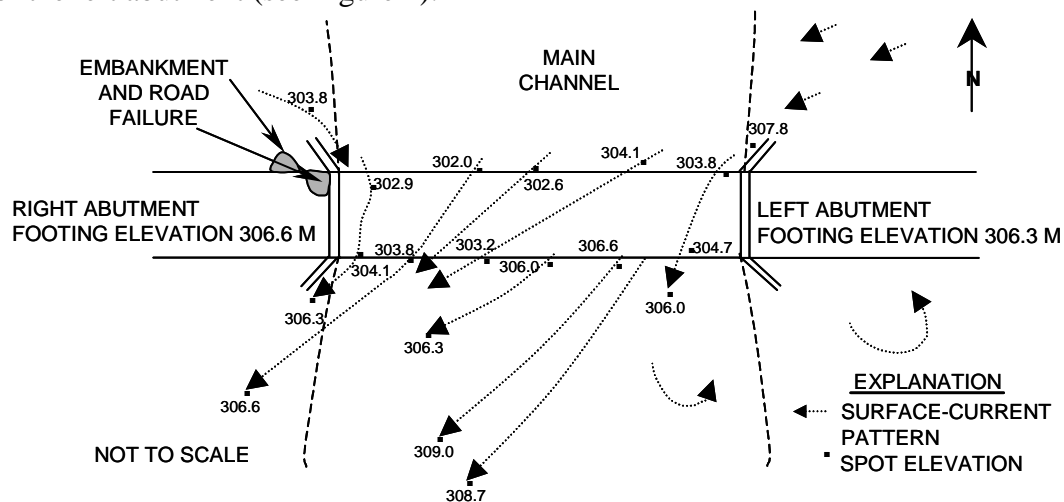


Figure 1. Sketch of U.S. Route 12 over Pomme de Terre River, Minnesota showing spot elevations and surface current patterns on April 9, 1997. (Elevations are in meters referenced to NGVD of 1929, 1 meter = 3.2808 feet)

Bridge Data

Structure #5359, at the time of the scour measurements, was an old truss bridge with a perpendicular alignment to the main channel. However, during the 1997 flood there was considerable skew as a significant amount of flow was coming from the left floodplain. The flow through the bridge opening in the center of the channel was skewed about 50 degrees. The U.S. 12 bridge was a single-span 88 ft wide structure with vertical abutments and wingwalls (type IV contracted opening). The low-chord elevation was 1023.85 ft above sea level. Bridge characteristics pertinent to scour are summarized in Table 2.

Table 2. Bridge data

Bridge Characteristic	Description
Structure Number	5359
Length (ft)	88.3
Width (ft)	27
Spans	1
Vertical Configuration	Sloping
Low Chord Elev (ft)	1023.85
Upper Chord Elev (ft)	1024.76
Overtopping Elev (ft)	1027.6
Skew (degrees)	0
Guide Banks	None
Waterway Classification	Main
Year Built	1933
Avg. Daily Traffic	Unknown
Plans on File	Yes
Parallel Bridges	No
Continuous Abutments	N/A

Geomorphic Setting

The U.S. 12 bridge is located in a relatively straight section of the Pomme De Terre river. A low-head dam (spillway elevation 1015 ft) is located approximately 300 ft upstream of the bridge. The right floodplain is forested and narrow relative to the left floodplain, which was less densely vegetated. A small park with picnic Tables and restroom facilities is located upstream of the U.S. 12 bridge on the left overbank. During the two site visits in April 1997, the floodplain flow was highly skewed through the bridge opening from the relatively wide left floodplain but the observed roadway and embankment failure was along the right abutment. A plan view of the U.S. 12 bridge site configuration is shown in Figure 2 and a USGS 7.5 minute quadrangle topographic map of the site is shown in Figure 3. Data characterizing the geomorphic setting is summarized in Table 3.

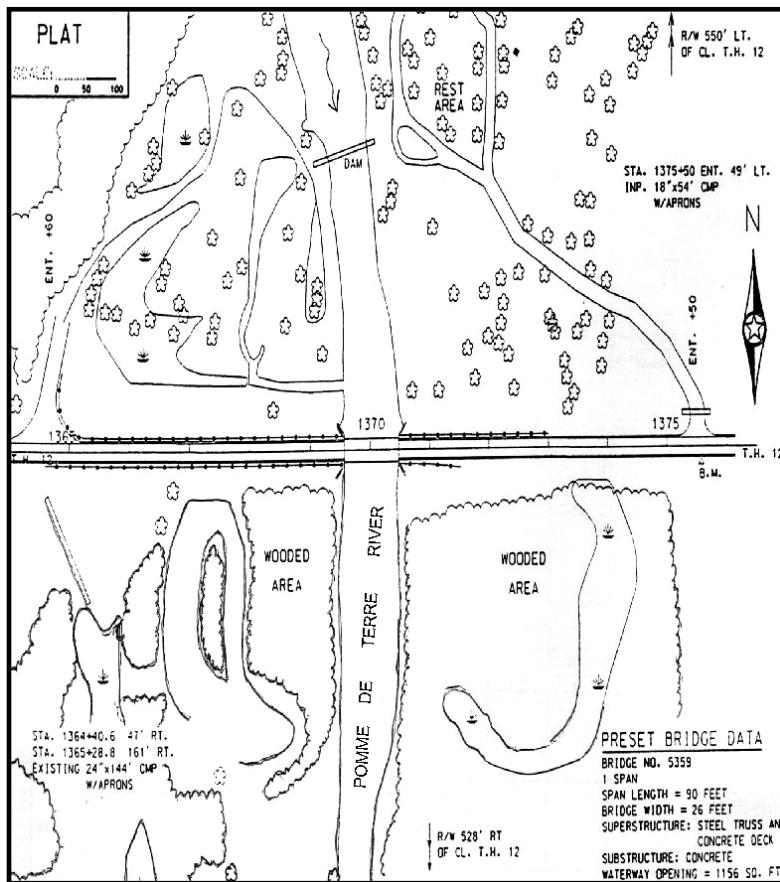


Figure 2. Plan view of U.S. 12 bridge site over the Pomme De Terre River.

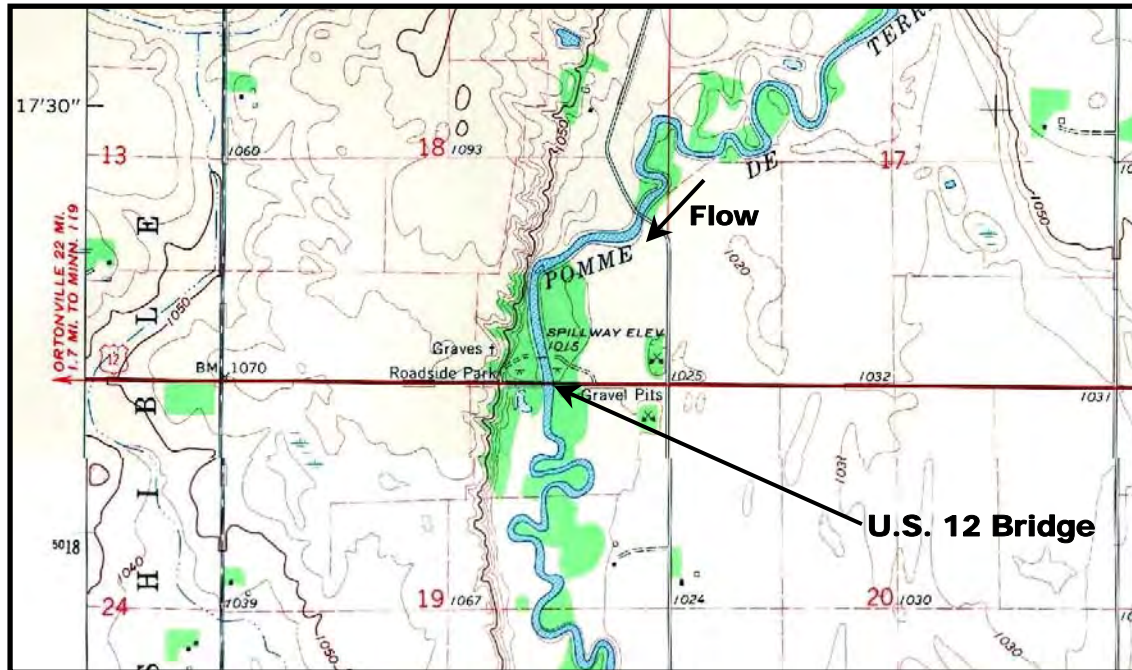


Figure 3. USGS topographic map of U.S. 12 bridge over the Pomme De Terre River near Holloway, MN.

Table 3. Geomorphic data

Geomorphic Characteristic	Description
Drainage Area (square miles)	845
Slope in Vicinity (ft/ft)	.0005
Flow Impact	Right
Channel Evolution	Pre-modified
Armoring	Unknown
Debris Frequency	Rare
Debris Effect	None
Stream Size	Small
Flow Habit	Perennial
Bed Material	Sand
Valley Setting	Low relief
Floodplain Width	Wide
Natural Levees	Unknown
Apparent Incision	None
Channel Boundary	Alluvial
Banks Tree Cover	Medium
Sinuosity	Straight
Braiding	None
Anabranching	None
Bars	Narrow
Stream Width Variability	Equiwidth

Bed Material Data

The bed material size distribution that is reported for the U.S. 12 bridge site are from information provided the Minnesota Department of Transportation (MnDOT). A review of the lithologic logs for the replacement bridge show that the subsurface material is primarily sands, silts, with some gravel with a $D_{50} = .15$ mm.

Roughness Coefficients

A distribution of Manning's n values is provided in Table 4.

Table 4. Manning's n values for the Pomme De Terre River at the U.S. 12 bridge. (fldpln, floodplain; chnl, channel; rt, right)

Upstream				Downstream			
Flow Type	Left Fldpln	Main Chnl	Rt Fldpln	Flow Type	Left Fldpln	Main Chnl	Rt Fldpln
High	0.08	0.035	0.08	High	0.1	0.035	0.1
Typical	--	0.030	--	Typical	0.08	0.030	0.08
Low	0.05	--	0.05	Low	--	--	--

Abutment Details

The U.S. 12 bridge had vertical abutments with wingwalls set at the edge of the channel (see Figure 4). The abutment characteristics are summarized in Table 5.

Table 5. Abutment data

Abutment Characteristic	Description
Left Station	35917.33
Right Station	35567.83
Left Skew (deg)	0
Right Skew (deg)	0
Left Abutment Length (ft)	67
Right Abutment Length (ft)	67
Left Abutment to Channel Bank (ft)	0
Right Abutment to Channel Bank (ft)	0
Left Abutment Protection	None
Right Abutment Protection	None
Contracted Opening Type	III*
Embankment Skew (deg)	-35
Embankment Slope (ft/ft)	.09
Abutment Slope (ft/ft)	2
Wingwalls	No
Wingwall Angle (deg)	N/A

* - Type III opening has sloping abutments and sloping spillthrough abutments.

Pier Details

There were no piers associated with the U.S. 12 bridge over the Pomme De Terre river.

Surveyed Elevations

Elevations are referenced to MSL based on values provided by MnDOT on their scour-monitoring plan. Plans for the new bridge developed by BRW showed elevations 30 ft higher. The scour report from BRW agreed with the MnDOT scour-monitoring plan and thus, that elevation reference was used. The top of curb near the east (left) abutment was used as a tape down location and was to have an elevation of 998.7 ft. The horizontal stationing of data collected from the bridge deck was also referenced to the east abutment then adjusted in post-processing to be consistent with stationing used in the BRW, Inc. WSPRO model. Distance of ADCP data from the bridge was visually estimated. Horizontal stationing for the ADCP is based on bottom tracking. The stationing was visually adjusted to agree with the BRW WSPRO model.

The elevations that were provided by MnDOT, and the elevations from the BRW sour report, when used to build a HEC-RAS model of the bridge section, were discovered to be inconsistent with the downstream gaging station (Appleton) elevations during the 1997 flood. MnDOT was again contacted and it was discovered that elevation 995 ft above MSL on the BRW scour report should actually be 1023.9 feet above MSL, thus validating the new bridge plan elevations.

Therefore, the elevation of the top of curb near the east abutment should actually be 1027.6 ft, making the bridge section more consistent with elevations upstream at the C.R. 22 bridge and downstream at the Appleton gaging station. A correction of +28.9 ft should be made to MnDOT's reference elevation on their sour monitoring plan and all elevations from the BRW sour report. The April 1997 field data, found in the supporting excel file (us12pdt-REV.xls), has already been corrected to reflect the new reference elevation. A summary of the measured water surface elevations is presented in the Table 7.

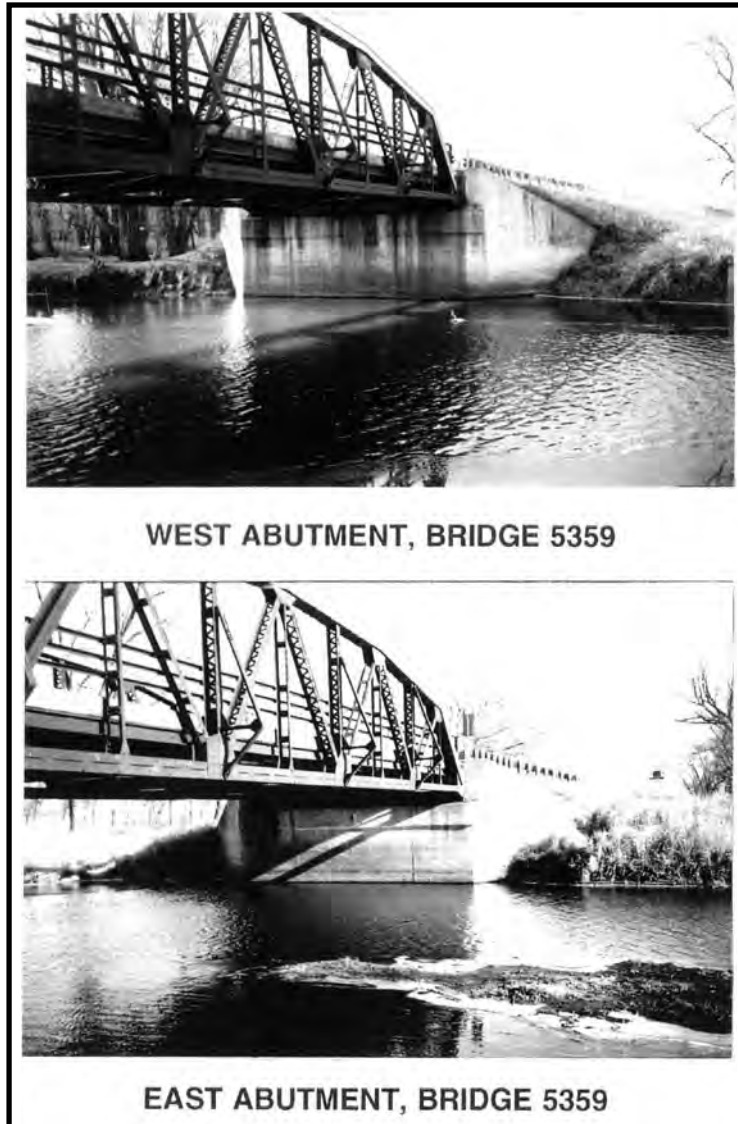


Figure 4. Pictures of the U.S. 12 bridge abutments taken during low-flow prior to the 1997 flood on the Pomme De Terre River.

Table 7. Water-surface elevation measured from the U.S. 12 bridge deck.

Date	Time	Upstream (ft)	Downstream (ft)
4/5/1997	--	1019.4	---
4/9/1997	--	1021.9	---

PHOTOS



Figure 5. Looking at the upstream U.S. 12 bridge face from right bank during the April, 1997 flood.



Figure 6. Scour measurement at upstream right wingwall of U.S. 12 bridge over the Pomme De Terre River; notice slump failure of embankment.



Figure 7. Looking upstream at U.S. 12 bridge over the Pomme De Terre River during low-flow prior to the April, 1997 flood.



Figure 8. Looking upstream from U.S. 12 bridge deck at the small dam on the Pomme De Terre River during low-flow prior to the April, 1997 flood.



Figure 9. Looking at upstream right abutment and embankment of U.S. 12 bridge during low-flow prior to April, 1997 flood.

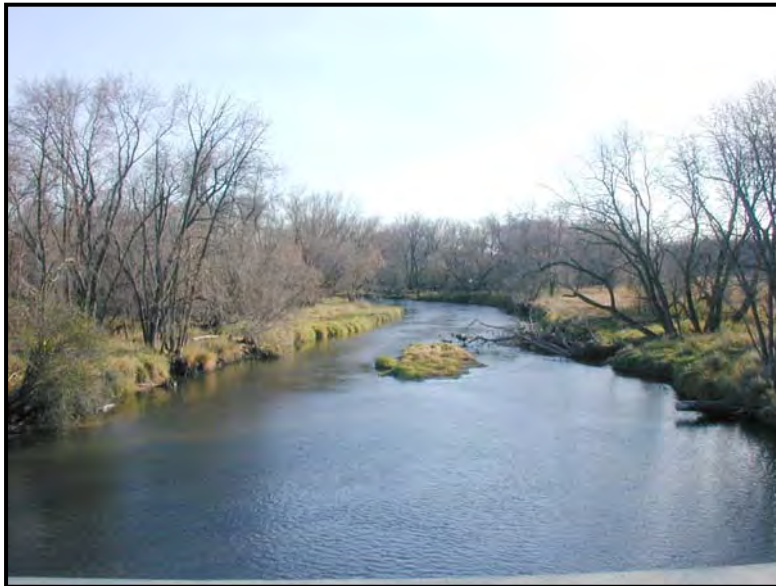


Figure 10. Looking downstream from replaced U.S. 12 bridge deck during low-flow following the April, 1997 flood.



Figure 11. Looking upstream from replaced U.S. 12 bridge deck during low-flow following the April, 1997 flood; notice the absence of the small upstream dam.

MEASURED SCOUR

All bathymetry data used to estimate the contraction and abutment scour were collected on 4/9/97 with both a sounding weight and transducer mounted on a knee-board. The knee-board was floated from upstream to downstream under the bridge to determine depth of flow through the bridge opening. Cross sections in the main channel were collected 300 feet upstream and downstream of the bridge on 4/5/97, but measurements on 4/9/97 were limited to the bridge opening. Data could not be collected in the

floodplains because of heavy vegetation and submerged structures in the park located on the left overbank, upstream of the bridge. A plot of measured cross-section in the bridge opening is illustrated in Figure 12.

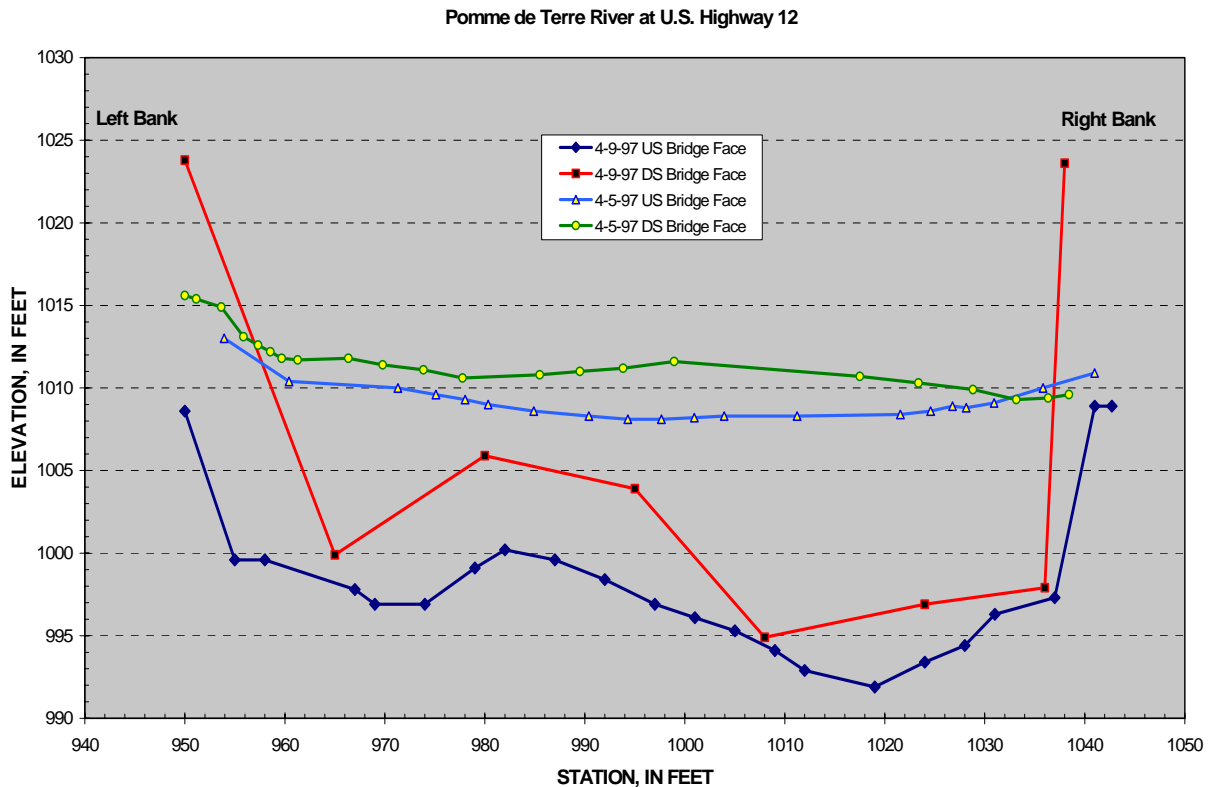


Figure 12. Cross-section data collected at the U.S. highway 12 bridge over the Pomme de Terre River on April 5, 1997 and April 9, 1997.

Abutment Scour

There was significant flow from the left upstream flood plain through the bridge opening. This flow from the left flood plain significantly skewed the flow through the bridge opening, about 50 degrees on the average. The reference surface used to determine the depth of abutment scour was the concurrent ambient bed. Therefore, the depth of abutment scour reported is the additional local scour below the depth of contraction scour. For this site, it appears that the scour holes may interact as there is only one or two depth measurement between the holes that define the ambient bed. Measurements numbers 1 and 4 were made with a sounding weight during a discharge measurement along the upstream face of the bridge. All other measurements were made using an echo sounder mounted on a knee-board.

The site characteristics pertinent to abutment scour are summarized in Table 8.

Table 8. Abutment scour data (--, not available; ft/s, feet per second; cfs, cubic feet per second; Abut, abutment; Avg, average; US, upstream; DS, downstream)

Measurement Number	Abutment	Date	Time	US/DS	Scour Depth (ft)	Accuracy (ft)
1	Right	4/9/1997	16:00	Upstream	8.0	2
2	Right	4/9/1997	14:00	Upstream	7.0	2
3	Right	4/9/1997	14:00	Downstream	11.0	2
4	Left	4/9/1997	16:00	Upstream	3.0	2
5	Left	4/9/1997	14:00	Upstream	1.5	2
6	Left	4/9/1997	14:00	Downstream	6.0	2

Measurement Number	Sediment Transport	Velocity at Abut (ft/s)	Depth at Abut (ft)	Discharge Blocked (cfs)	Avg Velocity Blocked (ft/s)	Avg Depth Blocked (ft)
1	Live-bed	4.2	30	--	--	--
2	Live-bed	4.2	31	--	--	--
3	Live-bed	4.2	27	--	--	--
4	Live-bed	3.8	25	--	--	--
5	Live-bed	3.8	25	--	--	--
6	Live-bed	3.8	22	--	--	--

Measurement Number	Embankment Length (ft)	Bed Material Cohesion	D50 (mm)	Sigma	Debris Effect
1	396	None	0.15	--	Insignificant
2	396	None	0.15	--	Insignificant
3	396	None	0.15	--	Insignificant
4	1006	None	0.15	--	Insignificant
5	1006	None	0.15	--	Insignificant
6	1006	None	0.15	--	Insignificant

Contraction Scour

Contraction scour was computed as the difference in average bed elevation between uncontracted and contracted sections, adjusted for bed slope.

The appropriate reference surface was determined from an analysis of cross sections collected by BRW on 6/5/95 and the USGS during the flood on 4/5/97. Cross sections on these two dates collected approximately 300 ft upstream from the bridge show only about a 0.5 ft difference in the channel bottom elevation. The flood section was the lower of the two. Downstream from the bridge the cross section surveyed on 6/5/95 (approximately 75 ft downstream) and the cross section surveyed on 4/5/97 (approximately 200 ft downstream) are similar, with less than 1 ft in variation in the channel bottom elevations. The 4/5/97 cross section 100 ft downstream was about 1.5 below the 6/5/97 cross section

at 75 ft downstream. It was assumed that the 4/5/97 cross section could have been affected by the scour at the bridge section. Thus, it was not considered in the setting of the reference surface. The WSPRO bridge section surveyed by BRW on 6/5/95 showed from 1 to 2 ft of abutment scour in the cross-section. However, the center of the channel at the bridge appears to be representative of consistent channel slope from the upstream section to the downstream section. Since little general scour was observed at the upstream and downstream sections the mean elevation of the unscoured portion of the WSPRO bridge section was used as the contraction scour reference surface, elevation 1010.4 ft.

The contracted section on 4/5/97 was measured under the bridge from data collected by an acoustic Doppler current profiler. The depths represent a weighted average of the four beam depths. Because a weighted-average was used it is possible that the local abutment scour was not detected. The maximum lowering of the streambed was actually 7.5 ft; however, when the entire bed below the bridge was averaged the depth of contraction scour was only 3.1 ft. The hydraulic data presented for measurement number 1 were collected with the ADCP. The ADCP data showed many missing ensembles that were estimated in the final processing. There was not clear delineation of the channel banks in the approach section, creating a degree of uncertainty in the approach discharge. Overall it is expected that the approach discharge is +/- 20% and the total discharge is +/- 10%.

Measurements number 2 was made during a discharge measurement along the upstream face of the bridge. The depths were measured with a sounding weight. Measurements 3 and 4 were made using an echo sounded mounted on a knee-board. The board was floated from upstream to downstream under the bridge. The measurements reflect the depths at the upstream or downstream face of the bridge.

The cross sections measured on 4/9/97 all showed a similar pattern with abutment scour holes on each side and a sharp mound in between the scour holes but skewed towards the left bank. It appears that the abutment scour holes may have overlapped. The highest elevation in the center of the cross section was subtracted from the reference surface to obtain the depth of contraction scour. No data in the approach section was collected on 4/9/97.

The site characteristics pertinent to contraction scour are summarized in Table 9.

Table 9. – Contraction scour data (--, not available; ft/s, feet per second; cfs, cubic feet per second; US, upstream; DS, downstream; Avg, average)

Measurement Number	Contracted Date	Contracted Time	Uncontracted Date	Uncontracted Time	US/DS	Scour Depth (ft)
1	4/5/1997	11:30	4/5/1997	--	US	3.1
2	4/9/1997	16:00	--	--	US	10.5
3	4/9/1997	14:00	--	--	US	12.5
4	4/9/1997	14:00	--	--	DS	4.5

Measurement Number	Accuracy (ft)	Contracted Avg Vel (ft/s)	Contracted Discharge (cfs)	Contracted Depth (ft)	Contracted Width (ft)
1	2	4.8	5000	12.1	88
2	2	2.7	5750	24	88
3	2	2.8	5750	23.6	88
4	2	3.8	5750	17.3	88

Measurement Number	Uncontracted Avg Vel (ft/s)	Uncontracted Discharge (cfs)	Uncontracted Depth (ft)	Uncontracted Width (ft)	Channel Contraction Ratio
1	3.4	1800	7.9	70	0.64
2	---	---	---	---	---
3	---	---	---	---	---
4	---	---	---	---	---

Measurement Number	Pier Contraction Ratio	Scour Location	Eccentricity	Sediment Transport	Bed Form	Debris Effect
1	---	Main Channel	---	Live-Bed	Unknown	Unknown
2	---	Main Channel	---	Live-Bed	Unknown	Unknown
3	---	Main Channel	---	Live-Bed	Unknown	Unknown
4	---	Main Channel	---	Live-Bed	Unknown	Unknown

Measurement Number	D95 (mm)	D84 (mm)	D50 (mm)	D16(m)	Sigma	Bed Material Cohesion
1	0.28	0.23	0.15	<.062	1.5	Non-cohesive
2	0.28	0.23	0.15	<.062	1.5	Non-cohesive
3	0.28	0.23	0.15	<.062	1.5	Non-cohesive
4	0.28	0.23	0.15	<.062	1.5	Non-cohesive

COMPUTED SCOUR

A calibrated HEC-RAS model of the site was developed to assess how accurately the scour for this flood could have been predicted. The pre-flood geometry of the bridge section was simulated with a HEC-RAS model utilizing the channel geometry from the original bridge plans and the low-flow survey conducted by BRW, Inc. on 6/5/1995. A separate model was developed with the main channel geometry data collected during the April, 1997 flood. The discharges measured during the April, 1997 flood were then modeled with the pre-flood and flood bathymetry to determine the hydraulic parameters needed for HEC-18 scour computations.

Abutment Scour

Abutment scour was computed in HEC-RAS by both the Froehlich equation and the HIRE equation. The hydraulic parameters taken from the HEC-RAS output were also used to calculate abutment scour using the Sturm abutment scour equation. The data contained in Table 10 show that the method of combining one dimensional model hydraulics and the scour equations grossly overpredicted the scour at the left and right abutments. Overall, the one dimensional step-backwater model was unable to accurately simulate the complex hydrodynamics.

Table 10. Comparison of observed to model-computed abutment scour at U.S. 12 over Pomme De Terre River near Holloway, MN.

Date	Abutment	Location	Local Scour Depth			
			Observed (ft)	Froehlich Equation (ft)	HIRE Equation (ft)	Sturm Equation (ft)
4/9/97	Right	Upstream	8	15.1	35.4	6.7
4/9/97	Right	Downstream	11	15.1	35.4	6.7
4/9/97	Left	Upstream	3	13.1	17.1	6.8
4/9/97	Left	Downstream	6	13.1	17.1	6.8

Contraction Scour

The contraction scour was computed in HEC-RAS by allowing the model to use the default equation (live-bed or clear-water) depending upon the hydraulic conditions computed by the model. The results of the model are compared with observed contraction scour in Table 11.

Table 11. Comparison of observed to model-computed contraction scour at U.S. 12 over Pomme De Terre River near Holloway, MN.

Date	Contraction Scour Depth	
	Observed (ft)	LiveBed (ft)
4/5/97	3.1	2.0

REFERENCES

Any questions regarding the U.S. 12 over Pomme De Terre River should be directed to the following points of contact:

1. David Mueller, U.S. Geological Survey
9818 Bluegrass Parkway
Louisville, KY 40299
Phone: (502) 493-1935
e-mail: dmueller@usgs.gov
2. Chad Wagner, U.S. Geological Survey
3916 Sunset Ridge Road
Raleigh, NC
Phone: (919) 571-4021
e-mail: cwagner@usgs.gov

SUPPORTING DATA

The following is a listing of supporting files that are associated with the U.S. 12 bridge:

us12pdt-REV.xls - contains the following data:

- Summary - Summary of basic site and scour data
- Hydrograph - Hydrograph from nearest USGS gaging station
- X-Sec – cross-section data

Site Photos:

The following photos were scanned from a black and white copy of the bridge scour evaluation report completed by BRW:

- pdt12-scrpt-ds-channel.jpg
- pdt12-scrpt-abuts.jpg
- pdt12-scrpt-bridge.jpg
- pdt12-scrpt-nwcorner-bridge.jpg
- pdt12-scrpt-us-channel.jpg
- pdt12-scrpt-us-dam.jpg

pdt12-brgpln-siteplan.jpg is a site plan scanned from the bridge plans provided by MnDOT.

The following photos/sketches were taken during the April, 1997 flood:

pdt12-flood-us-bridge.jpg is a photo taken during the flood, from the right bank looking across the face of the bridge to the left floodplain. Note the slump in the foreground.

pdt12-flowfield.jpg - sketch of flow field observed on 4-9-97

pdt12-rwingwall - photo of data collection along the right upstream wingwall. Note the slump in the embankment.

HEC-RAS Files

PreFlood_US12.zip – HEC-RAS model files with pre-flood bathymetry, includes scour computations.

Flood_US12.zip – HEC-RAS model files with main channel bathymetry collected during flooding on April 9, 1997; used as calibration model.

CASE STUDY #3

Minnesota River at State Route 25 near Belle Plaine, Minnesota

SITE OVERVIEW

The study site is located on the Minnesota River .7 miles north of the town of Belle Plaine on State Highway 25. The site is approximately 7.5 miles upstream from the USGS gaging station near Jordan (05330000) and 12 miles downstream from the USGS gaging station at Henderson (33032001). The period of record for the Jordan station is from October 1935 to the current year, with an annual mean flow of 4425 cfs, and an instantaneous peak flow of 117,000 cfs recorded on April 11, 1965. The USGS measured a discharge of 73,200 cfs and significant abutment and contraction scour at the site during real-time bridge scour measurements during the flood in April of 2001. Detailed discharge, velocity, and cross-section data were collected throughout a reach extending 1400 feet (ft) upstream and 1700 ft downstream of the bridge using an acoustic Doppler current profiler deployed on a manned boat during the flood on 4/17/2001.

The structure number for this site is 5260. The Minnesota Dept of Transportation (MnDOT) built the current bridge in 1934. The channel bottom at the time of construction was at approximately the same elevation as the top of footings (elevation 695 ft).

Eventually, the channel was scoured well below the footing bottoms, requiring re-stabilization of the channel bed around the piers and left abutment with rip-rap due to a flood in April of 1951 that caused extensive scouring of the channel. An underwater inspection was completed in 1991 and 2000. The 2000 inspection report contained upstream and downstream bridge face profiles, which reflected streambed elevations had been returned to levels similar to the initial construction conditions. Both inspections revealed the piers to be in generally good structural condition. Debris buildup at the piers appears to be a recurring problem, especially at pier 1.

Several measurements of scour have occurred at this site, by MnDOT and Collins Engineers, Inc. Collins Engineers, Inc. performed a series of investigations on the highway 25 bridge in the mid to late 1990's and found the bridge to be in good condition with minor scour depressions at the upstream end of pier #2. The USGS revisited the site in October 2001 to conduct a post-flood survey and noted that both abutments had been re-stabilized and lined with riprap as a result of the damage produced by the April 2001 flood. A summary of the general site information is found in Table 1.

A step-backwater hydraulic model (HEC-RAS) of the S.R. 25 site was developed as part of a bridge scour investigation report (consultant agreement no. 70490) for the Minnesota Department of Transportation in January, 1994. A separate HEC-RAS model was developed and calibrated by the USGS using channel geometry and field hydraulic measurements collected during the April, 2001 flood. Both models were used to predict the amount of abutment and contraction scour expected for the various geometric configurations using the techniques and equations from HEC-18.

Table 1. Site information

Site Characteristic	Description
County	Scott
Nearest City	Belle Plaine
State	Minnesota
Latitude	44°38'02''
Longitude	93°45'58''
Route Number	25
Route Class	State
Stream Name	Minnesota River

Hydrologic Conditions

Above normal rains in early November 2000 followed by snowfalls later in the month resulted in precipitation totals that were well above historical averages for the month, particularly in the central and southwestern portions of Minnesota. With additional snowfall throughout the winter, total accumulation in parts of southern Minnesota was 18 to 24 inches greater than for a normal winter (USGS MN District, Fact Sheet, 2002). Typically, the snow pack would lose much of its' water equivalence from later winter to early spring, before the arrival of spring rains. However, below-normal temperatures for February and March delayed the snowmelt and only compacted the existing snow cover. In April, heavy rains fell over much of the central and southern parts of the state which coupled with greater than normal snow-to-water equivalents to provide the excessive runoff that resulted in the April, 2001 flooding. A discharge of 73,200 cubic feet per second (cfs) was measured at the site during the visit, which has approximately a 35-year recurrence interval according to the peak flow frequency analysis developed for the Jordan, MN USGS gaging station.

DISCUSSION OF CONTRACTED SITE

The Minnesota River has a series of low radius bends that cause a slightly up-valley flow in the main channel upstream of the S.R. 25 bridge, which added complexity to the scour analysis. The upstream bends appear to be actively migrating longitudinally within the valley. A series of oxbow lakes are present on the left floodplain from which a significant part of the floodplain flow is blocked and forced through the bridge opening. A depiction of the hydraulics through the bridge opening during the April 1997 flood is shown in Figure 1.

Bridge Data

Structure #5260 is a metal truss bridge consisting of 3-150' continuous I-beam spans supported by two concrete column piers with partial web walls, and vertical abutments with wingwalls. Pier #1 is on the right, looking downstream, and is supported by 82 concrete pilings driven to elevations ranging from 660.28' to 637.28'. Pier #2 is

supported by 82 concrete pilings driven to elevations ranging from 665.96' and 654.96'. The south and north abutments are supported by creosoted piles driven to elevation 670.53' and 665.96', respectively. Both abutments are set back about 30-40 feet from the top of the channel banks and the bridge has a 1% downhill grade in the northbound direction. The bridge characteristics pertinent to scour are summarized in Table 2.



Figure 1. Sketch of site hydraulics during April, 2001 flood.

Table 2. Bridge data

Bridge Characteristic	Description
Structure Number	5260
Length (ft)	450
Width (ft)	28
Spans	3
Vertical Configuration	Sloping
Low Chord Elev (ft)	734
Upper Chord Elev (ft)	737
Overtopping Elev (ft)	740
Skew (degrees)	30
Guide Banks	None
Waterway Classification	Main
Year Built	1934
Avg. Daily Traffic	Unknown
Plans on File	Yes
Parallel Bridges	No
Continuous Abutments	No

Geomorphic Setting

The bridge is located in a sinuous reach of the river in between two small radius bends that flow directly across or even slightly up-valley. These bends are located immediately upstream of the bridge and appear to be actively migrating down-valley. The left floodplain is comprised of young forests and the barren oxbow lakes probably created during construction of the highway. The right floodplain consists of densely populated forests with some areas of un-maintained pastureland. During the site visit in April 2001, the floodplain flow was concentrated in the left floodplain. The concentration of left floodplain flow was attributed to the channel alignment upstream of the bridge. Inspection of the "approach" section (one bridge width upstream) revealed a large discharge relative to that of the contracted opening and a bed elevation similar to the contracted section. It was discovered that the upstream bend forced a majority of the left floodplain flow back into the main channel before the "approach" section, as defined by HEC-18.

The reattachment points along the right and left embankments during the flood were located approximately 630 ft and 1775 ft from the bridge, respectively. Data characterizing the geomorphic setting is summarized in Table 3. A topographic map of the site is shown in Figure 2.

Table 3. Geomorphic data

Geomorphic Characteristic	Description
Drainage Area (sq mi.)	16010
Slope in Vicinity (ft/ft)	.000063
Flow Impact	Left
Channel Evolution	Pre-modified
Armoring	Unknown
Debris Frequency	Occasional
Debris Effect	Local
Stream Size	Medium
Flow Habit	Perennial
Bed Material	Sand
Valley Setting	Low relief
Floodplain Width	Narrow
Natural Levees	Unknown
Apparent Incision	None
Channel Boundary	Alluvial
Banks Tree Cover	Medium
Sinuosity	Meandering
Braiding	None
Anabranching	None
Bars	Narrow
Stream Width Variability	Equiwidth

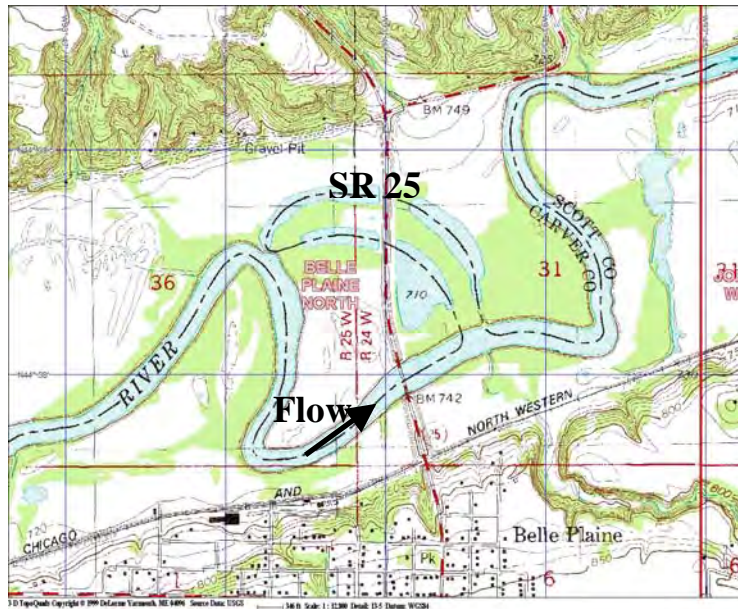


Figure 2. USGS topographic map of the CR 22 bridge scour site.

Bed Material Data

Bed material samples at the site were collected on 10/31/2001 with a BM-54H grab sampler from a manned boat at the following four locations in the vicinity of the bridge: 150 ft upstream of bridge in the center of the approach channel, 150 ft downstream of the bridge in the middle of the exit section, in the scour hole at the upstream left abutment in the bridge opening, and in the scour hole on the upstream left bank. The material sampled in the main channel approach section was sand with a $D_{50} = 0.36$ millimeters (mm). The grain size distribution of the bed material in the approach section is shown in Figure 3.

Roughness Coefficients

A complete distribution of Manning's n values is provided in Table 4.

Table 4. Manning's n values upstream and downstream of the CR 22 bridge. (fldpln, floodplain; chnl, channel; rt, right)

Upstream				Downstream			
Flow Type	Left Fldpln	Main Chnl	Rt Fldpln	Flow Type	Left Fldpln	Main Chnl	Rt Fldpln
High	0.085	0.045	0.065	High	0.085	0.05	0.08
Typical	0.05	0.032	0.052	Typical	0.052	0.044	0.052
Low	0.052	0.032	0.052	Low	0.052	0.044	0.052



Figure 3. Grain size distribution for CR 22 bed material samples

Abutment Details

The bridge has vertical abutments set back 30-40 ft from the edge of the main channel. Although the abutments were protected by riprap prior to the April, 2001 flood, a site reconnaissance in October, 2002 revealed that both abutments had been re-graded with intermediate breaks in the slope and new rip-rap had been placed (see Figure 4). The abutment characteristics are summarized in Table 5.

Table 5. Abutment data

Abutment Characteristic	Description
Left Station	4044.67
Right Station	3593
Left Skew (deg)	0
Right Skew (deg)	0
Left Abutment Length (ft)	77.4
Right Abutment Length (ft)	77.4
Left Abutment to Channel Bank (ft)	37
Right Abutment to Channel Bank (ft)	33
Left Abutment Protection	Riprap
Right Abutment Protection	Riprap
Contracted Opening Type	IV *
Embankment Skew (deg)	-30
Embankment Slope (ft/ft)	.17
Abutment Slope (ft/ft)	0
Wingwalls	Yes
Wingwall Angle (deg)	45

* - Type IV opening has sloping abutments and vertical abutments with wingwalls.



Figure 4. Picture of the re-stabilization done to the left abutment of the S.R 25 bridge over the Minnesota River near Belle Plaine, MN following April, 2001 flood.

Pier Details

Pier #1 is on the right, looking downstream, and is supported by 82 concrete pilings driven to depths ranging from 660.28' to 637.28'. Pier #2 is on the left, looking downstream, and is supported by 82 concrete pilings driven to elevations ranging from 665.96' and 654.96'. The foundation for both piers is dumbbell shaped with 15.5' square pads on each end connected by a 5' by 14' rectangle. In 1952, the piers were reinforced with stone rip-rap at a 2:1 slope from the top of the foundation due to a major scouring event that occurred in April, 1951. The remaining exposed channel bottom between the piers was lined with stone rip-rap paving to an elevation of 680'. Debris frequently accumulates in front of pier 1 and is a noted problem. The pier characteristics are summarized in Table 6.

Table 6. Pier data (--, not available)

Pier ID	Bridge Station (ft)	Alignment	Highway Station	Pier Type	# of Piles	Pile Spacing (ft)
1	-	0	37+42.75	Single	-	-
2	-	0	38+94.92	Single	-	-

Pier ID	Pier Width (ft)	Pier Shape	Shape Factor	Length (ft)	Protection	Foundation
1	6.5	Sharp	--	36.75	Riprap	Piles
2	6.5	Sharp	--	36.75	Riprap	Piles

Pier ID	Top Elevation (ft)	Bottom Elevation (ft)	Foot or Pile Cap Width (ft)	Cap Shape	Pile Tip Elevation (ft)
1	696.28	690.28	--	Other	637.3
2	694.76	688.76	--	Other	654.96

Surveyed Elevations

Water-surface elevations were measured from the bridge deck at the upstream left abutment. The vertical control for all surveyed elevations at the site was established from a benchmark (#7003 1973, elevation 741.75ft) located on the downstream right abutment and referenced to feet above mean sea level (MSL). The elevations used to dimension the bridge deck were determined from the bridge plans. A summary of the measured water surface elevations is presented in the Table 7.

Table 7. Water-surface elevation measured from the S.R. 25 bridge deck.

Date	Time	Upstream (ft)
4/17/2001	----	728.5

A local right-hand coordinate system was established with the positive y-axis in the upstream direction and the x-axis parallel to the upstream face of the bridge. This resulted in x-coordinates increasing from right to left. Since step backwater models typically use left to right coordinates, stationing was added which increases from left to right.

PHOTOS



Figure 5. Looking at flow contraction from left floodplain and location of upstream left overbank scour hole from right upstream abutment of S.R. 25 bridge during April, 2001 flood.



Figure 6. Looking at left upstream overbank scour hole (inside what appears to have been a much larger scour hole) from right bank along the upstream bridge face of S.R. 25 over the Minnesota River during low-flow.



Figure 7. Looking at turbulent flow and eddy fence attributed to severe contraction along the upstream left abutment of the S.R. 25 bridge during the April, 2001 flood.



Figure 8. Looking upstream at S.R. 25 bridge and left abutment during low-flow.

MEASURED SCOUR

All bathymetry data were collected with a 600 kHz ADCP and horizontally referenced with a differentially corrected global positioning system (DGPS). Cross sections in the main channel (tree line of right bank to tree line of left bank) were collected throughout the bridge reach at an approximate spacing of 225 ft upstream and 350 ft downstream of the bridge. The extents of the data collection upstream of the bridge was restricted due to downed power lines spanning the river. Data could not be collected in the floodplains because of heavy vegetation, but an approximation of the flow blocked by the road embankments was developed by cutting off the discharge entering the main channel from either floodplain with the ADCP. A survey of the floodplains and additional bathymetry data was collected in the approach, exit and bridge sections after the flood during a low-water site visit on October 31, 2001. A historic depiction of the scour through the S.R. 25 bridge opening is depicted in Figure 9 and a map of the bathymetric data collected during the April, 2001 flood is illustrated in Figure 10.

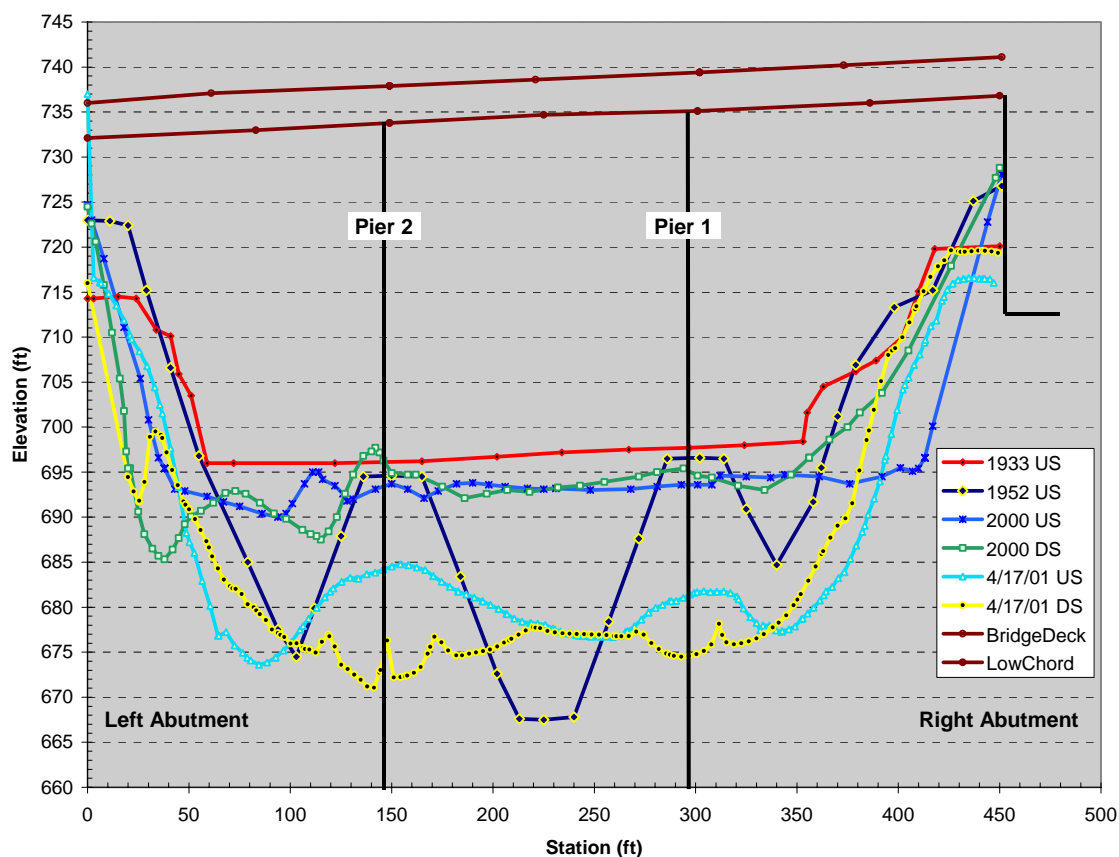


Figure 9. Historic cross-section data collected at the S.R. 25 bridge over the Minnesota River near Belle Plaine, MN.

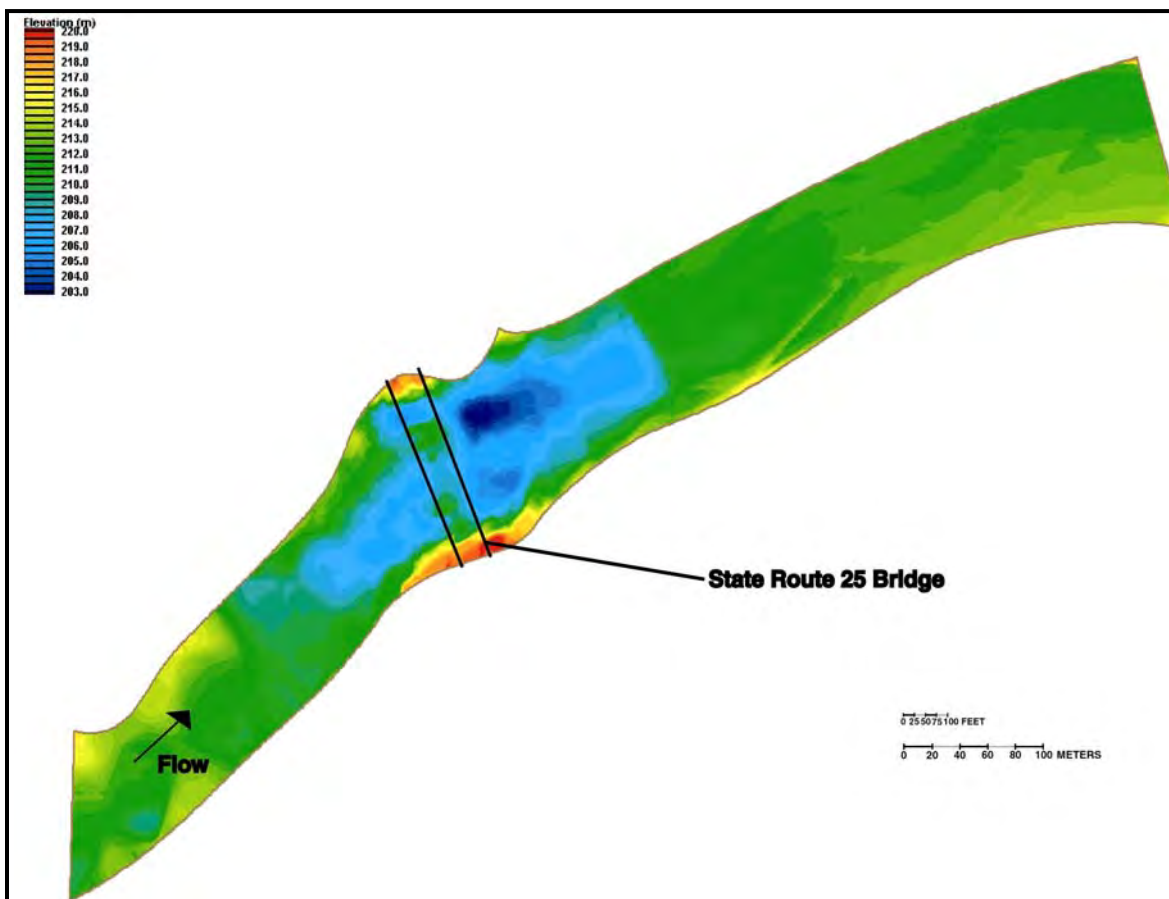


Figure 10. Bathymetric contour plot of Minnesota River in the vicinity of State Route 25 bridge, collected during April, 2001 flood.

Abutment Scour

The left upstream abutment was exposed to very high velocities coming out of the left floodplain. Intense boils and eddies were also present through the bridge opening at the left abutment. The left abutment slope and adjacent pier (#2) both had scour protection in the form of riprap. The maximum scour depth in the vicinity of the left abutment during the April, 2001 was actually measured downstream of the bridge (see Figure 9). Although it is difficult to determine the total effect that the riprap had on the depth of local abutment scour, it may have amplified the amount of scour in the channel downstream of the bridge. The riprap prevented scour and equilibrium sediment transport conditions to occur in the bridge opening and thereby shifting the scour process downstream to an unprotected portion of the channel.

The reference surface used to determine the depth of abutment scour was the concurrent ambient bed adjacent to the scour holes, which was established from bathymetry data collected upstream and downstream of the bridge during the flood (see Figures 9 and 10).

The velocity reported for “at the abutment” is the maximum velocity observed in the area of the scour hole. The site characteristics pertinent to abutment scour are summarized in Table 8.

Table 8. Abutment scour data (--, not available; ft/s, feet per second; cfs, cubic feet per second; Abut, abutment; Avg, average; US, upstream; DS, downstream)

Measurement Number	Abutment	Date	Time	US/DS	Scour Depth (ft)	Accuracy (ft)
1	Left	4/17/2001	11:10	Upstream	18.0	2
2	Left	4/17/2001	11:00	Downstream	13.0	3
3	Right	4/17/2001	11:00	Upstream	4.0	2
4	Right	4/17/2001	11:00	Downstream	3.0	2

Measurement Number	Sediment Transport	Velocity at Abut (ft/s)	Depth at Abut (ft)	Discharge Blocked (cfs)	Avg Velocity Blocked (ft/s)	Avg Depth Blocked (ft)
1	Live-bed	13.5	56	20800	2	16
2	Live-bed	--	52	20800	2	16
3	Live-bed	5.5	51.5	4200	0.67	10
4	Live-bed	--	50	4200	0.67	10

Measurement Number	Embankment Length (ft)	Bed Material Cohesion	D50 (mm)	Sigma	Debris Effect
1	1775	None	0.36	--	Insignificant
2	1775	None	0.36	--	Insignificant
3	630	None	0.36	--	Insignificant
4	630	None	0.36	--	Insignificant

Contraction Scour

From the data collected on 4/17/01 contraction scour was computed as the difference in average bed elevation between uncontracted and contracted sections (adjusted for bed slope). Inspection of the "approach" section (one bridge width upstream) revealed a large discharge relative to that of the contracted opening and a bed elevation similar to the contracted section. It was discovered that the upstream bend forced a majority of the left floodplain flow back into the main channel before the "approach" section. A cross section made further upstream showed much less discharge, which was consistent with channel discharge downstream of the bridge opening, and an average channel elevation approximately 15 higher than the contracted section. The widths and corresponding hydraulic characteristics for the uncontracted section is representative of the cross-section located just downstream of the upstream bend, rather than the conventional approach section (one bridge width upstream). If the ambient bed was taken at the cross-section one bridge width upstream, the resulting contraction scour would have been only 6ft.

Based on the measured elevation of the main channel between the abutment scour holes relative to the upstream ambient bed, there was approximately 15 ft of contraction scour. Comparisons of the center of the contracted section during the April, 2001 flood with the most recent bridge cross section collected on November 3, 2000 showed significant

change in elevation throughout the bridge opening that is consistent with the reported contraction scour depth (see Figure 9).

The average depth and velocity of the contracted section were computed from ADCP data collected throughout the bridge opening. The average depth included the abutment scour holes. The site characteristics pertinent to contraction scour are summarized in Table 9.

Table 9. Contraction scour data (--, not available; ft/s, feet per second; cfs, cubic feet per second; US, upstream; DS, downstream; Avg, average)

Measurement Number	Contracted Date	Contracted Time	Uncontracted Date	Uncontracted Time	US/DS	Scour Depth (ft)
1	4/17/2001	11:00	4/17/2001	11:55	--	15
Measurement Number	Accuracy (ft)	Contracted Avg Vel (ft/s)	Contracted Discharge (cfs)	Contracted Depth (ft)	Contracted Width (ft)	
1	2	4	69800	49	390	
Measurement Number	Uncontracted Avg Vel (ft/s)	Uncontracted Discharge (cfs)	Uncontracted Depth (ft)	Uncontracted Width (ft)	Channel Contraction Ratio	
1	2.9	32000	34	360	0.54	
Measurement Number	Pier Contraction Ratio	Scour Location	Eccentricity	Sediment Transport	Bed Form	Debris Effect
1	---	Main Channel	0.2	Live-Bed	Unknown	Unknown
Measurement Number	D95 (mm)	D84 (mm)	D50 (mm)	D16(m)	Sigma	Bed Material Cohesion
1	0.5	0.46	0.36	0.25	---	Non-cohesive

COMPUTED SCOUR

A calibrated HEC-RAS model of the site was developed to assess how accurately the scour for this flood could have been predicted. The pre-flood geometry of the bridge section was simulated with a HEC-RAS model developed in 1994 as part of a floodplain delineation project for Scott County, MN. A separate model was developed by the USGS with the geometry data collected during the April, 2001 flood and the subsequent low-flow floodplain survey. The discharge measured on 4/17/2001 (73,200 cfs) was then modeled with the pre-flood and flood bathymetry to determine the hydraulic parameters needed for HEC-18 scour computations.

Abutment Scour

Abutment scour was computed in HEC-RAS by both the Froehlich equation and the HIRE equation. The hydraulic parameters taken from the HEC-RAS output were also used to calculate abutment scour using the Sturm abutment scour equations. The data contained in Table 10 show although most equations grossly overpredicted the scour at the left and right abutments, the HIRE with hydraulic input from the one-dimensional

model incorrectly predicted more scour at the right abutments. The HIRE equation, which includes the velocity at the tip of the abutment, most likely predicted the more scour at the right abutment due to the inability of the HEC-RAS model to accurately simulate the extreme velocity magnitudes that were measured in the field at the left abutment. Overall, the one dimensional step-backwater model was unable to accurately simulate the complex hydrodynamics near the abutments attributed to the high level of flow contraction through the bridge opening.

Table 10. Comparison of observed to model-computed abutment scour at S.R. 25 over the Minnesota River near Belle Plaine, MN.

Date	Abutment	Location	Local Scour Depth			
			Observed (ft)	Froehlich Equation (ft)	HIRE Equation (ft)	Sturm Equation (ft)
4/17/01	Left	Upstream	18	40.3	31.0	40.5
4/17/01	Right	Upstream	4	30.7	38.3	17.4

Contraction Scour

The contraction scour was computed in HEC-RAS by allowing the model to use the default equation (live-bed or clear-water) depending upon the hydraulic conditions computed by the model. The results of the model are compared with observed contraction scour in Table 11.

Table 11. - Comparison of observed to model-computed contraction scour at S.R. 25 over the Minnesota River near Belle Plaine, MN.

Date	Contraction Scour Depth	
	Observed (ft)	LiveBed (ft)
4/17/01	15	35.4

REFERENCES

Any questions regarding the S.R. 25 bridge over the Minnesota River should be directed to the following points of contact:

1. David Mueller, U.S. Geological Survey
Louisville, KY
Phone: (502) 493-1935
e-mail: dmueller@usgs.gov

2. Chad Wagner, U.S. Geological Survey
Raleigh, NC
Phone: (919) 571-4021
e-mail: cwagner@usgs.gov

SUPPORTING DATA

The following is a listing of supporting files that are associated with the S.R. 25 bridge:
MN25.jpg – contour plot of detailed bathymetry data collected during April, 2001 flood.
MN25.lpk - contour plot of detailed bathymetry data collected during April, 2001 flood, displayed in AmTec's Tecplot software package.

Site Photos:

DSCN0068.jpg - DSCN0107.jpg - Photos taken during April, 2001 flood and description of each photo are documented in MN25_Photos.doc Word file.

HWY250041.jpg - HWY250068.jpg - Photos taken during October, 2001 low-flow survey, description for each is documented in MN25_Post-Flood_Photos.doc Microsoft Word file.

Minn25.jpg - USGS topo quad of the bridge site.

BellePlaine(Aerial).jpg - Aerial photo of MN 25 bridge site

BellePlaine(Aerial)2.jpg - Aerial photo of MN 25 bridge site

BellePlaine(Aerial)3.jpg - Aerial photo of MN 25 bridge site

BellePlaine(Aerial)4.jpg - Aerial photo of MN 25 bridge site

Surveyed Sections:

DS_xsection(HEC-RAS).xls - Excel spreadsheet containing surveyed data for the exit section used in a HEC-RAS model of the reach.

US_xsection(HEC-RAS).xls - Excel spreadsheet containing surveyed data for the approach section used in a HEC-RAS model of the reach.

100'_US.xls - Excel spreadsheet containing surveyed data for the section 100' upstream of bridge; location of overbank scour hole.

DS_Face.xls - Excel spreadsheet containing surveyed data for the downstream bridge face.

US_Face.xls - Excel spreadsheet containing surveyed data for the upstream bridge face.

Hwy25_HEC-Ras.xls - Excel spreadsheet summarizing the elev. and stationing for all sections in the HEC-RAS model of the reach.

MN25_GrainSizeDist.xls - Bed material grain size distribution for the site, determined by analysis of samples collected during post-flood survey.

ADCP_Data.zip - WinZip file containing all ADCP data collected in the reach during April, 2001 flood. The ADCP 3-D velocity data for each transect has been processed into depth-integrated 2-D velocity data and summarized in the .vel files.

CASE STUDY #4

State Route 37 over the James River near Mitchell, South Dakota

SITE OVERVIEW

The study site is located on the James River 20 miles north of the town of Mitchell on State Highway 37. The site is approximately 4.5 miles downstream from the USGS gaging station near Forestburg (06477000) and located in a highly rural/agricultural landscape with moderate topographic relief. High flow measurements for the Forestburg gaging station are actually made from the SR 37 bridge therefore a wire weight is installed on the upstream side of the bridge. The period of record for the station is from March 1920 to the current year, with an annual mean flow of 493 cfs, and an instantaneous peak flow of 25,600 cfs recorded on April 6, 1997. The South Dakota USGS measured an approximate peak of 17,100 cfs during the flood of April 2001 during which the USGS National Bridge Scour Team in cooperation with NCHRP and the University of Louisville made real-time bridge scour measurements at the site. A manned boat was deployed during the April 2001 flood and detailed scour data was collected with a 1200 kHz acoustic Doppler current profiler (ADCP). The site was revisited in October, 2001 during low-water to survey the floodplains, collect bed material samples and inspect for remnants of scour associated with the spring flood.

There was no road overtopping nor any relief bridges associated with the SR 37 bridge; therefore, all of the flow in the James River contracted and passed through the bridge opening. The bridge is a concrete girder, three span structure supported by two groups of cylindrical piers (3 in each group) which are both founded on steel piles. The upper 10-15' of the bed is comprised of a sandy-silt followed by 10-20 ft of silty-clay.

A summary of the general site information is found in Table 1.

A step-backwater hydraulic model (HEC-RAS) of the S.R. 37 site was developed and calibrated by the USGS using channel geometry and field hydraulic measurements collected during the April, 2001 flood. The model was used to predict the amount of abutment and contraction scour expected for various bathymetric configurations in the reach based on one-dimensional hydraulic parameters and equations from HEC-18.

Table 1. Site information

Site Characteristic	Description
County	Sanborn
Nearest City	Mitchell
State	South Dakota
Latitude	43°56'33''
Longitude	98°01'49''
Route Number	37
Route Class	State
Stream Name	James River

Hydrologic Conditions

Greater than normal precipitation starting with late fall rains in 2000, greater than normal snowfalls, a delayed snowmelt, and above average rains in April, all contributed to the upper Midwestern flooding in the spring of 2001. The James River basin received a surplus of 10 inches of precipitation through the winter of 2000-2001 and the early part of spring 2001. The temperatures in February, March and the first part of April were 10-15 degrees below normal, which delayed the typical period of snowmelt enough to coincide with a period of above average rainfall associated with a series of cyclonic weather systems characteristic of early spring.

A peak discharge of 17,100 cubic feet per second (cfs) was measured at the site during the April 10, 2001 flood, which has approximately a 45-year flood frequency according to the peak flow frequency analysis, developed for the Forestburg (06477000) USGS gaging station. The discharge measured by the USGS during the real-time scour measurements on April 15, 2001 was 15,200 cfs, which is approximately a 35-year discharge.

DISCUSSION OF CONTRACTED SITE

The bridge had a geometric contraction ratio of around 0.48, with a large majority of the contracted flow coming from the left floodplain. A berm located approximately 100 feet upstream of the bridge on the left overbank directed the contracting flow into the channel upstream of the left abutment (see Figure 1).



Figure 1. Looking upstream at left floodplain and berm, from S.R. 37 bridge deck during April, 2001 flood.

Bridge Data

The structure (#56-150-176) is a 42 ft wide, pre-stressed girder bridge with 3 - 120' spans supported by two piers, both located in the main channel of the James River. Pier #1 is

on the left, looking downstream, and consists of 3 separate 3.75 ft diameter cylindrical piles. Pier 2 is on the right and also consists of 3 separate 3.75 ft diameter cylindrical piles. The bridge has a type III contracted opening, meaning it has sloping embankments and sloping spillthrough abutments. The bridge has a 2.897% downhill grade in the northbound direction. The low-chord elevation is 1232.6 ft above sea level. The bridge characteristics pertinent to scour are summarized in Table 2.

Table 2. Bridge data

Bridge Characteristic	Description
Structure Number	56-150-176
Length (ft)	353
Width (ft)	42
Spans	3
Vertical Configuration	Sloping
Low Chord Elev (ft)	1232.6
Upper Chord Elev (ft)	1242.8
Overtopping Elev (ft)	1240.6
Skew (degrees)	-35
Guide Banks	None
Waterway Classification	Main
Year Built	1992
Avg. Daily Traffic	Unknown
Plans on File	Yes
Parallel Bridges	No
Continuous Abutments	N/A

Geomorphic Setting

The geomorphic setting and channel alignment of the James River at the SR 37 bridge is depicted in Figure 2 as well as a graphical representation of the effects of the roadway embankment on the flood-flow. Inspection of the "approach" section (one bridge width upstream) revealed a large discharge relative to that of the contracted opening. It was discovered that the blockage caused by the roadway embankment forced a majority of the left floodplain flow back into the main channel before the "approach" section.

A contour plot of the channel bathymetry collected during the April 2001 flood can be found in Figure 3 and a USGS 7.5 minute quadrangle topographic map of the site is shown in Figure 4. Data characterizing the geomorphic setting is summarized in Table 3.

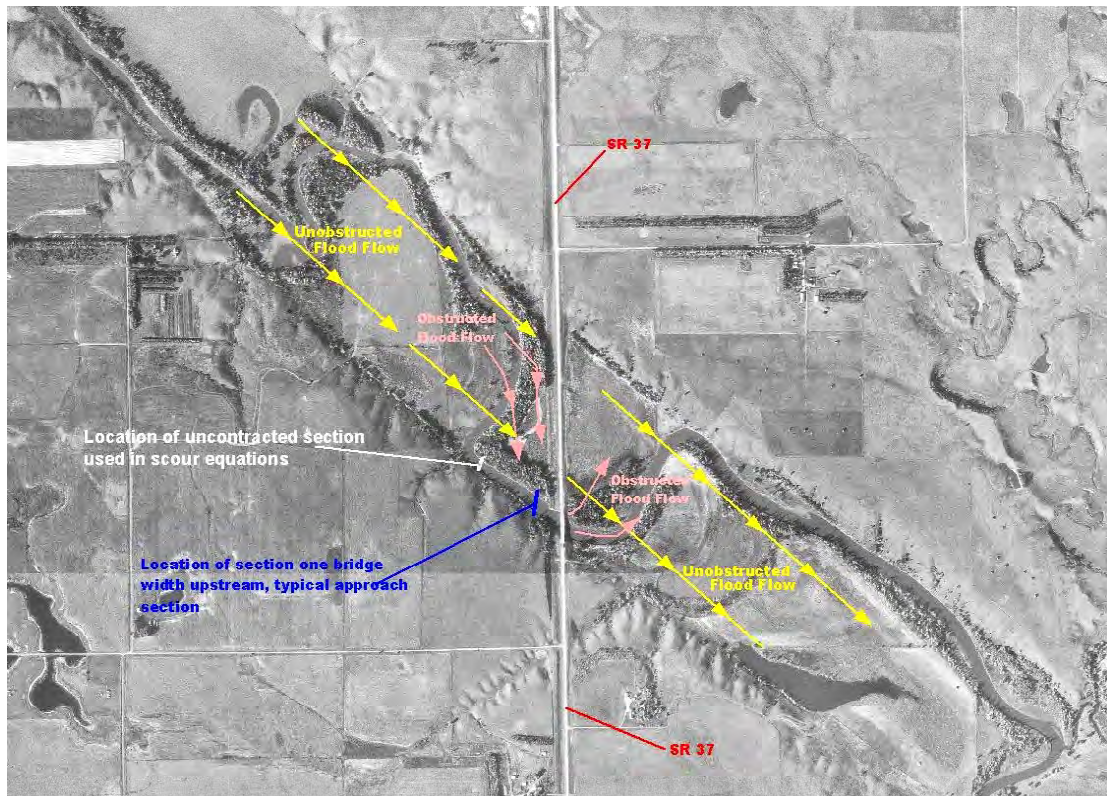


Figure 2. Geomorphic setting and channel alignment for the James River at SR 37 bridge near Mitchell, SD

Table 3. Geomorphic data

Geomorphic Characteristic	Description
Drainage Area	16010
Slope in Vicinity (ft/ft)	.000104
Flow Impact	Left
Channel Evolution	Pre-modified
Armoring	Unknown
Debris Frequency	Occasional
Debris Effect	Local
Stream Size	Medium
Flow Habit	Perennial
Bed Material	Silt
Valley Setting	Low relief
Floodplain Width	Narrow
Natural Levees	Unknown
Apparent Incision	None
Channel Boundary	Alluvial
Banks Tree Cover	Medium
Sinuosity	Meandering
Braiding	None
Anabranching	None
Bars	Narrow
Stream Width Variability	Equiwidth



Figure 3. Bathymetric contour plot of James River in the vicinity of S.R. 37 bridge, collected during April, 2001 flood.

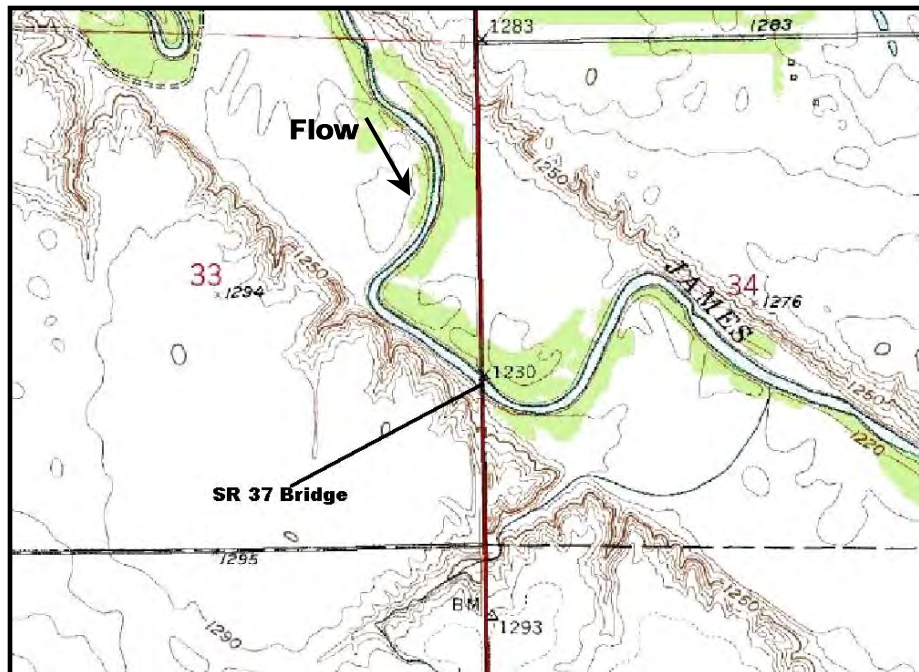


Figure 4. USGS topographic map of S.R. 37 bridge over the James River near Mitchell, SD

Bed Material Data

Bed material samples were collected at three locations in the main channel on 10/26/2001 with a BM-54H grab sampler; 150 feet upstream of the bridge, in the bridge opening, and 200 feet downstream of the bridge. The samples consisted primarily of a sandy clayey-silt and had a $D_{50} = .02$ mm. The grain size distribution of all the samples were very similar with the only difference found in the D_{95} of the samples in the bridge opening, which was larger (1.4 mm) than the D_{95} of the samples collected upstream and downstream of the bridge (.27 and .26 mm, respectively). The grain size distributions for the three sample locations are shown in Figures 5-7.

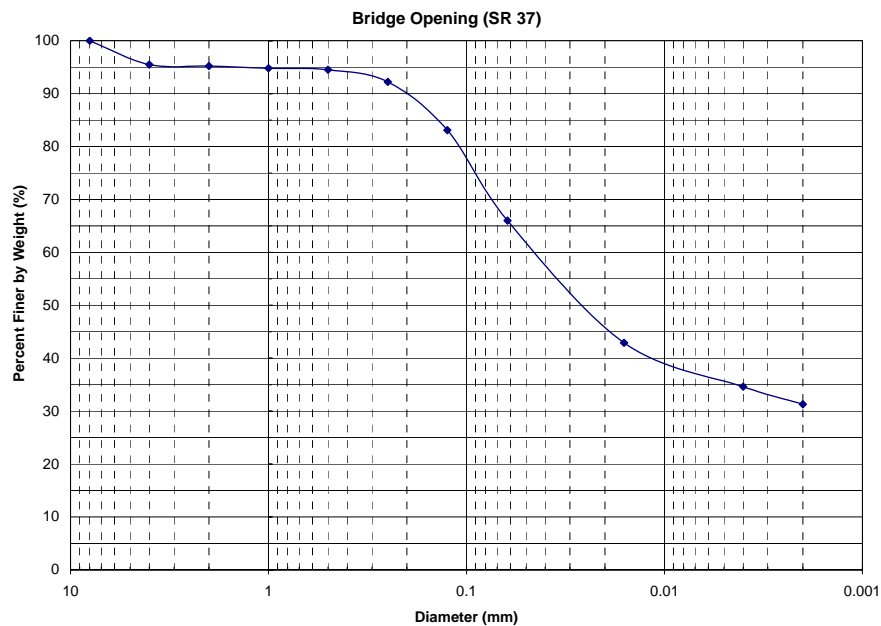


Figure 5. Grain size distribution for the bed material sample collected in the SR 37 bridge opening

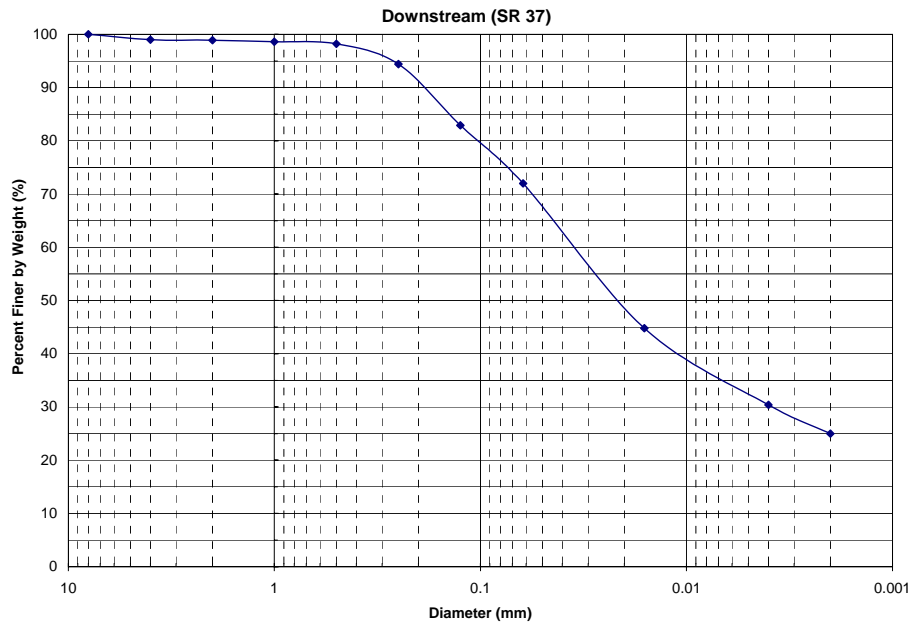


Figure 6. Grain size distribution for the bed material sample collected downstream of the SR 37 bridge.

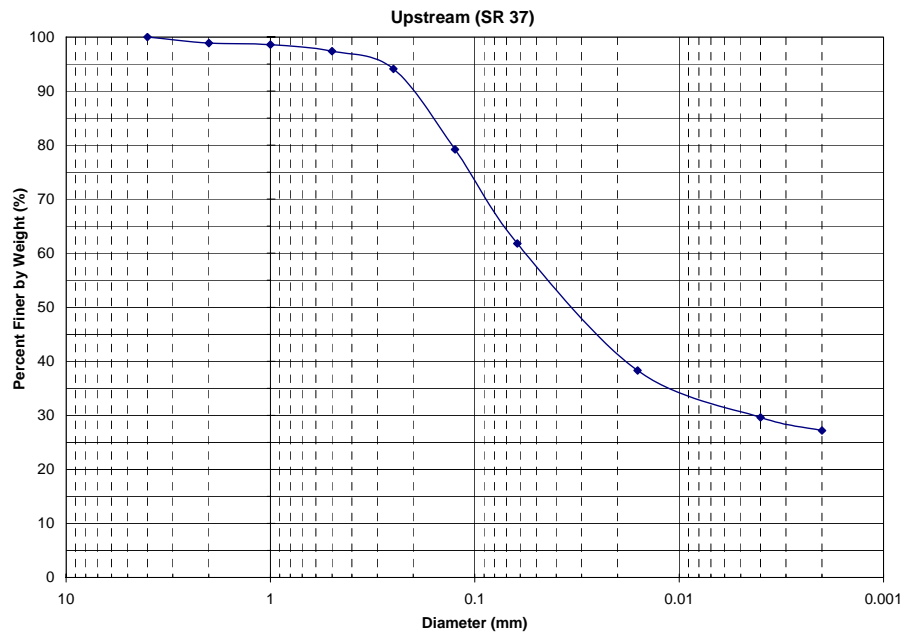


Figure 7. Grain size distribution for the bed material sample collected upstream of the SR 37 bridge.

Roughness Coefficients

A distribution of Manning's n values is provided in Table 4.

Table 4. Manning's n values for the James River at the S.R. 37 bridge. (fldpln, floodplain; chnl, channel; rt, right)

Left Fldpln	Main Cnhl	Rt Fldpln
0.08	0.034	0.065

Abutment Details

The bridge has sloping spill-through abutments with no scour protection. During the site reconnaissance in October, 2001 scour was observed on the left abutment (see Figure 8). The abutment characteristics are summarized in Table 5.

Table 5. Abutment data

Abutment Characteristic	Description
Left Station	35917.33
Right Station	35567.83
Left Skew (deg)	0
Right Skew (deg)	0
Left Abutment Length (ft)	67
Right Abutment Length (ft)	67
Left Abutment to Channel Bank (ft)	0
Right Abutment to Channel Bank (ft)	0
Left Abutment Protection	None
Right Abutment Protection	None
Contracted Opening Type	III*
Embankment Skew (deg)	-35
Embankment Slope (ft/ft)	.09
Abutment Slope (ft/ft)	2
Wingwalls	No
Wingwall Angle (deg)	N/A

* - Type III opening has sloping abutments and sloping spillthrough abutments.



Figure 8. Picture of the bank failure at the left abutment of the S.R 37 bridge over the James River near Mitchell, SD taken during low-flow survey following April, 2001 flood.

Pier Details

Pier #1 is on the left, looking downstream, and consists of three 3.75 ft diameter cylindrical piles. Pier #2 is on the right, looking downstream, and also consists of three 3.75 ft diameter cylindrical piles. The elevation at the foundation bottom of Pier #1 and Pier #2 is 1190.84 ft and 1190.83 ft, respectively. The foundation of each pier is supported by 13 steel H-piles pilings. The pier characteristics are summarized in Table 6.

Table 6. Pier data (--, not available)

Pier ID	Bridge Station (ft)	Alignment	Highway Station	Pier Type	# of Piles	Pile Spacing (ft)
1	-	35	35+80.3	Group	3	19.5
2	-	35	35+68.2	Group	3	19.5

Pier ID	Pier Width (ft)	Pier Shape	Shape Factor	Length (ft)	Protection	Foundation
1	3.75	Round	--	51	None	Piles
2	3.75	Round	--	51	None	Piles

Pier ID	Top Elevation (ft)	Bottom Elevation (ft)	Foot or Pile Cap Width (ft)	Cap Shape	Pile Tip Elevation (ft)
1	1194.84	1190.84	10.5	Square	--
2	1194.83	1194.83	10.5	Square	--

Surveyed Elevations

Water-surface elevations were measured from the bridge deck using a USGS wire-weight gage located on the upstream bridge face. The vertical control for all surveyed elevations at the site was established from the wire-weight gage check-bar (elevation 37.849 ft, 1246.189 ft above sea level). The elevations used to dimension the bridge deck were

determined from the bridge plans. A summary of the measured water surface elevations is presented in the Table 7.

Table 7. Water-surface elevation measured from the S.R. 37 bridge deck.

Date	Time	Upstream (ft)	Downstream (ft)
4/10/2001	----	1227.04	--
4/15/2001	12:30	1224.20	--

The low-water survey of the floodplains in the approach and exit sections utilized a local right-hand coordinate system, which was established with the positive y-axis in the upstream direction and the x-axis parallel to the upstream face of the bridge. This resulted in x-coordinates increasing from right to left. Since step backwater models typically use left to right coordinates, stationing was added which increases from left to right.

PHOTOS



Figure 9. Looking upstream towards left floodplain from bridge deck



Figure 10. Looking at upstream bridge face from berm on left bank



Figure 11. Looking at downstream left floodplain from bridge deck



Figure 12. Post-flood conditions, looking upstream at S.R. 37 bridge from right bank



Figure 13. Post-flood conditions, looking upstream from S.R. 37 bridge deck



Figure 14. *Post-flood conditions, looking at upstream left floodplain from S.R. 37 bridge.*



Figure 15. *Post-flood conditions, looking at downstream bendway from S.R. 37 bridge.*



Figure 16. *Post-flood conditions, looking at downstream left floodplain from S.R. 37 bridge.*

MEASURED SCOUR

All bathymetry data were collected with a 1200 kHz ADCP and horizontally referenced with a differentially corrected global positioning system (DGPS). Cross sections in the main channel (tree line of right bank to tree line of left bank) were collected throughout the bridge reach, which extended 1500 ft upstream and 1200 ft downstream of the S.R. 37 bridge. Data could not be collected in the upstream floodplain because of heavy vegetation, but an approximation of the flow blocked by the road embankments was developed by cutting off the discharge entering the main channel from left floodplain with the ADCP. A survey of the upstream and downstream floodplains was conducted after the flood during a low-water site visit October 28-29, 2001.

Abutment Scour

The flow separation point on the left valley wall was too far upstream to get a measurement and much of the floodplain flow re-entered the channel by the time it reached the section located one bridge-width upstream. As previously discussed, a section was made with the ADCP along the left bank of the channel to cut-off the floodplain flow entering the channel and gain insight to the amount of discharge that was being blocked by the roadway embankment. The measured live-bed abutment scour at the upstream left abutment was estimated to be 4 feet with accuracy of +/- 2 feet. No scour was detected at the right abutment.

The velocity reported for “at the abutment” is the maximum velocity observed in the area of the scour hole. The site characteristics pertinent to abutment scour are summarized in Table 8.

Table 8. Abutment scour data (--, not available; ft/s, feet per second; cfs, cubic feet per second; Abut, abutment; Avg, average; US, upstream; DS, downstream)

Measurement Number	Abutment	Date	Time	US/DS	Scour Depth (ft)	Accuracy (ft)
1	Left	4/15/2001	13:00	Upstream	4.0	2

Measurement Number	Sediment Transport	Velocity at Abut (ft/s)	Depth at Abut (ft)	Discharge Blocked (cfs)	Avg Velocity Blocked (ft/s)	Avg Depth Blocked (ft)
1	Live-bed	3.8	20	8200	2	6

Measurement Number	Embankment Length (ft)	Bed Material Cohesion	D50 (mm)	Sigma	Debris Effect
1	1500	Mildly	0.02	--	Insignificant

Contraction Scour

Inspection of the "approach" section (one bridge width upstream) revealed a large discharge relative to that of the contracted opening. It was discovered that the blockage caused by the roadway embankment forced a majority of the left floodplain flow back into the main channel at the "approach" section (see Figure 2). A cross section made further upstream showed much less discharge, which was consistent with channel discharge downstream of the bridge opening. Data from an ADCP section that cut-off the left floodplain flow accounted for all but 500 cfs of the difference in discharge between the "approach" section and the section further upstream. The section furthest upstream was used as the uncontracted section because it was most representative of the flow naturally carried by the main channel had the roadway embankment not be present. The following widths and corresponding hydraulic characteristics for both the contracted and uncontracted sections are representative of the portion of the channel in which live-bed transport would be expected. The measured live-bed contraction scour was estimated to be 3 feet with accuracy of +/- 1 foot. The site characteristics pertinent to contraction scour are summarized in Table 9.

Table 9. Contraction scour data (---, not available; ft/s, feet per second; cfs, cubic feet per second; US, upstream; DS, downstream; Avg, average)

Measurement Number	Contracted Date	Contracted Time	Uncontracted Date	Uncontracted Time	US/DS	Scour Depth (ft)
1	4/15/2001	12:30	4/15/2001	13:35	US	3

Measurement Number	Accuracy (ft)	Contracted Avg Vel (ft/s)	Contracted Discharge (cfs)	Contracted Depth (ft)	Contracted Width (ft)
1	1	4.2	13900	18	206

Measurement Number	Uncontracted Avg Vel (ft/s)	Uncontracted Discharge (cfs)	Uncontracted Depth (ft)	Uncontracted Width (ft)	Channel Contraction Ratio
1	3.5	6730	18.8	110	0.48

Measurement Number	Pier Contraction Ratio	Scour Location	Eccentricity	Sediment Transport	Bed Form	Debris Effect
1	---	Main Channel	0.05	Live-Bed	Unknown	Insignificant

Measurement Number	D95 (mm)	D84 (mm)	D50 (mm)	D16(m)	Sigma	Bed Material Cohesion
1	0.27	0.16	0.02	--	---	Mildly

COMPUTED SCOUR

A calibrated HEC-RAS model of the site was developed to assess how accurately the scour for this flood could have been predicted. The pre-flood geometry of the bridge section was simulated with a HEC-RAS model utilizing the channel geometry from the original bridge plans and the low-flow floodplain survey. A separate model was developed by the USGS with the geometry data collected during the April, 2001 flood and the subsequent low-flow floodplain survey. The discharges measured during the April, 2001 flood were then modeled with the pre-flood and flood bathymetry to determine the hydraulic parameters needed for HEC-18 scour computations.

Abutment Scour

Abutment scour was computed in HEC-RAS by both the Froehlich equation and the HIRE equation. The hydraulic parameters taken from the HEC-RAS output were also used to calculate abutment scour using the Sturm abutment scour equation. The data contained in Table 10 show the model grossly overpredicted the scour at the left abutment but correctly predicted no scour at the right abutment. Overall, the one dimensional step-backwater model was unable to accurately simulate the complex hydrodynamics associated with the relationship between the geomorphic setting and bridge alignment.

Table 10. Comparison of observed to model-computed abutment scour at S.R. 37 over the James River near Mitchell, SD.

Date	Location	Observed (ft)	Local Scour Depth			
			Froehlich Equation (ft)	HIRE Equation (ft)	Sturm Equation (ft)	
4/15/01	Left	Upstream	4	19.3	11.1	32.4
4/15/01	Right	Upstream	0	0	0	0

Contraction Scour

The contraction scour was computed in HEC-RAS by allowing the model to use the default equation (live-bed or clear-water) depending upon the hydraulic conditions computed by the model. The results of the model are compared with observed contraction scour in Table 11.

Table 11. Comparison of observed to model-computed contraction scour at S.R. 37 over the James River near Mitchell, SD.

Date	Contraction Scour Depth	
	Observed (ft)	LiveBed (ft)
4/15/01	3	14.7

REFERENCES

Any questions regarding the S.R. 37 bridge over the James River should be directed to the following points of contact:

1. David Mueller, U.S. Geological Survey
9818 Bluegrass Parkway
Louisville, KY 40299
Phone: (502) 493-1935
e-mail: dmueller@usgs.gov
2. Chad Wagner, U.S. Geological Survey
3916 Sunset Ridge Road
Raleigh, NC 27613
(919) 571-4021
e-mail: cwagner@usgs.gov

SUPPORTING DATA

The following is a listing of supporting files that are associated with the S.R. 37 bridge:

SR37_DetailExample.doc - detailed summary of the site and data collection during the April, 2001 flood.

SR37.lpk - contour plot of detailed bathymetry data collected during April, 2001 flood, displayed in AmTec's Tecplot software package.

SD37Contour.pdf - contour plot of detailed bathymetry data collected during April, 2001 flood in a PDF format.

Site Photos:

DSCN0003.jpg - DSCN0008.jpg & DSCN0034.jpg - DSCN0053.jpg - Photos taken during April, 2001 flood, description of each photo is documented in SR37_Photos.doc Word file.

SR370021.jpg - SR370037.jpg - Photos taken during October, 2001 low-flow survey, description for each is documented in Post-Flood_Photos.doc Microsoft Word file.

SR37(TopoQuad).jpg - Topo map of bridge reach

SR37.jpg - Descriptive Digital Ortho Quad image of the bridge site

SR37(ADCP_Data).xls - Excel file with multiple worksheets containing ADCP depth integrated velocities collected during April, 2001 flood.

Surveyed Sections:

SR37_(DS_Hec-Ras).xls - Excel spreadsheet containing surveyed data for the exit section used in a HEC-RAS model of the reach.

SR37_(US_Hec-Ras).xls - Excel spreadsheet containing surveyed data for the approach section used in a HEC-RAS model of the reach.

DS_Face.xls - Excel spreadsheet containing surveyed data for the downstream bridge face.

US_Face.xls - Excel spreadsheet containing surveyed data for the upstream bridge face.

HEC-RAS_Summary.xls - Excel spreadsheet summarizing the elev. and stationing for all sections in the HEC-RAS model of the reach.

GrainSizeDist.xls - Bed material grain size distribution for the site, determined by analysis of samples collected during post-flood survey.

CASE STUDY #5

State Route 35 over Conehoma Creek near Kosciusko, Mississippi

SITE OVERVIEW

The State Highway 35 crossing of Conehoma Creek is located in Attala County, approximately 3.7 miles south of Kosciusko, MS and 2.5 miles upstream from the confluence of the Yockanookany River (see Figure 1). The Yockanookany River USGS gaging station (02484000) is located on S.R. 35 approximately 1.5 miles north of Conehoma Creek. The S.R. 35 bridge over Conehoma Creek (No. 153.1) is 120 feet long near highway station 1642+58 with a span arrangement of 2 spans at 20 ft (feet), 1 span at 40 ft, and 2 spans at 20 ft. The drainage area at the site is about 10.3 mi² (square miles). The length of the channel from the site to the basin divide is about 6.0 mi (miles) and the average slope of the channel between points located at 10 and 85 percent of the length is about 17 ft/mi (feet per mile). Average channel and valley slopes in the vicinity of the crossing are about 5.4 ft/mi. The highway alignment is near perpendicular to the channel and the flood plain in the vicinity of the crossing.

The floods of April 12, 1979, and April 5, 2001, were significant at this site and lead to substantial contraction scour. The USGS, Mississippi District conducted post-flood scour surveys at the S.R. 35 bridge following both of the mentioned floods. Based on Mississippi Department of Transportation (MDOT) geotechnical reports in the area and the measured scour data, Conehoma Creek appears to have scoured down into or near the top of the Zilpha Clay formation during the floods of April 12, 1979, and the April 5, 2001.

The USGS recovered flood marks on May 9, 1979, along the upstream and downstream sides of the highway following the extreme flood of April 12, 1979. A private contractor took photographs and surveyed a bridge cross-section, an approach cross-section at the site in June 1979. This bridge cross-section and the surveyed approach cross section were used in a WSPRO step-backwater model to estimate the peak discharge that caused the surveyed upstream flood-mark elevation of 405.0 ft.

The MDOT obtained photographs and ground-to-grade information at the site on April 9, 2001, after the severe flooding that occurred on April 5, 2001. The USGS surveyed high-water marks and channel geometry S.R. 35 bridge reach on February 13, 2002. The bridge section was surveyed during a low-flow site visit on October 27, 1994, for a scour evaluation report provided to the MDOT on February 10, 1995. A pre-scour bridge section was approximated using the October 27, 1994, survey and the 1979 surveyed approach cross section to estimate (using the WSPRO model) the peak discharge that caused the surveyed April, 2001 flood-mark elevation of 404.6 ft. The surveyed approach cross section was modified where considered not representative and transferred upstream and downstream using the slope in the vicinity of the crossing to obtain the additional cross sections needed for the WSPRO analysis.

Scour estimates for both the 1979 and 2001 floods were also computed with the WSPRO simulations. A summary of the general site information on the site is found in Table 1.

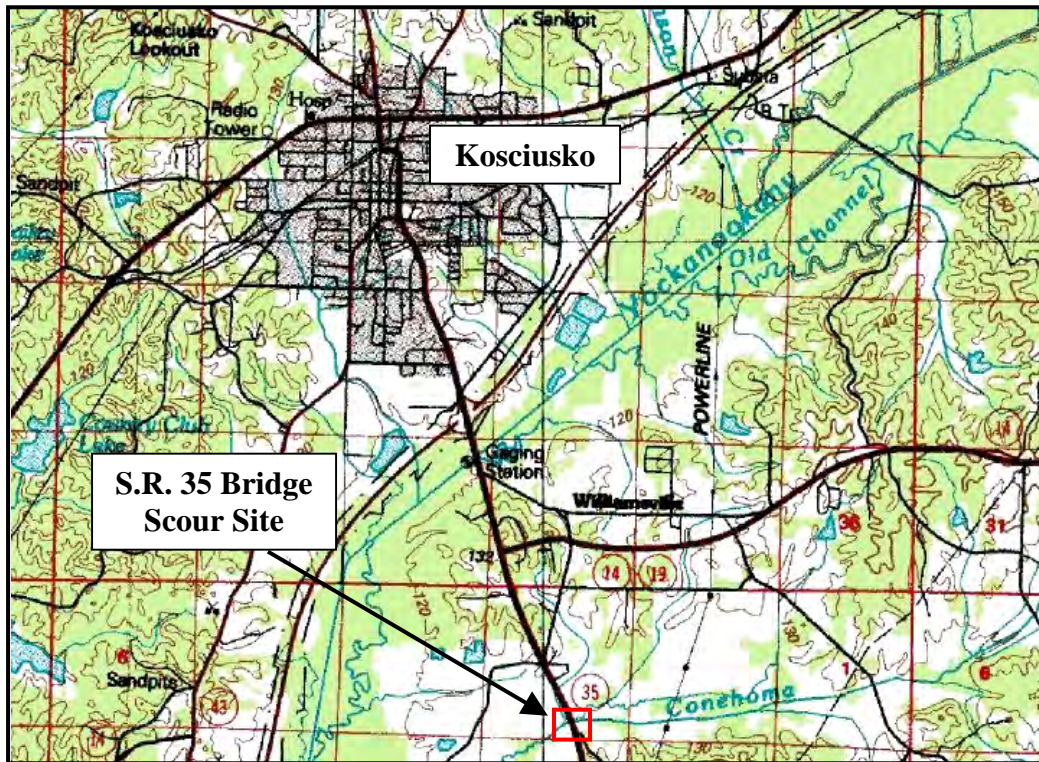


Figure 1. Location map for the S.R. 35 bridge scour site over Conehoma Creek near Kosciusko, MS

Table 1. Site information

Site Characteristic	Description
County	Attala
Nearest City	Kosciusko
State	Mississippi
Latitude	33°00'22''
Longitude	89°33'56''
Route Number	35
Route Class	State
Stream Name	Conehoma Creek

Hydrologic Conditions

The hydrologic conditions that were responsible for the 1979 and 2001 floods were associated with cyclonic precipitation that merged with an excessive amount of Gulf of Mexico moisture. Peak discharges of 10,200 cubic feet per second (cfs) and 6,750 cfs were estimated with WSPRO for the site during the April 12, 1979 and April 5, 2001

floods, respectively. The estimated peak discharges for both of these floods were greater than the 100-year flood estimated using procedures outlined in the 1991 USGS report, "Flood Characteristics of Mississippi Streams."

DISCUSSION OF CONTRACTED SITE

The cross section surveyed at the downstream side of the bridge in June 1979, April 2001 and February 2002 indicate scour occurred at the bridge during the 1979 and 2001 floods. The scour likely occurred as the flood was peaking and perhaps beginning to recede. When the surveyed bridge sections from 1979 and 1994 were compared, it was apparent that some repairs (probably consisting of some earthwork and riprap) had been made.

The bridge was under pressure flow conditions for both of the surveyed floods and there was substantial road overflow during the April 1979 flood. Results of the WSPRO simulation for the April 12, 1979 flood indicated that about 8,970 cfs flowed through the bridge opening and about 1,230 cfs flowed over the highway embankment.

Bridge Data

Structure No. 153.1 has five spans supported by 2 intermediate single-pile bents (nos. 2 & 5) and 2 intermediate double-pile bents (nos. 3 & 4). The S.R. 35 bridge was built in 1941 and has spill-through abutments (type III contracted opening) with partial riprap protection. The piers and the abutments are founded on piling; the piling is driven to an elevation of 374-376 ft. The abutments are set back from the top of the channel banks. The bridge characteristics pertinent to scour are summarized in Table 2.

Table 2. Bridge data

Bridge Characteristic	Description
Structure Number	153.1
Length (ft)	120
Width (ft)	27
Spans	5
Vertical Configuration	Horizontal
Low Chord Elev (ft)	401.0
Upper Chord Elev (ft)	401.8
Overtopping Elev (ft)	404.4
Skew (degrees)	0
Guide Banks	None
Waterway Classification	Main
Year Built	1941
Avg. Daily Traffic	4,200
Plans on File	Yes
Parallel Bridges	No
Continuous Abutments	N/A

Geomorphic Setting

Based on MDOT geotechnical reports in the area, the stream has very likely scoured down into or near the top of the Zilpha Clay formation during the floods of April 12, 1979, and the April 5, 2001. A 1997 MDOT geotechnical report for Yockanookany River at proposed State Highway 14 Bypass of Kosciusko, located about 1.9 mi northwest of this site, indicates that the top of the Zilpha formation possesses a cohesion of about 1,320 pounds per cubic foot (lb/ft^3), a friction angle of 31 degrees, and a unit weight of $119 \text{ lb}/\text{ft}^3$. The 1941 test-pile reports at the S.R. 35 site noted that soil borings indicated sand stone at elevation 377.0 ft above sea level, and indicated a significant increase in bearing capacity at about the same elevation. Therefore the top of the Zilpha formation at the S.R. 35 bridge is likely at about elevation 377 ft, which is a good approximation of the maximum depth of scour.

The Conehoma Creek has a straight alignment upstream and downstream of the S.R. 35 bridge. A USGS 7.5 minute quadrangle topographic map of the site is shown in Figure 2. The aerial photo of the site taken in 1993 is shown in Figure 3. and reveals very different land covers in the vicinity of the bridge. The overbanks have heavy vegetation immediately upstream of the bridge whereas the downstream overbanks are strictly agricultural. Data characterizing the geomorphic setting is summarized in Table 3.

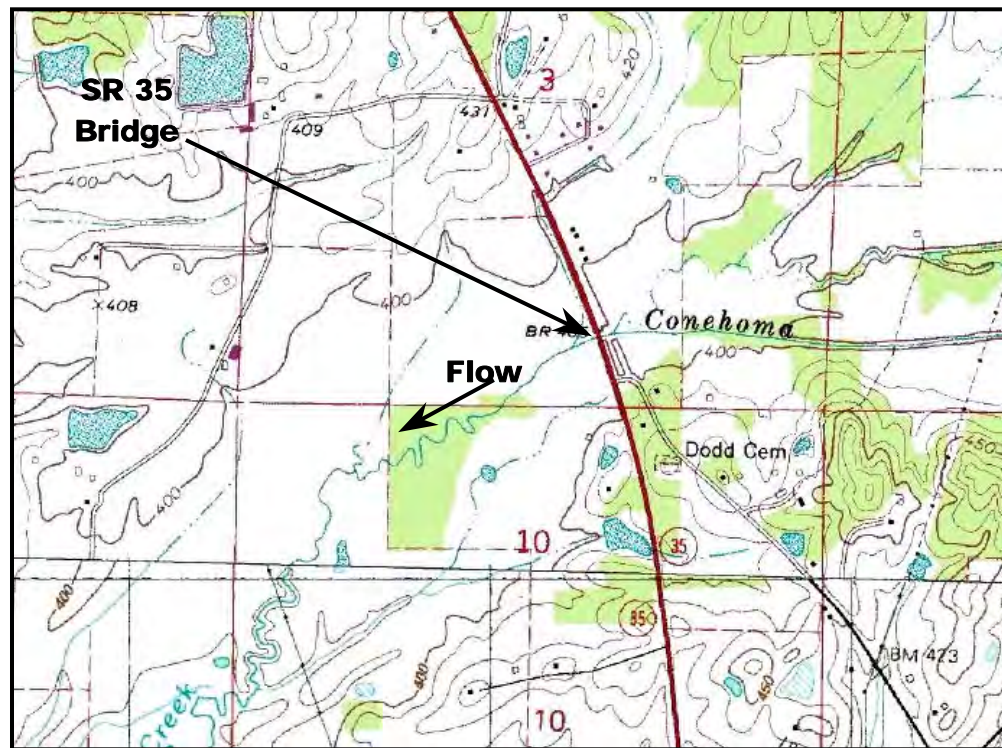


Figure 2. USGS topographic map of S.R. 35 bridge over the Conehoma Creek near Kosciusko, MS (elevations are in feet).

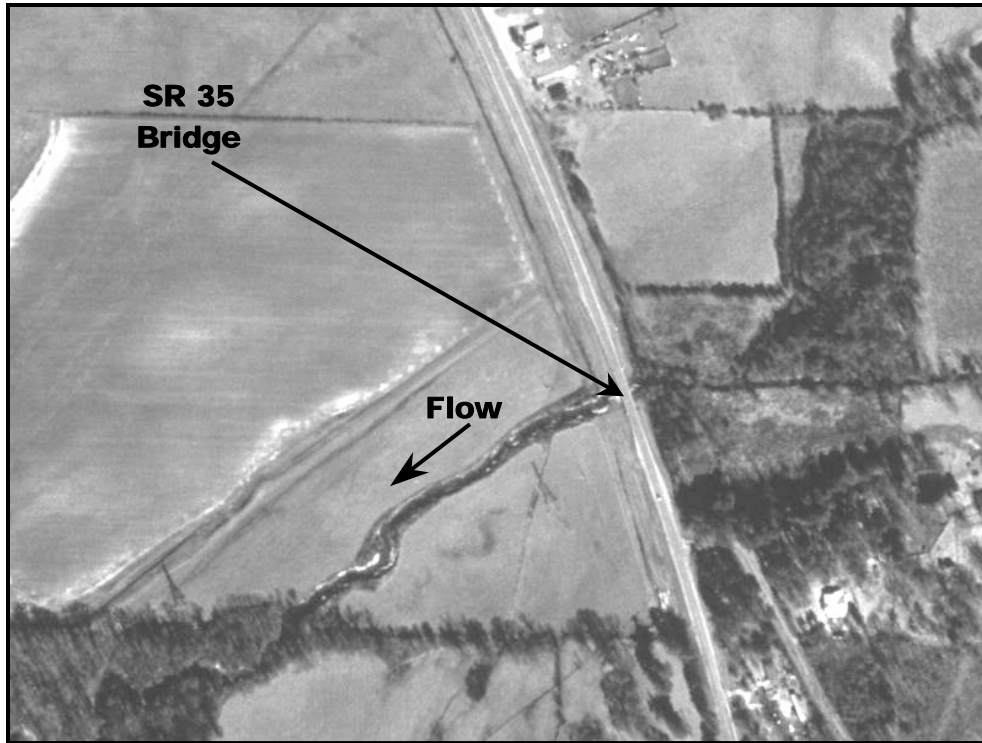


Figure 3. Aerial photo of the S.R. 35 bridge over Conehoma Creek near Kosciusko, MS.

Table 3. Geomorphic data

Geomorphic Characteristic	Description
Drainage Area	10.3
Slope in Vicinity (ft/ft)	.0010
Flow Impact	Straight
Channel Evolution	Unknown
Armoring	None
Debris Frequency	Unknown
Debris Effect	Unknown
Stream Size	Medium
Flow Habit	Perennial
Bed Material	Sand
Valley Setting	Low relief
Floodplain Width	Wide
Natural Levees	Unknown
Apparent Incision	None
Channel Boundary	Alluvial
Banks Tree Cover	Medium
Sinuosity	Sinuuous
Braiding	None
Anabranching	None
Bars	Unknown
Stream Width Variability	Unknown

Bed Material Data

Bed samples collected by the USGS on October 27, 1994, indicated the channel material was fine sand with a D_{84} of 0.29 mm, D_{50} of 0.10 mm, D_{16} of 0.017 mm, and a gradation coefficient of about 4.1. A 1997 MDOT geotechnical report for Yockanookany River at proposed State Highway 14 Bypass of Kosciusko, located about 1.9 mi northwest of this site, indicates that the top of the Zilpha clay formation has a D_{84} of about 0.37 mm, D_{50} of 0.16 mm, D_{16} of 0.026 mm, and a gradation coefficient of about 3.8.

Roughness Coefficients

A distribution of Manning's n values used in the WSPRO analyses is provided in Table 4.

Table 4. Manning's n values used in WSPRO model for Conehoma Creek at the S.R. 35 bridge. (fldpln, floodplain; chnl, channel; rt, right)

Location	Left Fldpln	Main Chnl	Rt Fldpln
Approach	0.10	0.050	0.10
Bridge	0.10	0.045	0.10
Exit	0.10	0.050	0.10

Abutment Details

The bridge has sloping spill-through abutments with partial scour protection. Bridge plans show that the abutments were partially protected with riprap, but photos taken after the 1979 flood are not clear enough to verify the presence of any type of scour protection. Photos of the abutments in 1994 (Figures 7 & 8) reveal that a dense layer of vegetation had been established on the top of the incised channel banks. The photo of the left abutment following the 2001 flood (Figure 8) illustrates that much of the vegetation had been removed, leaving behind exposed riprap. The length of the abutments and distance to channel for both abutments changed between 1979 and 2001 due to restabilization efforts of the Mississippi DOT. The abutment characteristics and the changes between 1979 and 2001 are summarized in Table 5.

Pier Details

The four piers are numbered from left to right, looking downstream and consist of groups of cylindrical timber piles. The piers are spaced at 20 ft intervals and aligned normal to the bridge and flow. Piers #1 and #4 are located on the overbank and Piers #2 and #3 are located in the main channel. The pier characteristics are summarized in Table 6.

Table 5. Abutment data

Abutment Characteristic	Description
Left Station	1642+58
Right Station	1643+78
Left Skew (deg)	0
Right Skew (deg)	0
Left Abutment Length (ft) 1979	674
Left Abutment Length (ft) 2001	707
Right Abutment Length (ft) 1979	1,397
Right Abutment Length (ft) 2001	1,344
Left Abut to Channel Bank (ft) 1979	708
Left Abut to Channel Bank (ft) 2001	741
Right Abut to Channel Bank (ft) 1979	1,441
Right Abut to Channel Bank (ft) 2001	1,388
Left Abutment Protection	Riprap
Right Abutment Protection	Riprap
Contracted Opening Type	III*
Embankment Skew (deg)	0
Embankment Slope (ft/ft)	1.5
Abutment Slope (ft/ft)	1.5
Wingwalls	No
Wingwall Angle (deg)	N/A

* - Type III opening has sloping abutments and sloping spillthrough abutments.

Table 6. Pier data (--, not available)

Pier ID	Bridge Station (ft)	Alignment	Highway Station	Pier Type	# of Piles	Pile Spacing (ft)
1	20	0	1642+78	Group	4	7
2	40	0	1642+98	Group	8	7
3	80	0	1643+38	Group	8	7
4	100	0	1643+58	Group	4	7

Pier ID	Pier Width (ft)	Pier Shape	Shape Factor	Length (ft)	Protection	Foundation
1	1.2	Cylindrical	--		Unknown	Piles
2	3	Cylindrical	--		Unknown	Piles
3	3	Cylindrical	--		Unknown	Piles
4	1.2	Cylindrical	--		Unknown	Piles

Pier ID	Top Elevation (ft)	Bottom Elevation (ft)	Foot or Pile Cap Width (ft)	Cap Shape	Pile Tip Elevation (ft)
1	--	--	--	N/A	374
2	--	--	--	N/A	375
3	--	--	--	N/A	376
4	--	--	--	N/A	376

Surveyed Elevations

Bridge data elevations were taken from MDOT plans, and are consistent with the 1929 National Geodetic Vertical Datum (NGVD) at the Conehoma Creek site. The Yockanookany River USGS gaging station's (02484000) gage datum is elevation 374.34 feet (NGVD). Water-surface elevations were determined by the USGS by post-flood surveys of high-water marks, which were flagged immediately following both floods. A summary of the measured water surface elevations and corresponding WSPRO estimated discharges is presented in Table 7.

Table 7. Water-surface elevations and corresponding estimated discharges for Conehoma Creek at the S.R. 35 bridge.

Date	Time	Upstream (ft)	Downstream (ft)	Discharge (cfs)
4/12/1979	----	405.0	402.6	10,200
4/5/2001	----	404.6	401.7	6,750

The low-water survey of the floodplains in the approach and exit sections utilized a local right-hand coordinate system, which was established with the positive y-axis in the upstream direction and the x-axis parallel to the upstream face of the bridge. This resulted in x-coordinates increasing from right to left. The WSPRO step backwater model requires the use of left to right coordinates (looking downstream), therefore stationing was added which increases from left to right.

PHOTOS

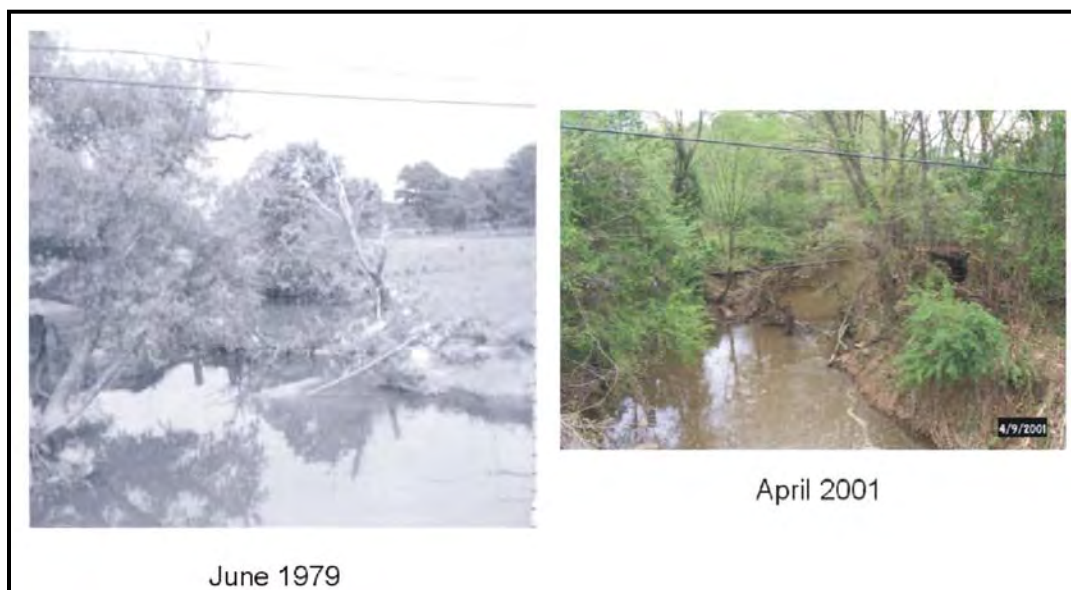


Figure 4. Photos looking upstream from S.R. 35 bridge following the floods in 1979 and 2001 on Conehoma Creek.

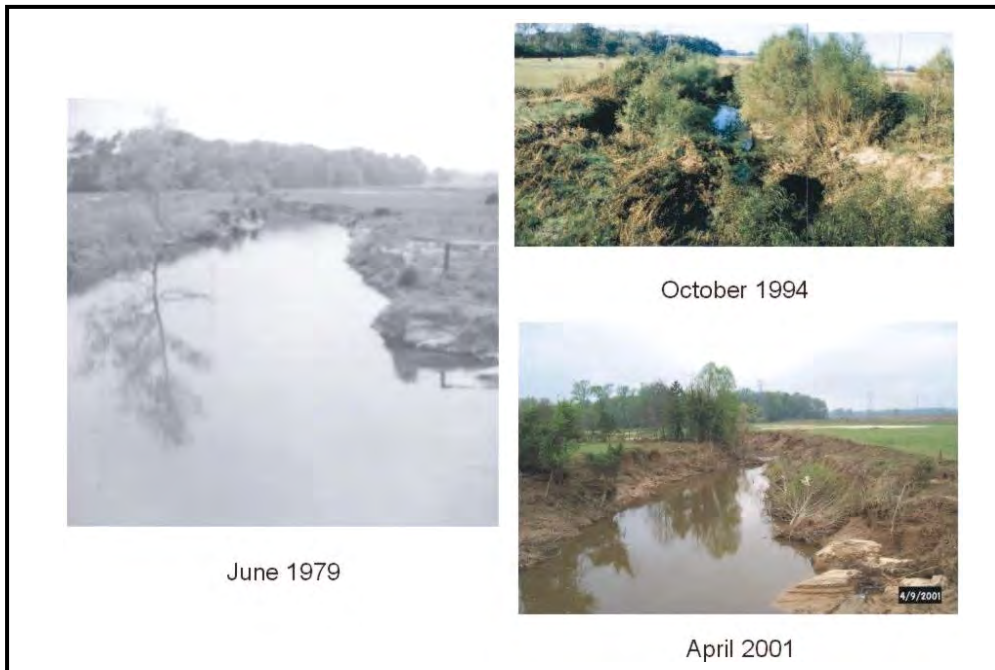


Figure 5. Looking downstream from the S.R. 35 bridge during the post-flood scour surveys in 1979 and 2001 and low-water survey in 1994 on Conehoma Creek.



Figure 6 Looking upstream through S.R. 35 bridge opening during October 24, 1994 survey on Conehoma Creek.



Figure 7. Looking downstream through the S.R. 35 bridge opening at left abutment and pile bent no. 2 following the 1979 and 2001 floods on Conehoma Creek.

MEASURED SCOUR

All measured scour data were collected during post-flood surveys of the S.R. 35 bridge section; therefore, the measured scour depths could be less than what actually occurred due to sediment infilling during the recession of both floods.

Abutment Scour

No measurements of abutment scour were made at the S.R. 35 bridge.

Contraction Scour

The contraction scour at this site was diminished during the April 12, 1979 flood due to a reduction in discharge and velocities through the bridge as a result of a substantial amount of road overflow. The S.R. 35 bridge was not subjected to road overflow during the 2001 flood and resulted in deeper contraction scour measurements despite a lower peak discharge. The measured contraction scour depths and modeled site characteristics pertinent to contraction scour are summarized in Table 9. The only approach cross-section data available for the site was surveyed just after the 1979 flood. Channelization of the reach downstream of the bridge has led to significant changes in the channel that is evident in the Figures 3-7. The accuracy of the scour observations, especially for the 2001 flood, is degraded due to the absence of a reliable reference surface.

Table 9. Contraction scour data (--, not available; ft/s, feet per second; cfs, cubic feet per second; US, upstream; DS, downstream; Avg, average)

Measurement Number	Contracted Date	Contracted Time	Uncontracted Date	US/DS	Scour Depth (ft)
1	4/12/1979	--	4/12/1979	--	4
2	4/5/2001	--	4/5/2001	--	6
Measurement Number	Accuracy (ft)	Contracted Avg Vel (ft/s)	Contracted Discharge (cfs)	Contracted Depth (ft)	Contracted Width (ft)
1	2	9.27	8973	21	76
2	3	9.25	6750	22.6	75
Measurement Number	Uncontracted Avg Vel (ft/s)	Uncontracted Discharge (cfs)	Uncontracted Depth (ft)	Uncontracted Width (ft)	Channel Contraction Ratio
1	0.95	10200	17.4	42	--
2	0.68	6750	17	42	--
Measurement Number	Pier Contraction Ratio	Scour Location	Eccentricity	Sediment Transport	Debris Effect
1	---	Main Channel	---	Live-Bed	Insignificant
2	---	Main Channel	---	Live-Bed	Insignificant
Measurement Number	D95 (mm)	D84 (mm)	D50 (mm)	D16 (mm)	Bed Material Cohesion
1	--	0.29	0.10	0.017	Non-cohesive
2	--	0.29	0.10	0.017	Non-cohesive

Pier Scour

None of the measured scour from the two floods is associated with pier scour. Although the presence of the 5 piers supporting the S.R. 35 bridge likely had an effect on the depth of contraction scour reported at the site, it is not possible to quantify the piers' contribution to the total scour.

COMPUTED SCOUR

A WSPRO model of the site was developed to estimate the peak flow during both the 1979 and 2001 floods and assess how accurately the scour for this flood could have been predicted using HEC-18 procedures. The pre-flood geometry of the bridge reach was simulated with the WSPRO model utilizing the channel geometry from the 1941 “as-built” plans and a 1977 inspection. The approach and exit sections used in the model were collected during the post-flood survey. The WSPRO estimated peak discharges for April 12, 1979 and April 5, 2001 floods were modeled with the pre-flood bathymetry to determine the hydraulic parameters needed for HEC-18 scour computations.

Abutment Scour

Abutment scour was not computed with the HEC-18 equations for the S.R. 35 bridge over Conehoma Creek.

Contraction Scour

Contraction scour computations were performed according to procedures outlined in the May 2001, 4th edition of the Federal Highway Administration's Hydraulic Engineering Circular No. 18 (HEC-18). The sub-area stationing limits for the post-scour section were kept the same as those used for the pre-scour section so that a consistent top width could be determined; the average depths for pre- and post-scour conditions were determined for the overbank and the main channel. These pre- and post-scour depths were used to determine average contraction (mostly) scour depths in the overbank and main-channel areas.

Contraction scour was estimated for the floods of April 12, 1979, and April 5, 2001, and compared to measured scour (Figures 8 and 9). The HEC-18 estimated post-scour elevations suggest that the bridge pilings would have been undermined during both the 1979 and 2001 floods. The measured and computed contraction scour depths are summarized in Tables 11 and 12.

Table 11. Measured contraction scour depths at S.R. 35 over Conehoma Creek near Kosciusko, MS.

Date	Contraction Scour Depth		
	Measured Left Bank (ft)	Measured Channel (ft)	Measured Right Bank (ft)
4/12/1979	0	4	5
4/5/2001	0	6	2

Table 12. Computed contraction scour depths at S.R. 35 over Conehoma Creek near Kosciusko, MS using HEC-18 procedures.

Date	Flow Condition	Contraction Scour Depth		
		Computed Left Bank (ft)	Computed Channel (ft)	Computed Right Bank (ft)
4/12/1979	Free Surface	3	19	3
4/12/1979	Pressure	2	27	0
4/5/2001	Free Surface	3	19	4
4/5/2001	Pressure	1	19	2

REFERENCES

Any questions regarding the S.R. 35 bridge over Conehoma Creek should be directed to the following point of contact:

K. Van Wilson, Hydrologist, P.E.
 U.S. Geological Survey
 308 South Airport Road
 Pearl, MS 39208-6649
 Phone: (601) 933-2922
 E-mail: kvwilson@usgs.gov

A-81

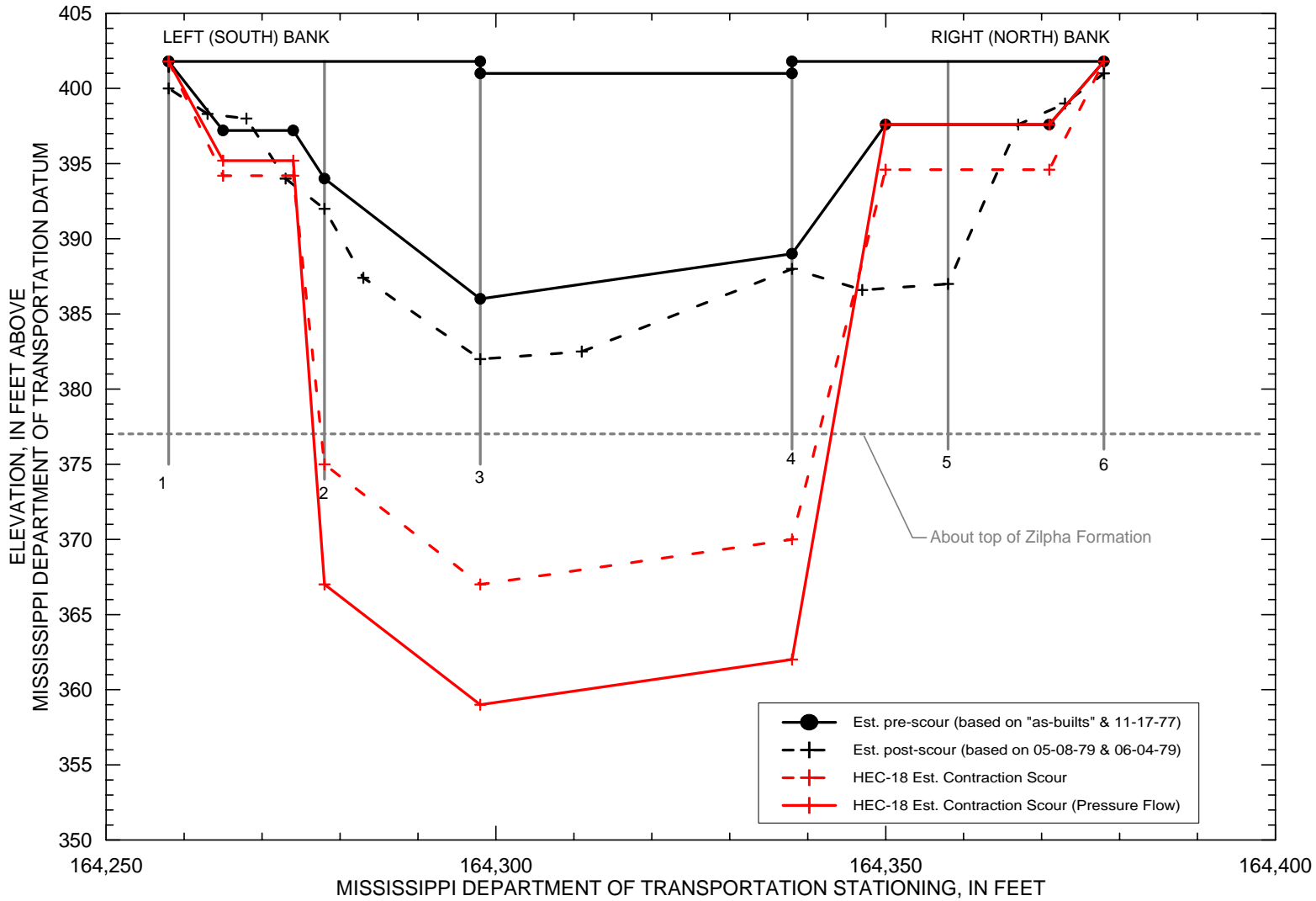


Figure 8. Comparison of the measured and computed scour on Conehoma Creek at S.R. 35 for the April 12, 1979 flood.

A-82

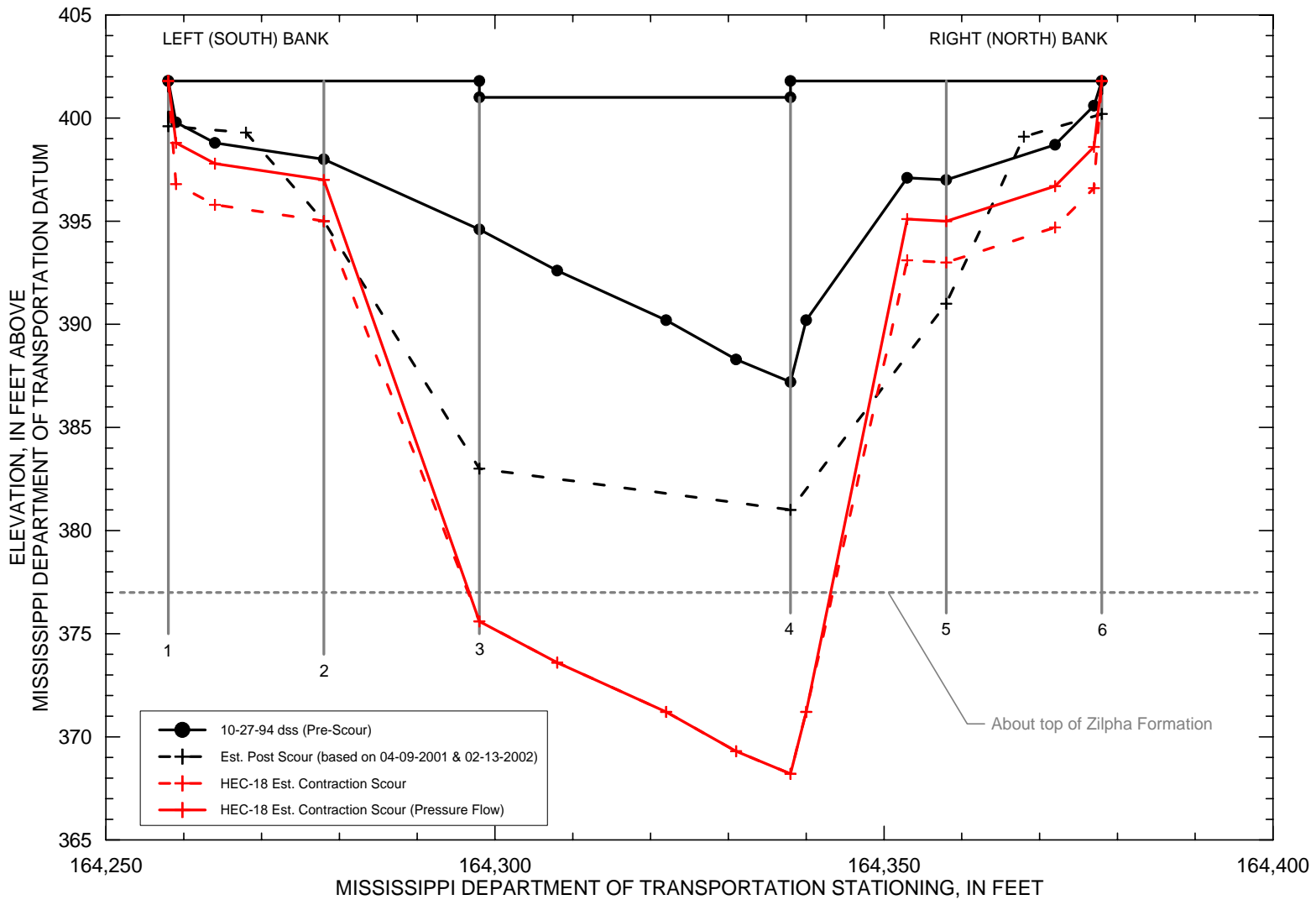


Figure 9. Comparison of the measured and computed scour on Conehoma Creek at S.R. 35 for the April 5, 2001 flood.

SUPPORTING DATA

WSPRO Model Files:

1979post.prt – Model output file for simulation of April 12, 1979 flood using scoured geometry.

1979post.wsp – Model input file for simulation of April 12, 1979 discharge using scoured geometry.

1979pre.prt – Model output file for simulation of April 12, 1979 flood using pre-flood geometry.

1979pre.wsp – Model input file for simulation of April 12, 1979 discharge using pre-flood geometry.

2001post.prt – Model output file for simulation of April 5, 2001 flood using scoured geometry.

2001post.wsp – Model input file for simulation of April 5, 2001 discharge using scoured geometry.

2001pre.prt – Model output file for simulation of April 5, 2001 flood using pre-flood geometry.

2001pre.wsp – Model input file for simulation of April 5, 2001 discharge using pre-flood geometry.

CASE STUDY #6

Bear Creek at U.S. 70 near Mays Store, North Carolina

SITE OVERVIEW

The U.S. 70 crossing of Bear Creek is located in Lenoir County, approximately 0.7 miles west of Mays Store, NC and 4.5 miles upstream from the confluence with the Neuse River (see Figure 1). The crossing consists of an upstream west bound bridge and a downstream east bound bridge that share the same embankment. The site is approximately 1.7 miles upstream from the USGS gaging station near Mays Store (03020202). Records were kept for the Mays Store station from October 1987 to September 2001, with an annual mean flow of 75.87 cubic feet per second (cfs), and an instantaneous peak flow of 1,550 cfs recorded on October 9, 1996. Using indirect methods, the USGS measured an approximate peak of 11,000 cfs during Hurricane Floyd in September 1999. A summary of the general site information is found in Table 1.

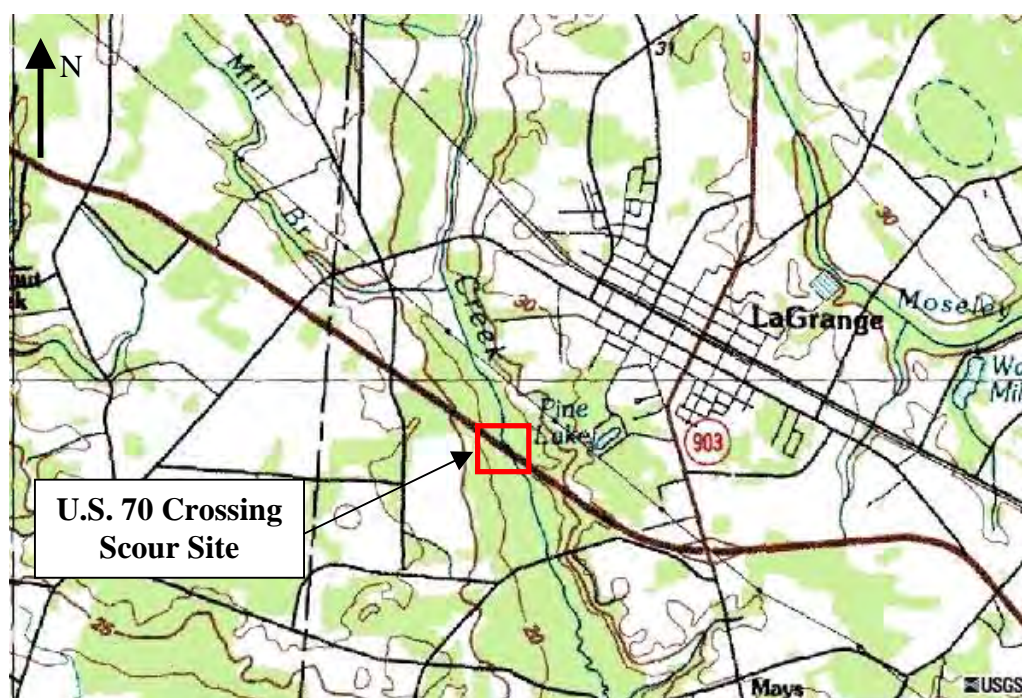


Figure 1. Location map for the U.S. 70 crossing scour site over Bear Creek near LaGrange, North Carolina.

Hydrologic Conditions

The flooding was the result of heavy rainfall on September 15 and 16, 1999 associated with Hurricane Floyd. Soils had already been saturated from rainfall associated with Hurricane Dennis, which had passed through the area approximately 10 days earlier on September 4 and 5, 1999. During Hurricane Floyd, the Nahanta Swamp Basin received more than 12 inches of rainfall over a 24-36 hour period. Widespread flooding, some in excess of 500-year recurrence intervals, occurred throughout eastern North Carolina in

most of the major basins including the Neuse River Basin. The estimated peak discharge of 11,000 cfs for this flood was greater than the 500-year flood estimate of 8,480 cfs.

Table 1. Site information

Site Characteristic	Description
County	Lenoir
Nearest City	Mays Store
State	North Carolina
Latitude	35°17'45"
Longitude	77°48'29"
Route Number	70
Route Class	U.S.
Stream Name	Bear Creek

DISCUSSION OF CONTRACTED SITE

Bridge Data

Both structures consisting of three spans (1 at 63'-2", 1 at 80'-9", and 1 at 64'-4") with a clear roadway width of 40' (42'-5" out to out) and having a concrete deck on continuous concrete I-beams are supported by a substructure of reinforced concrete caps on concrete pile bents. Each of the interior pile bents (piers) consisted of 11-1.5 ft diameter piles spaced at 6.4 ft. The structural components of the abutments consisted of end pile bents and abutment pile caps. The U.S. 70 crossing was built in 1968, and has a type III contracted opening, meaning it has sloping embankments and sloping spill-through abutments. The bridge characteristics pertinent to scour are summarized in Table 2.

Table 2. Bridge data

Bridge Characteristic	Description
Structure Number	11 & 13
Length (ft)	208.25
Width (ft)	42.4
Spans	3
Vertical Configuration	Horizontal
Low Chord Elev (ft)	76.25
Upper Chord Elev (ft)	80
Overtopping Elev (ft)	80
Skew (degrees)	54
Guide Banks	None
Waterway Classification	Main
Year Built	1968
Avg. Daily Traffic	16,600
Plans on File	Yes
Parallel Bridges	Yes
Continuous Abutments	Yes

Geomorphic Setting

Bear Creek is generally straight with the exception of two bends directly upstream of the U.S. 70 crossing. A USGS 7.5 minute quadrangle topographic map of the site is shown in Figure 2. The aerial photo of the site taken in 1993 is shown in Figure 3. The entire overbank area in the project reach is heavily vegetated by trees. Data characterizing the geomorphic setting are summarized in Table 3.

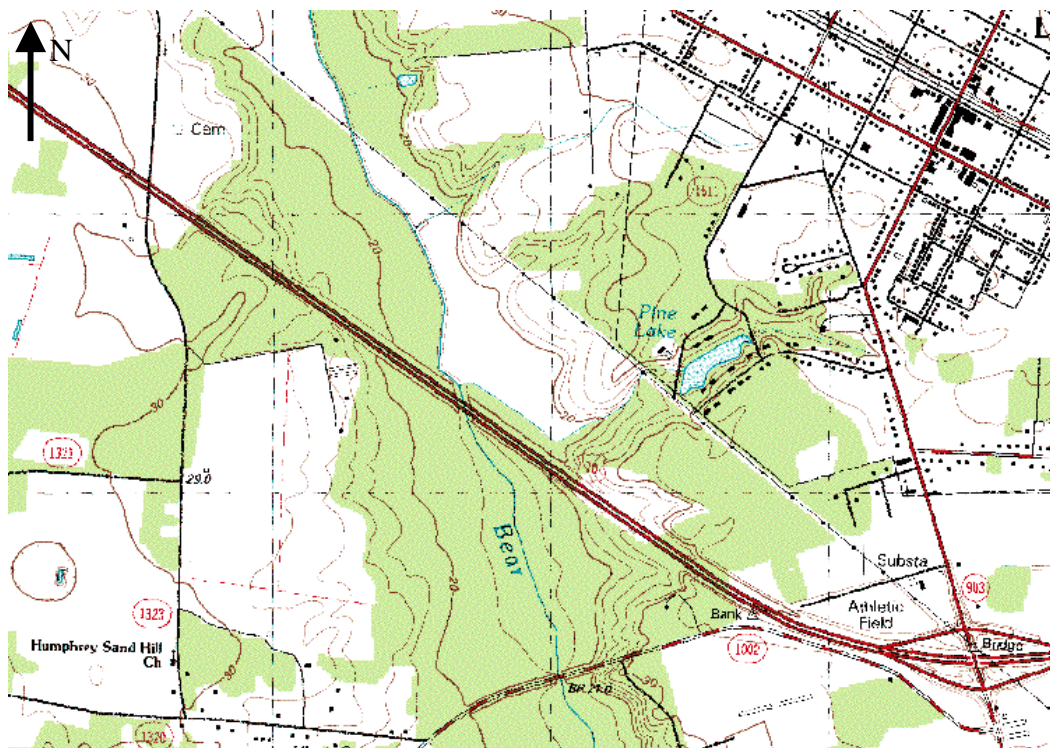


Figure 2. USGS topographic map of the U.S. 70 crossing over the Bear Creek near LaGrange, NC (elevations are in meters).



Figure 3. – Aerial photo of the U.S. 70 crossing over Bear Creek near LaGrange, NC.

Table 3. Geomorphic Data

Geomorphic Characteristic	Description
Drainage Area	54.2
Slope in Bridge Vicinity (ft/ft)	.00025
Flow Impact	Skewed
Channel Evolution	Unknown
Armoring	None
Debris Frequency	Unknown
Debris Effect	Unknown
Stream Size	Small
Flow Habit	Perennial
Bed Material	Medium Sand
Valley Setting	Low relief
Floodplain Width	Very Wide
Natural Levees	Yes
Apparent Incision	Yes
Channel Boundary	Alluvial
Banks Tree Cover	Heavy
Sinuosity	Straight
Braiding	None
Anabranching	None
Bars	Small/None
Stream Width Variability	Equiwidth

Bed Material Data

Streambed was collected from a location immediately downstream of the east bound bridge by the USGS on February 24, 2003. The size distribution of the bed material sediment is shown in Figure 4. The characteristics of the sediment are given in Table 4.

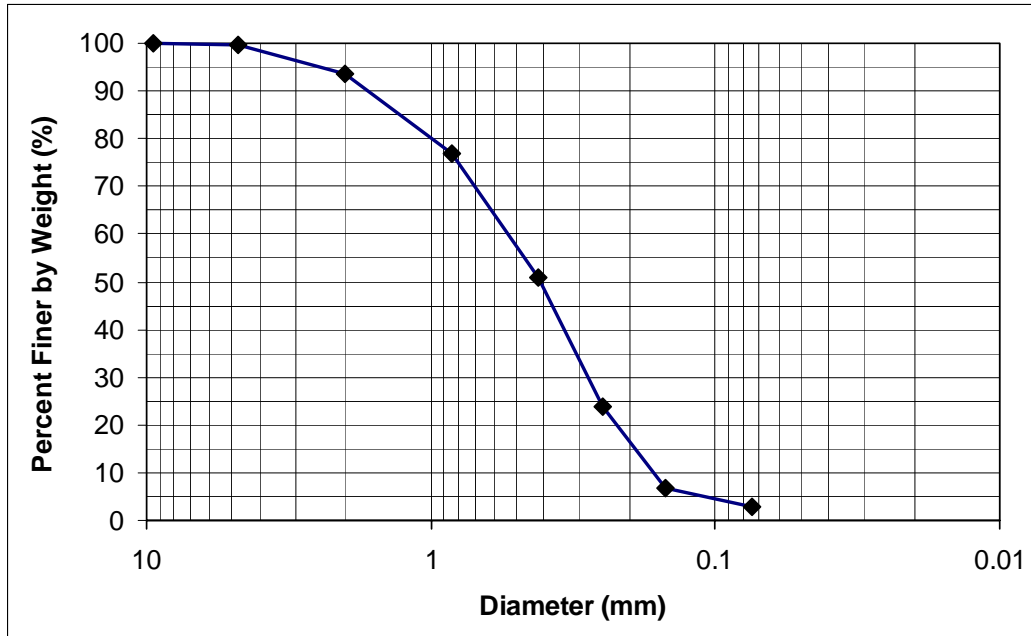


Figure 4. – Bed material sediment sample gradation curve.

Table 4. Sediment Characteristics

D16	0.20 mm
D35	0.32 mm
D50	0.41 mm
D84	1.34 mm
D95	2.58 mm

Information from boring logs obtained during the construction of a replacement bridge indicate that sediment below the active bed layer was fine silty sand with traces of small clay lenses. Although coarse sands were present in the borings, they were typically located more than 10 ft below the elevation of the scoured channel bottom. A dense clay also existed, but it was located more than 40 ft below the scoured hole minimum elevation.

Roughness Coefficients

A distribution of Manning n values used in the HEC-RAS analysis is provided in Table 5.

Table 5. Manning n values used in HEC-RAS model for Bear Creek at the U.S. 70 crossing. (fldpln, floodplain; chnl, channel; rt, right)

Location	Left Fldpln	Main Chnl	Right Fldpln
Approach	0.10	0.045	0.10
Bridge	0.10	0.045	0.10
Exit	0.10	0.045	0.10

Abutment Details

The crossing has sloping spill-through abutments with concrete slope protection. The abutment characteristics are summarized in Table 6.

Table 6. Abutment Data

Abutment Characteristic	Description
Left Station #11	32+30.75
Left Station #13	31+59.25
Right Station #11	29+60.75
Right Station #13	28+89.25
Left Skew (deg)	?
Right Skew (deg)	?
Left Abutment Length (ft)	881
Right Abutment Length (ft)	980
Left Abut to Channel Bank (ft)	18
Right Abut to Channel Bank (ft)	18
Left Abutment Protection	Concrete
Right Abutment Protection	Concrete
Contracted Opening Type	III*
Embankment Skew (deg)	54
Embankment Slope (ft/ft)	0.68
Abutment Slope (ft/ft)	0.57
Wingwalls	No
Wingwall Angle (deg)	N/A

* - Type III opening has sloping abutments and sloping spillthrough abutments.

Pier Details

The piers are pile bents consisting of 11, 18-inch diameter concrete piles spaced 6.4 feet apart in a single line. The four piers are numbered from left to right, looking downstream. The pier characteristics are summarized in Table 7.

Table 7. Pier Data (--, not available)

Pier ID	Bridge Station (ft)	Alignment	Highway Station	Pier Type	# of Piles	Pile Spacing (ft)
1	3069.25	0	--	Group	11	6.4
2	2979.25	0	--	Group	11	6.4
3	3140.75	0	--	Group	11	6.4
4	3050.75	0	--	Group	11	6.4
Pier ID	Pier Width (ft)	Pier Shape	Shape Factor	Length (ft)	Protection	Foundation
1	1.5	Round	--	--	None	Piles
2	1.5	Round	--	--	None	Piles
3	1.5	Round	--	--	None	Piles
4	1.5	Round	--	--	None	Piles
Pier ID	Top Elevation (ft)	Bottom Elevation (ft)	Foot or Pile Cap Width (ft)	Cap Shape	Pile Tip Elevation (ft)	
1	--	--	--	Square	--	
2	--	--	--	Square	--	
3	--	--	--	Square	--	
4	--	--	--	Square	--	

Surveyed Elevations

Bridge data elevations were taken from NCDOT bridge plans, and are consistent with the 1929 National Geodetic Vertical Datum (NGVD) at the Bear Creek site.

PHOTOS



Figure 5. Looking upstream at the east bound bridge abutment during low-flow.



Figure 6. Looking downstream from the east bound bridge deck during low-flow.



Figure 7. Looking at the east abutment from the top of the west abutment.



Figure 8. West bound bridge left abutment.



Figure 9. West bound left pile group with temporary steel soldier piles.

MEASURED SCOUR

All measured scour data were collected during post-flood surveys of the U.S. 70 crossing; therefore, the measured scour depths could be less than what actually occurred due to sediment infilling during the flood recession or subsequent bankfull flow events.

Combined Abutment and Contraction Scour

The embankments of U.S. 70 block approximately 90% of the Bear Creek valley submerged by the 1999 flood. This severe contraction caused backwater upstream of the U.S. 70 crossing, in which upstream approach flow average velocities were very low (0.6 fps modeled). Flow accelerated around abutment corners (14.0 fps modeled) and into the bridge opening. One continuous scour hole formed between the spill-through abutments of the embankments; however, the deepest portions of the scour hole were highly skewed toward the left abutment for the westbound bridge and the right abutment for the eastbound bridge. No distinct separation of “local abutment”, “local pier” or “contraction” scour could be determined from the topography of the scour hole. A combination of scour and abutment slope failure caused the destruction of the westbound left abutment slope and slope protection as shown in Figure 8. Figure 9 shows the settled westbound left concrete pile bent and the temporary steel soldier piles used to restore the structural integrity of the bridge. Figure 10 shows the inferred sequence of progressive scour and slope failure that is considered to have resulted in the observed slope and scour hole geometry.

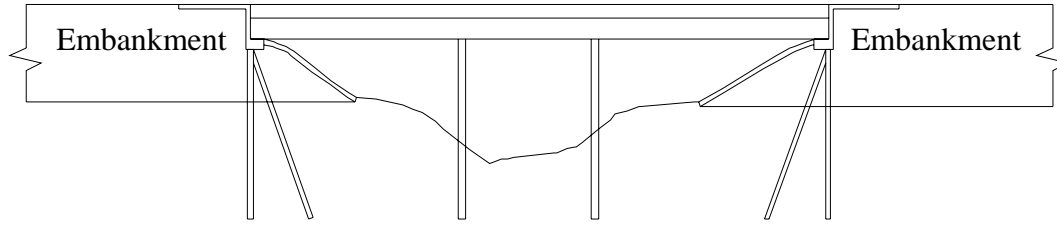
The influence of skew of the upstream face of the embankments with respect to the face of the abutments in the bridge opening and the relatively long distance through the bridge

opening (220 ft) is apparent in the measured scour pattern and locations of maximum scour depth. The last image of Figure 10 shows that sediment accumulated on the right floodplain and along the right main channel bank upstream and under the west bound bridge while deep scour (15.5 ft) occurred on the left side of the channel. The pattern of scour was opposite on the downstream side of the east bound bridge: deposition occurred along the left side of the channel (Figure 5) and deep scour destroyed the right abutment embankment slope and caused settlement of the right pile bent (Figure 6).

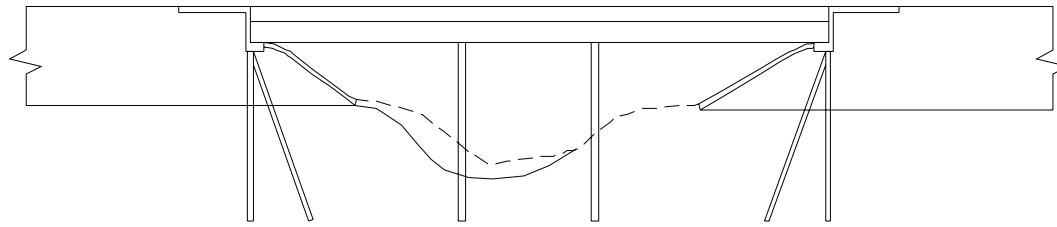
The location of deepest scour did not occur at the toe of the left bridge abutment, despite the apparently high skewing of flow toward that abutment. Possible reasons for the shift of the maximum depth in the scour pattern include the following:

- 1) the influence of slope failure processes as illustrated in Figure 10
- 2) the initiation of scour at the pile bents and along the erodible non-vegetated channel banks
- 3) the general tendency for the maximum scour location to move away from the toe of the abutment as flow along the abutment upstream face increases.

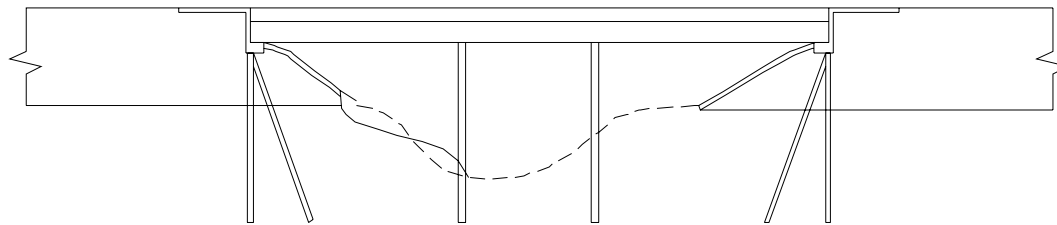
Although this site illustrates the important influence of embankment skew to the axis of the bridge opening, the components of scour could not be separated by any standard method; therefore, only total observed scour was compared to the total scour computed.



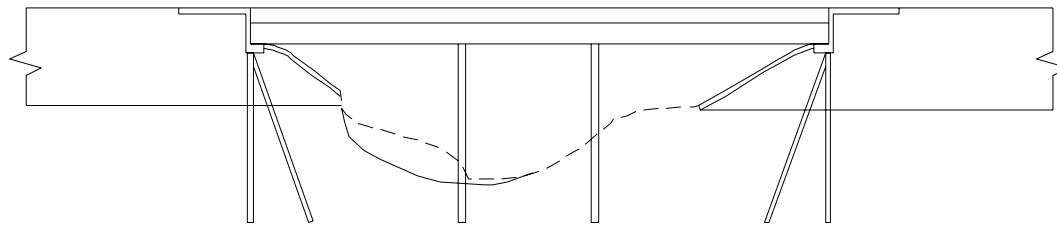
Stage 1



Stage 2

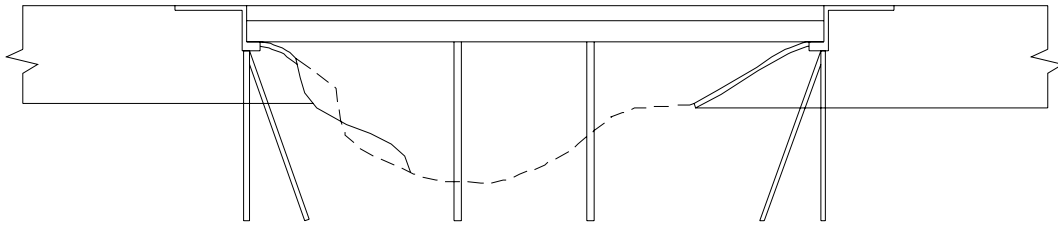


Stage 3

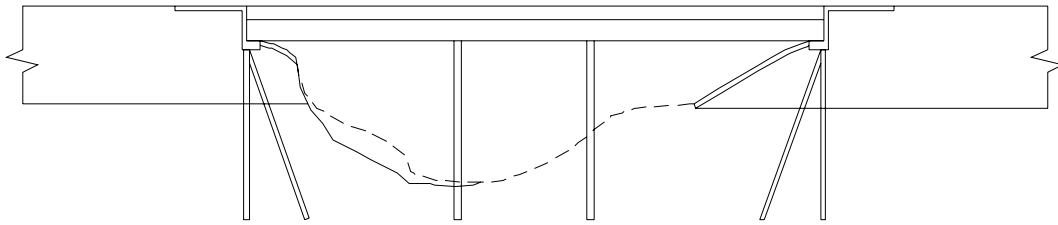


Stage 4

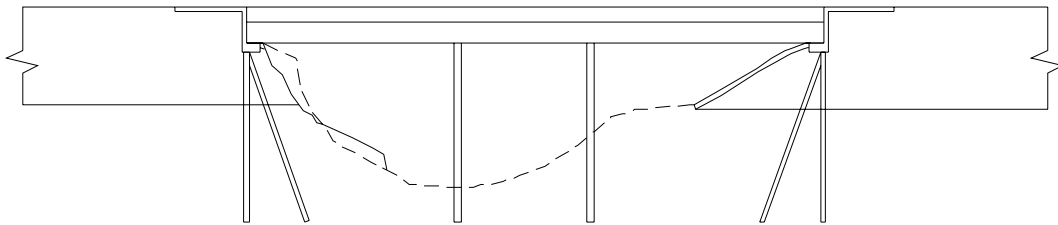
Figure 10. Progression of geometric change at spill through abutments caused by scour.



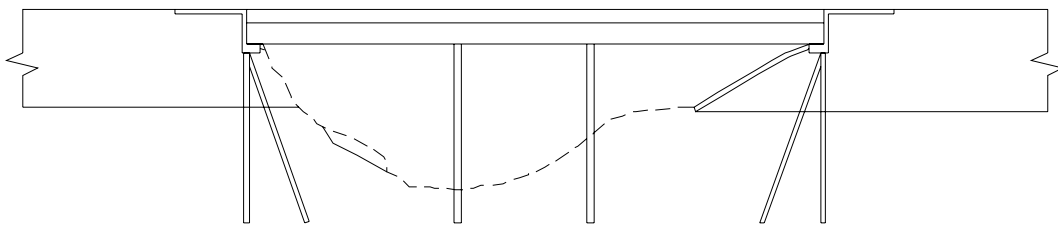
Stage 5



Stage 6

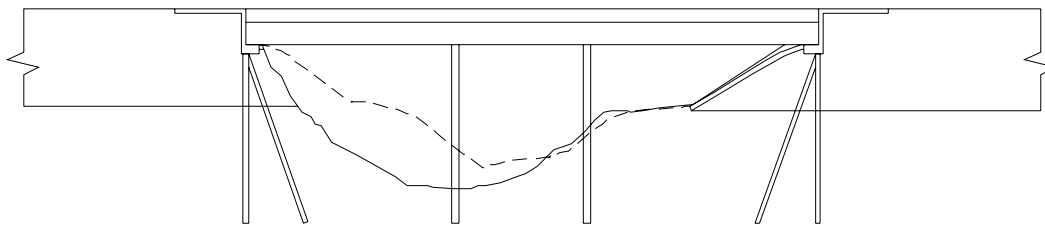


Stage 7



Stage 8

Figure 10(cont'd). Progression of geometric change at spill through abutments caused by scour.



Stage 9

Figure 10(cont'd). Progression of geometric change at spill through abutments caused by scour.

Table 8. Progression of Geometric Change at Spill Through Abutments Caused by Scour

Stage	Description
1	Bridge cross section at the US 70 crossing of Bear Creek surveyed during a site visit in 1986.
2	Initial channel geometric change primarily driven by scour.
3	Bank and embankment slope failure driven by mass slope instability. Partial filling of scour hole with slope failure debris including concrete slope protection.
4	Erosion of slope failure debris and continued erosion of embankment toe causing lateral migration of scour hole.
5	Progressive failure of streambank and embankment slope with partial filling of scour hole with failure debris.
6	Erosion of slope failure debris and continued erosion of embankment toe causing lateral migration of scour hole.
7	Progressive failure of embankment slope with partial filling of scour hole with failure debris.
8	Erosion of slope failure debris and continued erosion of embankment toe causing lateral migration of scour hole.
9	Final scoured bridge cross section compared to 1986 bridge geometry.

COMPUTED SCOUR

Flow conditions for the estimated peak discharge for the September 16, 1999 flood were modeled with pre-flood bathymetry to determine the hydraulic parameters necessary for estimating scour using HEC-18 prediction methods. Flow conditions for the pre-flood geometry of the bridge reach were simulated with the HEC-RAS model utilizing the

channel geometry from the 1968 “as-built” plans and a 1986 inspection. The approach and exit sections used in the model were collected during the post-flood survey.

Hydraulic Parameters

Peak flow conditions were obtained from the USGS North Carolina District and the North Carolina Department of Transportation. The peak discharge was estimated by the USGS using indirect methods. Water-surface elevations at the bridge (assumed to be given at the downstream face of the east bound bridge) were obtained from the North Carolina DOT. The downstream water surface elevation was assumed to be within 1.6 ft of a roadway crossing located 0.6 miles downstream that was overtopped.

A 2-D model (FESWMS 2D-H version 3.0) was also used to examine the effect of flow distribution through the bridge and to infer potential impacts of skewed flow on scour pattern. Figure 11 shows the velocity distribution produced by the model in the vicinity of the bridge and significant features observed in post-flood site assessments. Figure 12 shows the location of transects from which the velocity distributions shown in Figures 13, 14 and 15 were obtained from the 2-D model. Average channel velocities from HEC-RAS are also shown in Figures 13, 14 and 15. The impact of skew on the flow distribution is shown in these figures. Locations of observed scour, deposition and embankment failure are indicated by the variation of flow velocity produced by the model.

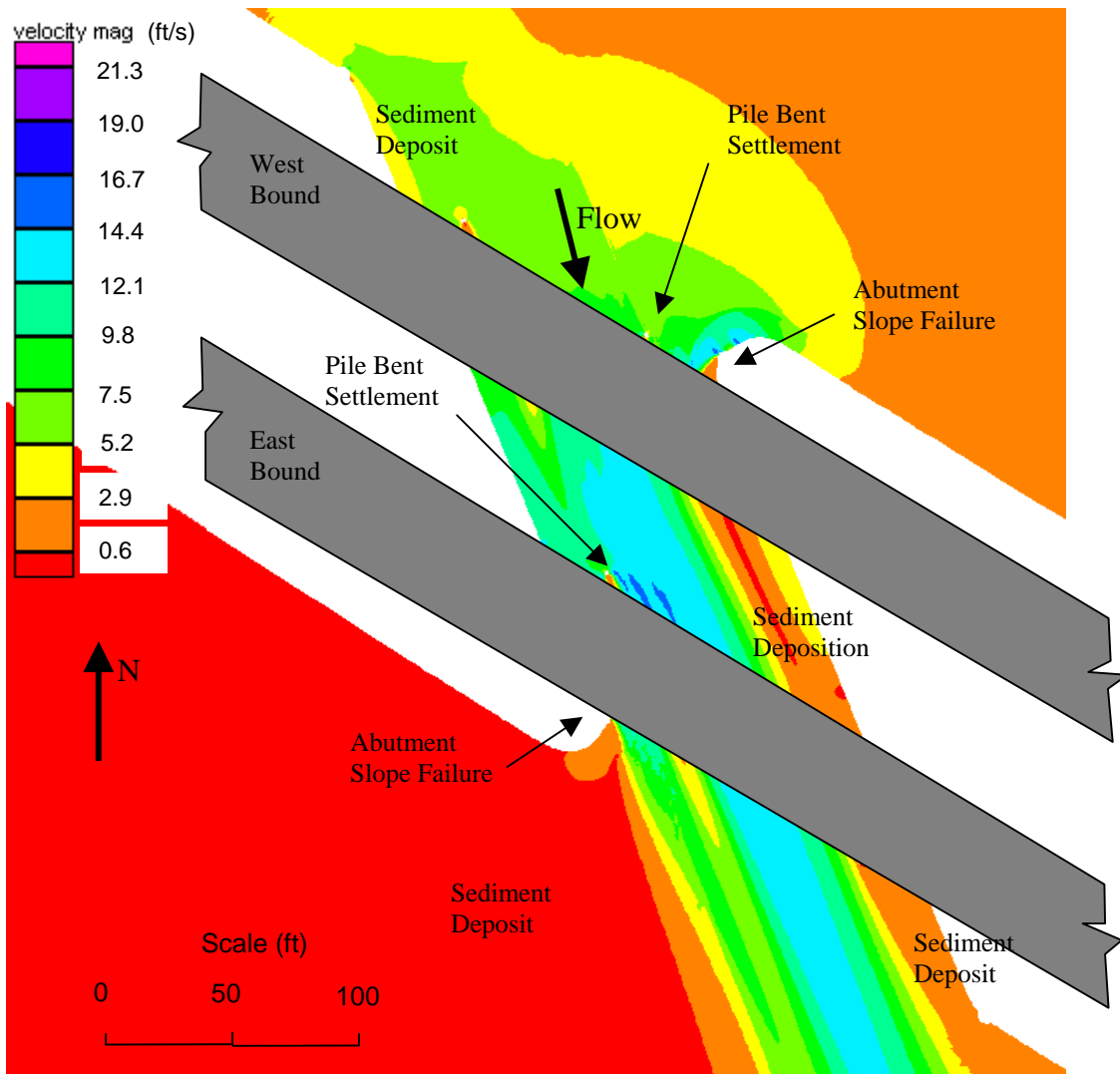


Figure 11. Velocity magnitudes from the 2-D model and significant features of post-flood assessment of the U.S. 70 crossing over Bear Creek.

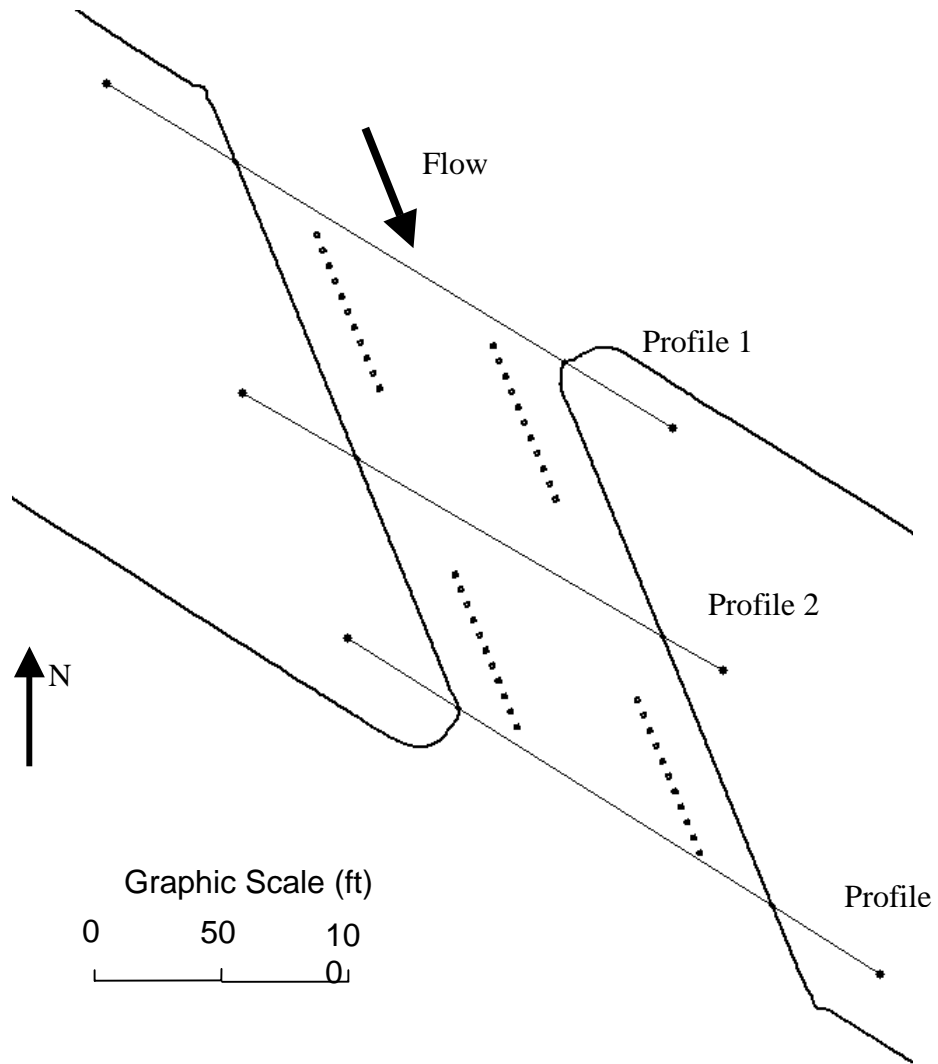


Figure 12. Location of velocity distribution transects obtained from the 2-D model.

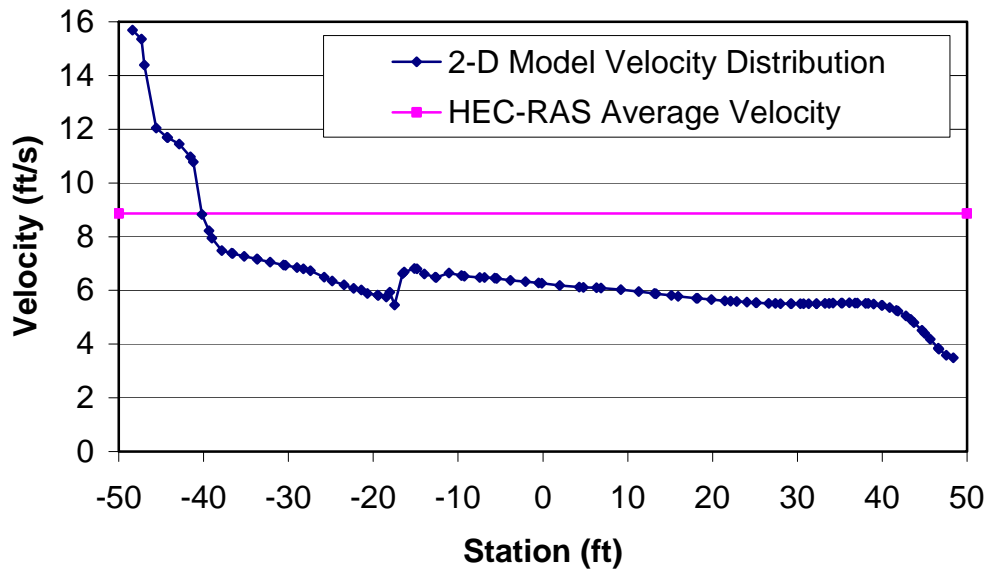


Figure 13. Upstream transect velocity distribution (Profile 1).

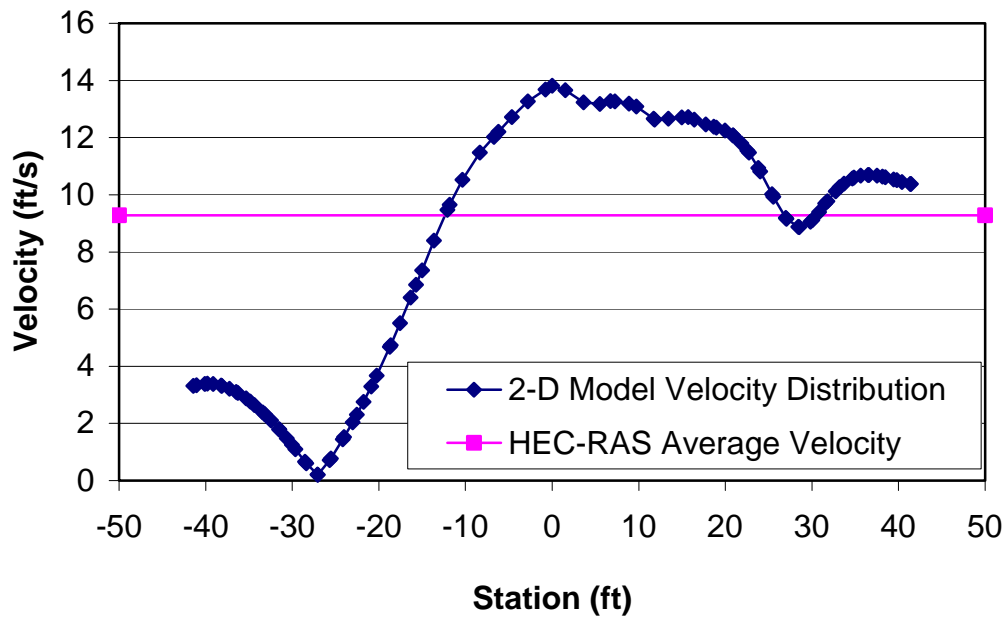


Figure 14. Midbridge transect velocity distribution (Profile 2).

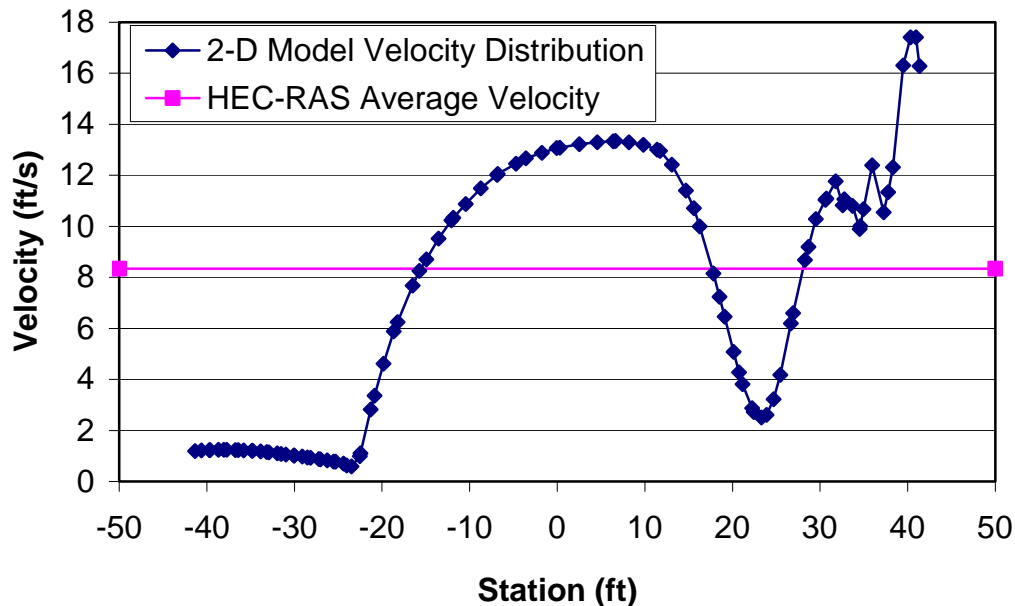


Figure 15. Downstream transect velocity distribution (Profile 3).

Computed Abutment Scour

Abutment scour was computed using the Froehlich, HIRE, Sturm and Maryland equations. The hydraulic parameters required for each equation were taken from the HEC-RAS output. The Froehlich and HIRE methods were computed using the functions available in HEC-RAS, and the Sturm method utilized a spreadsheet developed by the USGS.

Table 9. Abutment Scour Data

Date	Location	Observed (ft)	Local Scour Depth		
			Froehlich Equation (ft)	HIRE Equation (ft)	Sturm Equation (ft)
2/24/03	Left Upstream	--	18.0	15.7	20.5
2/24/03	Right Upstream	--	18.8	18.0	31.6

Computed Contraction Scour

Contraction scour was computed using the Laursen Clear-water equation. The hydraulic parameters required for the equation were taken from the HEC-RAS output. The Laursen Clear-water method was computed using the function available in HEC-RAS.

Table 10. Contraction Scour Data

Date	Contraction Scour Depth	
	Observed (ft)	Laursen Clear-water
		HEC-18 (ft)
2/24/03	--	45.1

Comparison of Maximum Total and Computed Scour

The maximum scour measured from the surface of the pre-flood geometry was 15.5 ft and was located between the upstream left abutment and the left pile bent. The scour depth was considered the total scour depth for the left abutment. Sediment deposition on the pre-flood ground surface was observed on the floodplain surface located between the upstream right abutment and the right pile bent (deposition, rather than scour near the right abutment). The observed total scour at the left upstream abutment was less than the abutment scour computed by any of the equations in Table 9. Addition of contraction scour estimates by the Laursen method and Sturm abutment scour estimates by the Sturm method produces total scour depths that were 4.2 times the observed total scour depth.

CASE STUDY #7

Old Glenn Highway (State Route 1) over the Knik River near Palmer, Alaska

SITE OVERVIEW

The Old Glen Highway (State Route 1) over the Knik River is located approximately 35 miles northeast of Anchorage near the town of Palmer (Figure 1). The river emanates from the Knik Glacier approximately 17 miles upstream from the bridges and drains into Knik Arm, the northern most extent of Cook Inlet, approximately 8 miles downstream of the bridge. At the mouth of the glacier, the river is anastomosing, but reduces to a single strand through the bridge reach. Branching of the channel resumes downstream of the bridge, but not to the extent found in the headwaters. A daily station (station 15281000) was operational at this site from 1958-1988, 1991-1992, and was reactivated in 2001. The gage is located at the new bridge on the right upstream bank. Average annual mean flow (from 1960-1987) is 6904 cubic feet per second (cfs), with annual peaks occurring in August-September and averaging 37,000 cfs (excluding outburst floods). High volume (up to 359,000 cfs) glacial outburst floods occurred annually on the Knik River up until 1966. Due to recession of the Knik glacier these flows no longer occur.

Two bridges are located in the study reach (Figure 2). The upstream bridge was built to accommodate the high volume outburst floods and extends across the entire channel. The newer downstream bridge (the focus of this analysis) was built after the cessation of the outburst floods and its embankments constrict the flow. The abutments and embankments for the new bridge are rip rapped and spur dikes extend upstream beyond the old bridge.

The USGS, Alaska District surveyed the site in 1999 and conducted a level 2-scour analysis for the new bridge. A step-backwater hydraulic model (HEC-RAS) of the Old Glenn Highway site was developed as part of the analysis to predict the amount of pier and contraction scour expected for flood measurements at the site based on one-dimensional hydraulic parameters and equations from HEC-18. Alaska District staff also was deployed to the site in 2001 to collect real-time bridge scour measurements during a glacial-melt event on the Knik River (July 31- August 3 and August 7). Real-time data was collected from a manned boat using an ADCP to collect velocity and discharge data and a fathometer to collect bathymetry data. A summary of the general site information on the site is found in Table 1.

Table 1. Site information

Site Characteristic	Description
County	Matnuska Susitna
Nearest City	Palmer
State	Alaska
Latitude	61° 30' 18"
Longitude	149° 01' 48"
Route Number	1
Route Class	State
Stream Name	Knik River

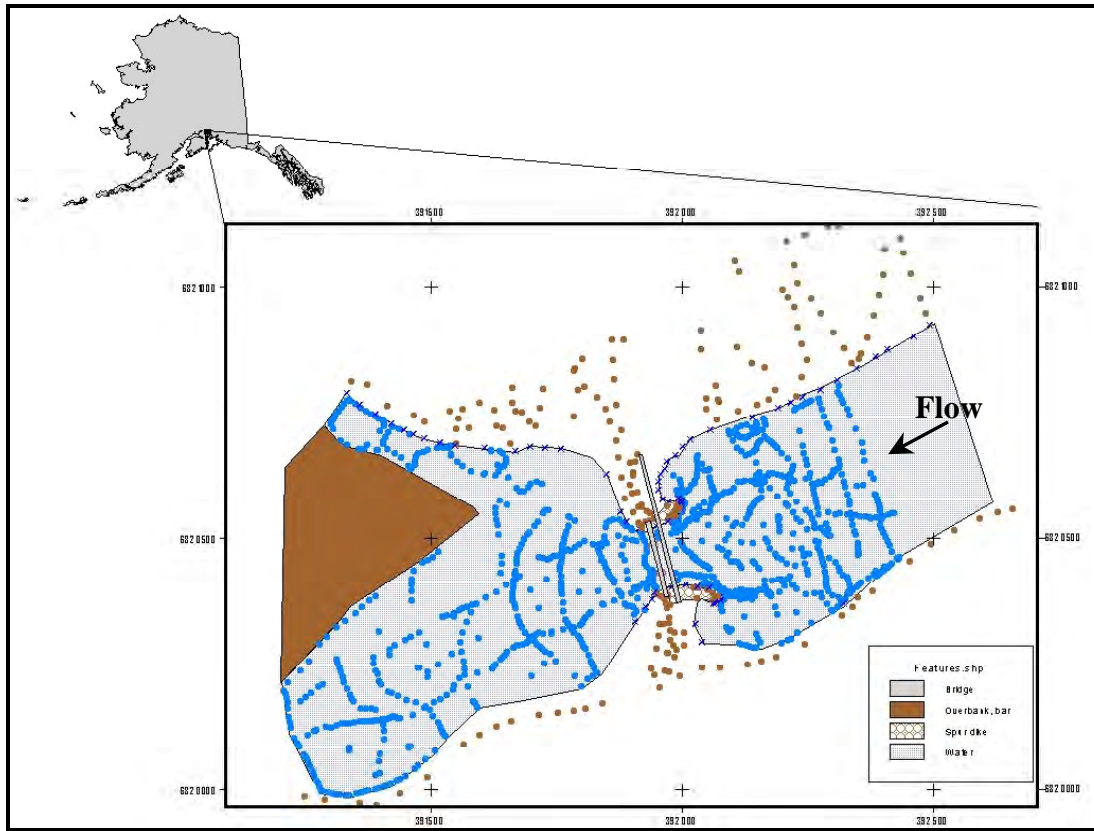


Figure 1. Location of study site and map of collected data points.



Figure 2. Aerial photo of the Old Glenn Highway (S.R. 1) over the Knik River.

Hydrologic Conditions

The hydrologic events responsible for the measured floods were typical summer glacial melt runoff from the Knik glacier. The peak discharge that was measured during the 1999 survey was 23,000 cubic feet per second (cfs) on July 13, 1999. The discharge measured in 2001 during the real-time measurements was 22,100 cfs on August 1, 2001.

DISCUSSION OF CONTRACTED SITE

The Knik River is highly braided upstream of the Old Glen Highway bridge and contracts to a single channel through the new bridge opening. The spur dikes assist in contracting the flow upstream of the bridge therefore by definition in HEC-18, all scour through the bridge opening will be associated with either contraction or pier scour, not abutment scour. A review of measurements at the site in 1999 and 2001 indicates that the bed fills in after spring and summer runoff events and that the elevation through the bridges has deepened by about 4 ft adjacent to the left abutment/spur dike (see Figure 3). The hump that is evident at pier #3 is attributed to the presence of riprap that was placed to protect the old bridge from scour. All measurements were made at the upstream face of the old bridge.

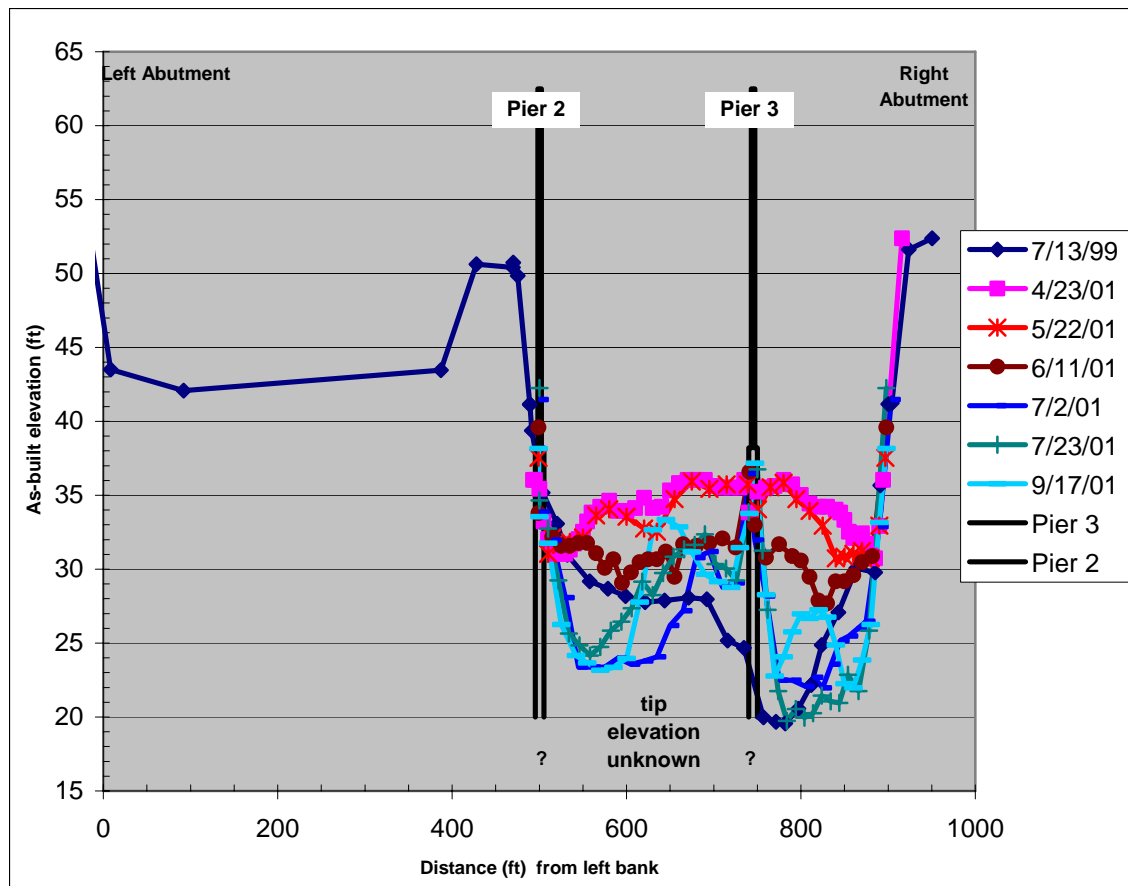


Figure 3. Comparison of bathymetry data collected in the contracted opening under the old Old Glenn Highway bridge on the Knik River.

Bridge Data

The new structure (#539) consists of three continuous composite steel box girder spans supported by two concrete webbed piers, and spill-through abutments (type III contracted opening). The piers and the abutments are founded on piling; the pier and abutment piling is driven to an estimated elevation of -14.0 ft. Spur dikes extend upstream of the new bridge and have a bank slope of 2:1. The abutments, spur dikes and roadway embankments are protected with riprap. The bridge characteristics pertinent to scour are summarized in Table 2.

Table 2. Bridge data

Bridge Characteristic	Description
Structure Number	539
Length (ft)	505.5
Width (ft)	28
Spans	3
Vertical Configuration	Horizontal
Low Chord Elev (ft)	63.0
Upper Chord Elev (ft)	63.0
Overtopping Elev (ft)	71.0
Skew (degrees)	0
Guide Banks	Elliptical
Waterway Classification	Main
Year Built	1975
Avg. Daily Traffic	Unknown
Plans on File	Yes
Parallel Bridges	Yes
Continuous Abutments	No

Geomorphic Setting

A review of flood measurement notes from 1999 and 2001 indicated that this site experienced a substantial deformation during the two-year period. The Knik River is a course grained, braided stream common to Alaska's geomorphology and subject to lateral migration, especially upstream of the bridge. Extreme (>Q500) discharges were common during annual outburst floods from the glacially dammed Lake George. The glacier has receded and outburst floods have not occurred since 1966.

The progression of scour through the bridges shown in Figure 3 reveals the tendency for the channel to aggrade and degrade a considerable amount over the course of an annual hydrograph. The channel is constantly changing, as can be seen by the multiple shifts observed in numerous measurements at the site made by USGS staff over the years. A USGS 7.5 minute quadrangle topographic map of the site is shown in Figure 4 but keep in mind the map was developed in 1960 prior to the retreat of the Knik glacier, therefore many of the braided channels depicted north of the bridge site no longer are actively

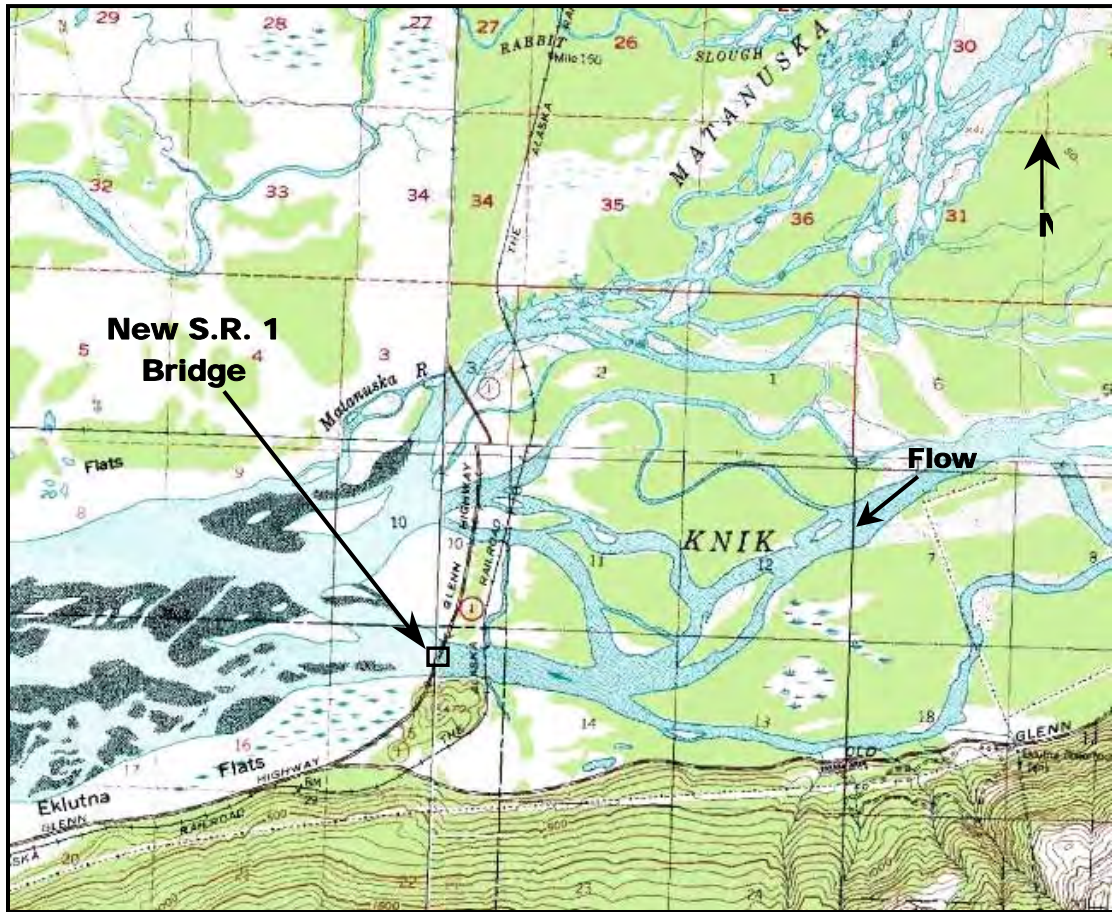


Figure 4. USGS topographic map of Old Glenn Highway (S.R. 1) bridge over the Knik River near Palmer, AK (elevations are in feet).



Figure 5. Aerial photo of the site taken in 1996 showing the geomorphic setting of the Knik River at the Old Glenn Highway (Route 1) bridge near Palmer, AK.

conveying flow. An aerial photo of the site taken in 1996 is shown in Figure 5. Data characterizing the geomorphic setting is summarized in Table 3.

Table 3. Geomorphic data

Geomorphic Characteristic	Description
Drainage Area (mi ²)	1200
Slope in Vicinity (ft/ft)	.00069
Flow Impact	Straight
Channel Evolution	Unknown
Armoring	Partial
Debris Frequency	Unknown
Debris Effect	Unknown
Stream Size	Wide
Flow Habit	Perennial
Bed Material	Gravel
Valley Setting	Moderate
Floodplain Width	Unknown
Natural Levees	Unknown
Apparent Incision	Unknown
Channel Boundary	Alluvial
Banks Tree Cover	High
Sinuosity	Sinuuous
Braiding	Generally
Anabranching	Generally
Bars	Wide
Stream Width Variability	Wider

Bed Material Data

Observations since the recession of the Knik glacier indicate that the bed material and suspended sediment is almost entirely composed of very fine glacial silt. In fact, wading measurements at the site are avoided because the bed is a mud 'soup' that acts similar to quick sand. There is a fair amount of sand and gravel that is transported along the bed at high flows, but it is insignificant compared to the quantities of silt being scoured and deposited. The only bed material samples that are recorded at the site were collected in 1965, prior to the retreat of the Knik glacier, as part of a USGS scour investigation. The bed material was classified as gravel with a $D_{50} = 1.6$ mm, however that sample is not representative of the current bed material.

Roughness Coefficients

A distribution of Manning's n values is provided in Table 4.

Table 4. Manning's n values for the Knik River at the Old Glenn Highway bridge. (fldpln, floodplain; chnl, channel; rt, right)

Flow Type	Left Fldpln	Main Chnl	Rt Fldpln
High	--	0.037	--
Typical	0.08	0.030	0.08
Low	--	0.027	--

Abutment Details

The bridge has sloping spill-through abutments with dumped riprap as scour protection. Spur dikes, with a top of berm elevation of 51.0 ft, extend upstream of the new bridge and preclude abutment scour as defined in HEC-18. The abutment characteristics are summarized in Table 5.

Table 5. Abutment data

Abutment Characteristic	Description
Left Station	0
Right Station	505.5
Left Skew (deg)	0
Right Skew (deg)	0
Left Abutment Length (ft)	46
Right Abutment Length (ft)	46
Left Abutment to Channel Bank (ft)	0
Right Abutment to Channel Bank (ft)	0
Left Abutment Protection	Riprap
Right Abutment Protection	Riprap
Contracted Opening Type	III
Embankment Skew (deg)	0
Embankment Slope (ft/ft)	Unknown
Abutment Slope (ft/ft)	2
Wingwalls	No
Wingwall Angle (deg)	N/A

* - Type III opening has sloping abutments and sloping spillthrough abutments.

Pier Details

The two piers are numbered from left to right, looking downstream and consist of single concrete columns with partial web walls. The piers have square foundations supported by steel piles drive to an estimated elevation of -14.0 ft. The pier characteristics are summarized in Table 6.

Table 6. Pier data (--, not available)

Pier ID	Bridge Station (ft)	Alignment	Highway Station	Pier Type	# of Piles	Pile Spacing (ft)
1	155	0	106+45.5	Single	-	-
2	345	0	108+35.5	Single	-	-

Pier ID	Pier Width (ft)	Pier Shape	Shape Factor	Length (ft)	Protection	Foundation
1	4.33	Sharp	--	26	None	Piles
2	4.33	Sharp	--	26	None	Piles

Pier ID	Top Elevation (ft)	Bottom Elevation (ft)	Foot or Pile Cap Width (ft)	Cap Shape	Pile Tip Elevation (ft)
1	21	16	--	Square	-14
2	21	16	--	Square	-14

Surveyed Elevations

A gage (station 15281000) was operational at this site from 1958-1988 and from 1991-1992. Gage datum is tied to a Corps of Engineers benchmark (elevation 62.67 ft above MSL) on the upstream side of the left abutment of the old bridge. Elevation to gage datum for this point is 32.50 ft. To correct elevations to gage datum adjust by 30.17 ft. A summary of the measured water surface elevations and corresponding discharges at the new bridge is presented in Table 7.

Table 7. Water-surface elevations and corresponding discharges measured on the Knik River at the new Old Glenn Highway bridge.

Date	Discharge (cfs)	Water Surface Elevation (ft)
7/13/1999	23,000	41.57
8/1/2001	21,700	41.13

The low-water survey of the floodplains in the approach and exit sections utilized a local right-hand coordinate system, which was established with the positive y-axis in the upstream direction and the x-axis parallel to the upstream face of the bridge. This resulted in x-coordinates increasing from right to left. The HEC-RAS step backwater model requires the use of left to right coordinates (looking downstream), therefore stationing was added which increases from left to right.

PHOTOS



Figure 7. Looking downstream at the Old Glenn Highway (S.R. 1) bridge over the Knik River near Palmer, AK on 7/16/2001.

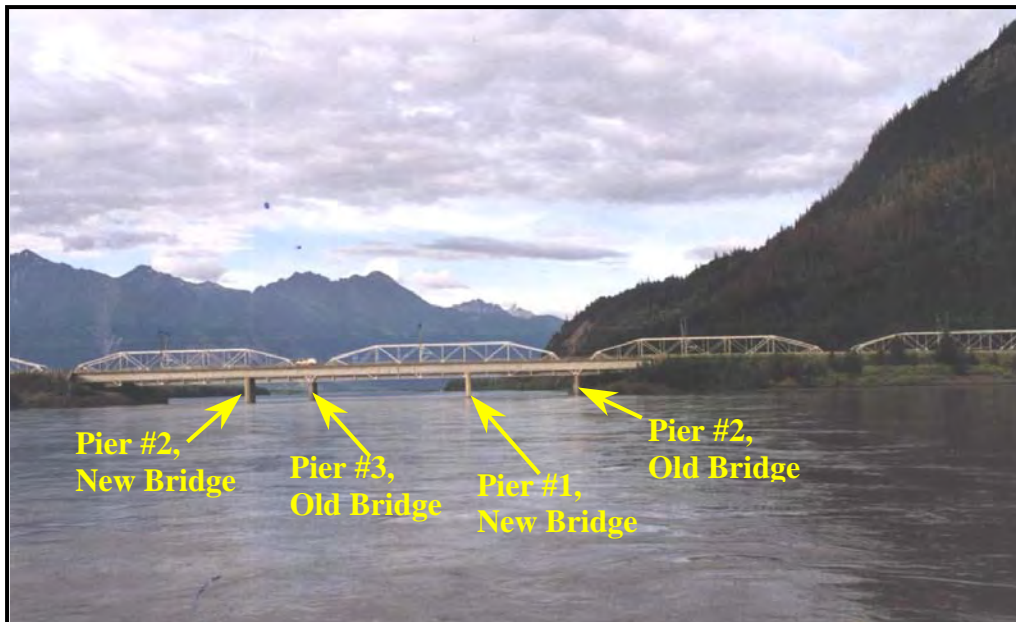


Figure 8. Looking upstream at Old Glenn Highway (S.R. 1) bridge from a boat on the Knik River, 8/1/2001.

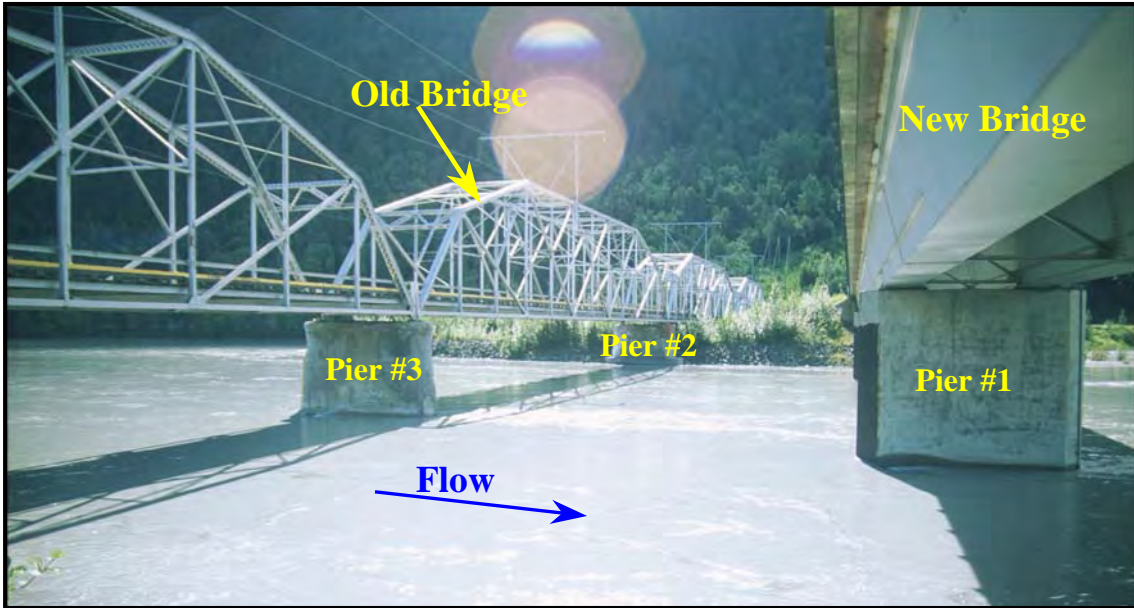


Figure 9. Looking from right bank to left bank between the two Old Glenn Highway bridges (new bridge is on the right) over the Knik River.



Figure 10. Looking along upstream face of the old Old Glen Highway bridge over the Knik River at the left bank and spur dike.



Figure 11. Looking along downstream face of the new Old Glen Highway bridge over the Knik River, field crew and survey boat are in shown in the foreground.

MEASURED SCOUR

All reported bathymetry data were collected with a fathometer on a manned boat. Discharge and velocity data were collected with a traditional AA price current meter during the 1999 survey and with an ADCP during the 2001 survey. ADCP data were collected at 13 cross sections (Figure 12). Topographic, bathymetric, and ADCP data were all geo-referenced with a base station corrected GPS receiver. GPS coverage in this area is extremely poor. The northern latitude in conjunction with the 6,400 ft Pioneer Peak located on the left bank of the river resulted in low space vehicle availability. During optimal surveying times, only seven space vehicles were visible. These conditions resulted in high PDOPs and multi-pathing. The estimated post processed vertical and horizontal precisions range from 1.2-2.9 ft and 0.7-2.7 respectively. All data points with a PDOP in excess of 4.0 were eliminated from the data set. Outlying points (i.e. extreme high or low elevation) were also eliminated from the data set. The GPS unit was interfaced to WinRiver and used in the collection of ADCP data. The processed data using the GPS for bottom tracking are variable and the ship tracks are erratic. This is thought to be the result of intermittent DGPS signal resulting from poor satellite coverage. A summary plot of the surveyed topographic and bathymetric data points collected in 1999 and 2001 are depicted in Figures 13 and 14, respectively. It is important to note that all scour measurements were made at the upstream face of the old bridge.

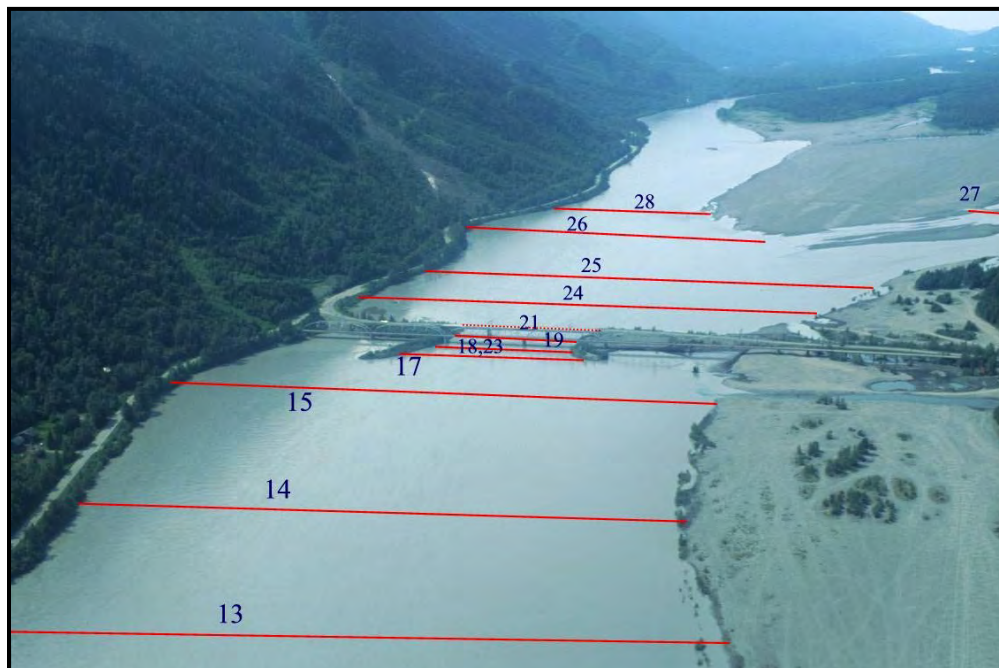


Figure 12. Looking downstream at location of ADCP cross-sections on the Knik River at Old Glenn Highway (S.R.1).

Abutment Scour

No measurement of abutment scour were made at the Old Glenn Highway bridge.

Contraction Scour

The contraction at this site is attributed to the reduction of the Knik River from numerous braided channels upstream to a single channel through the bridge opening. The observed contraction scour represents depths computed from an "equilibrium bed" elevation measured prior to the spring and summer runoff period. A direct relationship between the progression of contraction scour and the discharge hydrograph during the snowmelt period is depicted in Figure 15. The measured contraction scour depth and site characteristics pertinent to contraction scour that were collected during the detailed bridge scour survey July 31-August 3, 2001 are summarized in Table 9. The contracted width in the Table does not include the width of the riprap protection (~75 ft) around pier #3 of the old bridge and the scour depth is cumulative over the snowmelt period prior to the measurement (April – August, 2001).

Pier Scour

Scour at pier #3 of the old bridge is a concern of the AkDOT and therefore it has been protected with riprap. None of the measured scour is associated with pier scour. Although the presence of pier #3 supporting the old bridge likely had an effect on the depth of contraction scour reported at the site, it is not possible to accurately quantify the pier's contribution to the total scour.

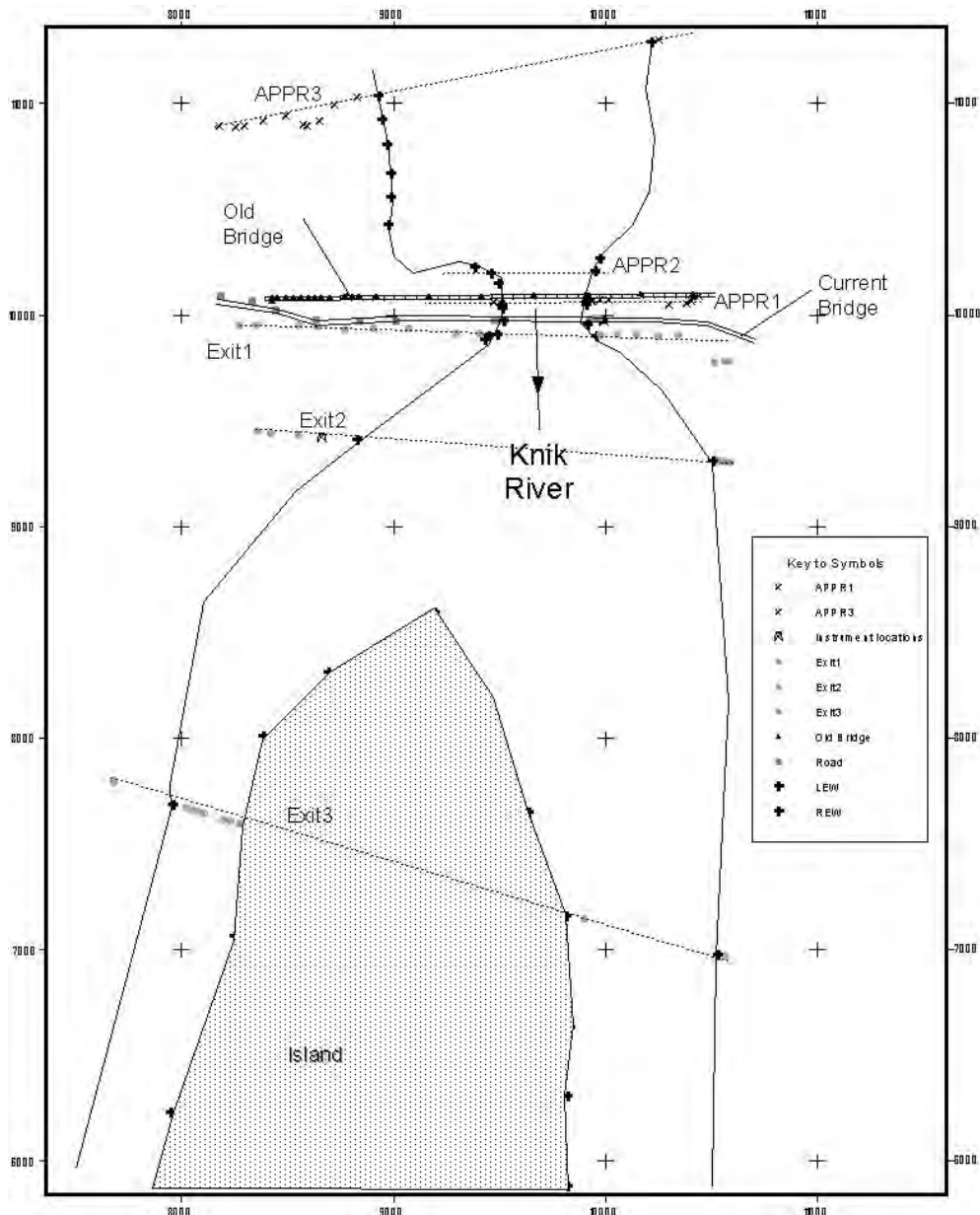


Figure 13. Schematic of survey data for bridge 539 at Knik River near Palmer, AK, collected during 1999-scour survey (Coordinate system is arbitrary).

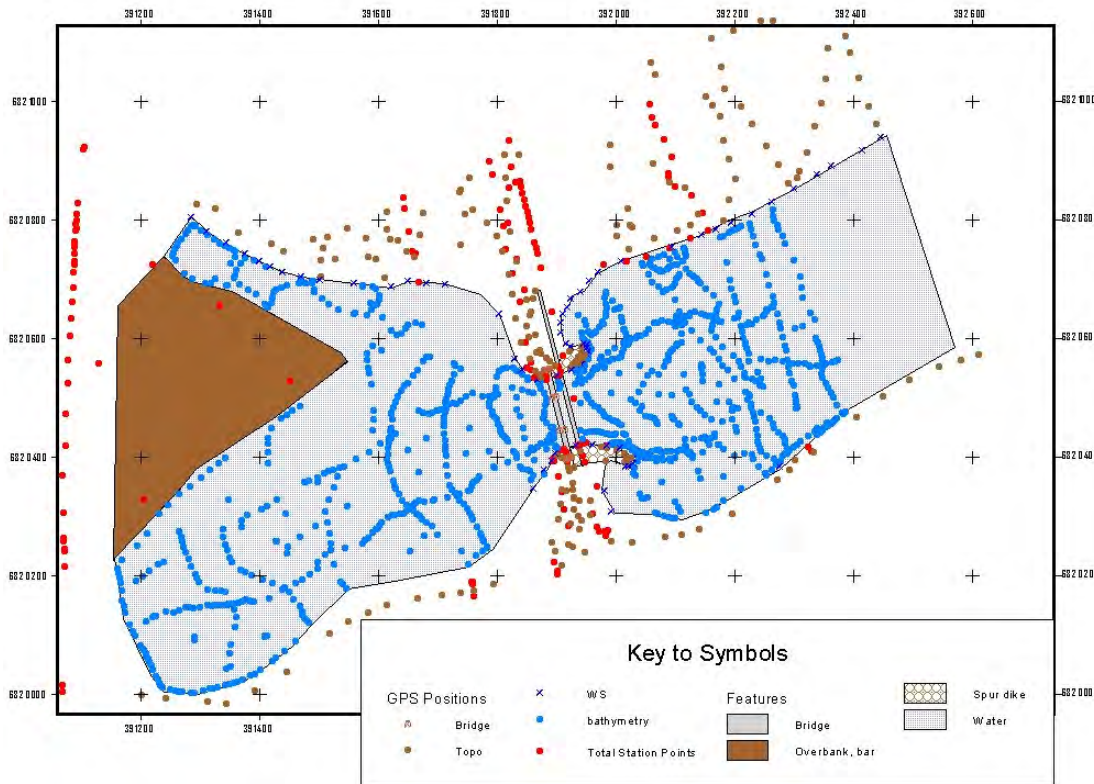


Figure 14. Schematic of survey data for bridge 539 at Knik River near Palmer, AK, collected during 2001-scour survey (Coordinate system is UTM Zone 6, NAD27 Alaska datum).

Table 9. Contraction scour data (--, not available; ft/s, feet per second; cfs, cubic feet per second; US, upstream; DS, downstream; Avg, average)

Measurement Number	Contracted Date	Contracted Time	Uncontracted Date	Uncontracted Time	US/DS	Scour Depth (ft)
1	8/1/2001	12:00	8/1/2001	12:00	US	7.5
Measurement Number	Accuracy (ft)	Contracted Avg Vel (ft/s)	Contracted Discharge (cfs)	Contracted Depth (ft)	Contracted Width (ft)	
1	2	4.2	21700	15	335	
Measurement Number	Uncontracted Avg Vel (ft/s)	Uncontracted Discharge (cfs)	Uncontracted Depth (ft)	Uncontracted Width (ft)	Channel Contraction Ratio	
1	3.7	17400	7.5	625	---	
Measurement Number	Pier Contraction Ratio	Scour Location	Eccentricity	Sediment Transport	Bed Form	Debris Effect
1	---	Main Channel	---	Live-Bed	Unknown	Insignificant
Measurement Number	D95 (mm)	D84 (mm)	D50 (mm)	D16(m)	Sigma	Bed Material Cohesion
1	11	5	1.6	0.5	--	Non-cohesive

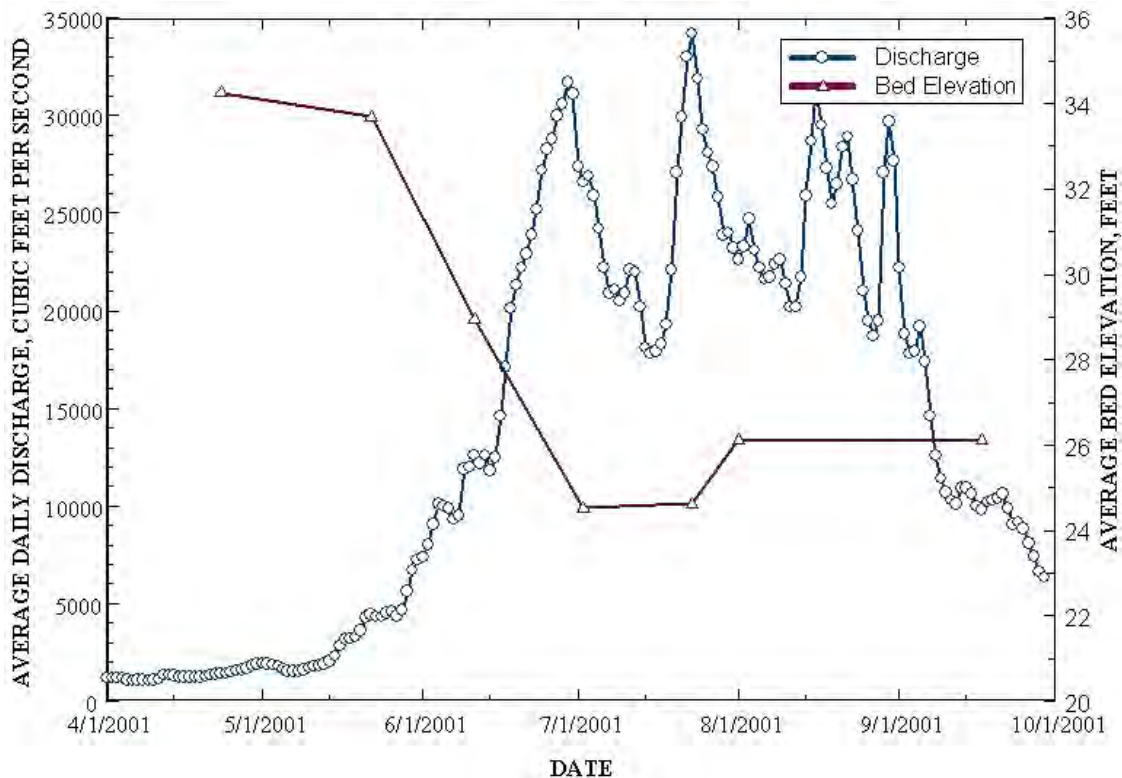


Figure 15. Plot of average bed elevation change (across the entire bridge opening) relative to the 2001 snowmelt runoff hydrograph on the Knik River at the Old Glenn Highway bridge.

COMPUTED SCOUR

A HEC-RAS model of the site was developed as part of a level 2-scour analysis of the new Old Glenn Highway (S.R. 1) bridge to predict the scour at this site under various hydraulic conditions. Bathymetric and topographic data collected in 1999 was supplemented with information from the as-built bridge plans in order to develop the HEC-RAS model of the site. The hydraulic conditions measured during on July 13, 1999 as well as the Q100 and Q500 were modeled to determine the hydraulic parameters needed for HEC-18 scour computations. Discharge estimates for the 100- and 500-year events were taken from the Phase 1 analysis at the site, which determined the flood frequency magnitudes using methods outlined by Jones and Fahl (1994). High volume (up to 359,000 cfs) glacial outburst floods occurred annually on the Knik River up until 1966. Due to recession of the Knik glacier these flows no longer occur and were therefore not included in the calculations of the Q100 and Q500 discharges. The model was run as subcritical using the standard step energy method. Initial boundary condition for the July 13, 1999 calibration survey was a known water surface elevation of 39.92 ft. at the location of the EXIT3 cross-section (see Figure 13), while the initial condition for the Q100 and Q500 events was a normal depth with a slope of 0.0005. This is the slope of the energy gradient at the downstream cross section for the calibration discharge. Model variables are summarized in Table 10.

Roughness values of 0.08 for the overbanks and 0.03 for the channel were initially selected and the channel values were adjusted to as low as .027 and as high as 0.037 to calibrate the modeled water surface elevation to the observed. Using these values the modeled water surface elevations are equal to the observed for sections EXIT2, EXIT1, and APPR1. Section APPR2 has a modeled elevation of 41.3 ft and an observed of 41.57 ft and section APPR3 has a modeled elevation of 42.0 ft with an observed water surface at 42.53 ft. The discrepancy between modeled and observed water surfaces for the approach sections could be attributed to templating survey data upstream. This may present a situation in which the templated elevations are lower than actual elevations. This would result in modeled water surfaces that are lower than observed. The model errors indicate the need for more cross sections to reduce velocity head drops and conveyance ratios between sections. Addition of interpolated cross sections would eliminate these errors, but not significantly affect the water surface profiles or the scour computations.

Using the methodology from HEC-18 (Richardson and Davis, 1995) contraction (live-bed) and pier scour were calculated using HEC-RAS for bridge 539. Larry S. Leveen (unpublished U.S. Geological Survey administrative report, 1967) determined a D50 of 1.08 mm and measured dunes up to 4 ft in height and 10 ft in wavelength at the Knik River crossing on the new Glen Highway. Although these data were downstream of bridge 539 they are thought to be representative and were used in the scour calculations.

Abutment Scour

No abutment scour was computed with the HEC-RAS model.

Contraction Scour

The reported contraction scour for each measured flood was computed using the HEC-RAS hydraulic parameters and HEC-18 live-bed equations. The results of the computed contraction scour are summarized in Table 11.

Pier Scour

Pier scour was computed using the CSU equation. Water temperature used for the calculations was 45° Fahrenheit. Angle of attack was left at zero because the piers are aligned to the direction of flow. The results of the scour computations are presented in Table 11.

POINT OF CONTACT

Any questions regarding the Old Glenn Highway (S.R. 1) bridge over the Knik River should be directed to the following point of contact:

Jeff Conaway, Hydrologist
U.S. Geological Survey, Water Resources Division
4230 University Drive, Suite 201
Anchorage, Alaska 99508-4664
(907)-786-7041
jconaway@usgs.gov

Table 10. Summary of selected model parameters used for the level 2-scour analysis of the new Old Glenn Highway bridge.

Variable	Value	Notes
Manning's roughness	.027-.037 (channel), 0.08 (overbank)	Calibrated to observed water surface elevation
Discharge (7/13/1999)	23,000 ft ³ s ⁻¹	Calibration condition
Q100	79,400 ft ³ s ⁻¹	
Q500	104,000 ft ³ s ⁻¹	
Elevation (7/13/1999)	39.92 ft	At downstream cross section
Slope of water surface	0.0007	Determined from surveyed WS
Slope of energy gradient	0.0005	At downstream cross section for calibration discharge
D50	1.08 mm or 0.0035 ft.	Leveen scour report
Water temperature	45° Fahrenheit	Estimated
Pier dimensions for scour calculation	4.3 ft wide, 26 ft long	
Pier Shape	Sharp nosed	
Bed condition	Medium dunes (K3=1.1)	Leveen scour report

Table 11. Summary of computed scour results for the new Old Glenn Highway bridge over the Knik River near Palmer, AK (All scour values are in feet).

	1999 Survey Q=23,000 ft ³ /s	Q100 Q=79,400 ft ³ /s	Q500 Q=104,000 ft ³ /s
<i>Bridge 539</i>	Channel	Channel	Channel
Contraction	0.26	0.55	0.77
Pier 1 (left bank)	7.61	11.65	12.91
Pier 2 (right bank)	7.61	11.65	12.91
Total scour	7.87	12.20	13.69

REFERENCES CITED

Jones, S.H., and Fahl, C.B., 1994, Magnitude and frequency of floods in Alaska and conterminous basins of Canada: U.S. Geological Survey Water-Resources Investigations Report 93-4179, 122 p.

Richardson, E.V., and Davis, S.R., 1995, Evaluating scour at bridges (3d ed.): U.S. Federal Highway Administration, FHWA-IP-90-017 HEC-18, 204 p.

SUPPORTING DATA*1999 Level 2-scour analysis files:*

File name	File description and software
539_knik_ics.txt 539_knik_printed	Raw data files from the data logger in Northing, Easting, Elevation (ics) and full information formats.
539_knik_survey.xls	Excel spreadsheet containing transformation of points, surveyed cross sections, interpolated cross sections, and data exported to HEC-RAS
539_knik_writeup.doc	Document summarizing 1999 analysis
539_knik.g02	Final HEC-RAS geometry file
539_knik.h01	Final HEC-RAS hydraulic design file
539_knik.f02	Final HEC-RAS flow file
539_knik.p02	Final HEC-RAS plan file
539_knik.prj	Final HEC-RAS project file (details of files used, units, default parameters, etc.)
539_knik.r02	Final HEC-RAS run file

2001 Survey Files:

File name	File description and software
finalTable.txt	All bathymetry, topo and bride survey data from 1999 survey, in a text file format.
gps points.txt	Summary of all bathymetry, topo and bride gps data from 1999 survey, in a text file.
Hydrographic data collection on the Knik River.doc	Document summarizing 2001 survey.
GPS_data.xls	GPS and Total Station data for the overbanks and channel, contains historic plot of old bridge x-sec bathymetry 1999-2001.
Total_translate.txt	Total station data in a text file format.
Knik_stage.prn	Stage data from USGS gaging station at the site (7/23/01 – 8/3/01).
Edited ADCP (folder)	ADCP measurements at the following locations: Knik013 1330 ft upstream of old bridge Knik014 800 ft upstream of old bridge Knik015 350 ft upstream of old bridge Knik017 upstream of spur dike Knik018 immediately upstream of old bridge Knik019 between bridges Knik021 immediately downstream of new bridge Knik023 immediately upstream of old bridge Knik024 400 ft downstream of new bridge Knik025 800 ft downstream of new bridge Knik026 1200 ft downstream of new bridge Knik027 tributary channel 1200 ft downstream Knik028 1500 ft downstream of new bridge

Description of Photos taken in 2001:

Photo Name	Description
Knik_002	Downstream view to bridge piers
Knik_003	Upstream view to bridges
Knik_004	ADCP/GPS mount
Knik_005	Tributary, US Right bank above spur dike
Knik_006	Old bridge pier
Knik_007	Right bank to left bank downstream of bridges
Knik_008	Downstream right bank from new bridge
Knik_009	Downstream channel from new bridge
Knik_010	Right bank to left bank from new bridge
Knik_011	Right bank to left bank between bridges
Knik_012	Old bridge from new
Knik_013	Left bank downstream of bridges
Knik_014	Right bank to left bank under new bridge
Knik_016	Tributary from end of right bank spur dike
Knik_017	Right bank to left bank under old bridge
Knik_018	Upstream from right bank spur dike
Knik_019	Upstream view to bridges
Knik_020	Right bank approach to bridge
Knik_021	Upstream left bank
Knik_air1	Aerial view of bridges looking downstream
Knik_air2	Aerial view of bridges looking downstream
Knik_air3	Aerial view of bridges looking downstream

CASE STUDY #8

Cedar River at U.S. 218 near Janesville, Iowa

SITE OVERVIEW

U.S. 218 over the Cedar River was relocated from the north edge of Janesville, IA to a location further north in 1997. Maps from Delorme do not have the bridge in the correct (new) location. The highway now crosses the Cedar River near the apex of a river bend. This new location consists of two parallel bridges, each with two lanes of traffic and wide shoulders. Each bridge has six round-nose piers. The piers of the downstream bridge are located directly downstream of the piers on the upstream bridge. The piers are hammerhead-type piers that are 18 ft long at the water surface and hammerheads are 40 ft long. There was a rock dike (berm) about 100 ft upstream extending from the left abutment out the top of bank. Although the concrete portion of the abutments is not continuous between the bridges, there is only a short distance and shallow ditch between the two bridges, so the abutments have been treated for hydraulic purposes as if they were continuous abutments. The right abutment has a guidebank on the upstream side to help redirect flow from the right floodplain.

This site is used by the USGS for making streamflow measurements. The Cedar River at Janesville stream gage (05458500) is located in a park about 0.25 miles downstream from the bridge and has been operational from 1904 - 2003.

The bridge is located near the apex of a bend in the river. Standing on the bridge looking upstream reveals a straight channel for about 500 ft and looking downstream, a straight channel for a much longer distance. Beyond 500 ft upstream, several islands divide the channel. The description of the USGS gaging station states that the streambed is composed of sand, gravel, and rock.

The left floodplain is fairly narrow, high, and thinly wooded. The right floodplain is low with trees and bushy undergrowth. A small field is located on the upstream right floodplain and a residence with large yard is located on the downstream right floodplain. In both situations the field and yard are several hundred feet from the streambank and the area between the streambank and the field or yard is covered by trees with bushy undergrowth. The narrow left floodplain is almost completely spanned by the bridge, but there is a significant contraction on the right side.

The USGS collected real-time data at this site on 7-23-99. During this visit the stage was just past the peak and receding. A second visit was made on 7-25-99. By this time the stage had fallen to within the top banks. A low-flow visit was completed on 8-10-99. A WSPRO step-backwater model was developed for the site to estimate the amount of scour using HEC-18 methods.

A summary of the general site information on the site is found in Table 1.

Table 1. Site information

Site Characteristic	Description
County	Bremer
Nearest City	Janesville
State	Iowa
Latitude	42°39'13"
Longitude	92°27'52"
Route Number	218
Route Class	US
Stream Name	Cedar River

Hydrologic Conditions

The peak discharge that was measured during the 1999 flood was approximately 42,200 cfs on July 23, 1999. The 1999 flood produced the peak of record for the site, over 5,000 cfs more than the next highest recorded discharge. The bridge plans for the new bridges indicates that the 100-year discharge is 41,000 cfs representative of data through 1990.

DISCUSSION OF CONTRACTED SITE

The new bridges are located in the apex of a bend in the Cedar River north of Janesville, IA. A guide bank extending approximately 100 feet upstream of the left abutment and a drainage ditch on the left floodplain concentrated the contraction of the left overbank flow upstream of the bridge sections. A rock wall on the right bank adjacent to the abutment also prevented the contraction of floodplain flow at the abutment directing the flow into the main channel upstream of the bridge. A majority of the floodplain flow was in the main channel prior to being conveyed through the bridge openings. The left and right abutments were set back 200 and 60 feet, respectively, from the channel and the overbanks were heavily vegetated. A contour map of the Cedar River bathymetry surveyed during the flood on July 23, 1999 is illustrated in Figure 2.

Bridge Data

This is a relatively new bridge built in 1994. Maps from Delorme do not have the bridge in the correct (new) location. This site has two parallel bridges. Each bridge has six round-nose piers. The piers of the downstream bridge are located directly downstream of the piers on the upstream bridge. The piers are hammerhead type piers that are 18 ft long at the water surface and hammerheads are 40 ft long. There was a rock dike (berm) about 100 ft upstream extending from the left abutment out the top of bank. Although the concrete portion of the abutments is not continuous between the bridges, there is only a short distance and shallow ditch between the two bridges, so the abutments have been treated for hydraulic purposes as if they were continuous abutments. The right abutment had a short guidebank on the upstream side. The bridge characteristics pertinent to scour are summarized in Table 2.

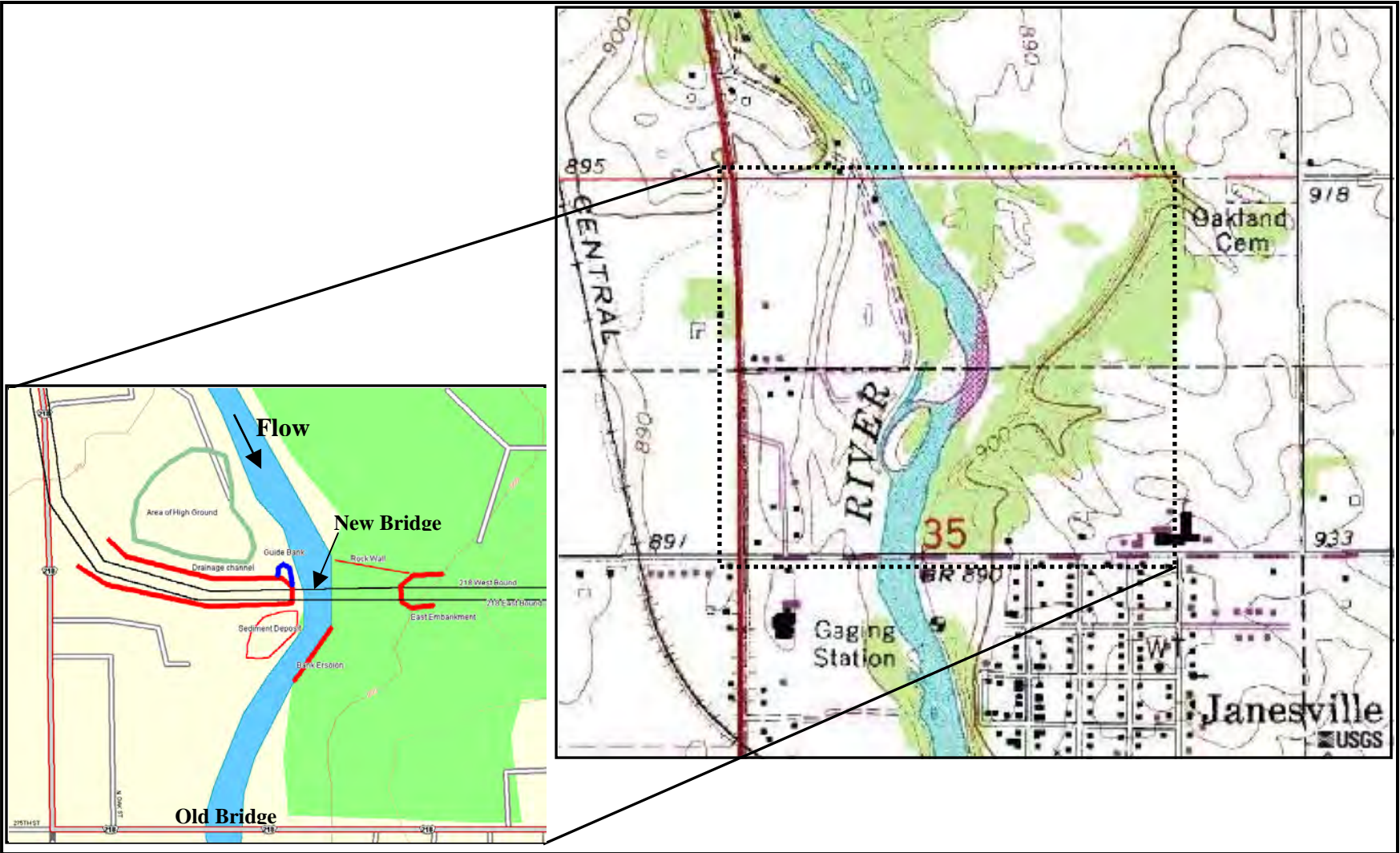


Figure 1. USGS topographic map (1984) of US 218 bridge site over the Cedar River with inset of new bridge configuration.

Table 2. Bridge data

Bridge Characteristic	Description
Structure Number	F 218-8(20)
Length (ft)	674
Width (ft)	40
Spans	7
Vertical Configuration	Sloping
Low Chord Elev (ft)	895
Upper Chord Elev (ft)	902.8
Overtopping Elev (ft)	901.8
Skew (degrees)	0
Guide Banks	Elliptical
Waterway Classification	Main
Year Built	1997
Avg. Daily Traffic	Unknown
Plans on File	Yes
Parallel Bridges	Yes
Continuous Abutments	Yes
Dist betwn Centerlines (ft)	124
Dist betwn Pier Faces (ft)	62

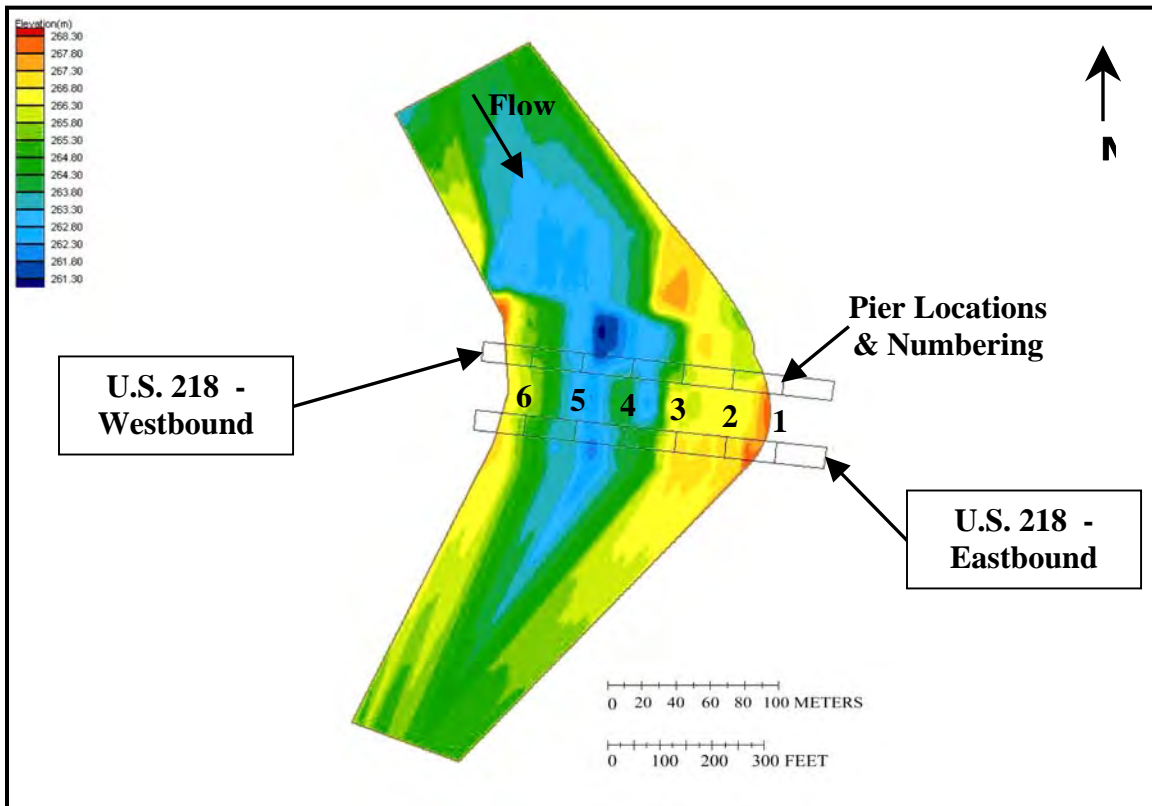


Figure 2. Contour plot of Cedar River bathymetry surveyed during flood on July 23, 1999.

Geomorphic Setting

The Cedar River streambed is composed of sand, gravel, and rock and has narrow floodplains in the vicinity of the U.S. 218 bridge. The location of the bridges in a bend of the Cedar River complicates the determination of an ambient streambed for scour estimations due to the natural tendency for long-term channel degradation in bends. The channel is straight for approximately 500 feet upstream, after a minor second bend, it is straight for a much longer distance looking downstream. Beyond 500 ft upstream, several islands divide the channel.

A portion of the USGS 7.5 minute quadrangle topographic map of the site with the old bridge is shown in Figure 1 and an aerial photo of the site taken in 1994 with the new bridges is shown in Figure 3. Data characterizing the geomorphic setting is summarized in Table 3.



Figure 3. Aerial photo of the U.S. 218 bridge site over the Cedar River, taken in 1994.

Bed Material Data

The description of the USGS gaging station states that the streambed is composed of sand, gravel, and rock. Bed material samples were collected just upstream of the bridge revealed a D_{50} of 0.53 mm. A full grain size distribution of the bed material sample collected in the area around the scour hole is shown in Figure 4.

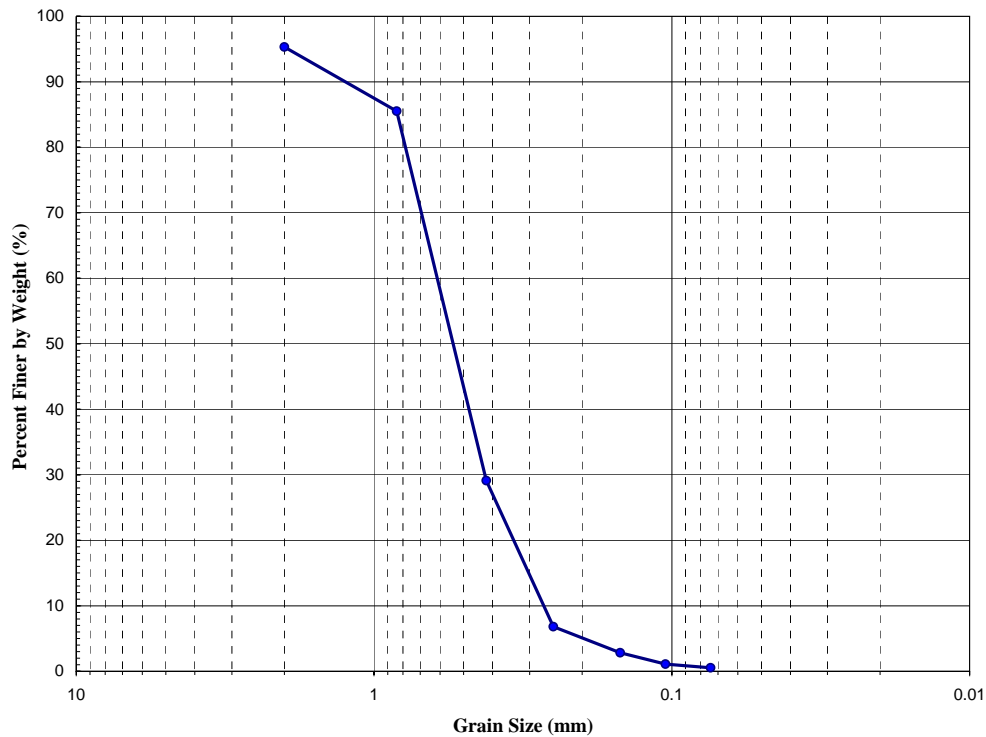


Figure 4. Grain size distribution for the bed material sample collected upstream of US 218 in the Cedar River near Janesville, IA.

Table 3. Geomorphic data

Geomorphic Characteristic	Description
Drainage Area (mi ²)	1661
Slope in Vicinity (ft/ft)	.000379
Flow Impact	Left
Channel Evolution	Unknown
Armoring	Unknown
Debris Frequency	Occasional
Debris Effect	Local
Stream Size	Medium
Flow Habit	Perennial
Bed Material	Sand
Valley Relief	Low
Floodplain Width	Narrow
Natural Levees	Little
Apparent Incision	Unknown
Channel Boundary	Alluvial
Banks Tree Cover	Medium
Sinuosity	Straight
Braiding	None
Anabranching	Locally
Bars	Narrow
Stream Width Variability	Random

Roughness Coefficients

A distribution of Manning's n values is provided in Table 4.

Table 4. Manning's n values for the Cedar River at US 218 near Janesville, IA. (fldpln, floodplain; chnl, channel; rt, right)

Flow Type	Left Fldpln	Main Chnl	Rt Fldpln
High	0.15	0.034	0.15
Typical	0.1	0.03	0.106
Low	.05	.024	.084

Abutment Details

The bridge has sloping spill-through abutments with no scour protection. Both abutments are setback from the main channel and the overbanks through the bridge are heavily vegetated. The abutment characteristics are summarized in Table 5.

Table 5. Abutment data

Abutment Characteristic	Description
Left Station	0
Right Station	673.75
Left Skew (deg)	0
Right Skew (deg)	0
Left Abutment Length (ft)	142
Right Abutment Length (ft)	142
Left Abutment to Channel Bank (ft)	200
Right Abutment to Channel Bank (ft)	60
Left Abutment Protection	None
Right Abutment Protection	None
Contracted Opening Type	III*
Embankment Skew (deg)	0
Embankment Slope (ft/ft)	6
Abutment Slope (ft/ft)	2.5
Wingwalls	No
Wingwall Angle (deg)	N/A

* - Type III opening has sloping abutments and sloping spillthrough abutments.

Pier Details

Piers are numbered from left to right looking downstream and all have a uniform vertical profile; 18 feet long, with hammerhead design at top. The pier characteristics are summarized in Table 6.

Surveyed Elevations

Water surface elevations at the site were measured from the upstream and downstream sides of the US 218 bridge during the real-time scour measurements on July 23, 1999. The measurements were made at the beginning and end of the data collection and revealed that the river stage was falling throughout the day (Table 7).

Table 6. Pier data (--, not available)

Pier ID	Bridge Station (ft)	Alignment	Highway Station	Pier Type	# of Piles	Pile Spacing (ft)
1	95.75	0	---	Single	--	--
2	192.25	0	---	Single	--	--
3	288.75	0	---	Single	--	--
4	385.25	0	---	Single	--	--
5	481.75	0	---	Single	--	--
6	578.25	0	---	Single	--	--

Pier ID	Pier Width (ft)	Pier Shape	Shape Factor	Length (ft)	Protection	Foundation
1	3	Round	--	18	None	Poured
2	3	Round	--	18	None	Poured
3	3	Round	--	18	None	Poured
4	3	Round	--	18	None	Piles
5	3	Round	--	18	None	Piles
6	3	Round	--	18	None	Piles

Pier ID	Top Elevation (ft)	Bottom Elevation (ft)	Foot or Pile Cap Width (ft)	Cap Shape	Pile Tip Elevation (ft)
1	868.40	865.40	9	Square	---
2	862.89	859.90	9	Square	---
3	858.04	855.04	9	Square	---
4	864.08	860.08	9	Square	839
5	863.82	859.82	9	Square	820
6	863.96	859.96	9	Square	860

Table 7. Summary of surveyed water-surface elevations at the US 218 bridge over the Cedar River on July 23, 1999.

Location	Time	APPENDIX A Water Surface Elevation (ft)
Upstream	10:41	886.42
Downstream	10:49	886.17
Upstream	17:15	885.85
Downstream	17:19	885.58

PHOTOS



Figure 5. Looking west across upstream face of US 218 bridge over the Cedar River near Centralia, WA on 7/23/1999.



Figure 6. Looking upstream at wake around Pier 5 of upstream US 218 bridge over the Cedar River, 7/23/1999.



Figure 7. Looking downstream from downstream US 218 bridge deck, 7/23/1999.



Figure 8. Looking upstream at right guide bank, floodplain and drainage ditch on 7/23/1999.



Figure 9. Looking upstream from upstream US 218 bridge over the Cedar River, 7/23/1999.



Figure 10. Looking at upstream left floodplain from upstream US 218 bridge over the Cedar River, 7/23/99.



Figure 11. Looking upstream at right guide bank, floodplain and drainage ditch from upstream US 218 bridge over Cedar River during low flow, 8/10/99.



Figure 12. Looking upstream at left overbank and areas of clear-water scour from downstream US 218 bridge over Cedar River during low flow, 8/10/99.



Figure 13. Looking downstream at right overbank and Pier 5 of US 218 bridge over Cedar River during low flow, 8/10/99.

MEASURED SCOUR

The most substantial scour occurred in the main channel upstream of the bridges between piers 4 and 5 (Figure 2). The scour hole was approximately 100 feet long in the longitudinal direction of flow beginning near the upstream face of the westbound bridge and extending upstream. A minimal depression was observed around pier 5 on the right overbank for both the upstream and downstream bridges (Figure 12).

Abutment Scour

No measurement or computations of abutment scour were made at the US 218 bridge over the Cedar River.

Contraction Scour

The reference surface used to determine the reported contraction scour of 2 feet was established by inspection of a longitudinal profile through the SR 218 surveyed bridge reach. The plot (shown Figure 13) illustrates a natural degradation of the channel bed through the bridge opening due to the bend rather than contraction scour. The contraction scour was measured below the bed elevation in the bend rather than average

channel elevation in uncontracted sections further upstream and downstream (Figure 2). A spur dike extending upstream of the bridge's right abutment forced the right floodplain flow to enter the channel approximately 100 feet upstream of the bridge at which point scour in the channel was observed. The reference surface was established from a cross-section located upstream of the convergence between the floodplain and main channel flow. The maximum contraction scour depth was ~5.7 feet and observed upstream of the bridges between pier #4 and #5.

The measured contraction scour depth and modeled site characteristics pertinent to contraction scour are summarized in Table 9.

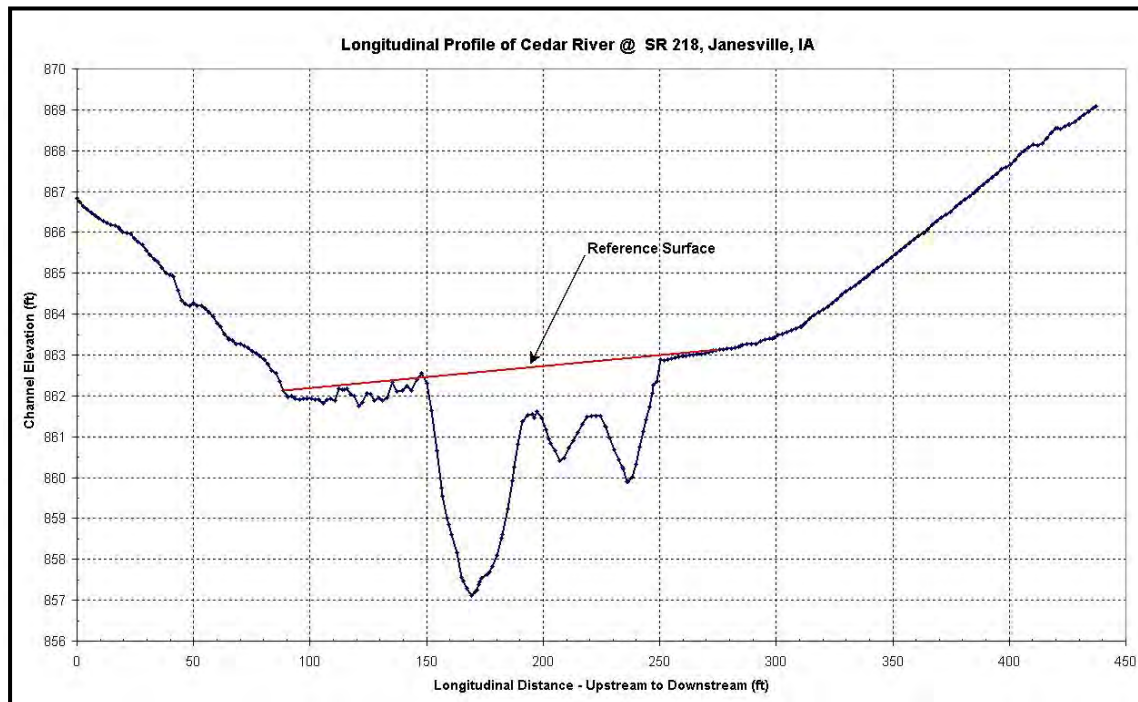


Figure 14. Surveyed longitudinal streambed profile of Cedar River at US 218 on 7/23/1999, used to estimate measured contraction scour.

Pier Scour

No local pier scour was reported in the bridge scour database (BSDMS) although some minor depressions were observed around the base of pier 5 during the low-flow inspection.

Table 9. Contraction scour data (---, not available; ft/s, feet per second; cfs, cubic feet per second; US, upstream; DS, downstream; Avg, average)

Measurement Number	Contracted Date	Contracted Time	Uncontracted Date	Uncontracted Time	US/DS	Scour Depth (ft)
1	7/23/1999	15:15	7/23/1999	14:45	US	2
Measurement Number	Accuracy (ft)	Contracted Avg Vel (ft/s)	Contracted Discharge (cfs)	Contracted Depth (ft)	Contracted Width (ft)	Channel Contraction Ratio
1	0.5	5.6	24,200	24.6	190	
Measurement Number	Uncontracted Avg Vel (ft/s)	Uncontracted Discharge (cfs)	Uncontracted Depth (ft)	Uncontracted Width (ft)	Channel Contraction Ratio	
1	5.2	24,800	22.6	210	0.29	
Measurement Number	Pier Contraction Ratio	Scour Location	Eccentricity	Sediment Transport	Bed Material Cohesion	Debris Effect
1	0.032	Main Channel	---	Live-Bed	Non-cohesive	Unknown

COMPUTED SCOUR

A WSPRO model of the site was developed as part of a post-scour analysis of the US 218 bridge. The model was calibrated to surveyed high-water marks and discharge utilizing the topographic data from the low-flow floodplain survey and channel bathymetry collected during the flood. Pre-flood channel geometry was then input to the calibrated model to estimate the bridge scour using methods outlined in HEC-18 (Richardson and Davis, 1995).

Abutment Scour

Abutment scour was computed utilizing the WSPRO model and Froehlich and HIRE design scour equations but not reported due to the increased erosion resistance of heavy vegetation present on the overbanks adjacent to the abutments.

Contraction Scour

Contraction scour was estimated for the main channel using the live-bed equation and for the overbanks using the Laursen Clear –Water contraction scour equation methodologies from HEC-18 (Richardson and Davis, 1995). The results of the computed contraction scour are summarized in Table 10. No measurable scour was observed on the overbanks due to the primarily due to the presence of heavy vegetation.

Pier Scour

Pier scour was computed at piers 4, 5 and 6 but pier scour measurements were not detailed enough to build a comparison and beyond the scope of the project.

Table 10. Summary of computed and observed contraction scour for U.S. 218 over the Cedar River near Janesville, IA.

	Type	HEC-18 Computed (ft)	Observed (ft)
Main Channel Contraction Scour	Live-Bed	2.5	2
Left Overbank Contraction Scour	Clear-Water	10.6	< 1
Right Overbank Contraction Scour	Clear-Water	11.6	< 1

POINTS OF CONTACT

Any questions regarding the U.S. 218 bridge over the Cedar River should be directed to the following point of contact:

1. Chad Wagner, Hydraulic Engineer
U.S. Geological Survey, Water Resources Division
3916 Sunset Ridge Road
Raleigh, NC 27613
(919) 571-4021
e-mail: cwagner@usgs.gov
2. Dave Clamon, Hydraulic Engineer
Iowa Department of Transportation
(515) 239-1487

SUPPORTING DATA

saab.meas.outp - scour calculations output worksheet

wsp_calb.prt - WSPRO output file for calibration model using surveyed high-water marks and discharge

wsp_prel.prt - WSPRO output file for model using pre-flood geometry for scour calculations.

AllSections.xls - Excel spreadsheet with all surveyed channel bathymetry

f218.xls - Excel spreadsheet with all surveyed floodplain topography.

Janesville_Topo.jpg - plot of surveyed channel bathymetry on July 23, 1999.

LongProfile.jpg - longitudinal profile of surveyed channel reach used to establish contraction scour reference surface.

NewBridgeLocation.jpg - sketch of new bridge location and alignment relative to old bridge.

Photos:

DCP00172.jpg - DCP00207.jpg - photos taken during 1999 flood

DCP00252.jpg-DCP00344.jpg - photos taken during after 1999 flood receded.

DSCN0123.jpg-DSCN0138.jpg - photos taken during low-flow/floodplain survey (2000).

Janesville photos.doc - Word document description of all site photos.

Iowa_Janesville_3-25-90.jpg - Aerial photo of site taken in 1990, prior to construction of new bridges

Iowa_Janesville_5-01-94.jpg - Aerial photo of site taken in 1994, after construction of new bridges

ADCP Data Files:

IOWA003.vel - IOWA 031.vel - output files of ADCP data collected on at site 7-23-99.

CASE STUDY #9

Galvin Road Overflow Bridge for the Chehalis River near Centralia, Washington

SITE OVERVIEW

The Galvin Road Overflow bridge is approximately 2.5 miles northwest of the town of Centralia, WA and serves as a relief opening on the east floodplain of the Chehalis River during high-flow events (Figure 1). The current bridge at the site is 382 feet (ft) long and consists of 10 spans supported on 11 piers. A low spot in the embankment fill 500 ft east of the bridge overtops during major floods and prevents pressure flow at the overflow bridge. The bridge was damaged on February 9, 1996, when the Chehalis River experienced a major flood. The flood produced a massive scour hole under the western one-third of the bridge and undermined the timber piles of one intermediate pier, which caused the bridge deck to sag 18 inches.

A USGS gaging station (12027500) on the Chehalis River at Grand Mound has been operational four miles downstream of the Galvin Road Overflow bridge from 1929 - 2002.

Three hydraulic reports involving the Galvin Road Overflow bridge were developed prior to the 1996 flood: 1) FEMA Flood Insurance Study Report for Unincorporated Lewis County (FEMA, 1991); 2) Galvin Road Overflow Bridge Hydraulics Study dated November 1986 by Robert E. Meyer Consultants (REM 1986); 3) a second Galvin Road Overflow Bridge Hydraulics Study dated October 1991, also by REM (1991). The purpose of the November 1986 study was to provide Lewis County with the hydraulic information necessary to select a replacement design for the Galvin Road Overflow bridge. Due to the bridge being within FEMA's regulatory floodway, a hydraulic study had to be completed to show that the new bridge would "not increase" the 100-yr flood water surface elevation. REM developed a HEC-2 model of the Chehalis River and used it to show that with minor channel bed excavation, the overflow bridge could be shortened from 530 ft to about 360 ft and still meet FEMA's requirements. In 1991, a 382 ft long bridge was selected and REM completed a second study, which showed that the proposed bridge satisfied FEMA's "no increase" requirement (Northwest Hydraulic Consultants 1996).

The REM studies were restricted to satisfying FEMA's "no increase" requirement, and did not give a realistic picture of the hydraulic conditions that could develop during major flood, and did not accurately address scour as a potential problem at the site. A review of the HEC-2 input and output by Northwest Hydraulic Consultants prior to the 1996 flood revealed several problems. The major problem involved the use of non-representative Manning's n roughness coefficients in the vicinity of the bridge. The REM model used an n value of 0.015 for the main channel of the Chehalis River and 0.104 for the Overflow bridge opening. The n value is too low in the main channel and too high for the overflow waterway; reasonable values for both model sections range from 0.03 – 0.05. This, along with other problems in the model, caused the model to significantly underestimate the flow through the overflow bridge. The REM output indicated that for

the FEMA 100-yr flood (56,000 cubic feet per second (cfs)), less than 3,800 cfs was conveyed through the overflow and average velocities were less than 1 foot per second (fps). A simplified HEC-2 model of the site was developed by Northwest Hydraulic Consultants using surveyed high-water marks and cross-sections from the 1996 flood. The model developed from field data showed that 25,000 to 30,000 cfs passed under the overflow bridge with average velocities ranging from 8 to 10 fps.

A summary of the general site information on the site is found in Table 1.

Table 1. Site information

Site Characteristic	Description
County	Lewis
Nearest City	Centralia
State	Washington
Latitude	46°44'09"
Longitude	123°01'08"
Route Number	Galvin Road
Route Class	County
Stream Name	Chehalis River

Hydrologic Conditions

The hydrologic event responsible for the 1996 flood was an intense winter storm that hit southwestern Washington. The peak discharge that was measured during the 1996 flood was approximately 74,900 cfs on February 9. Northwest Hydraulic Consultants conducted a flood frequency analysis on the historical data (1929-1996) from the Grand Mound gaging station. Estimates of the 100- and 500-year discharges are 73,600 cfs and 99,800 cfs, respectively. The existing FEMA flood insurance study lists the 100-yr and 500-yr discharges as 56,000 cfs and 70,000 cfs; however these were based upon a shorter period of record (1929-1976).

DISCUSSION OF CONTRACTED SITE

The main channel of the Chehalis River is 1200 ft west of the overflow bridge and is spanned by a 400 ft concrete bridge. The Main bridge, overflow bridge, and low spot in the fill are the only places where flood flows can pass to downstream of Galvin Road. From surveyed high-water marks of the February 9, 1996 flood, it appears that 45,000 to 50,000 cfs remained in the Chehalis River main channel and 25,000 to 30,000 cfs passed through the overflow bridge. As the floodplain flow approached the new overflow bridge, the new western approach fill significantly blocked the flow and intensified the contraction and velocities at the left (western) portion of the overflow bridge (Figure 2).

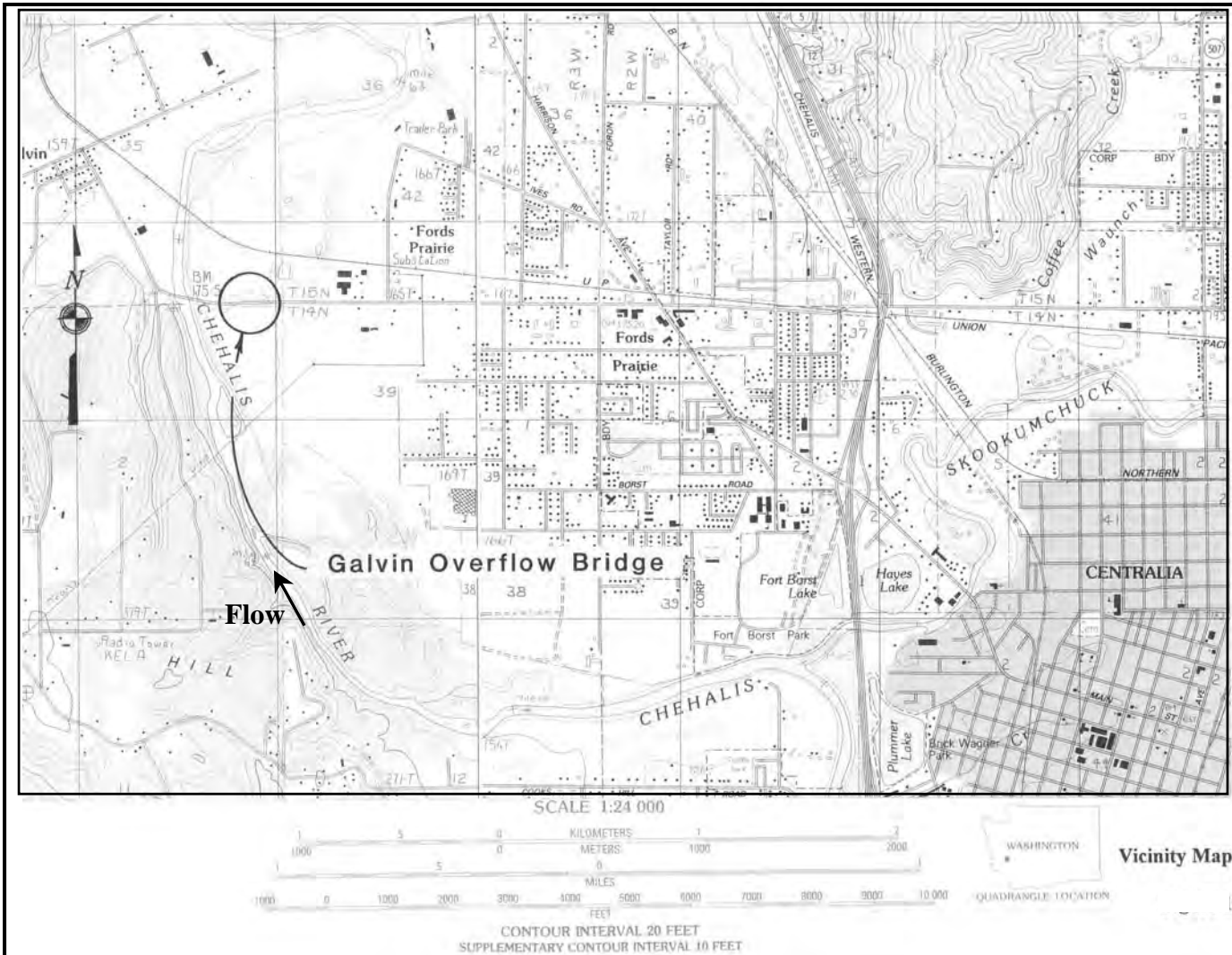


Figure 1. Location and topographic map of Galvin Road Overflow bridge site.

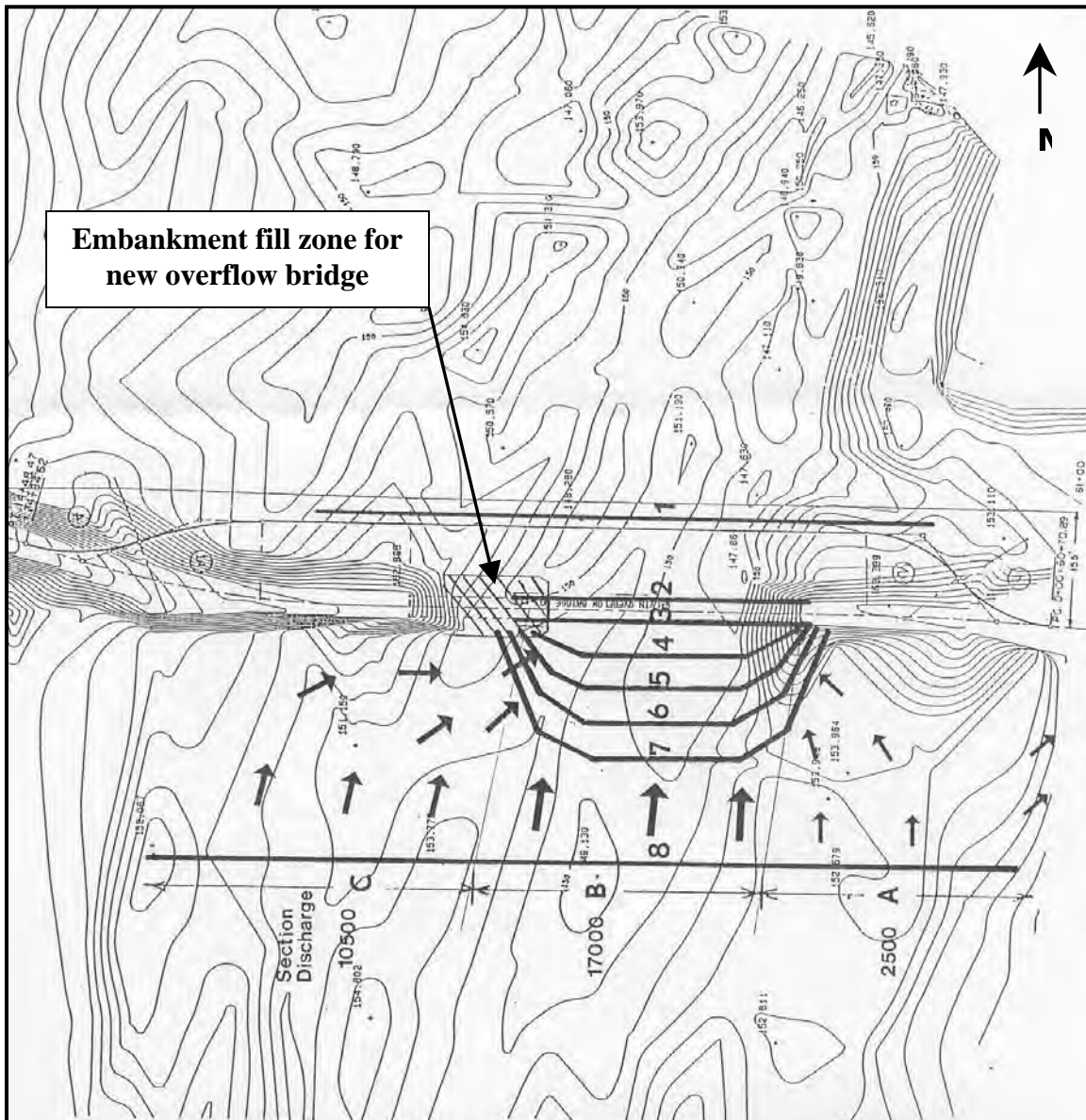


Figure 2. Sketch of flow patterns and HEC-2 model sections through Galvin Road overflow bridge during February 1996 flood.

Bridge Data

The Galvin Road overflow bridge (structure #112) was constructed in 1993 and replaced a previous 530 ft long bridge at the same location. The current bridge is 382 ft long and consists of ten composite glue-lam timber/concrete spans supported by 11 piers. When the previous bridge was removed and replaced by the new shorter structure, the west approach fill was extended 146 feet and greatly increased the contraction of the floodplain flow path. Piers 1 and 11 at the ends of the bridge are completely buried in the approach fills. Piers 2 and 10 are intermediate piers. The approach fills at the ends of the bridge are 15 to 20 ft high and block the floodplain. The end slopes of both approach fills are sloped 1.5H to 1V and protected by riprap ($D_{50} = 12$ inches). The bridge characteristics pertinent to scour are summarized in Table 2.

Table 2. Bridge data

Bridge Characteristic	Description
Structure Number	112
Length (ft)	382
Width (ft)	28
Spans	10
Vertical Configuration	Sloping
Low Chord Elev (ft)	161.8
Upper Chord Elev (ft)	163.8
Overtopping Elev (ft)	165.6
Skew (degrees)	0
Guide Banks	None
Waterway Classification	Overflow
Year Built	1993
Avg. Daily Traffic	Unknown
Plans on File	Yes
Parallel Bridges	No
Continuous Abutments	No

Geomorphic Setting

The Chehalis River is a fine- to medium-grained sand channel with a wide floodplain in the vicinity of the Galvin Road overflow bridge. The Galvin site is more complicated than most other bridge sites in the area because of a wide flood plain, upstream overbank flow diversion, off-channel storage and backwater effects from the downstream reaches of the Chehalis River. The backwater effects stems from an adverse channel gradient in the vicinity of the bridge crossing. Rather than a uniformly sloping channel in the downstream direction, the main channel of the Chehalis River between river miles 61.7 and 62.9 (the Galvin Road bridge is located upstream at river mile 64.08) has an adverse slope of .0005 ft/ft. The adverse slope of the channel in the vicinity of Galvin Road is attributed to an abrupt narrowing (pinch) of the Chehalis River valley topography approximately 3.5 river miles downstream of the Galvin Road crossing. The severe pinch in the river valley creates backwater during high flow events and leads to frequent flooding of Centralia and Interstate 5. Under most hydraulic conditions, the backwater created by the pinch in the valley topography is just as or more severe than the backwater caused by the Galvin Road overflow bridge contraction.

A portion of the USGS 7.5 minute quadrangle topographic map of the site is shown in Figure 1 and an aerial photo of the site taken in 1990 is shown in Figure 3. Data characterizing the geomorphic setting is summarized in Table 3.



Figure 3. Aerial photo of the Galvin Road Overflow bridge site taken in 1990.

Bed Material Data

From the soil logs for four test holes the bed material in the top layer consists of 6 to 10 feet of fine to medium sand underlain by 4 to 10 feet of coarser material, composed of 50% sand and 50% gravel up to 2.5-in size.

Table 3. Geomorphic data

Geomorphic Characteristic	Description
Drainage Area (mi ²)	675
Slope in Vicinity (ft/ft)	.00074
Flow Impact	Straight
Channel Evolution	Unknown
Armoring	Partial
Debris Frequency	Unknown
Debris Effect	Unknown
Stream Size	Wide
Flow Habit	Perennial
Bed Material	Organic Sand
Valley Relief	Low
Floodplain Width	Narrow
Natural Levees	Unknown
Apparent Incision	None
Channel Boundary	Alluvial
Banks Tree Cover	Low
Sinuosity	Meandering
Braiding	None
Anabranching	Generally
Bars	Unknown
Stream Width Variability	Unknown

Roughness Coefficients

A distribution of Manning's n values is provided in Table 4.

Table 4. Manning's n values for the Chehalis River overflow bridge waterway. (fldpln, floodplain; chnl, channel; rt, right)

<u>Flow Type</u>	<u>Left Fldpln</u>	<u>Main Chnl</u>	<u>Rt Fldpln</u>
High	0.05	0.05	0.05
Typical	0.03	0.03	0.03
Low	--	--	--

Abutment Details

The bridge has sloping spill-through abutments with dumped riprap as scour protection. The abutment characteristics are summarized in Table 5.

Table 5. Abutment data

Abutment Characteristic	Description
Left Station	68+05.04
Right Station	64+22.96
Left Skew (deg)	0
Right Skew (deg)	0
Left Abutment Length (ft)	60
Right Abutment Length (ft)	60
Left Abutment to Channel Bank (ft)	0
Right Abutment to Channel Bank (ft)	0
Left Abutment Protection	Riprap
Right Abutment Protection	Riprap
Contracted Opening Type	III*
Embankment Skew (deg)	0
Embankment Slope (ft/ft)	6.75
Abutment Slope (ft/ft)	1.5
Wingwalls	Yes
Wingwall Angle (deg)	45

* - Type III opening has sloping abutments and sloping spillthrough abutments.

Pier Details

The piers are numbered from right to left, looking downstream and consist of a group of 5-6 creosoted timber piles. The piles do not have foundations but rather driven into the bed material until refusal (penetration averaged 12.3 feet). The pier characteristics are summarized in Table 6.

Surveyed Elevations

The hydraulic analysis of the February 1996 flood by Northwest Hydraulic Consultants is based on high-water marks surveyed by Lewis County following the flood. From the high-water marks NHC reported that approximately 25,000 – 30,000 cubic feet per second (cfs) passed through the Gavin Road overflow bridge. A summary of the measured high-water marks and corresponding modeled discharges at the overflow bridge is presented in Table 7.

Table 6. Pier data (--, not available)

Pier ID	Bridge Station (ft)	Alignment	Highway Station	Pier Type	# of Piles	Pile Spacing (ft)
1	0	0	64+22.96	Group	5	7.1875
2	39.04	0	64+62.0	Group	6	5.75
3	77.04	0	65+00	Group	6	5.75
4	115.04	0	65+38	Group	6	5.75
5	153.04	0	65+76	Group	6	5.75
6	191.04	0	66+14	Group	6	5.75
7	229.04	0	66+52	Group	6	5.75
8	267.04	0	66+90	Group	6	5.75
9	305.04	0	67+28	Group	6	5.75
10	343.04	0	67+66	Group	6	5.75
11	382.08	0	68+05.04	Group	5	7.1875

Pier ID	Pier Width (ft)	Pier Shape	Shape Factor	Length (ft)	Protection	Foundation
1	1.42	Round	--	28	None	Piles
2	0.67	Round	--	28.75	None	Piles
3	0.67	Round	--	28.75	None	Piles
4	0.67	Round	--	28.75	None	Piles
5	0.67	Round	--	28.75	None	Piles
6	0.67	Round	--	28.75	None	Piles
7	0.67	Round	--	28.75	None	Piles
8	0.67	Round	--	28.75	None	Piles
9	0.67	Round	--	28.75	None	Piles
10	0.67	Round	--	28.75	None	Piles
11	1.42	Round	--	28	None	Piles

Pier ID	Top Elevation (ft)	Bottom Elevation (ft)	Foot or Pile Cap Width (ft)	Cap Shape	Pile Tip Elevation (ft)
1	--	--	--	None	142.1
2	--	--	--	None	136.6
3	--	--	--	None	137.4
4	--	--	--	None	137.6
5	--	--	--	None	137.8
6	--	--	--	None	138.8
7	--	--	--	None	138.9
8	--	--	--	None	137.7
9	--	--	--	None	137.7
10	--	--	--	None	135.8
11	--	--	--	None	139.9

Table 7. Surveyed high-water mark elevations and corresponding modeled discharges modeled at the Galvin Road overflow bridge.

Location	Discharge (cfs)	Water Surface Elevation (ft)
Upstream	25-30,000	160.8
Downstream	25-30,000	159.4

PHOTOS



Figure 4. Looking east across upstream face of Galvin Road Overflow Bridge for Chehalis River near Centralia, WA on 2/9/1996.



Figure 5. Looking east at Pier 10 (foreground) and Pier 9 (the pier that failed) of Galvin Road Overflow Bridge, 2/9/1996.



Figure 6. Looking east along downstream side of Galvin Road overflow bridge into scour hole during dewatering.



Figure 7. Looking downstream (north) to the Galvin Road overflow bridge.



Figure 8. Looking downstream at piers 8, 9 (the pier that failed) and 10 following the February 1996 flood.



Figure 9. Looking east at failed pier #9 following the February 1996 flood.



Figure 10. Looking west toward sag in bridge deck due to failure of pier #9 during the February 1996 flood.

MEASURED SCOUR

The limits and depth of the scour hole are depicted in Figure 11. The hole was 130 feet long in the longitudinal direction of flow beginning 10 feet upstream and extending 90 feet downstream from the bridge. Piers 7-10 are encompassed by the 110-foot wide scour hole. Observations following the dewatering of the scour hole indicated that the bottom was armored with a layer of gravel.

Abutment Scour

No measurement of abutment scour was made at the Galvin Road overflow bridge.

Contraction Scour

The contraction at this site is most notably attributed to the severe constriction in the floodplain flow width created by extending the western approach fill 146 feet to accommodate the new shorter Galvin Road overflow bridge. Although the hydraulic analysis for the new bridge revealed that the shorter structure would meet the Federal Emergency Management Agency's (FEMA) requirement of less than 1-foot increase in the floodplain depth, the analysis did not consider the potential for scour.

The measured contraction scour depth and modeled site characteristics pertinent to contraction scour are summarized in Table 9. The maximum contraction depth was approximately 14 feet measured adjacent to piers #8 and #9 near the downstream bridge face.

Pier Scour

Although local pier scour around the base of the piles may have contributed to the total scour depth and failure of the piles, it was determined by NHC to be insignificant compared to the contraction scour. Therefore, no measurement or computations of pier scour were made at the Galvin Road overflow bridge.

Table 9. Contraction scour data (--, not available; ft/s, feet per second; cfs, cubic feet per second; US, upstream; DS, downstream; Avg, average)

Measurement Number	Contracted Date	Contracted Time	Uncontracted Date	Uncontracted Time	US/DS	Scour Depth (ft)
1	2/9/1996	--	2/9/1996	--	US	3
2	2/9/1996	--	2/9/1996	--	US	3
Measurement Number	Accuracy (ft)	Contracted Avg Vel (ft/s)	Contracted Discharge (cfs)	Contracted Depth (ft)	Contracted Width (ft)	Channel Contraction Ratio
1	2	7.6	25,000	9.31	359	--
2	2	9.1	30,000	9.33	360	--
Measurement Number	Uncontracted Avg Vel (ft/s)	Uncontracted Discharge (cfs)	Uncontracted Depth (ft)	Uncontracted Width (ft)	Channel Contraction Ratio	
1	2.7	13,990	6.31	400	--	
2	3.0	16,600	6.33	400	--	
Measurement Number	Pier Contraction Ratio	Scour Location	Eccentricity	Sediment Transport	Bed Material Cohesion	Debris Effect
1	---	Overflow Bridge	---	Clear-water	Non-cohesive	Unknown
2	---	Overflow Bridge	---	Clear-water	Non-cohesive	Unknown

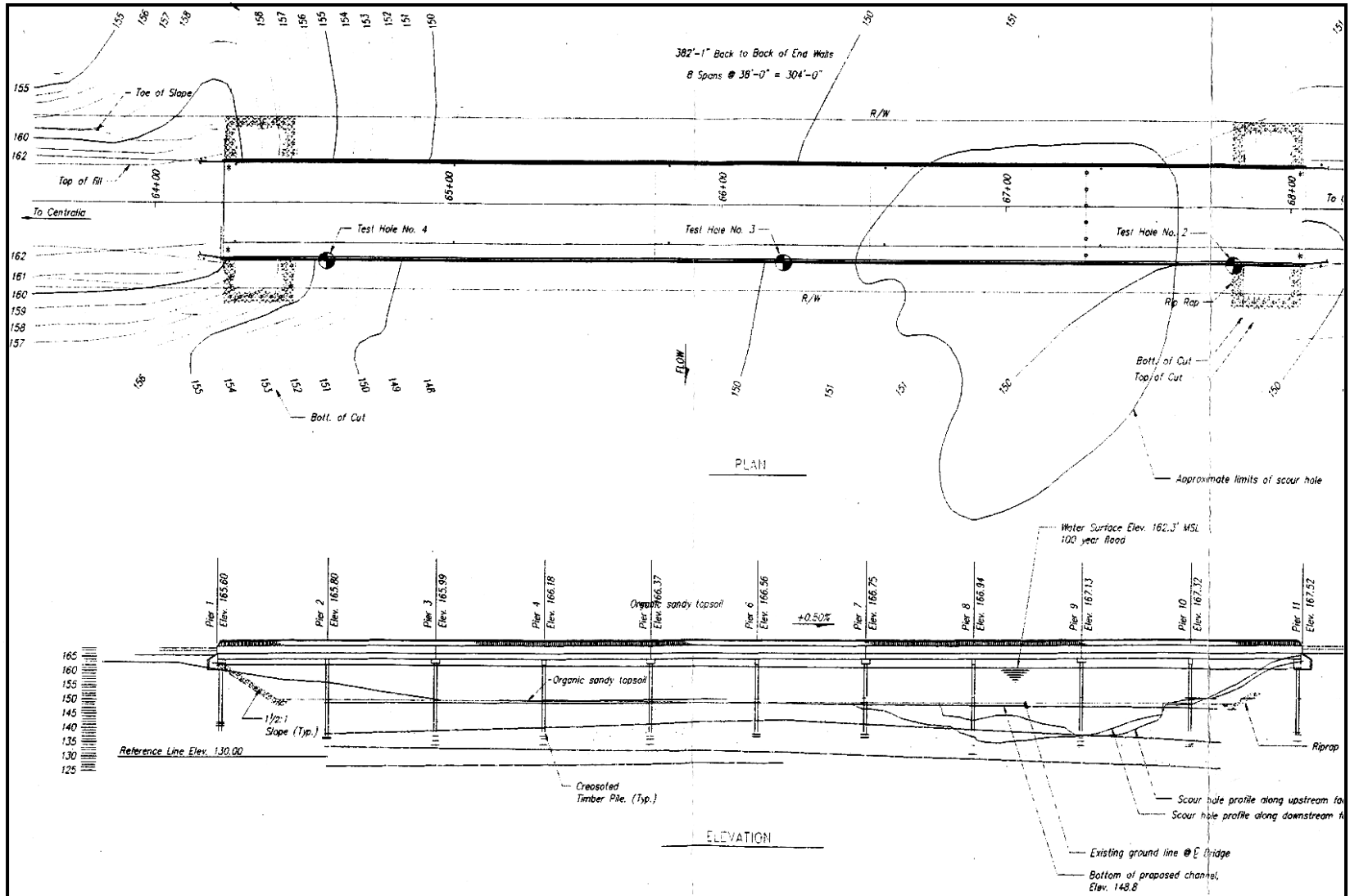


Figure 11. Plan and profile plots of scour hole location at Galvin Road overflow bridge for the Chehalis River, Centralia, WA.

COMPUTED SCOUR

A HEC-2 model of the site was developed as part of a post-scour analysis of the Galvin Road overflow bridge to determine the cause of the scour at this site and suggest mitigation procedures. As discussed previously, from the high-water marks the HEC-2 model predicted that 45,000 – 50,000 cfs remained in the Chehalis River channel and 25,000 – 30,000 cfs passed through the overflow bridge. The model indicated that at cross section 8 in Figure 2, the flow distribution across the floodplain was as follows: Zone A 2,500 cfs, Zone B 17,000 cfs, and Zone C 10,500 cfs. The combination of flows in zones B and C greatly increased the discharge and velocity near the left abutment (looking downstream) and produced the large scour hole (Northwest Hydraulic Consultants, 1996). The model indicated that just prior to the scour hole development, velocities through the western section of the bridge might have exceeded 12 feet per second (fps).

Abutment Scour

No abutment scour was computed with the HEC-RAS model.

Contraction Scour

Using the methodology from HEC-18 (Richardson and Davis, 1995) Laursen Clear – Water contraction scour equation was used to compute the maximum scour at the site given the February 9, 1996 flood conditions. The results of the computed contraction scour are summarized in Table 12.

Pier Scour

No pier scour was computed.

Table 12. Summary of computed and observed contraction scour for the Galvin Road Overflow bridge of the Chehalis River near Centralia, WA.

	Type	HEC-18 Computed (ft)	Observed (ft)
Contraction Scour	Clear-Water	30.6	3

POINTS OF CONTACT

Any questions regarding the Galvin Road overflow bridge for the Chehalis River should be directed to the following point of contact:

1. Chad Wagner, Hydraulic Engineer
U.S. Geological Survey, Water Resources Division
cwagner@usgs.gov
2. Rod Lakey, Senior Engineer
Lewis County Department of Public Works
350 N. Market Boulevard
Chehalis, WA 98532
(360) 740-1123

REFERENCES

Northwest Hydarulic Consultants, 1996, Galvin Road Overflow Bridge Failure – Scour and Hydraulic Investigation, Report prepared for Lewis County Department of Public Works. Tukwila, Wash. 9 p.

Robert E. Meyer Consultants, Inc., 1986, Bridge Hydraulics Study for Galvin Overflow Bridge and Scheuber Road Bridge Chehalis River, Washington, Report prepared for Lewis County Department of Public Works. Beaverton, Oregon. 22 p.

Robert E. Meyer Consultants, Inc., 1991, Bridge Hydraulics Study for Galvin Overflow Bridge and Scheuber Road Bridge Chehalis River, Washington, Report prepared for Lewis County Department of Public Works. Beaverton, Oregon. 20 p.

Richardson, E.V., and Davis, S.R., 1995, Evaluating scour at bridges (3d ed.): U.S. Federal Highway Administration, FHWA-IP-90-017 HEC-18, 204 p.

SUPPORTING DATA

Photo2.jpg - Looking east across upstream face of Galvin Road Overflow Bridge for Chehalis River near Centralia, WA on 2/9/1996.

Photo3.jpg - Looking east at Pier 10 (foreground) and Pier 9 (the pier that failed) of Galvin Road Overflow Bridge, 2/9/1996.

Photo4.jpg - Looking east along downstream side of Galvin Road overflow bridge into scour hole during dewatering.

Photo5.jpg - Looking downstream (north) to the Galvin Road overflow bridge.

Photo6.jpg - Looking east at failed pier #9 following the February 1996 flood.

Photo7.jpg - Looking upstream at left abutment and area of failure from downstream of bridge.

Photo8.jpg - Looking downstream at piers 8, 9 (the pier that failed) and 10 following the February 1996 flood.

Photo10.jpg - Looking west toward sag in bridge deck (from bridge deck) due to failure of pier #9 during the February 1996 flood.

GalvinRdFlowPatterns.jpg - Sketch of flow patterns and HEC-2 model sections through Galvin Road overflow bridge during February 1996 flood.

GalvinRdScourHole.jpg - Plan and profile plots of scour hole location at Galvin Road overflow bridge for the Chehalis River, Centralia, WA.

ChehalisMap.jpg - Location and topographic map of Galvin Road Overflow bridge site.

AerialPhoto.jpg - Aerial photo of the Gavin Road Overflow bridge site taken in 1990

CASE STUDY #10

Chariton River at State Route 129 near Prairie Hill, Missouri

SITE OVERVIEW

The study site is located on the Chariton River at mile 11.73 of State Route 129, about 9 miles north of the town of Salisbury (at the intersection of State Route 129 and U.S. Route 24), and about 18 mile south of the intersection of State Route 129 and U.S. Route 36. A USGS streamflow gaging station (06905500) is located at the study site. The period of record for this station (06905500) is from October 1928 to the current year, with an annual mean flow of 1,273 cfs, and an instantaneous peak flow of 33,600 cfs recorded on May 27, 1996 (stage 22.33 ft, gage datum). The Chariton River basin above the bridge covers approximately 1,870 square miles, and is partially regulated by Rathbun Lake in Iowa (station 06903880) built in 1969.

The structure number for this site is L-344 and consists of 60'-70'-70'-60' continuous I-beam spans supported by three dual-conical concrete column piers with partial web walls, and spill-through abutments. The Missouri Dept of Transportation (MoDOT) built the current bridge in 1949 and channelized the Chariton River, replacing a structure over the old channel on the current right floodplain. The channel has been regularly dredged, evidenced by the dredge piles observed on both banks. Apparently due to channelization, this site is prone to catch drift. Several of the flood measurements on record indicate a large debris drift pileup on the central pier and the consequent scour that occurs as a result of the raft. The propensity to catch debris and the resulting scour are what make this site an interesting case study.

The USGS National Bridge Scour Team and Missouri District in cooperation with NCHRP and the University of Louisville made real-time limited-detail bridge scour measurements at the site during the flooding on May 24, 1995. All of the data used in the analysis of the 1995 flood were collected from the bridge deck with a current meter, sounding weight and echo sounder. Prior to the 1995 flood, several other scour measurements have been made at the Chariton River site (1960, 1973, 1978, and 1993). A summary of the general site information on the site is found in Table 1.

Table 1. Site information

Site Characteristic	Description
County	Chariton
Nearest City	Prairie Hill
State	Missouri
Latitude	39°32'25''
Longitude	92°47'23''
Route Number	129
Route Class	State
Stream Name	Chariton River

A step-backwater hydraulic model (WSPRO) of the S.R. 129 site was developed to predict the amount of pier and contraction scour expected for flood measurements at the site based on one dimensional hydraulic parameters and equations from HEC-18.

Hydrologic Conditions

The hydrologic events responsible for the measured floods were typical springtime cyclonic fronts that merged with an excessive amount of Gulf of Mexico moisture to produce heavy rainfall in the Chariton River basin. The peak discharge that was measured during the five scour measurements was 31,300 cubic feet per second (cfs) on April 22, 1973. The peak discharge in April, 1973 has approximately an 83-year return period according to the peak flow frequency analysis, developed for the Chariton River at Prairie Hill (06905500) USGS gaging station.

DISCUSSION OF CONTRACTED SITE

A review of flood measurement notes at the site seems to indicate that bed elevations in cases where the debris raft is not present are consistently steady, matching the ground line at the time of construction of L-344 and a channel survey taken in November 1999 during low flow. However, for floods where a debris raft forms on the central pier, the bed elevations drop by as much as 20 feet in what appears to be a combination of contraction scour (caused by the reduced flow area due to the raft) and local scour effects caused by the raft and pier. For example, during the July 8, 1993 flood, the streambed was lowered by about 19 ft at the downstream side of the bridge in comparison to streambed levels recorded on June 9, 1993 (see Figure 1). This temporary degradation is attributed to combined effects of contracted flow at the bridge and partial blockage of the bridge opening by woody debris. A cross section obtained on August 19, 1993 (Figure 1) indicated that the streambed was reestablished at a level slightly higher than that of June 9, 1993. A picture of the debris raft formed at the left pier in 1995 is shown in Figure 2.

Bridge Data

Structure L-344 consists of 60'-70'-70'-60' continuous I-beam spans supported by three dual-conical concrete column piers with partial web walls, and spill-through abutments (type III contracted opening). The piers and the abutments are founded on piling; the pier piling is driven to an elevation of 585-590 ft, and the abutment piling is driven to an elevation of 607 ft. The right abutment extends into the channel and the left abutment is set back about 35 feet from the top of the left bank. Both the left bank and the right abutment are covered with large chunks of concrete debris and riprap. The bridge characteristics pertinent to scour are summarized in Table 2.

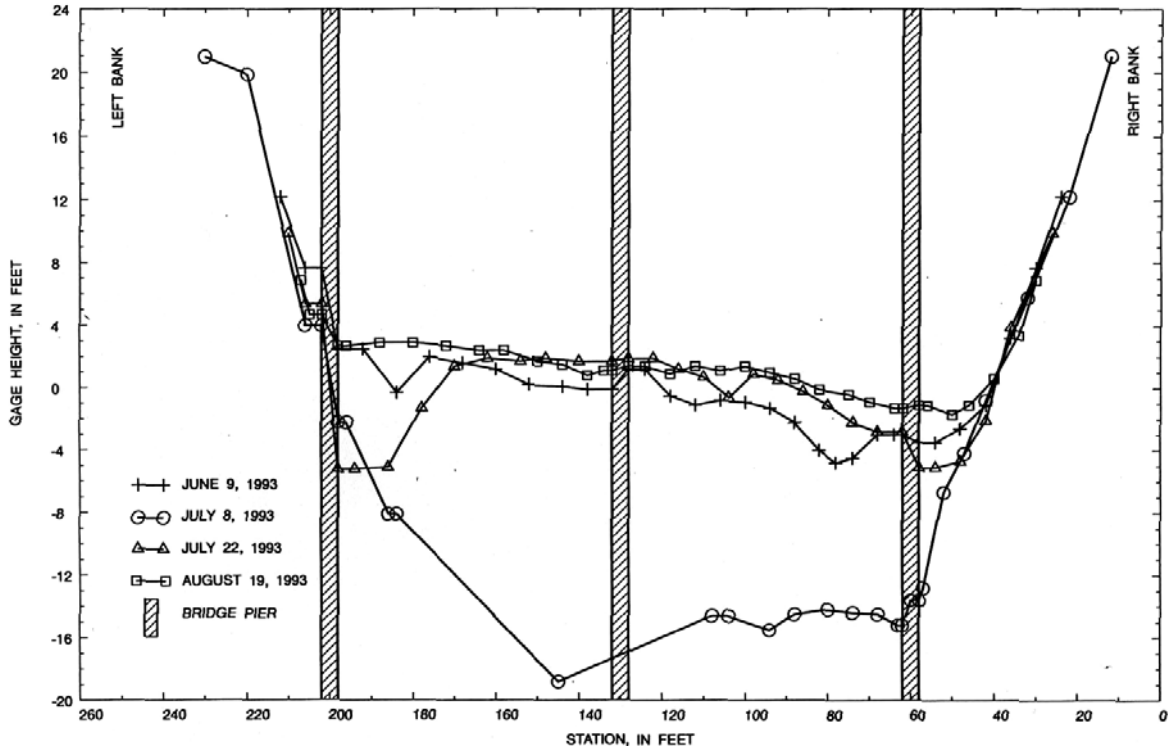


Figure 1. Streambed cross-sections at the downstream face of the SR 129 bridge over the Chariton River near Prairie Hill, MO.

Table 2. Bridge data

Bridge Characteristic	Description
Structure Number	L-344
Length (ft)	264
Width (ft)	24.5
Spans	4
Vertical Configuration	Horizontal
Low Chord Elev (ft)	657.85
Upper Chord Elev (ft)	664.25
Overtopping Elev (ft)	662.17
Skew (degrees)	0
Guide Banks	None
Waterway Classification	Main
Year Built	1949
Avg. Daily Traffic	600
Plans on File	Yes
Parallel Bridges	No
Continuous Abutments	N/A



Figure 2. – Looking upstream at the remnants of the debris raft formed in front of the middle pier (#2) of the S.R. 129 bridge over the Chariton River during the May 24, 1995 flood.

Geomorphic Setting

A review of flood measurement notes seems to indicate that this site does not experience substantial scour of any form when there is no debris raft. The bed elevations in these cases are consistently steady, matching the ground line at the time of construction of L-344 and a channel survey taken in November 1999 during low flow. The only change in the channel from the time of construction is a widening and lateral migration of the channel. The channel configuration--with the dredge banks on either side and low road embankments on both floodplains--is such that for flows less than bank-full, flow direction is straight through the bridge opening with little contraction of flow, resulting in no contraction scour and minimal pier scour. A USGS 7.5 minute quadrangle topographic map of the site is shown in Figure 3. Data characterizing the geomorphic setting is summarized in Table 3.

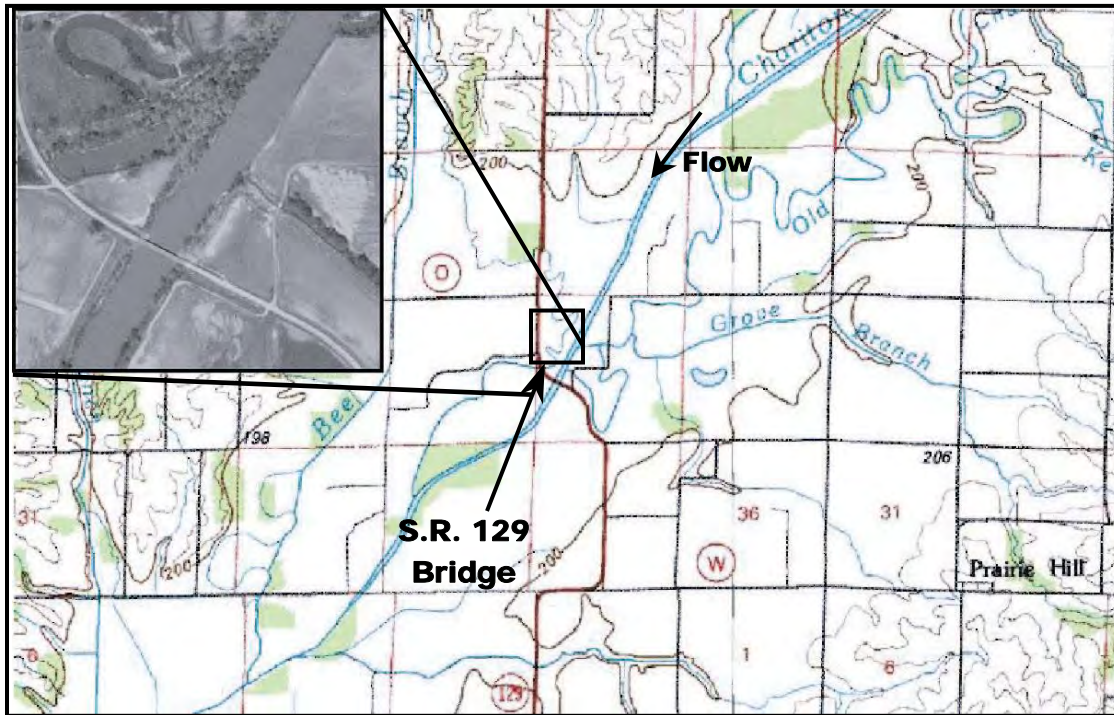


Figure 3. – USGS topographic map of S.R. 129 bridge over the Chariton River near Prairie Hill, MO (elevations are in meters).

Table 3. Geomorphic data

Geomorphic Characteristic	Description
Drainage Area	16010
Slope in Vicinity (ft/ft)	.000063
Flow Impact	Left
Channel Evolution	Channelized
Armoring	Unknown
Debris Frequency	Occasional
Debris Effect	Local
Stream Size	Medium
Flow Habit	Perennial
Bed Material	Sand
Valley Setting	Low relief
Floodplain Width	Narrow
Natural Levees	None
Apparent Incision	Deep
Channel Boundary	Alluvial
Banks Tree Cover	Medium
Sinuosity	Meandering
Braiding	None
Anabranching	None
Bars	Narrow
Stream Width Variability	Equiwidth

Bed Material Data

Bed material samples were collected in the main channel and on the left overbank with a grab sampler at low-flow. The sample in the main channel was sand with a $D_{50} = .32$ mm. The overbank sample was silty fine sand with a $D_{50} = .088$ mm. The grain size distributions for the two samples are shown in Figures 4-5.

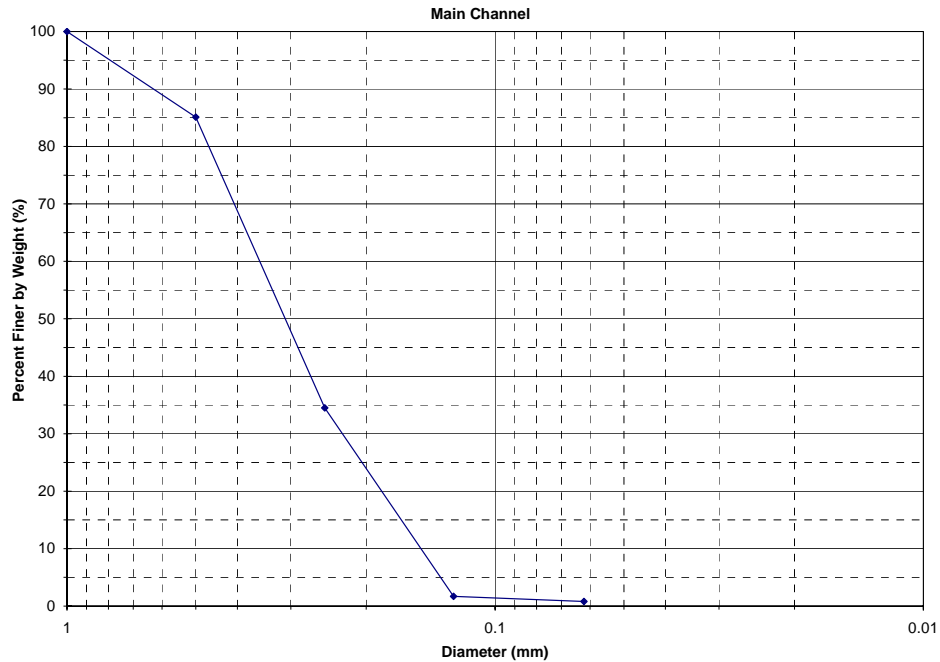


Figure 4. Grain size distribution for the bed material sample collected in the main channel of the Chariton River at the SR 129 bridge.

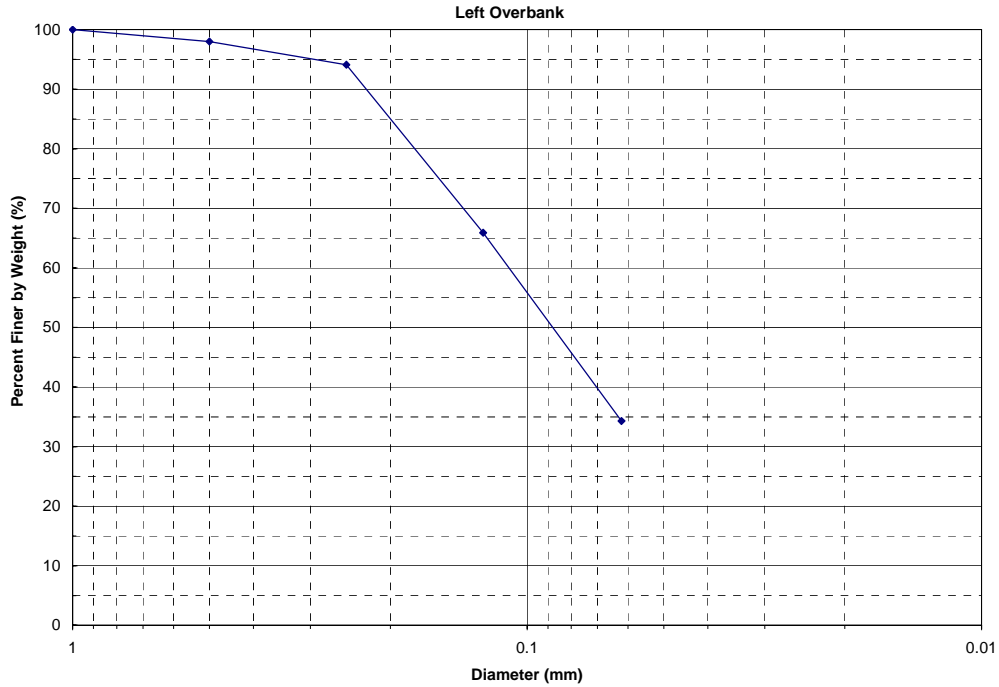


Figure 5. Grain size distribution for the bed material sample collected on the left overbank upstream of the SR 129 bridge over the Chariton River.

Roughness Coefficients

A distribution of Manning's *n* values is provided in Table 4.

Table 4. Manning's *n* values for the Chariton River at the S.R. 129 bridge. (fldpln, floodplain; chnl, channel; rt, right)

Flow Type	Left Fldpln	Main Chnl	Rt Fldpln
High	0.075	0.045	0.075
Typical	0.06	0.035	0.06
Low	0.045	0.030	0.045

Abutment Details

The bridge has sloping spill-through abutments with dumped concrete and riprap as scour protection. Substantial road overflow areas on both floodplains and dredge banks on both tops of banks preclude abutment scour. The abutment characteristics are summarized in Table 5.

Table 5. Abutment data

Abutment Characteristic	Description
Left Station	0
Right Station	264.75
Left Skew (deg)	0
Right Skew (deg)	0
Left Abutment Length (ft)	24.5
Right Abutment Length (ft)	24.5
Left Abutment to Channel Bank (ft)	35
Right Abutment to Channel Bank (ft)	-10
Left Abutment Protection	Riprap
Right Abutment Protection	Riprap
Contracted Opening Type	III*
Embankment Skew (deg)	0
Embankment Slope (ft/ft)	1.5
Abutment Slope (ft/ft)	2
Wingwalls	No

* - Type III opening has sloping abutments and sloping spillthrough abutments.

Pier Details

The three piers are numbered from left to right, looking downstream and consist of dual concrete columns with partial web walls. Each column has the following configuration, from bottom up: 9' x 6' x 4.5' (WxLxH) footings over 6 concrete piles (30' average in place); cylindrical sub-column 4.625' in diameter and 11.5' high with conical column above tapering from 4.625' to 3' in 19.625'; 3.5' x 23.5' x 2' cap; webwall from elevation 642.0' to cap. The pier characteristics are summarized in Table 6.

Table 6. Pier data (--, not available)

Pier ID	Bridge Station (ft)	Alignment	Highway Station	Pier Type	# of Piles	Pile Spacing (ft)
1	61.75	0	--	Single	-	-
2	113.75	0	--	Single	-	-
3	201.75	0	--	Single	-	-
Pier ID	Pier Width (ft)	Pier Shape	Shape Factor	Length (ft)	Protection	Foundation
1	4.63	Round	--	24.63	None	Piles
2	4.31	Round	--	24.75	None	Piles
3	4.63	Round	--	24.63	None	Piles
Pier ID	Top Elevation (ft)	Bottom Elevation (ft)	Foot or Pile Cap Width (ft)	Cap Shape	Pile Tip Elevation (ft)	
1	623.5	619	9	Square	590	
2	623	619	11.5	Square	586	
3	623.5	619	9	Square	591	

Surveyed Elevations

Bridge data elevations were taken from MoDOT plans, but are consistent with gage datum (elevation 632.05 feet above sea level). Water-surface elevations were determined using the data from the USGS gaging station at the site and a USGS wire-weight gage located on the upstream bridge face. A historical summary of the measured water surface elevations and corresponding discharges is presented in Table 7.

Table 7. Water-surface elevations and corresponding discharges measured on the Chariton River at the S.R. 129 bridge.

Date	Discharge (cfs)	Return Period (yrs)	Elevation (ft)
3/29/1960	18,200	4.5	650.51
4/22/1973	31,300	83	653.89
5/8/1978	27,500	33	651.31
7/8/1993	24,300	15	653.01
5/24/1995	28,200	42	653.97

The low-water survey of the floodplains in the approach and exit sections utilized a local right-hand coordinate system, which was established with the positive y-axis in the upstream direction and the x-axis parallel to the upstream face of the bridge. This resulted in x-coordinates increasing from right to left. The WSPRO step backwater model requires the use of left to right coordinates (looking downstream), therefore stationing was added which increases from left to right.

PHOTOS



Figure 6. Looking upstream at debris raft formed in front of right pier (#3) in June, 1963.



Figure 7. Looking at upstream S.R. 129 bridge face from right bank during low-flow on 5/26/1976.



Figure 8. Looking along upstream S.R. 129 bridge face from right bank at debris raft in front of middle pier (#2) during July 1993 flood.



Figure 9. Looking along upstream S.R. 129 bridge face from left bank at debris raft in front of middle pier (#2) during July 1993 flood.

MEASURED SCOUR

All reported bathymetry data were collected with either a sounding weight or echo sounder from the S.R. 129 bridge deck. Cross section data could not be collected with an ADCP throughout the bridge reach due to a moving bed condition, meaning that a layer of sediment was being rapidly transported along the streambed, which creates a negative bias (underestimation) in the measured discharge and velocity data. The discharge in the road overflow sections was measured by USGS personnel during the 1995 flood. A survey of the upstream and downstream floodplains was conducted after the flood during a low-water site visit in November, 1999.

Abutment Scour

No measurement or computations of abutment scour were made at the S.R. 129 bridge due to substantial road overflows and dredge banks on the tops of both the right and left banks at the bridge, which precluded any abutment scour.

Contraction Scour

The contraction at this site is mainly attributed to the large debris raft that typically collects in front of the middle pier during high flow conditions. The observed contraction scour represents depths computed from an "equilibrium bed" elevation (established in Nov, 1999, based on survey and historical data).

The measured contraction scour depths and site characteristics pertinent to contraction scour are summarized in Table 9.

Pier Scour

Scour is reported only at the middle pier (#2) for all of the scour measurements made at the S.R. 129 bridge. These pier scour depths represent depth from an "equilibrium bed" elevation (established in Nov, 1999, based on survey and historical data). The effective pier diameter is calculated using Melville & Dongel (1992) wherein the effect of a debris raft is converted to an effective pier diameter based on the thickness of the raft (assumed to be the approach depth divided by 3.4) and the diameter of the raft (approximated from discharge notes). The computed pier scour depths and site characteristics pertinent to pier scour were extracted from the WSPRO output file and summarized in Table 10.

A decision was made not to attempt to separate the total scour measurement into components due to the complexity and uncertainty that was introduced to the system by the large debris raft at the pier.

COMPUTED SCOUR

A WSPRO model of the site was developed to assess how accurately the scour at this site could have been predicted and attempt to estimate the components of the measured total scour. The pre-flood geometry of the bridge section was simulated with the WSPRO model by utilizing the channel geometry from the original bridge plans and the low-flow survey of the Chariton River in November, 1999. The discharges reported during the five measured floods were then modeled with the pre-flood bathymetry to determine the hydraulic parameters needed for HEC-18 scour computations.

Abutment Scour

No abutment scour was computed with the WSPRO model.

Contraction Scour

The reported contraction scour for each measured flood was computed using the WSPRO hydraulic parameters and HEC-18 live-bed equations. The results of the computed contraction scour are summarized in Table 11.

Pier Scour

The reported pier scour for each measured flood was computed using the WSPRO hydraulic parameters and HEC-18 pier scour equations. To determine the contribution of the debris raft on pier scour, Melville & Dongel (1992) recommends incorporating the effect of the debris into an effective pier diameter based on the thickness and diameter of the raft. The thickness of the debris raft was assumed to be a value equal to the approach depth divided by a constant (constant = 3.4 provided the best fit of observed versus HEC-18 computed scour for all (5) scour measurements) and the diameter of the raft, which was approximated from discharge notes taken during each flood. The computed pier scour and total scour measured for each flood is summarized in Table 11.

Table 9. Contraction scour data (--, not available; ft/s, feet per second; cfs, cubic feet per second; US, upstream; DS, downstream; Avg, average)

Measurement Number	Contracted Date	Contracted Time	Uncontracted Date	Uncontracted Time	US/DS	Scour Depth (ft)
1	3/29/1960	--	3/29/1960	--	--	1.2
2	4/22/1973	--	4/22/1973	--	--	6.8
3	5/8/1978	--	5/8/1978	--	--	2.3
4	7/8/1993	--	7/8/1993	--	--	0.4
5	5/24/1995	--	5/24/1995	--	--	3.1
Measurement Number	Accuracy (ft)	Contracted Avg Vel (ft/s)	Contracted Discharge (cfs)	Contracted Depth (ft)	Contracted Width (ft)	Channel Contraction Ratio
1	--	6.49	18176	17.1	163.7	0.818
2	--	4.94	17339	20.9	167.8	0.839
3	--	6.68	21330	19.7	162	0.81
4	--	7.45	22578	18.8	160.9	0.804
5	--	6.36	20579	20	161.9	0.81
Measurement Number	Uncontracted Avg Vel (ft/s)	Uncontracted Discharge (cfs)	Uncontracted Depth (ft)	Uncontracted Width (ft)	Channel Contraction Ratio	Bed Form
1	5.7	17952	15.7	200	0.818	Unknown
2	7.46	28324	19	200	0.839	Unknown
3	7.29	26351	18.1	200	0.81	Unknown
4	6.88	23913	17.4	200	0.804	Unknown
5	7.34	26795	18.3	200	0.81	Unknown
Measurement Number	Pier Contraction Ratio	Scour Location	Eccentricity	Sediment Transport	Bed Form	Debris Effect
1	---	Main Channel	---	Live-Bed	Unknown	Substantial
2	---	Main Channel	---	Live-Bed	Unknown	Substantial
3	---	Main Channel	---	Live-Bed	Unknown	Substantial
4	---	Main Channel	---	Live-Bed	Unknown	Substantial
5	---	Main Channel	---	Live-Bed	Unknown	Substantial
Measurement Number	D95 (mm)	D84 (mm)	D50 (mm)	D16 (mm)	Sigma	Bed Material Cohesion
1	0.725	0.49	0.32	0.18	--	Mildly
2	0.725	0.49	0.32	0.18	--	Mildly
3	0.725	0.49	0.32	0.18	--	Mildly
4	0.725	0.49	0.32	0.18	--	Mildly
5	0.725	0.49	0.32	0.18	--	Mildly

Table 10. Pier scour data

Measurement Number	Pier ID	Date	Location	Scour Depth (ft)	Accuracy (ft)	Effective Pier Width (ft)
1	2	3/29/1960	Upstream	15.3	0.50	9.58
2	2	4/22/1973	Upstream	17.1	0.50	13.28
3	2	5/8/1978	Upstream	19.2	0.50	13.36
4	2	7/8/1993	Upstream	21.1	0.50	14.34
5	2	5/24/1995	Upstream	12.8	0.50	7.23

Measurement Number	Approach Velocity (ft/s)	Approach Depth (ft)	Skew (deg)	Sediment Transport	Cohesion	Debris Effects
1	7.2	15.4	0	Live-Bed	Non-cohesive	Substantial
2	5.33	19.1	0	Live-Bed	Non-cohesive	Substantial
3	7.03	18	0	Live-Bed	Unknown	Substantial
4	8	17.1	0	Live-Bed	Unknown	Substantial
5	6.84	18.2	0	Live-Bed	Unknown	Substantial

Measurement Number	Comments
1	Effective pier diameter based on the thickness of the raft (assumed to be the approach depth divided by 3.4 = $(17.1/3.4) = 5.03$) and the diameter of the raft (approximated from discharge notes as 70 feet). The computed contraction scour was 0.4 feet, for a total scour of 21.5 feet. The actual measured total scour on this date was 20.0 feet.
2	Effective pier diameter based on the thickness of the raft (assumed to be the approach depth divided by 3.4 = $(19.1/3.4) = 5.62$) and the diameter of the raft (approximated from discharge notes as 70 feet). The computed contraction scour was 0.0 feet, for a total scour of 17.1 feet. The actual measured total scour on this date was 17.1 feet
3	Effective pier diameter based on the thickness of the raft (assumed to be the approach depth divided by 3.4 = $(18.0/3.4) = 5.30$) and the diameter of the raft (approximated from discharge notes as 70 feet). The computed contraction scour was 0.0 feet, for a total scour of 19.2 feet. The actual measured total scour on this date was 20.0 feet.
4	Effective pier diameter based on the thickness of the raft (assumed to be the approach depth divided by 3.4 = $(17.1/3.4) = 5.03$) and the diameter of the raft (approximated from discharge notes as 70 feet). The computed contraction scour was 0.4 feet, for a total scour of 21.5 feet. The actual measured total scour on this date was 20.0 feet
5	Effective pier diameter based on the thickness of the raft (assumed to be the approach depth divided by 3.4 = $(19.1/3.4) = 5.62$) and the diameter of the raft (approximated from discharge notes as 70 feet). The computed contraction scour was 0.0 feet, for a total scour of 12.8 feet. The actual measured total scour on this date was 11.8 feet

Table 11. Comparison of model-computed and measured scour at S.R. 129 over the Chariton River near Prairie Hill, MO.

Date	Computed Contraction Scour (ft)	Computed Pier Scour (ft)	Total Computed Scour (ft)	Total Measured Scour (ft)
3/29/60	1.2	15.3	16.5	17.2
4/22/73	0.0	17.1	17.1	17.1
5/8/78	0.0	19.2	19.2	20.0
7/8/93	0.4	21.1	21.5	20.0
5/24/95	0.0	12.8	12.8	11.8

REFERENCES

Any questions regarding the S.R. 129 bridge over the Chariton River should be directed to the following points of contact:

1. Richard J. Huizinga, U.S. Geological Survey
1400 Independence Road, MS 200
Rolla, MO 65401
Phone: (573) 308-3570
e-mail: huizinga@usgs.gov
2. Paul Rydlund, U.S. Geological Survey
1400 Independence Road, MS 200
Rolla, MO 65401
Phone: (573) 308-3572
e-mail: prydlund@usgs.gov

SUPPORTING DATA

Model Files:

wsp_complev3.dat - Input file, WSPRO model of measured flows with no road overflow.
wsp_complev3.prt - Output file WSPRO model of measured flows w/ no road overflow.
wsp_complev2.dat - Input file, WSPRO model of measured flows with road overflow.
wsp_complev2.prt - Output file WSPRO model of measured flows with road overflow.

Survey Data and Scour Calculations:

CharitonBridgeSection.xls – Excel file with bridge face cross-section plots of all scour measurements.
CharitonSurey.xls – Excel file with raw data of topographic survey of approach, full valley and exit sections.
Debrisflood.xls – Excel file of scour calculations using HEC-18 and New Zealand methods.